An aerial photograph of a mountain valley. The foreground shows steep, rocky slopes with patches of green vegetation. A winding road is visible in the middle ground, leading down to a small village with red-roofed buildings. The background features more mountain ranges under a clear blue sky.

# **Numerical Modeling as a Means to Enhance Genetic Sedimentary Basin Interpretation: A Case Study of the Southern Cantabrian Basin (NW Spain)**

**Birgit Dietrich  
2005**



Numerical Modeling as a Means to Enhance  
Genetic Sedimentary Basin Interpretation:  
A Case Study of the Southern Cantabrian Basin  
(NW Spain)

INAUGURAL - DISSERTATION

zur Erlangung der Doktorwürde der  
Naturwissenschaftlich - Mathematischen  
Gesamtfakultät der  
Ruprecht - Karls - Universität  
Heidelberg

Vorgelegt von  
Diplom - Geologin Birgit Dietrich  
aus Frankfurt am Main



Gutachter 1: **HD Dr. Rainer Zühlke**

Geologisch-Paläontologisches Institut, Ruprecht-Karls-Universität Heidelberg  
Im Neuenheimer Feld 234, 69120 Heidelberg

Gutachter 2: **Prof. Dr. Peter Kukla**

Geologisches Institut, RWTH Aachen  
Wüllnerstr. 2, 52056 Aachen

Tag der mündlichen Prüfung: 04.07.2005



a) Ich erkläre hiermit, dass ich die vorgelegte Dissertation selbst verfasst und mich dabei keiner anderen als der von mir ausdrücklich bezeichneten Quellen und Hilfen bedient habe.

b) Ich erkläre hiermit, dass ich an keiner anderen Stelle ein Prüfungsverfahren beantragt bzw. die Dissertation in dieser oder anderer Form bereits anderweitig als Prüfungsarbeit verwendet oder einer anderen Fakultät als Dissertation vorgelegt habe.

Heidelberg, den 12.05.2005

## ACKNOWLEDGEMENTS

First of all, I would like to thank Thilo Bechstädt for providing the opportunity to do my doctoral studies at the University of Heidelberg and allocating the topic of my work that comprised so many interesting parts of geology. I am grateful for him reading and revising the thesis, which certainly enhanced the final version.

Rainer Zühlke supervised my work and was always open for discussion and widening the modeling horizon. I am grateful for revisions of the thesis and continuous motivation during my time in Heidelberg.

I am indebted to Peter Kukla for kindly accepting to referee the thesis and being a member of the committee.

Thanks go to the DFG (German Research Foundation) for financial support of the project, including travel and material cost and also providing transportation to carry out field work; to the IPP for travel money, sponsoring courses and social events.

I would like to thank everybody who invaluablely added more information to the project and helped improving my thesis:

To Elisa Villa, who kindly shared her paleontological knowledge to determine foraminifers of my field area.

To Jürgen Adam, who gave support in constructing admissible cross-sections and to Reinhard Greiling and Jens Grimmer for further discussions.

To Scott Bowman and Chris Kendall for providing support with the modeling programs and rushing in as a last-minute help.

To Elias Samankassou, Luis Pedro Fernández González, Giovanna della Porta, Jeroen Kenter and Juan Bahamonde for sedimentological discussions.

Special thanks go to Naomi Veselovsky for kindly improving the English text, and also to Adrienne Patterson for last-minute English revisions.

I thank the assistants Lena and Christian for taking some of the tedious work off my back.

The time in Heidelberg was stimulated in many ways by the “team 113a”: Axel Emmerich, Michael Seeling, and Zbynek Veselovsky - thanks, guys! I am glad about discussing “Cantabrian issues” with Thomas Angerer, Fernando Ayllón, Kevin Carrière, Marta Gasparrini, Jochen Schneider, and Kai Frings. Let me also say “thank you” to the following “geos” (sorry for ignoring various non-geo backgrounds of all the people who came together at our multicultural institute!) for upgrading the time in and outside the institute: Anja, Asher, Bonsai, Carsten, Fabio, Francisco, Frank, Gesine, Guy, Ibi, Isabelle, Jana, Jutta, Kirsten, Manu, Ralph, Rike, Rolf, Roswitha and to everybody who I may have forgotten to mention!

I would like to particularly thank all my friends motivating me and sharing time with me during the last years, especially Franziska, Michela and Ohle.

„The Spanish Team“ sweetened everyday-life in the Spanish Mountains: Igor, José, Nora, Luis, Ricardo and Estelle - thanks for safety backup and having a great time together in Spain - ¡Todos los días sale el sol!

Last but not least, I am grateful that my parents and brothers were always there to support me.





# TABLE OF CONTENTS

## ACKNOWLEDGEMENTS

## ABSTRACT

## ZUSAMMENFASSUNG

<b>CHAPTER 1: INTRODUCTION</b>	<b>1</b>
<b>1.1 THE OROGENIC CYCLE</b>	<b>3</b>
<b>1.1.1 Wilson - Cycle</b>	<b>3</b>
<b>1.1.2 Foreland Basins</b>	<b>4</b>
<i>Tectonic Model</i>	4
Spatial Dimension of Depositional Zones	5
Visco-Elastic or Elastic Lithospheric Model?	6
<i>Antitectonic Model</i>	6
<i>Sedimentary Evolution</i>	7
<b>1.2 Sequence Stratigraphy</b>	<b>8</b>
<b>1.3 Structural Balancing</b>	<b>8</b>
<b>1.3.1 History</b>	<b>9</b>
<b>1.3.2 Principle</b>	<b>9</b>
<b>1.4 Numerical Basin Modeling</b>	<b>10</b>
<b>1.4.1 Basin Fill Succession: Controlling Factors</b>	<b>10</b>
<b>1.4.2 Reverse Modeling (2D-Backstripping)</b>	<b>11</b>
<b>1.4.3 Forward Modeling</b>	<b>12</b>
 <b>Chapter 2: Geological Framework</b>	 <b>13</b>
<b>2.1 GEODYNAMIC OVERVIEW</b>	<b>13</b>
<b>2.1.1 Late Neoproterozoic to Silurian</b>	<b>13</b>
<i>Neoproterozoic</i>	13
<i>Cambrian to Silurian</i>	13
<b>2.1.2 Devonian and Carboniferous: European Variscides and the Cantabrian Zone</b>	<b>14</b>
<i>Evolution of the Asturian Arc</i>	16
<i>Deep Structure of the Orogen</i>	18
<i>Metamorphism</i>	18
<b>2.1.3 Permian to Recent: Post-Variscan Deformation History</b>	<b>19</b>
<b>2.2 Sedimentary Development of NW-Iberia</b>	<b>19</b>
<i>Cambrian and Ordovician</i>	19
<i>Silurian</i>	21
<i>Devonian</i>	22
<i>Carboniferous</i>	23

<b>CHAPTER 3: CANTABRIAN BASIN FILL</b>	<b>25</b>
<b>3.1 Cambrian to Upper Devonian Deposits</b>	<b>26</b>
<i>Herrería Formation</i>	26
<i>Láncara Formation</i>	26
<i>Oville Formation</i>	26
<i>Barrios Formation</i>	27
<i>Capas de Getino</i>	27
<i>San Pedro Formation</i>	28
<i>La Vid Group</i>	28
<i>Santa Lucía Formation</i>	28
<i>Huergas Formation</i>	28
<b>3.2 Upper Devonian to Carboniferous Deposits</b>	<b>28</b>
<i>Ermita Formation</i>	30
<i>Baleas Formation</i>	30
<i>Vegamián Formation</i>	31
<i>Alba Formation</i>	32
<i>Barcaliente Formation</i>	33
<i>Olleros Formation</i>	37
<i>Valdeteja Formation</i>	38
Slope	40
Platform Margin	44
Platform Interior	46
Intra-Platform Basin	49
<i>Forcoso Zone</i>	49
<i>San Emiliano Formation</i>	52
<b>3.3 Post-Westphalian Deposits</b>	<b>58</b>
 <b>Chapter 4: Integrated Tectono-Sedimentary and Sequence Stratigraphic Model</b>	
<b>for the Serpukhovian to Moscovian</b>	<b>61</b>
<b>4.1 TECTONO-SEDIMENTARY MODEL</b>	<b>61</b>
<b>4.1.1 Fault-bounded Basin</b>	<b>61</b>
<b>4.1.2 Orogenic Foreland Basin</b>	<b>61</b>
<b>4.2 Bashkirian and Moscovian Sequence Stratigraphy</b>	<b>63</b>
<i>Pre-Bas 1 (Barcaliente Fm.)</i>	63
<i>Bas 1 (ca. 321Ma - 317.5Ma, Barcaliente Fm. - Valdeteja Fm.)</i>	63
<i>Bas 2 (317.5Ma - 315Ma, Valdeteja Fm., Forcoso Zone, San</i>	
<i>Emiliano Fm.)</i>	75
<i>Mos 1 (315Ma - 313.5Ma, Valdeteja Fm., Forcoso Zone, San</i>	
<i>Emiliano Fm.)</i>	77
<i>Mos 2 (&lt;313.5, San Emiliano Fm.)</i>	77

<b>CHAPTER 5: STRUCTURAL BALANCING</b>	79
<b>5.1 CONSTRAINTS</b>	79
<i>Deformation Mechanism</i>	83
<i>Out-of-Sequence Deformation</i>	84
<b>5.2 Construction of Cross-Sections</b>	84
<i>Choice of Line</i>	84
<i>Sedimentary Thickness Changes</i>	85
<i>Internal Deformation</i>	85
<i>Detachment</i>	85
<i>Duplexes and Imbricate Thrust System</i>	85
<b>5.2.1 Cross-Section A-B</b>	87
<b>5.2.2 Cross-Section E-F</b>	90
<b>5.3 Restoration of Cross-Sections</b>	92
<b>5.4 Results and Discussion</b>	92
 <b>Chapter 6: Subsidence Analysis</b>	97
<b>6.1 DATABASE</b>	97
<i>Time Lines</i>	97
<i>Sedimentary Thickness</i>	97
<i>Flexural Parameters</i>	98
<i>Lithologies and Compaction</i>	101
<b>6.2 Pre-Carboniferous Basin Fill</b>	102
<b>6.2.1 Results</b>	102
<b>6.2.2 Discussion</b>	106
<b>6.3 Carboniferous Basin Fill</b>	109
<b>6.3.1 Results</b>	109
<i>Bas 1 (ca.321Ma - 317.5Ma)</i>	111
<i>Bas 2 (317.5Ma - 315Ma)</i>	111
<i>Mos 1 (315Ma - 313.5Ma)</i>	113
<i>Mos 2 (&lt;313.5Ma)</i>	113
<b>6.3.2 Discussion</b>	114
<i>Spatial and Temporal Patterns</i>	114
The Bodón Unit	115
 <b>CHAPTER 7: STRATIGRAPHIC FORWARD MODELING</b>	117
<b>7.1 MODELING SOFTWARE: OVERVIEW</b>	117
<b>7.2 Software Specifics: SEDPAK</b>	117
<b>7.2.1 Siliciclastics</b>	118
<i>Clastic supply</i>	118
<b>7.2.2 Carbonates</b>	118



<b>7.3 Data Input</b>	119
<i>Facies Distribution</i>	120
<i>Porosity and Density</i>	120
<i>Eustatic Sea-Level Curve and Subsidence</i>	120
<i>Resolution</i>	120
<i>Initial Topography</i>	121
<i>Limitations of the Model</i>	121
<b>7.4 Results</b>	122
<b>7.4.1 Carbonate Deposition</b>	122
<i>Valdeteja Fm.: Platform Patterns</i>	123
<b>7.4.2 Siliciclastic Deposition</b>	127
<b>7.4.3 Eustatic Sea-Level Curve</b>	130
<b>Chapter 8: Synt hesis</b>	131
<b>8.1 SOUTHERN CANTABRIAN BASIN: THE PRE-CARBONIFEROUS</b>	131
<b>8.2 The Carboniferous</b>	131
<b>8.2.1 Serpukhovian - Moscovian: Regional Setting</b>	131
<b>8.2.2 Serpukhovian</b>	132
<b>8.2.3 Bashkirian and Moscovian</b>	132
<b>8.2.4 Spatial and Temporal Patterns and their Implications</b>	133
<b>Chapter 9: Concl usions</b>	137
<b>9.1 SEDIM ENTOLOGICAL MODEL</b>	137
<b>9.2 Structural Balancing</b>	137
<b>9.3 Subsidence Analysis</b>	138
<b>9.4 Forward Modeling</b>	138
<b>References</b>	141
<b>LIST OF FIGURES</b>	159
<b>LIST OF TABLES</b>	162
<b>LIST OF STRATIGRAPHIC PROFILES</b>	162
<b>LIST OF MOVIES</b>	163
<b>LIST OF ABBREVEATIONS</b>	163
<b>APPENDIX I</b>	165
<i>Stratigraphic Profiles</i>	165
<b>APPENDIX II</b>	258
<i>Biostratigraphic Data</i>	258
<i>Stratigraphic Data</i>	261
<b>APPENDIX III</b>	
<i>Architectural and Stratigraphic Development of the Basin Fill</i>	CD-ROM

## ABSTRACT

The objective of this work was to quantify factors controlling the development of the Southern Cantabrian Basin (NW Spain). A sedimentological and sequence stratigraphic model was established for the syn-orogenic Carboniferous basin fill, and subsequently analyzed and calibrated by a combined approach of reverse basin and stratigraphic forward modeling.

The basin fill comprises Cambrian to Carboniferous deposits that were deformed and displaced along thrust planes by thin-skinned tectonics within the Variscan fold-and-thrust belt. In order to carry out stratigraphic modeling, structural balancing was employed to determine initial distances between the recorded stratigraphic columns. Surface data only were available, therefore a family of structures was determined for the Southern Cantabrian Zone to construct admissible cross-sections. Within the thrust sheets, minimum shortening rates range from 19% to 54%, depending on the extent to which individual tectonic units were deformed. Minimum shortening rates range between 44% and 64%, including displacement along the thrust planes.

The Carboniferous deposits reflect the development from a simple underfilled foreland basin to a segmented and subsequently filled foreland basin system. Within the field area, distal siliciclastic foredeep deposits successively onlap and terminate the Valdeteja carbonate platform that developed in the position of the forebulge. The cratonward margin of the platform and the transition to the basinal backbulge deposits are well exposed. The margin exhibits excellent stratification patterns that

were able to be traced within aerial photographs due to the overly subvertical dip of the sedimentary package.

Sequence stratigraphic analysis was based on stratigraphic columns measured during field work, thin section analysis, biostratigraphic data and aerial photographs. It was used to reach a higher time-resolution within the carbonate platform and to correlate the stages of platform development with the progressively approaching, predominantly siliciclastic, deposits of the San Emiliano Formation. Platform termination proceeded from the west and south to the east by increasing subsidence rates and terrigenous input. The change in depositional environment from a shallow-water platform to a mixed carbonate-siliciclastic basinal deposition reflects the response of the lithosphere to the progressively approaching Variscan Orogen.

Reverse basin modeling was applied to two restored, north-south oriented transects and also to a third, west-east oriented transect connecting them. Subsidence rates were obtained for the complete Paleozoic basin fill. These data cover the development of the basin from an early Paleozoic extensional to a late Paleozoic compressional setting that resulted in the creation of the Variscan Orogen. Due to the proximal position of the transects, pre-Carboniferous data show uniformly low subsidence rates with a maximum of 80m/Ma.

Thermo-tectonic subsidence rates of 740m/Ma at maximum created the necessary space to accommodate the siliciclastics shed during the orogenic foredeep stage during the Carboniferous. Subsidence rates within the

internal parts of the forebulge depozone reach a maximum of 110m/Ma, whereas subsidence in the outer parts of the forebulge reaches 270m/Ma.

Spatial and temporal distribution patterns of subsidence values at the time of platform termination point to a complex non-linear setting in front of the Variscan Orogen that could be indicative of an orogenic recess or an oblique collision.

Stratigraphic forward modeling highlighted the importance of geometrical constraints as one of the controlling factors for platform progradation into the basin. During aggradation, the carbonate repose angle increased to up to 45°. Carbonate production rates for the platform of the Valdeteja Formation reached a maximum of 260m/Ma. Furthermore, the Carboniferous eustatic sea-level curve was calibrated by the model.

**KEYWORDS:** Southern Cantabrian Basin, structural balancing, Carboniferous foreland basin system, carbonate platform, sequence stratigraphy, reverse basin modeling, stratigraphic forward modeling, orogenic recess, oblique collision



## ZUSAMMENFASSUNG

Das Ziel der Arbeit war die Quantifizierung der Kontrollfaktoren für die sedimentologische Entwicklung des südlichen Kantabrischen Beckens (NW Spanien). Ein sedimentologisches und sequenzstratigraphisches Modell wurde für die synorogene karbonische Beckenfüllung erstellt und mittels einer kombinierten stratigraphischen Rückwärts- und Vorwärtsmodellierung analysiert und kalibriert.

Die Beckenfüllung umfasst kambrische bis karbonische Abfolgen, die während der Variszischen Orogenese in einzelne Überschiebungseinheiten zerstückelt und entlang von Überschiebungshorizonten verlagert wurden. Als Grundlage für die stratigraphische Modellierung wurde eine strukturelle Bilanzierung durchgeführt um die ursprünglichen Abstände zwischen den gemessenen Profilen zu bestimmen. Da nur Oberflächendaten zur Verfügung standen, wurde eine Gruppe von Strukturelementen für die südliche Kantabrische Zone aufgestellt, die als Rahmenbedingung für die Erstellung der Profile gedient haben. Minimale Verkürzungsbeträge innerhalb der einzelnen Überschiebungspakete betragen 19% bis 54%, abhängig von dem jeweiligen Grad der Verformung der strukturellen Einheiten. Bei Einberechnung der Überschiebungsweiten in die minimalen Verkürzungsbeträge ergeben sich Werte zwischen 44% und 64%.

Im Laufe der Orogenese kam es zur Differenzierung des Vorlandbeckens in ein zentrales, tieferes Becken vor dem Orogen (Vortiefe) und einen gehobenen Bereich in distaler Position ("forebulge") sowie ein

angrenzendes, kleineres Becken ("backbulge") zwischen *forebulge* und Kraton. In der Position des *forebulge* bildete sich die Karbonatplattform der Valdeteja-Formation. Die Vortiefe wurde sukzessive mit Siliziklastika der San Emiliano-Formation verfüllt, die mit fortschreitender Orogenese auf die Karbonatplattform übergriffen. Der Übergang zwischen Karbonatplattform und angrenzendem Becken auf der Seite des Kratons sind gut aufgeschlossen. Exzellente Schichtungsmuster sind im Luftbild aufgrund des überwiegend subvertikalen Einfallens der Schichtung verfolgbar.

Für die sequenzstratigraphische Analyse wurden die Luftbildinterpretation, sowie im Gelände gemessene stratigraphische Profile, Dünnschliffanalyse und biostratigraphische Daten genutzt. Die Sequenzstratigraphie ermöglichte die Verbesserung der zeitlichen Auflösung innerhalb der Plattform und der Korrelation zu den distalen siliziklastischen Sedimenten der Vortiefe.

Aufgrund der zunehmenden flexurellen Biegung der Lithosphäre durch das Herannahen des Orogens wurde die Karbonatplattform zunehmend zurückgedrängt und Klastika verfüllten den neu geschaffenen Akkommodationsraum. Eine Rückwärtsmodellierung ermittelte Subsidenzwerte für die komplette paläozoische Beckenfüllung entlang der zwei bilanzierten nord-süd verlaufenden Transekten und eines weiteren, west-ost gerichteten Transektes, der die anderen beiden Transekte verbindet. Die Subsidenzdaten umfassen die extensionsdominierte Entwicklung während des frühen Paläozoikums und die anschließende Inversion

des Spannungsfeldes bis hin zur Variszischen Orogenese. Geringe Subsidenzwerte von maximal 80m/Ma im prä-orogenen Becken sind auf die proximale Lage der Transekte zurückzuführen.

Während des Karbons erreichten die thermo-tektonischen Subsidenzraten einen Maximalwert von 740m/Ma bei Einsetzen der klastischen Sedimentation im westlichen Arbeitsgebiet. Interne Bereiche des *forebulge* weisen maximale Subsidenzwerte von 110m/Ma auf, während externe Bereiche maximale Werte von 270m/Ma erreichen.

Die zeitliche und räumliche Subsidenzentwicklung deutet auf eine komplexe, nicht-lineare Verteilung der Faziesgürtel vor dem Variszischen Orogen hin. Aufgrund der Faziesverteilung und der Subsidenzentwicklung wird ein nicht-linearer, gebogener Verlauf des Orogens oder, alternativ, eine schräge Kollision angenommen.

Die stratigraphische Vorwärtsmodellierung verdeutlichte den bedeutenden Einfluss von geometrischen Parametern auf das Progradationsmuster der Plattform. Während Zeiten hoher Aggradation versteilte sich der Neigungswinkel des Plattformhanges auf bis zu 45°. Die Karbonatproduktionsraten innerhalb der Valdeteja Formation erreichten Werte bis zu 260m/Ma. Die eustatische Meeresspiegelkurve wurde aufgrund der Modellierungsergebnisse modifiziert.

**SCHLÜSSELWÖRTER:** Südliches Kantabrisches Becken, strukturelle Bilanzierung, Karbon, Vorlandbecken, Karbonatplattform, Sequenzstratigraphie, Rückwärtsmodellierung, Vorwärtsmodellierung, nicht-lineares Orogen, schräge Kollision

## CHAPTER 1: INTRODUCTION

This doctoral thesis has been conducted within the context of an inter-university research group working in the Southern Cantabrian Basin of NW Spain, funded by the DFG (German Research Foundation). Within the Graduiertenkolleg 273 (Research Training Group) of the University of Heidelberg, several research areas were approached, such as structural geology and sedimentology, including chronological, stratigraphical, paleontological, and diagenetic studies. The Cantabrian Basin provides an excellent study area: outcropping strata comprise successions from the uppermost Precambrian to the Mesozoic. Due to deformation, strata often dip subvertically, which permits an investigation of the whole basin fill conveniently in the field.

Within this thesis, the overall sedimentological development of the basin is investigated and subsequently quantified by a combination of reverse basin and stratigraphic forward modeling. The available stratigraphic record allows the quantification of subsidence rates for the whole Paleozoic succession of the proximal part of the Southern Cantabrian Basin. This covers the sedimentary development during an extensional tectonic setting close to the northern margin of the Gondwanan continent and during the inversion of the tectonic regime resulting in the Variscan Orogeny.

The special focus of the thesis is on the pattern within the foreland basin system in front of the approaching Variscan Orogen during the Carboniferous. Spatial and temporal geometries within this system of a carbonate platform interfingering with siliciclastic systems provide

further constraints on the complex interplay of thrust emplacement, rotating tectonic stress fields and contemporaneous sedimentation. The quantification of subsidence rates in combination with the sedimentary genetic model enables to gain further information about the overall evolution of the area.

Moreover, quantification of depositional parameters responsible for the growth pattern of the investigated Carboniferous carbonate platform is of general interest for studies of ancient platform systems. Carbonate platforms are sensitive to various, interacting factors such as sea-level changes, subsidence, sediment production and erosion, biogenic factors, geometrical constraints, and climatic constraints. Because forward modeling considers the principal genetic factors and provides minimum and maximum genetic models, it is a powerful tool for testing the developed stratigraphic model by matching modeled geometries with the outcrop analogues. A graphical display of spatial and temporal relationships helps to reveal quantitative inconsistencies within the existing genetic model, which then can be adjusted. Additionally, the relative importance of several variables in generating the depositional system can be examined.

This study focuses on three transects: the north-south directed Torío and Curueño Transects and the west-east directed Bodón Transect, which connects the north-south directed transects with each other. This set-up provides the basis of the documentation and evaluation of the basin development of this area.



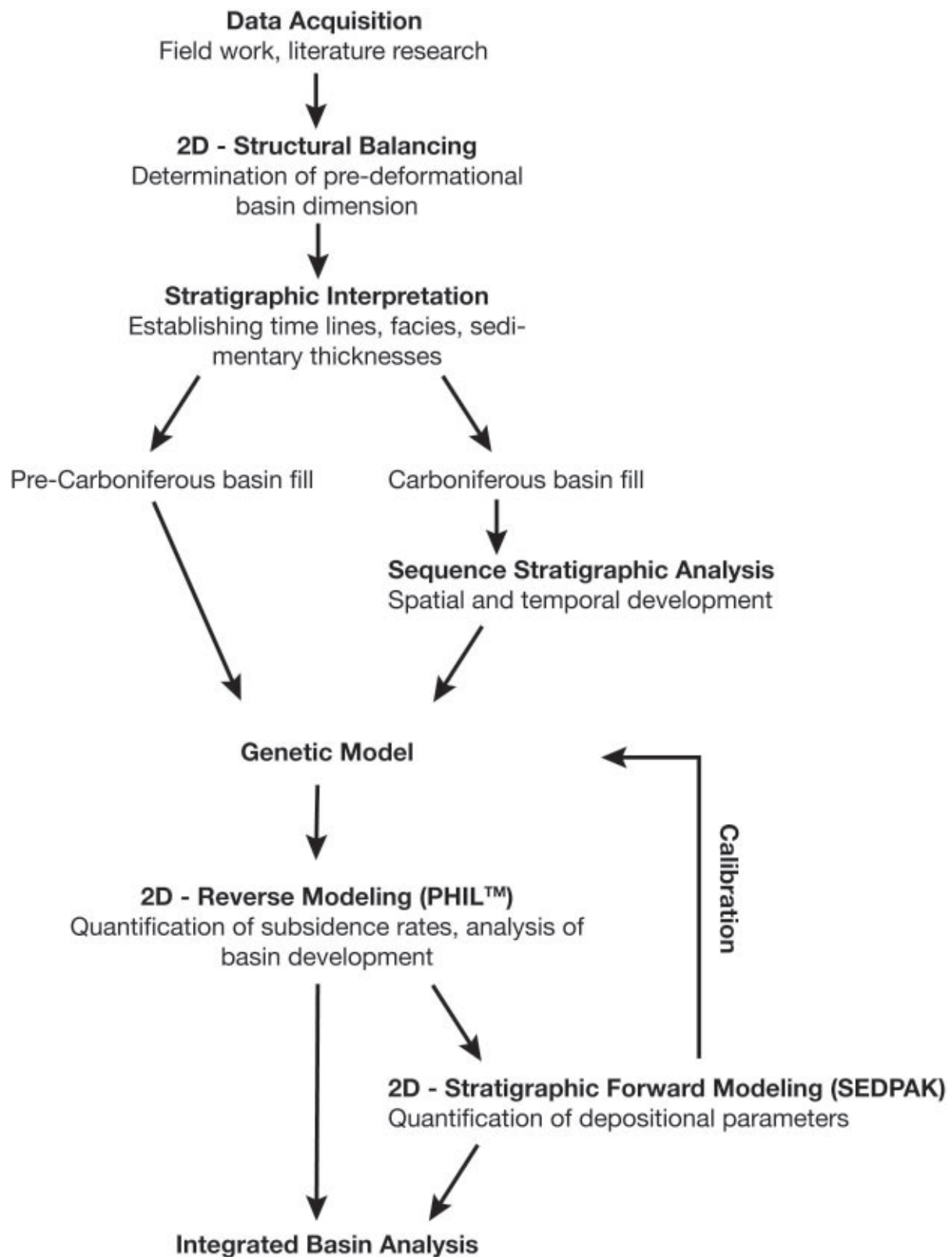


Fig. 1.1: Schematic workflow of this study.

Figure 1.1 shows a workflow of the approach taken within this work. First, due to strong deformation within the fold-and-thrust belt setting, 2D-structural balancing had to be carried out to determine initial distances between measured stratigraphic profiles prior to basin analysis. The stratigraphic interpretation is based on extensive field work, literature research, analysis of aerial photographs and thin sections. For the Carboniferous succession of the field area, a sequence stratigraphic model was developed. The subsidence development of the basin is quantified by reverse basin modeling. The numerical results and the facies information served as the basis for the stratigraphic forward model built for the Carboniferous succession of the west-east directed Bodón Transect. Forward modeling further calibrated the deployed genetic model and also validated the facies distribution and basin architecture. A synthesis will outline the results in the context of the paleogeographic development.

Within Chapter 1, an introduction to the orogenic cycle and the foreland setting in particular is presented. Furthermore, an overview of the sequence stratigraphic concept and sedimentary modeling will be given.

## 1.1 The Orogenic Cycle

### 1.1.1 Wilson - Cycle

Wilson (1970) first proposed that several plate tectonic settings belong to one genetic cycle. The cycle consists of the rifting of basins that evolve into ocean basins bordered by passive margins. Subsequently, after tens or hundreds of millions of years, the tectonic regime changes from extensional to compressional and the ocean basin closes, generating subduc-

tion zones around the margins. Closure of the oceans eventually leads to continent-continent collision and consequently to the development of an orogenic belt (Fig. 1.2). The cycle may be repeated.

Although this cycle is still considered to be valid, Wilson did not integrate the role of accreted terranes. Additionally, oblique and strike-slip plate motions modify this scheme (Mitchell & Reading 1986).

A sedimentary basin often underwent several of these stages. Therefore, the term “polyhistory basin” was used by e.g. Kingston et

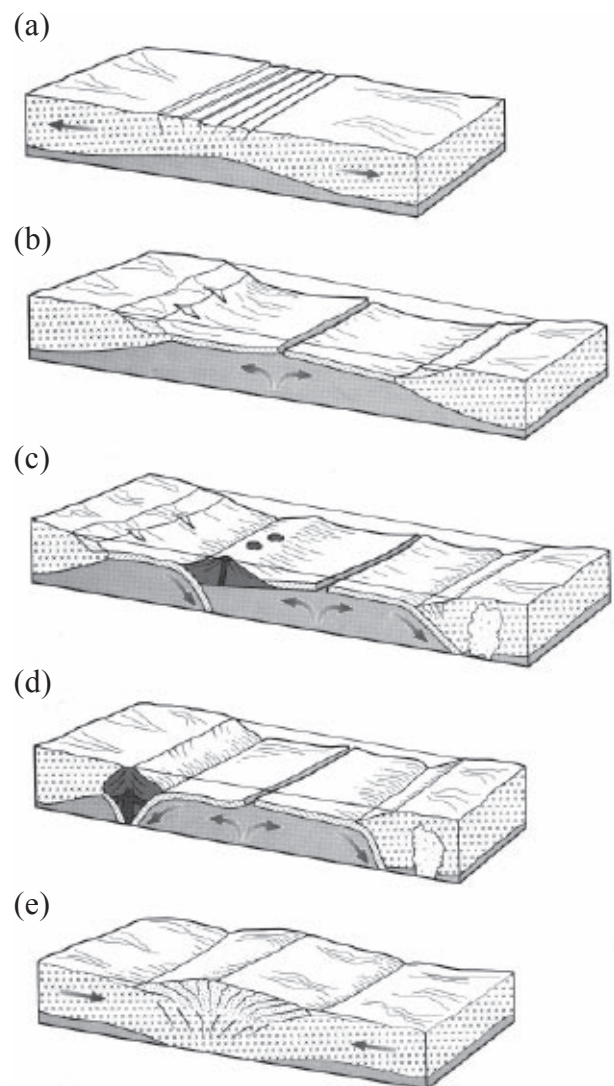


Fig. 1.2: Sketch of the orogenic cycle as introduced by Wilson 1966 (modified by Duff 1993). (a) Rift basin, (b) ocean basin, (c) arc and trench formation, (d) ocean closure, (e) mountain belt.

al. (1983) and Klein (1987). A record of the stages a basin went through is reflected by the stratigraphy, which displays the evolution and transitions of a basin.

The early rifting stage has predominantly continental deposits, succeeded by shallow-marine deposits. Subsequently, an elongated graben develops with hemipelagic sediments. During the early stage of passive margins bordering the ocean basin, sediments are largely siliciclastics deposited on a narrow shelf margin. This is followed by an increase in shale and carbonate buildups are established, depending on climatic conditions (Einsele 2000).

During subsequent closure, basin inversion takes place, and this may be partial or entire. Partial inversion results in structural highs, which are subjected to erosion. However, differentiation of the area may elsewhere cause the environment to deepen. The basin floor may be deformed and tilted (Einsele 2000).

Eventually, an orogenic belt with a foreland basin is established.

### 1.1.2 Foreland Basins

#### *Tectonic Model*

Major loads (e.g. the orogen and sedimentary load) cause downwarping of the lithosphere in order to re-establish isostatic equilibrium (Fig. 1.3). Essentially, a flexural depression builds up around the load. The amount of deflection decreases away from the load (Einsele 2000). This results in the classic architecture of a simple foreland basin, whose cross-section shows a wedge-shaped geometry (Beaumont 1981, Dickinson 1974, Jordan 1995, Price 1973). The depocenter is located adjacent to the orogenic load, thinning gradually from the orogen towards the hinterland (Miall 1999).

During progressive deformation of the foreland, a segmentation into foredeep and forebulge zone develops due to decreasing flexural

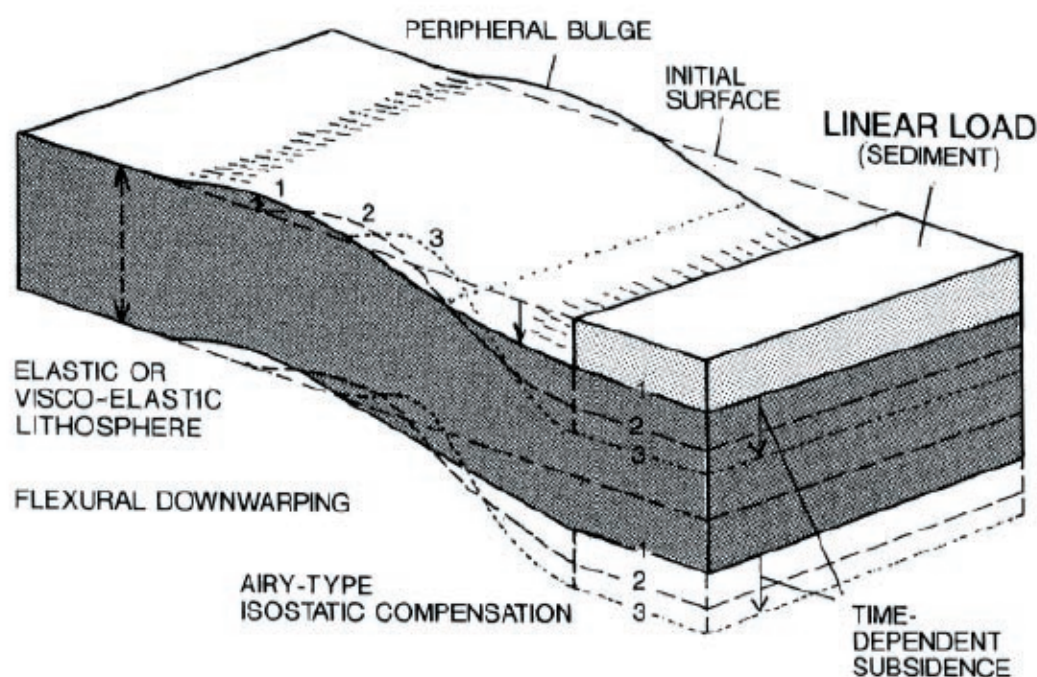


Fig. 1.3: Successive (step 1 to 3) flexural response of the lithosphere to an applied linear load corresponding to an applied orogenic load (Einsele 2000, Quinlan & Beaumont 1984). The peripheral forebulge is shown to migrate toward the applied load. Note the spatial linear distribution of the components of the system.

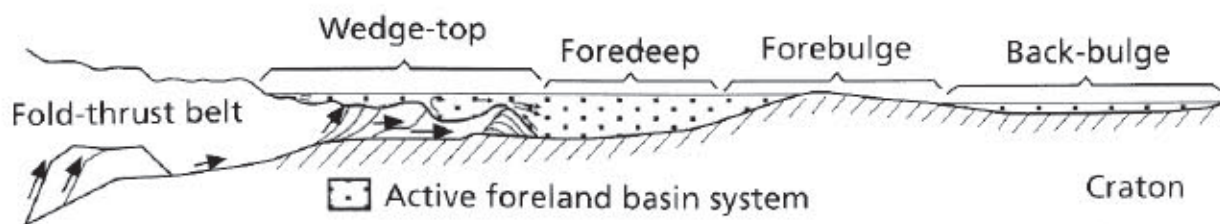


Fig. 1.4: Schematic zonation within a segmented, four-component foreland basin system (Horton & DeCelles 1997).

strength of the bending crust away from the load (Fig. 1.4). A thin, saucer-shaped back-bulge zone may also develop, which acts as a sedimentary basin (Leeder 1999). The nature of the lithospheric processes generating the back-bulge depozone are poorly understood to date (Leeder 1999). Subsidence within the back-bulge depozone was predicted to be relatively low once it is established. However, dynamic effects may increase subsidence (Horton & DeCelles 1997). Continuing deformation and migration of the thrust front can eventually result in stacked depozones such as a vertical sequence of upward-coarsening deposits of back-bulge, forebulge, foredeep and wedge-top deposits (DeCelles & Currie 1996). In concordance with that, Jordan (1995) suggested the presence of an overtopped forebulge from the modern Subandean fold-thrust belt in Peru and Bolivia.

#### Spatial Dimension of Depositional Zones

The dimension of foreland systems essentially depends on the flexural rigidity of the subducted plate and the orogenic plus sedimentary load. DeCelles & Giles stated that foredeep depozones are typically 100 - 300km wide and 2 - 8km thick.

For the Cretaceous North American Western Interior Basin of central Colorado, White et al. (2002) calculated a distance of approximately 340km between the Sevier thrust front and the

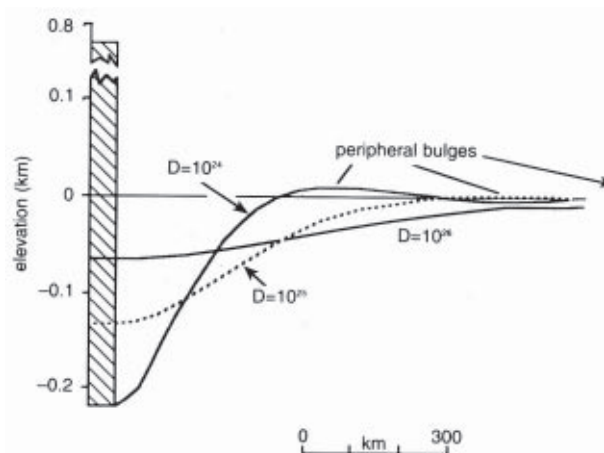


Fig. 1.5: Experimental results for compensation of an applied load (Beaumont 1981). The amount of flexural downwarping and the width of the foredeep depend on the flexural rigidity  $D$  of the plate. A thick plate results in minor downwarping, for a thin plate vice versa. Vertical exaggeration factor is 2000.

assumed forebulge crest.

The modern Great Pearl Bank Barrier in front of the Zagros fold-thrust belt is interpreted by DeCelles & Giles (1996) as a subdued forebulge. The approximate distance to the thrust front is 200km.

Lugo & Mann (1995) proposed a width of 100 - 150km for the foredeep zone of the Venezuelan Maracaibo Basin during the early Eocene, narrowing to 50 - 80km during the middle Eocene.

Holt & Stern (1994) presented the Oligo-Miocene Taranaki foreland basin (New Zealand) with an approximated distance between the thrust front and the forebulge of only 60km and an back-bulge area within another 40km.



The depth of the depocenter varies in relation to the width: the maximum depth of the Taranaki foredeep reaches 2200m, whereas the maximum depth of the central basin in front of the Zagros fold-thrust belt amounts to up to 80m. The experimental setup of Beaumont (Fig. 1.5; 1981) shows the relationship between the applied load, flexural rigidity of the plate, i.e. the lithospheric thickness, and the distance between the load and the peripheral bulge, which corresponds to the forebulge. The higher the lithospheric thickness, the wider is the foredeep.

#### Visco-Elastic or Elastic Lithospheric Model?

Nowadays, a visco-elastic model of the lithosphere is generally applied to a foreland basin setting (Miall 1999). A cycle of flexural loading and associated cratonward migration of the forebulge, visco-elastic relaxation and rebound is assumed (Fig. 1.5; Beaumont 1981, Einsele 2000). During visco-elastic relaxation, effective rigidity is reduced and the forebulge migrates (Miall 1999). Uplift, erosion and the formation of unconformities occur. Relaxation time is a value less than infinity; Beaumont (1981) set the relaxation time to 27.5Ma for the Alberta Basin, based on stratigraphic analysis and recognized changes in the architecture of the basin.

However, Flemings and Jordan (1990) suggested an elastic lithosphere model without migration of the forebulge in the direction of the hinterland during tectonic quiescence. The relaxation time for the elastic model would equal infinity. The early Proterozoic Kilohigok Basin in northern Canada and the Tertiary Apennine foreland basin systems possess stationary forebulges (Waschbusch & Royden

1992). The authors suggested weak zones within the lithosphere to be responsible for localized flexural bulges.

The tectonic model outlined above represents the common interpretation of subsidence development within a foreland basin. The recognized stratigraphic and basin evolution is interpreted to be related to crustal flexure and subsidence in response to thrusting and supracrustal loading (syntectonic model of sedimentation). In this model, the basin fill would record a progressively shallowing depositional environment that is related to increasing tectonism.

#### Antitectonic Model

In contrast, the antitectonic model suggests the time of tectonic activity being a time of basin deepening. The effects of crustal loading and flexure may be outpaced by the development of an organized drainage net, which supplies detritus from the uplifted zone into the basin. Therefore, gradual shallowing may be related

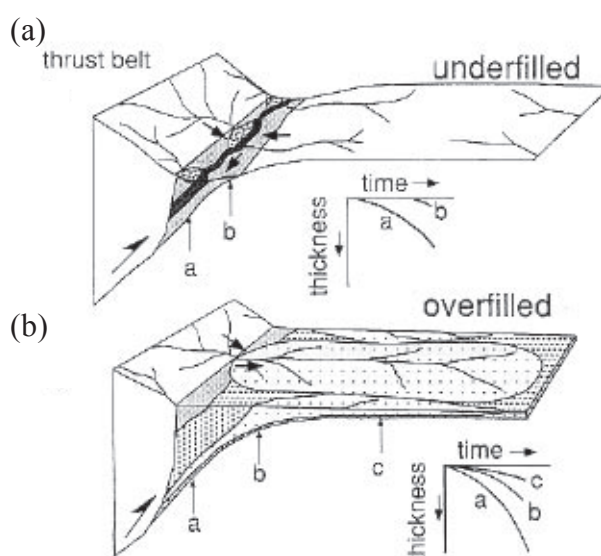


Fig. 1.6: Underfilled (a) and overfilled (b) basin stages by Jordan (1995). Insets show subsidence plots for designated points within the basin. Note the linear distribution of facies belts parallel to strike of the orogen within the underfilled stage.



to the establishment of drainage nets and the progradation of coastal-plain deposits into the basin. Maximum tectonism possibly ceased long before a basin fill reached conglomeratic deposits (Heller et al. 1988, Heller & Paola 1992).

### *Sedimentary Evolution*

The sedimentary infill of foreland basins is defined by the amount of sediment accumulation in relation to the available accommodation space. Foreland basins are classified to evolve from underfilled, then filled and subsequently into an overfilled stage (Covey 1986, Flemings & Jordan 1989, Jordan 1995). Nevertheless, a basin does not necessarily undergo all stages. During the initial development of the mountain belt, the relief and therefore sediment supply is low. Sediments are mostly fine-grained, turbiditic sediments. This relates to the underfilled basin stage with limited sediment supply; the rate of subsidence exceeds the rate of supply (Nichols 1999). Trunk rivers may have axial drainage through the basin (Fig. 1.6a, Jordan 1995). Later deposits are predominantly shallow water or continental deposits. Overfilled basins have a high sediment supply due to the high topography of the mountain chain in the hinterland. However, the amount of sediment supply also depends on the prevailing lithology within the source area. Sediments predominantly derive from the orogen in the hinterland, but also from erosion within the forebulge zone. River systems may extend over the whole basin and the forebulge area (Jordan 1995). The filled stage is the equilibrium between these stages. According to a definition by Sinclair (1997), facies used to identify an underfilled basin state must have been depo-

sited in significant (more than 200m) water depths.

Sedimentation rates in proximal areas are significantly higher than in distal areas. Average rates within the depocenter of the foreland basin range from 100 to >1,000m/Ma (Einsele 2000). Facies changes within the foreland basin may also follow the basin axis (Fig. 1.6a). Transport directions of gravity mass flows and turbidites in deeper water may be parallel to the strike of the orogen (Covey 1986, Einsele 2000, Sinclair & Allen 1992).

Mostly, the forebulge zone is subjected to uplift and, hence, to erosion, which could result in an erosional unconformity. However, if the foredeep depozone is not filled, carbonate platforms may develop on the forebulge (Allen et al. 1991, Dorobek 1995). Dorobek (1995) proposed that carbonate platforms mostly have homoclinal ramp profiles, independent of available reef organisms. Lithospheric flexure is thought to be the primary factor influencing platform morphology in foreland basins. It controls the depositional gradient, subsidence rate and water depth of the platform. Lithospheric flexure produces a gentle, basinward-dipping surface in the forebulge zone. Ramp profiles mimic this surface and hence, do not develop steep slopes (Dorobek 1995). During migration of the depozone cratonward, carbonate ramps either backstep or drown (Dorobek 1995, Schlager 1981). The orientation of the platform margin determines the direction of a platform's backstepping. Synorogenic backstepping will be highly diachronous if there are major salients or an oblique collision (Bradley 1989, Davies et al. 1989, Pigram et al. 1989). Only if the platform margin is subparallel to the basin axis will there be backstepping of the entire margin (Davies et al. 1989).

Furthermore, platform development may be strongly influenced by non-flexural deformation.

Within the back-bulge depozone, the sedimentation rate is significantly lower than in the foredeep depozone. Flemings & Jordan (1989) and DeCelles & Burden (1992) reported sub-parallel time planes over lateral distances of several hundred kilometers away from the orogen. The depositional environment is mainly shallow marine (<200m; Ben Avraham & Emery 1973, Holt & Stern 1994). Due to the fact that the principal sediment source is located in the distant orogenic belt, fine-grained sediments dominate. A subordinate amount of sediments may originate from the cratonward side.

## 1.2 Sequence Stratigraphy

Sequence stratigraphy is a means to recognize and interpret genetically related packages of sedimentary strata, which can be delineated by unconformities and/or conformities within a framework of time surfaces (Nystuen 1998).

The sequence stratigraphic concept roots back to the middle of the last century (e.g. Sloss et al. 1949, Wheeler 1958), but modern sequence stratigraphy as a predictive tool in petroleum exploration was initiated by the Exxon Production Research Co. in the seventies of the 20th century (e.g. Vail et al. 1977a-c). The fundamental unit used to describe a succession is the stratigraphic sequence. Mitchum (1977) defined a depositional sequence to be a relatively conformable succession of genetically related strata bounded at its top and base by unconformities and their correlative conformities. It is composed of a succession of systems tracts and

is interpreted to be deposited between eustatic-fall inflection points (Posamentier et al. 1988). Systems tracts are recognizable by transgressive, progradational and aggradational patterns of the sedimentary deposits within one sequence (Nichols 1999). They are related to the stages in the cycle of sea-level fall and rise (Posamentier et al. 1988, Van Wagoner et al. 1988). Therefore, the sequence stratigraphic concept relates the creation and destruction of accommodation space to sea-level rise and fall based on the simplified assumption that subsidence was constant over the time interval considered.

Contrastingly to the Exxon scheme, Galloway (1989) defined genetic stratigraphic sequences bound by maximum flooding surfaces. Within this model, unconformity surfaces are included within the genetic sequence.

Overviews regarding the modern sequence stratigraphy were given by Emery & Myers (1996), Haq (1991), Posamentier (1991), Van Wagoner (1995) and others.

The Exxon scheme is most commonly used and also applied within this study.

## 1.3 Structural Balancing

Due to north-south directed (according to today's coordinates) thrusting in the working area, the tectonic units must be structurally restored to accomplish stratigraphic modeling. Facies relationships cannot be understood without a knowledge of the initial distance between the recorded stratigraphic columns. Hence, structural balancing was applied to the north-south directed Torío and Curueño Transects (Fig. 5.1a). Furthermore, restoration of a cross-section validates the interpreted structural geometries. Elliott (1983) defined

balanced sections as follows: “... If a section can be restored to an unstrained state, it is a viable cross-section. By definition, a balanced cross-section is both viable and admissible.”

In this study, the objective of balancing is to achieve both a viable and an admissible balanced cross-section in order to determine values for minimum shortening. The construction of the cross-section is based on surface data. A detailed, three-dimensional structural analysis of the area is not available. Hence, constraints for reconstructing the cross-sections are inferred from regional data and geometric constraints (see Chapter 5.1). Structural balancing focuses on medium- to large-scale deformation (hundreds of meters to kilometers). Small-scale deformation has not been accounted for.

### 1.3.1 History

Dahlstrom (1969) wrote the first comprehensive overview on the subject of structural balancing. He defined and evaluated the technique and geometrical constraints for restoring cross-sections.

Previous work of other authors had been using the concept in other structural techniques such as the calculation of depth-to-detachment (Bucher 1933, Chamberlain 1910, 1919). A strongly simplified, initial form of balancing was already used by Buxtorf (1907) to balance the fold-and-thrust belt of the Jura Mountains applying equal bedding lengths. Bally et al. (1966), Carey (1962), Goguel (1952), and Hunt (1957) applied structural balancing, however they did not give a detailed evaluation of the technique.

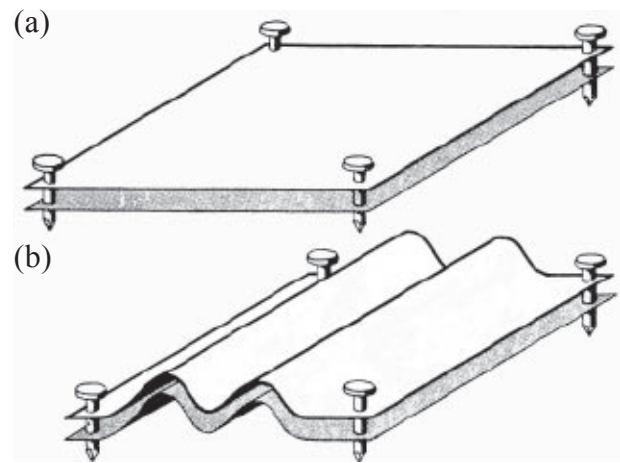


Fig. 1.7: Consistency of bed length due to fixed pins, here shown as restraining a block at its corners (a) before and (b) after deformation (Dahlstrom 1969).

### 1.3.2 Principle

Goguel (1952) introduced the law of conservation of volume during deformation, based on the principal of mass-maintenance. A bed might reduce its thickness due to load compaction but it does not change its areal extent. Dahlstrom (1969) eliminated one dimension of this three-dimensional law by stating that fold axes and fault strikes are parallel, folds are concentric (Price 1964) and faults are dip-slip thrusts in the fold-and-thrust belt regime. He concluded, that “in concentric regimes the cross-sectional length of a bed remains constant during deformation.”

In a regime without considerable tectonic thinning (such as in the studied area and comparable structural suites), the volume of a bed is not altered during deformation. Therefore, it is possible to apply this law, which refers to a three-dimensional continuum, also to the two-dimensional area bed length and establish that the bed lengths remain constant during deformation. Consequently, restoration is done by measuring each bed length. A basic assumption for applying this method is plane strain deformation. Material transport oblique to the

chosen cross-section would create an open system and interfere with the law of mass-maintenance. According to Woodward et al. (1989), the amount of shortening was calculated:

$$(x - x_0) * 100 / x_0 = e$$

$x_0$  = undeformed bed length

$x$  = deformed bed length

$e$  = amount of shortening (in percent)

To restore a 2D cross-section by the equal-length method, pin lines were used as reference lines (Fig. 1.7). A pin line was positioned perpendicular to bedding in each deformed thrust unit. Pin lines should be placed in areas where it is presumed that there is minimal interbed shear. Ideally, a pin line is positioned in the undeformed hinterland. However, in the field area this was not available. Therefore, positioning of pin lines along axial planes of folds is a good alternative method (Woodward et al. 1989). If hanging wall cutoffs and the corresponding ramp folds of thrust sheets are not preserved, local pin lines were used, which were placed in the trailing edge of each thrust sheet (Woodward et al. 1989).

Deformed beds were straightened out using the pin lines as fixed points of no slip. The unpinned parts of the thrust sheet were restored assuming simple shear. The layers slide back into layercake geometry while line length is conserved (Woodward et al. 1986).

After restoration of each single thrust sheet, the respective thrust sheets were stitched along the common ramps. To control the validity of restoration, common ramp angles should match and the position of pin lines should be perpendicular to bedding in the undeformed state.

## 1.4 Numerical Basin Modeling

Numerical basin modeling is applied to understand and quantify the factors controlling the development of a sedimentary basin and its infill. It defines the vertical motion of the lithosphere in response to extension and compression, sedimentation, eustatic sea-level variations, in-plane force variations, erosion, and magmatic underplating. Modeling follows sequence stratigraphic concepts of the creation and destruction of accommodation space as the main factors influencing sedimentary systems (Bowman & Vail 1999, Jervey 1988).

Computer simulations employ algorithms that intend to describe all geological factors influencing the basin development. However, the quality of a quantified model strongly depends on the quality of the input data and the computer program.

### 1.4.1 Basin Fill Succession: Controlling Factors

Primarily, the stratigraphic basin fill depends on the accommodation space available and sediment supply. Accommodation space is the amount of space available for sediment to accumulate. It can be created or destroyed by sea-level rise and fall, respectively, or by subsidence and uplift, respectively (Fig. 1.8).

Sediment is supplied from outer sources by erosion and denudation, which depend on the climate, antecedent topographic relief and bathymetry. The amount of sediment transported to a location also depends on the transport distance and the geometry of the basin. In situ biogenic production is a significant factor within carbonate systems. Additionally, sedimentary redistribution within the basin has to be considered.



Subsidence and uplift of the basin are controlled by tectonic subsidence rates, by the flexural response of the lithosphere, and by the compaction of the sedimentary load. Within stratigraphic studies, compaction induced subsidence rates are generally not evaluated. Flexurally induced subsidence and thermo-tectonic subsidence are mostly not differentiated.

### 1.4.2 Reverse Modeling (2D-Backstripping)

Backstripping is a technique to calculate the subsidence rates of a sedimentary basin using the sedimentary basin fill. The backstripping process removes sedimentary layers iteratively. In doing so, it calculates and removes the effects of compaction, sediment loading, changing paleo-bathymetry, and sea-level variations for each layer. It begins with the youngest layer and ends with the oldest layer whose base is the detachment horizon underneath the paleozoic sedimentary pile of the

Southern Cantabrian Basin.

Reverse modeling uses time lines for calculation. Mostly, they represent formation boundaries of synchronous age. For the Carboniferous succession, time lines are further refined within formations by available biostratigraphical data and using the sequence stratigraphic data as discussed in Chapter 4.

Output values are total subsidence rates, which are separated into compaction and flexurally induced subsidence rates, and thermo-tectonic subsidence rates. Compaction induced subsidence rates correct the subsidence curve for a value, which approximates the effects of sedimentary load. Additionally, it corrects the amount of compaction the sedimentary load of the removed unit inflicts on the underlying sediments. The flexurally induced subsidence rate is a value for the (elastic) bending of the lithosphere due to loading or unloading. The thermo-tectonic value is calculated by adding

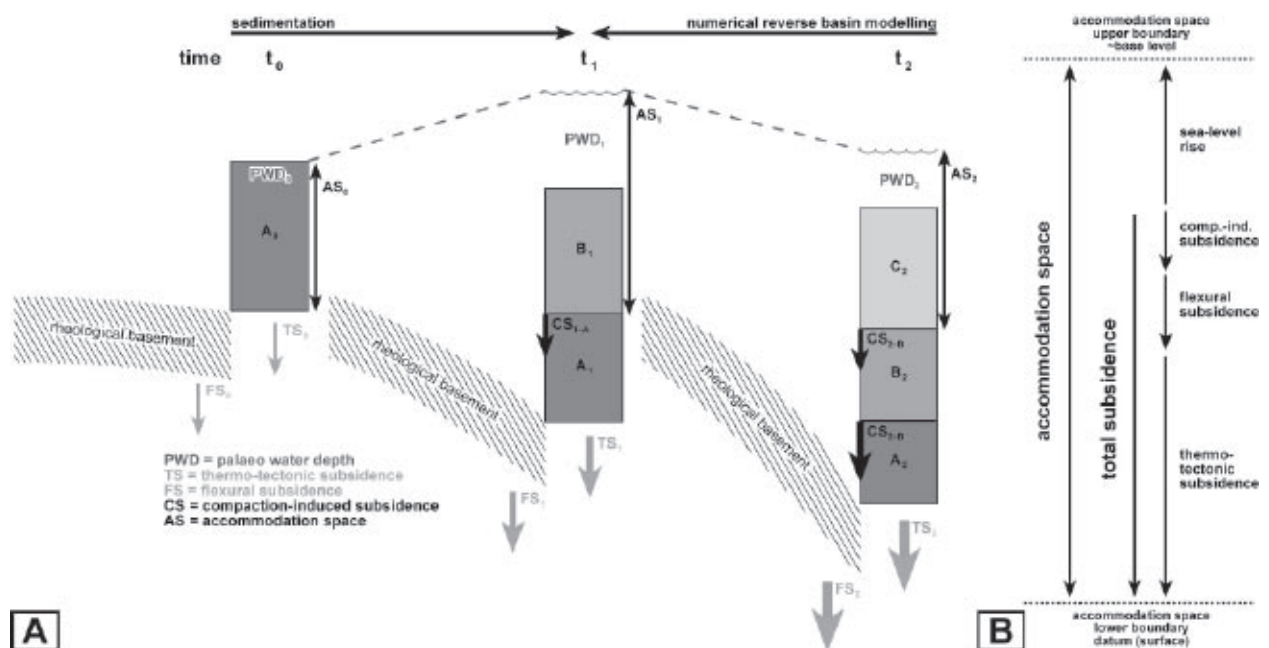


Fig. 1.8: The concept of reverse basin modeling is based on the creation of accommodation space. A: Successive accumulation of sedimentary layers A - C and related subsidence. X-axis: time, y-axis: burial depth. Arrows indicate semi-quantitative vectors of subsidence. B: Sketch showing the factors influencing the accommodation space. (Emmerich 2004, Veselovsky 2004).

the rate of change necessary to produce the thickness changes in the recorded sediment column and changes in paleowaterdepth, minus the effect of compaction and flexural loading (Bowman & Vail 1999). The relevant geologic processes may be thermo-tectonic, or fault motion. Thermo-tectonic subsidence is the main factor responsible for the creation of accommodation space. Hence, the analysis will focus on thermo-tectonic subsidence values.

### **1.4.3 Forward Modeling**

Stratigraphic forward modeling simulates sedimentation processes. Initial input parameters, such as seismic data, well data and outcrop data, constrain the numerical model of the basin architecture and sediment infill. Forward modeling quantifies controlling factors responsible for basin development and enables the importance of single parameters to be tested in order to create the recorded depositional setting. It provides the means to calibrate and refine an existing sedimentary model and therefore validates the model as a possible genetic interpretation. Geological processes have to be quantified as input parameters, which enforces the modeler to identify important gaps in the process understanding (Griffiths 2001). The graphical display of spatial and temporal relationships helps to understand the system and reveals possible flaws within the genetic model. Forward modeling is used by the industry to predict architecture and facies distributions of a sedimentary basin and to constrain interpretations of subsurface data (Lawrence et al. 1990).



## CHAPTER 2: GEOLOGICAL FRAMEWORK

The study area is located in NW Iberia within the Cantabrian Mountains. The stratigraphic succession modeled ranges from the Neoproterozoic - Cambrian boundary to the Carboniferous to the Meso-/Cenozoic cover rocks. The geodynamic and sedimentary history of NW Iberia from the Late Neoproterozoic to recent times is briefly outlined below, with the main emphasis placed on Variscan events.

### 2.1 Geodynamic Overview

#### 2.1.1 Late Neoproterozoic to Silurian

##### *Neoproterozoic*

Authors generally agreed that Iberia was part of the northern margin of Gondwana during the late Neoproterozoic/early Paleozoic. However, the tectonic setting of the margin is a matter of controversial discussion. Nägler et al. (1995) proposed an active margin setting during the Neoproterozoic to lowermost Cambrian. However, due to the lack of coeval volcanics and the geochemical maturity of Neoproterozoic-Cambrian sediments, various authors suggested a Gondwanan passive margin at that time (Bauluz et al. 2000, Beetsma 1995, Ugidos et al. 1997a,b, 1999, Valladares et al. 1999, 2000, 2002).

Of regional interest is the angular unconformity separating Neoproterozoic and Cambrian sediments. It is present in the Cantabrian Zone (CZ) as well as in the West Asturian-Leonese Zone (WALZ) and in some areas of the Central Iberian Zone (CIZ). It separates Neoproterozoic and Cambrian sediments. A Cadomian compressive deformation phase may have caused the unconformity (Díez Balda et al. 1990,

Marcos 1973, San José et al. 1990). Liñán et al. (2002) related the unconformity to an extensional event and associated fall in relative sea-level. Aramburu (1995) proposed a rifting phase being related to the opening of the Iapetus Ocean around the Precambrian to Cambrian boundary.

In the CZ and WALZ, the surface of the unconformity largely coincides with the basal thrust plane of the Variscan thin-skinned deformation (Chapter 5).

##### *Cambrian to Silurian*

Cambrian and late Neoproterozoic, paleogeographical positions of NW and SW Iberia are subject to discussion. The Iberian Peninsula is commonly regarded as a promontory extending the Moroccan part of the North Gondwanan shelf (Cocks 2000, Cocks & Fortey 1990, Young 1990). Considering similarities in benthic fauna, a better fit would be to those of the NE Algerian Sahara and of Saudi Arabia than to those of Morocco (Liñán et al. 2002). Another theory by Bergström & Massa (1992) and Massa & Bourrouilh (2000) proposed that Iberia was possibly located adjacent to Libya. This theory is based on resemblances between late Ordovician limestones of the Iberian Peninsula and Djeffara Formation of NE Libya.

In the Upper Ordovician, further extension on the margin led to the opening of the Rheic Ocean, which evolved between the Avalonian terrane and the Iberian block (Fig. 2.1; Fernández-Suárez et al. 2002, Robardet 2002, Tait et al. 1997). According to Leeder (1988),

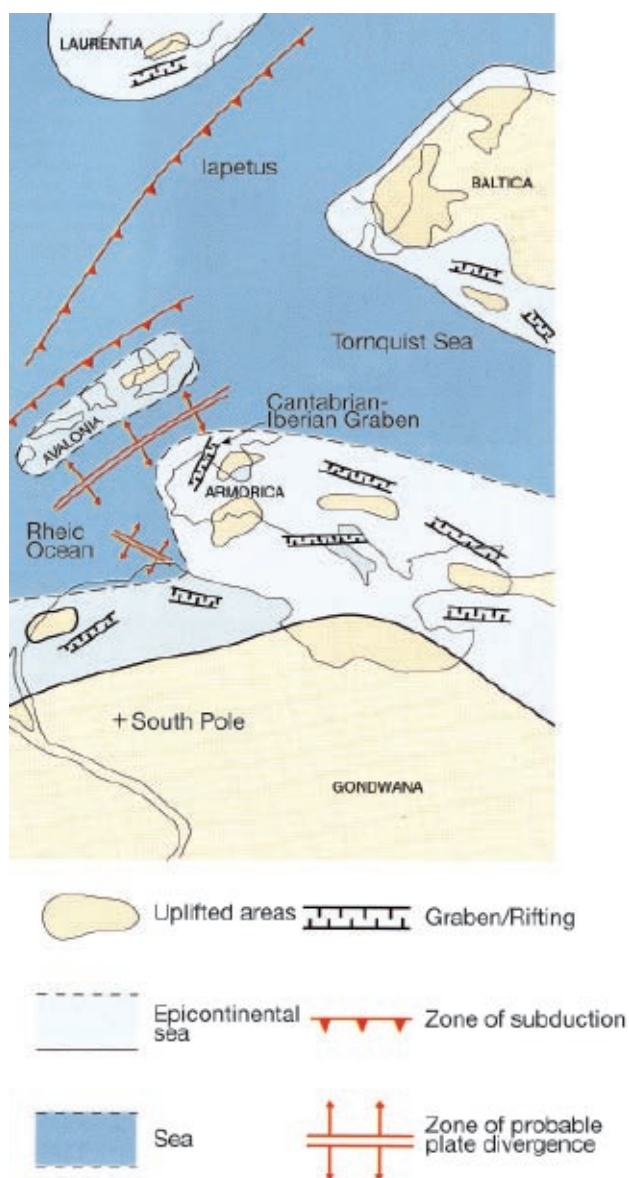


Fig. 2.1: Paleogeographical sketch of land-to-sea distribution in Europe during Lower Ordovician (Aramburu & Bastida 1995).

Linnemann & Heuse (2000), Matte (1991), Matte (2001), and Tait et al. (1997), the Iberian block was part of the Armorican terrane and apart from the Iapetus Ocean and the Rheic Ocean, another ocean was assumed to have existed between the Armorican terrane and the northern Gondwanan margin named Galicia-Massif Central Ocean (Matte 1991) or proto-Tethys (Fig. 2.2; Leeder 1988, Matte 1986). Contrastingly, Gutiérrez-Marco et al. (2002), Lorenz & Nichols (1984), and Robardet (2002)

dismissed the existence of the proto-Tethys and the idea that Armorica was a microplate independent from Gondwana (Fig. 2.1; Gutiérrez-Marco et al. 2002, Lorenz & Nichols 1984, Robardet 2002).

During the Silurian, the overall extensional stress regime continued, the Iberian Peninsula drifted further northward (Tait et al. 1997). According to Robardet & Gutiérrez-Marco (2002), Iberia still belonged to the North Gondwanan shelf.

### 2.1.2 Devonian and Carboniferous: European Variscides and the Cantabrian Zone

The European Variscides (Fig. 2.3) developed in the Devonian and Carboniferous as the Rheic Ocean and the proto-Tethys closed creating an amalgamation of microplates between Laurussia and Gondwana (e.g. Gutiérrez-Marco et al. 2002, Matte 1991). The Rheic Ocean probably closed during Late Devonian (Tait et al. 2000). The continental collision occurred around 380Ma at the boundary Eifelian - Givetian, which is indicated by metamorphism and crustal melting in Brittany, Massif Central and southern Spain along the southern suture generating thrust-thickened crust (Windley 1995). Subduction probably started in the SW of Iberia, then progressively moved on to the north (Dias & Ribeiro 1995). The subduction zone was directed to the north-east, indicated by I-type magmatism north and east of the suture zone (Ribeiro et al. 1990). The collision was interpreted as being the result of a crustal wedge moving to the north and northwest, respectively (Dias & Ribeiro 1995, Matte 1986, 1991). Accordingly, the supporters of the proto-Tethys theory proposed that

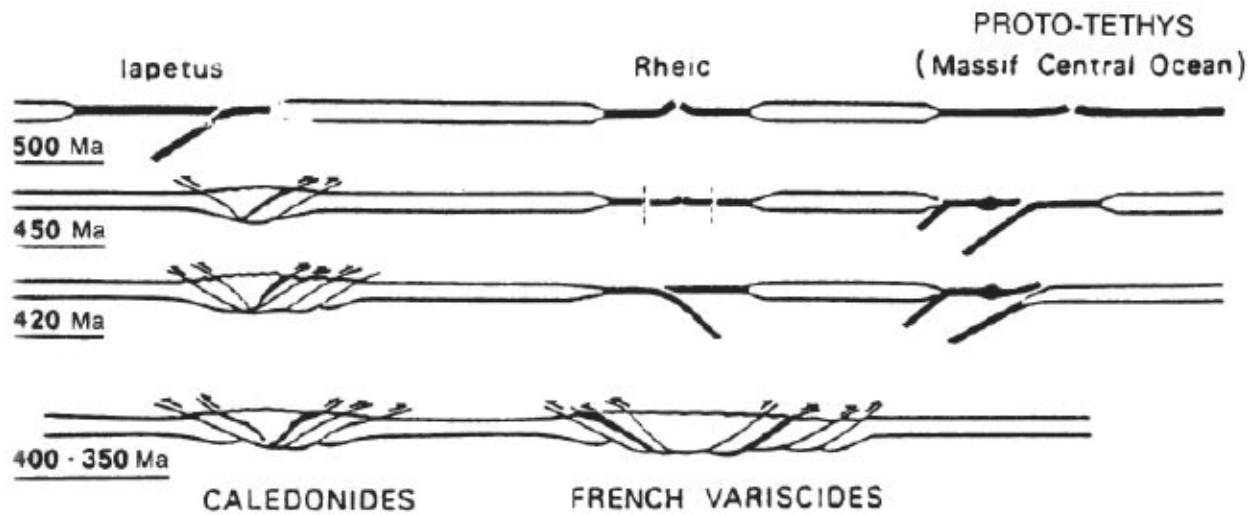


Fig. 2.2: Schematic plate tectonic setting of the Mid-European Variscides assuming two oceans (Matte 1986). See text for discussion.

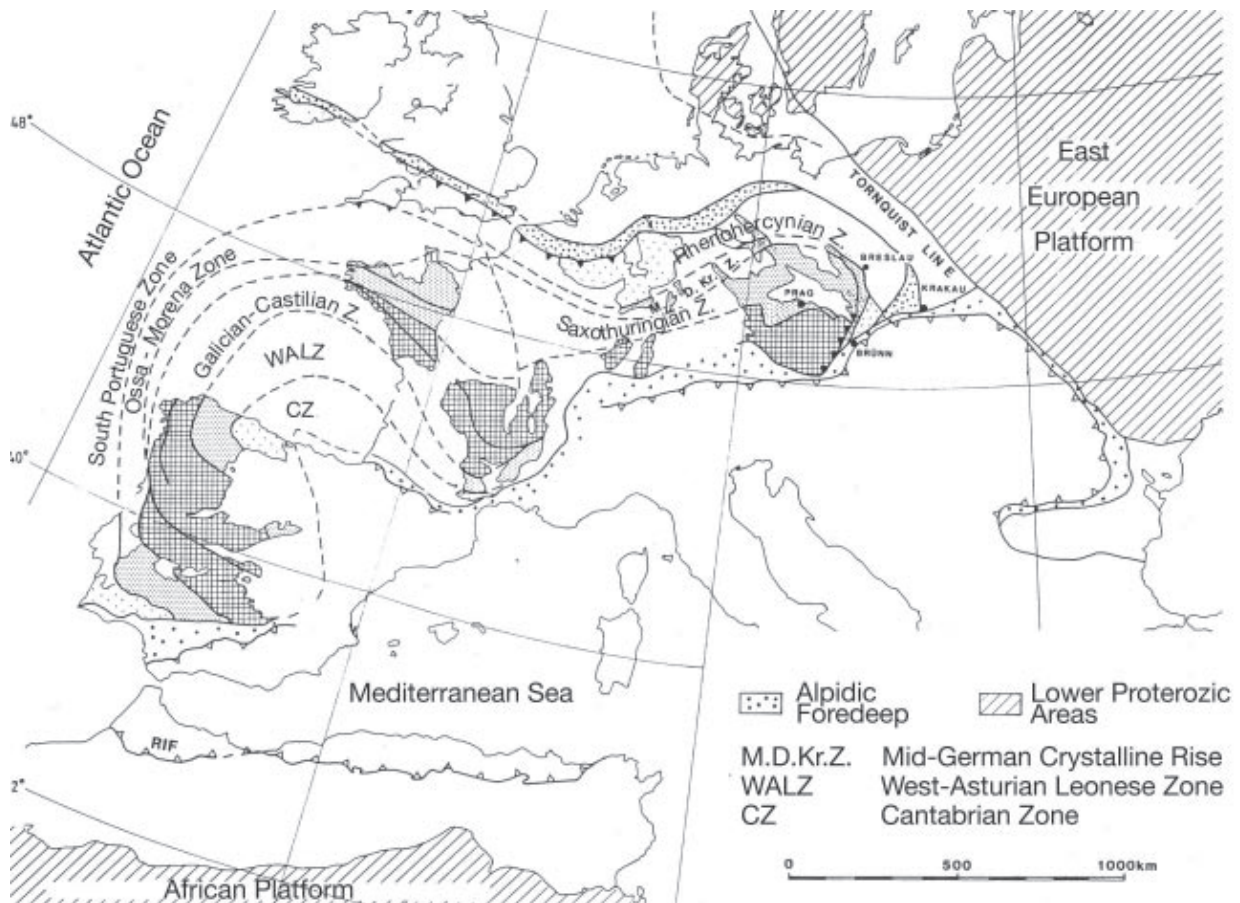


Fig. 2.3: Overview of the structure of the European Variscides (modified after Schönerberg & Neugebauer 1997). The field area is located within the Southern Cantabrian Zone (CZ).



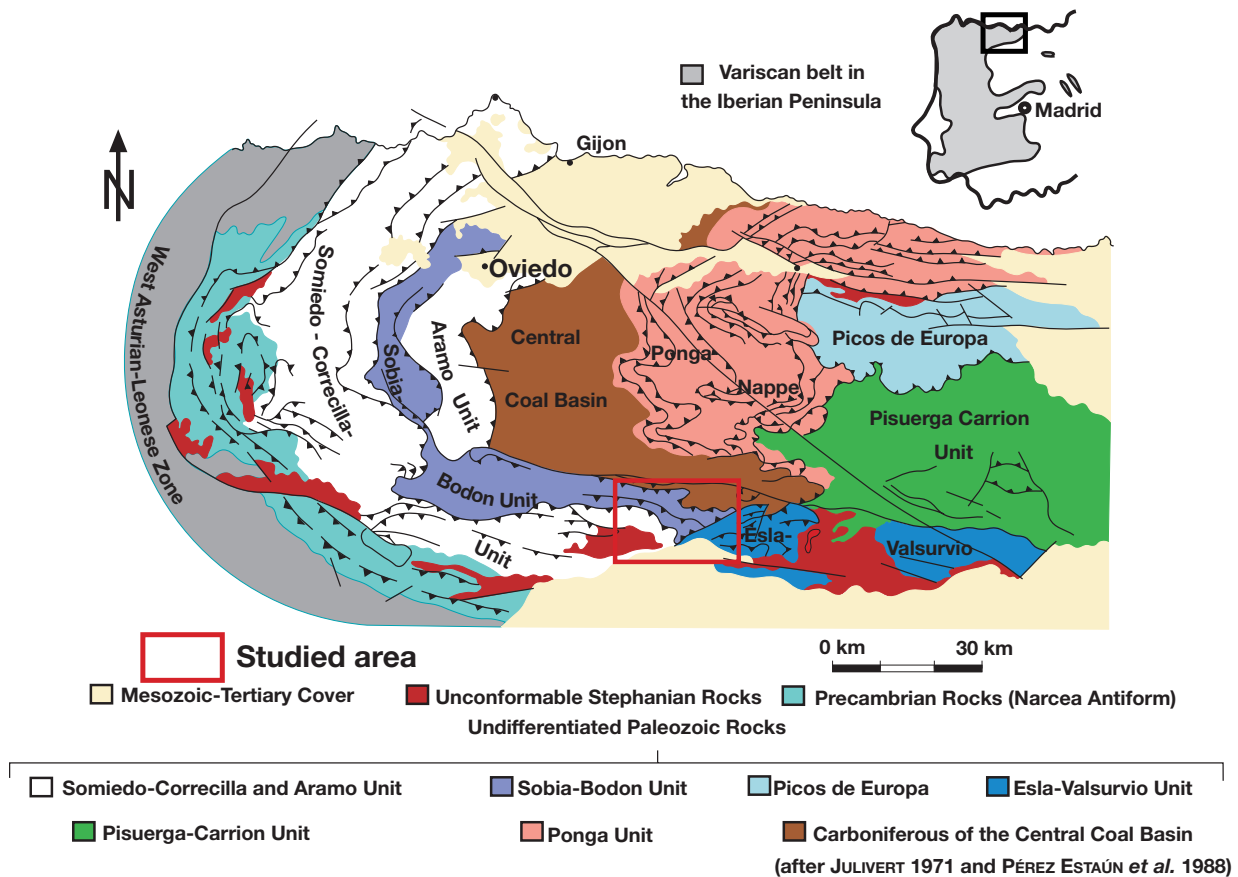


Fig. 2.4: Zonation of the western European Variscan belt (Cantabrian Mountains, NW-Spain; after Julivert 1971 and Pérez-Estaún *et al.* 1988).

the orogen evolved by symmetrical subduction of opposed lithospheric plates. Therefore, deformation and metamorphism migrated progressively northwards and southwards from the suture towards the orogenic forelands from 380Ma (Eifelian-Givetian boundary) to 300Ma (Moscovian). Authors agreed on the predominance of a transpressive, sinistral strike-slip system in NW Iberia.

The Cantabrian Zone belongs to the Western European Variscan fold-and-thrust belt (Fig. 2.3). It has an overall arcuate shape and is generally referred to as “Asturian Arc”. Julivert (1971) introduced the zonation of the Cantabrian Orogen into tectonic units based on stratigraphic and structural characteristics and timing of thrusting (Fig. 2.4). The first units to

be emplaced were the westernmost Somiedo, La Sobia, and Aramo Units in the Namurian to early Westphalian. More external structures originated during the Stephanian (Dallmeyer *et al.* 1997, Julivert 1978, Pérez-Estaún *et al.* 1988). The timing is indicative for a forward-propagating emplacement (Alonso *et al.* 1992). The time span of emplacement of the units is in the range of approximately 15-20Ma (Dallmeyer *et al.* 1997). Dallmeyer *et al.* (1997) compared isotopic ages and used hypothetical values for orogenic shortening of 50 to 75% to propose an average propagation rate of approximately 5km/Ma. This corresponds to an average convergence rate of 1-2cm/year.

#### *Evolution of the Asturian Arc*

The origin of the arc is the subject of extensive

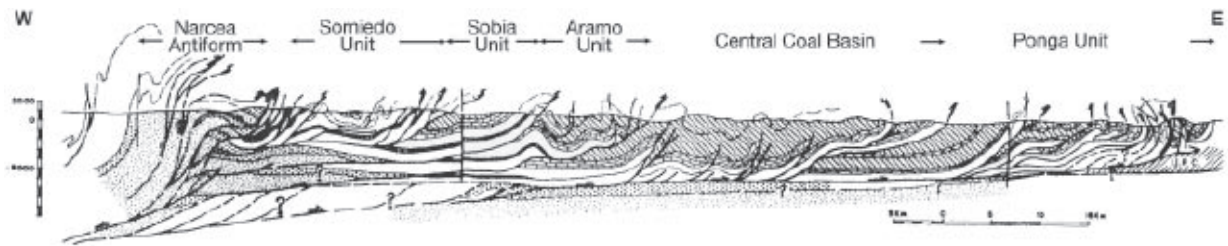


Fig. 2.5: Cross-section through the Cantabrian fold-and-thrust belt (Pérez-Estaún et al. 1988).

dispute. The discussion focuses on the timing of the thrust emplacement in relation to the bending of the arc. The most popular theories are outlined below.

Pérez-Estaún & Bastida (1990) and Pérez-Estaún et al. (1988) proposed two phases for the emplacement of the tectonic units: (i) thrusting of westernmost units, (ii) development of a deeper situated thrusting system associated with the emplacement of eastern units (Fig. 2.5), the latter causing steepening, local overturning of the thrust planes. A progressive series of rotational displacements led to a final disposition of the major units similar to that of the leaves of a photographic iris (Pérez-Estaún et al. 1988, in accordance with Matte 1986, Matte & Ribeiro 1975, Nijman & Savage 1989). Folds developed contemporaneously with thrusts, mimicking subsurface structures. Due to the radial transport direction of the thrust units, prominent strike-slip systems were reactivated as fault systems such as the León Line and Sabero-Gordón Line (Alonso 1987b).

Essentially, Julivert (1971), Julivert & Arboleya (1984, 1986) and Julivert & Marcos (1973) agreed with the above. However, they defined a first phase with thrusting and development of an arched set of folds, and a second phase generating a radial set of folds and overall tightening. The radial set of folds vanishes to the west, which is indicative of the increasing

curvature of the arc as the orogeny progresses. Paleomagnetic measurements by Hirt et al. (1992) supported this theory.

Other paleomagnetic studies confirmed that the curvature of the arc was at least partly of secondary origin (Bachtadse & Van der Voo 1986, Bonhommet et al. 1981, Perroud 1986, Perroud & Bonhommet 1981, Parés et al. 1994, Stewart 1995, Tait et al. 1997, Van der Voo et al. 1997). The extent and timing of the curvature remains a matter of discussion.

Kollmeier et al. (2000) proposed an initially linear, generally north-south trending fold-thrust belt. However, the southern branch was interpreted as rotating in a mild foreland-progressive counter-clockwise movement in successively younger thrust sheets (calcite twinning analysis). The evolution comprised two phases: (i) E-W horizontal compression acting on a stable margin, (ii) N-S horizontal compression, which led to clockwise bending in the northern branch, radial folding in the western part of the arc and tightening of the thrusts in the southern branch.

Paleomagnetic studies by Weil et al. (2000, 2001, 2003) and work by Gutiérrez-Alonso et al. (2004) corroborated this. The authors suggested a completely linear, N-S directed orogen during thrusting and post-orogenic bending. Weil et al. (2000, 2001, 2003) pro-

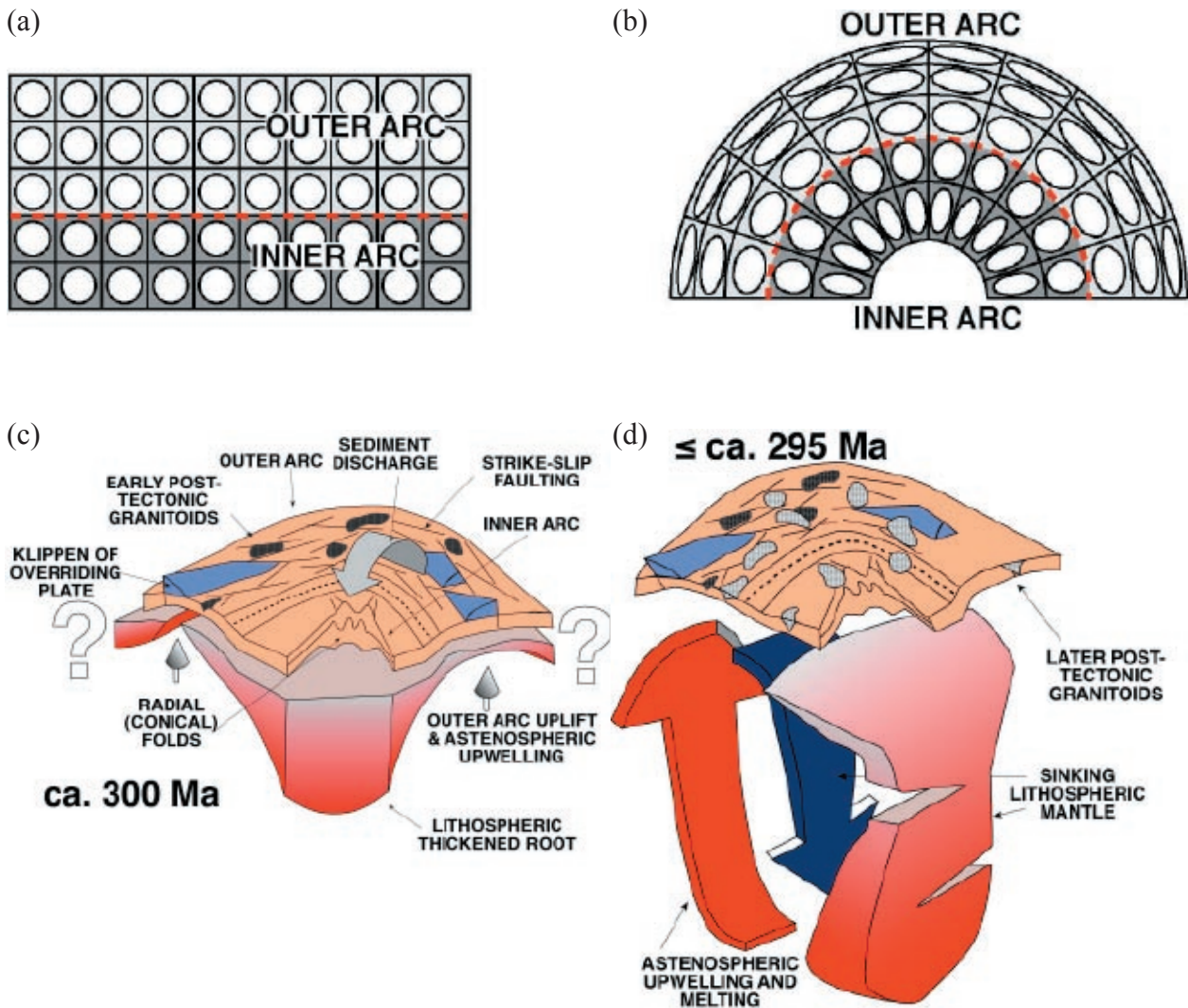


Fig. 2.6: (a) and (b) Sketch showing tangential longitudinal strain accommodating lithospheric bending of the Asturian Arc around a vertical axial plane, creating an inner and outer arc with arc-parallel stretching in the outer arc and shortening in the inner arc. (c) Thickened lithospheric root due to shortening in the inner arc, thinned lithosphere beneath the outer arc. (d) Delamination and collapse. The sinking lithosphere is displaced by upwelling asthenosphere (Gutiérrez Alonso et al. 2004).

posed three folding phases, the phase during Namurian to Stephanian being E-W directed, the younger phase during Early Permian being N-S directed. According to Gutiérrez-Alonso et al. (2004), the orogen was bent around a vertical axial plane (Fig. 2.6a, b).

#### *Deep Structure of the Orogen*

Gutiérrez-Alonso et al. (2004) proposed, that crust and lithospheric mantle experienced coupled deformation during oroclinal bending around a vertical axis (Fig. 2.6a, b) causing

thickening of the lithospheric root in the inner arc and thinning of the lithospheric root in the outer arc of the Cantabrian Orogen (Fig. 2.6c). This subsequently led to delamination of the lithospheric mantle (Fig. 2.6d).

Fernández-Suárez et al. (2000) favored the delamination model to explain the high heat flow, which is reflected by an associated voluminous and widespread magmatic event.

#### *Metamorphism*

The Cantabrian part of the Variscan Orogen



developed under shallow crustal conditions. Metamorphism stages generally increase to the western parts of the Cantabrian Orogen, reaching anchizonal (Bastida et al., 1999) to epizonal metamorphism stages (Aller et al. 1987, Raven & Van der Pluijm 1986, Van der Pluijm & Kaars-Sijpesteijn 1984). The CZ belongs to the mostly unmetamorphosed part of the Variscan Belt (Julivert et al. 1972, Lotze 1945, Marcos & Pulgar 1982). Cleavage developed only in the basal part of the Herrería Fm. but is otherwise locally restricted and does not display any relationship to compressional structures (Aller et al. 1987).

### 2.1.3 Permian to Recent: Post-Variscan Deformation History

Along NE-SW striking faults, rifting and associated volcanism developed within a trans-tensional system during Permian and Triassic (Lepvrier & Martínez García 1990, Martínez García et al. 1983). During the early Jurassic to early Cretaceous, the Atlantic Ocean and the Bay of Biscay opened, a NE-SW directed extensional regime prevailed (Lepvrier & Martínez-García 1990, Verhoef & Srivastava 1989). It then experienced counterclockwise rotation and an independent Iberian microplate existed until it was integrated into the European plate by Alpidic compression.

Within the Cantabrian Orogen, Alpidic compression generated the Southern Boundary Fault along which the Paleozoic succession of the Cantabrian Orogen was faulted above the Cretaceous and Tertiary sediments of the Duero Basin causing a dip of the Cretaceous and Tertiary deposits. The vertical offset along the fault was estimated to amount to up to 400 – 1,000m, the resulting angle between the

Cretaceous/Tertiary and Paleozoic successions is approximately 30° (Evers 1967, Rupke 1965).

## 2.2 Sedimentary Development of NW-Iberia

The stratigraphic columns within Figure 2.7 give an overview of the Proterozoic/Paleozoic formations occurring within the Cantabrian Zone (Fig. 2.7a) and the ones being present within the northern (Fig. 2.7b) and southern study area (Fig. 2.7c).

### *Cambrian and Ordovician*

The beginning of the Cambrian marked the start of the transgressive phase of the first major Phanerozoic flooding cycle (Vail et al. 1991). In the CZ, the Herrería, Láncara, Oville Fm. and the lower part of the Barrios Fm. were deposited (Fig. 2.7). From the Cambrian to Silurian, sedimentation in the CZ occurred on a shelf area with shallow marine sedimentation (Fernández-Suárez et al. 2002). However, the regional setting was that of an elongated graben structure during the Ordovician, being limited by normal faults (Cantabrian-Iberian Graben; Fig. 2.8) and subdivided by numerous minor horsts and grabens (Aramburu 1995, Aramburu et al. 1992, Aramburu & García-Ramos 1993). Sedimentary thicknesses within the Cantabrian Basin reach up to 4,500m in the east, whereas thicknesses increase to up to 10,000m in the west (Fig. 2.9). Generally, grain size decreases to the west (Aramburu & Bastida 1995, Tait et al. 2000). Sediments were derived from an uplifted area in the northeast, named the Cantabrian-Iberian High (Fig. 2.8; Aramburu & García-Ramos 1993). An overall continuity of lithofacies and faunas existed from the Central Iberian Zone to

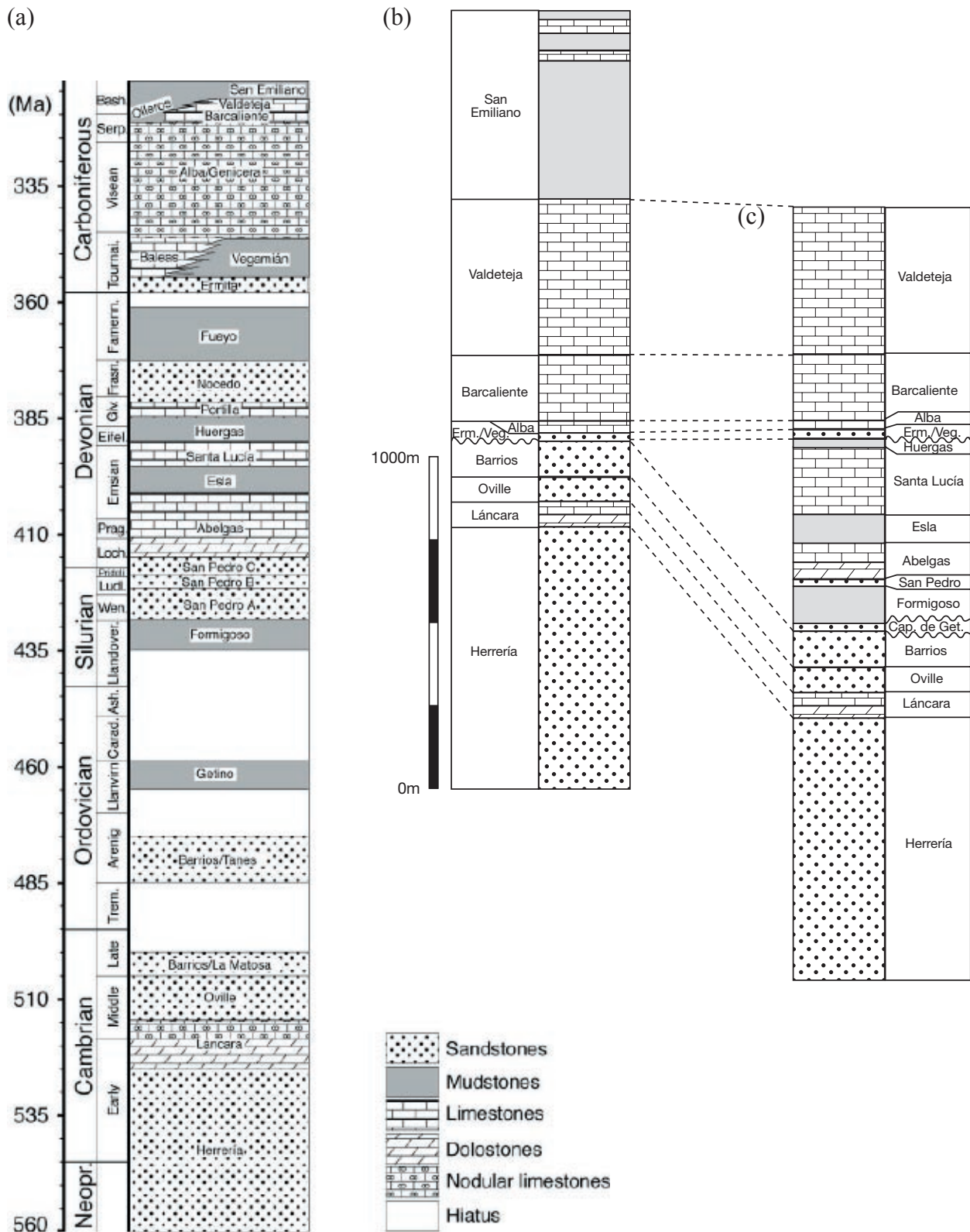


Fig. 2.7: (a) Stratigraphic chart of the formations occurring in the Southern Cantabrian Basin (Veselovsky 2004). (b) Stratigraphic profile at location Lavandera (Bodón Unit) in the northern part of the field area. (c) Stratigraphic profile at Las Hoces de Vegacervera (Correcilla Unit) in the southern part of the field area. Note the diminishing thickness and disappearance of Ordovician to Devonian formations from the southern towards the northern profile. Formation names are placed within the lithologic column (a) and aside the lithologic column (b, c), respectively. Cap. de Get.: Capas de Getino, Erm.: Ermita, Veg.: Vegamián.

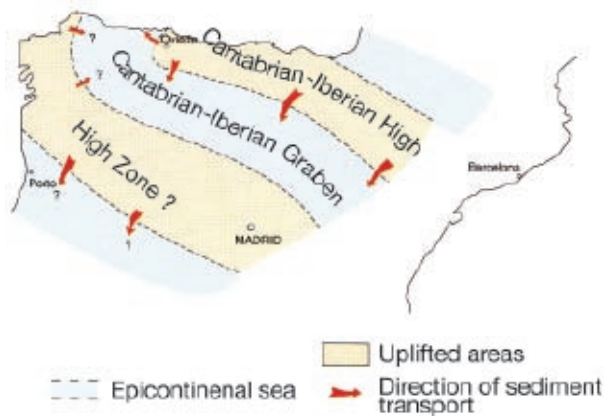


Fig. 2.8: Lower Ordovician paleogeography of the northern Iberian Peninsula (Aramburu et al. 1992, Aramburu & Bastida 1995).

the NNW, which probably reflects an original paleogeographical and biogeographical continuity within the North Gondwanan marine shelf. Considering the whole Iberian Peninsula during the Ordovician, an overall SE to NW deepening trend was attributed to its position on the northward deepening, more unstable shelf of the northern Gondwanan margin (Gutiérrez-Marco et al. 2002).

During and following the deposition of the Barrios Fm., major stratigraphic hiatus over the Cantabrian, West Asturian-Leonese, northernmost Central Iberian Zones and Iberian Cordillera were recorded, caused by high zones

(Aramburu et al. 1992, Aramburu & García-Ramos 1988). Uplifting of the high zones was interpreted as being related to the Sardic movements in the shelf-to-basin transitional zone (Gutiérrez-Marco et al. 2002). Hence, the sedimentary thickness of the Ordovician to Devonian sediments decreases significantly to the north within the Southern CZ (Fig. 2.7).

### Silurian

Across most of the CIZ, Iberian Cordillera, in some units of the WALZ, CZ and western Pyrenees, deposition began with sandstone units at the Ordovician-Silurian transition. In the field area, following a long stratigraphic hiatus, the sedimentary record starts with the euxinic black shales of the Llandoveryian Formigoso Fm. Thick units of alternating sandstones, siltstones and shales of the San Pedro Fm. follow, which were situated close to the terrestrial source areas (Gutiérrez-Marco et al. 1998, Paris 1993, Robardet et al. 1994). It is assumed that a land mass existed, probably situated between the CZ and the western Pyrenees (Fig. 2.8), but speculations regarding the character and position of the land-mass vary significantly. Heddebaut (1975) and

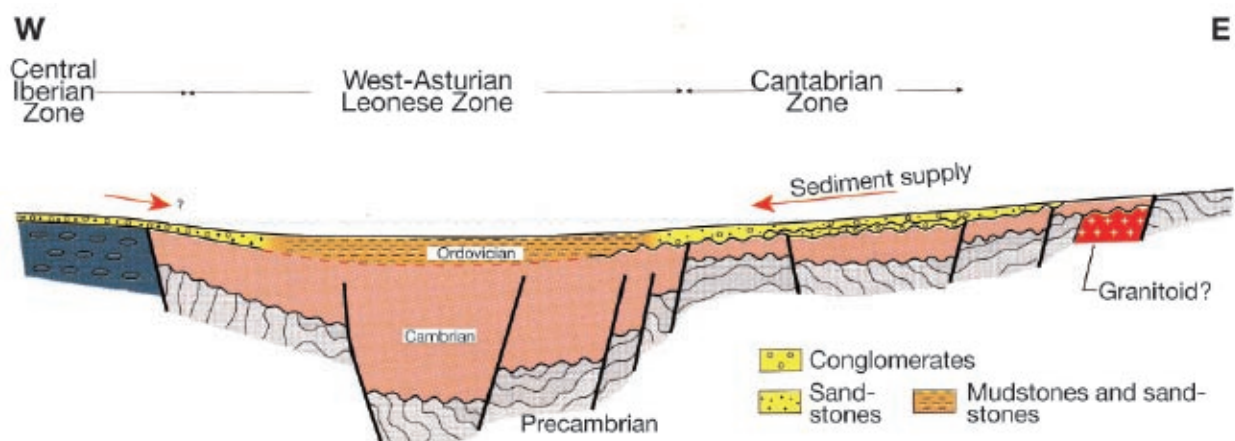


Fig. 2.9: Schematic cross-section through the Lower Ordovician sedimentary setting of the WALZ and CZ (Aramburu & Bastida 1995). Note the decrease of sedimentary thickness to the east.



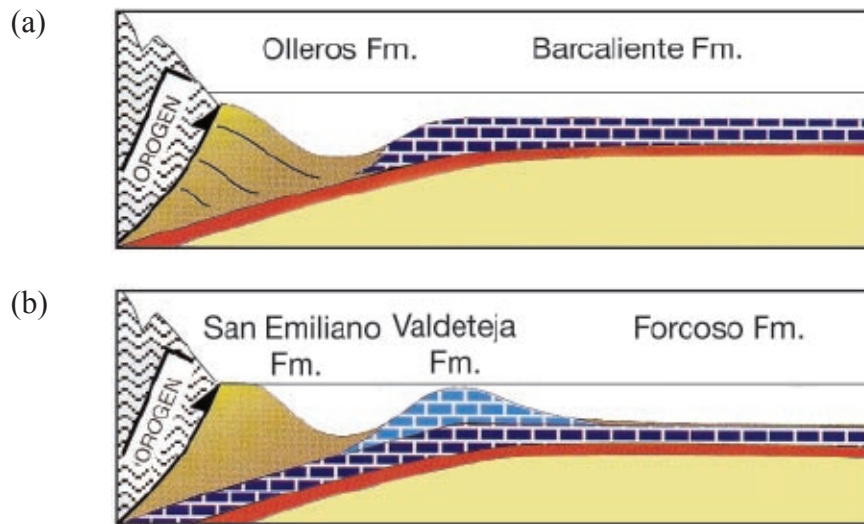


Fig. 2.10: Sketch of the paleogeographic setting during (a) lowermost Bashkirian and (b) lower and upper Bashkirian. See text for further explanation. Modified after Aramburu & Bastida (1995).

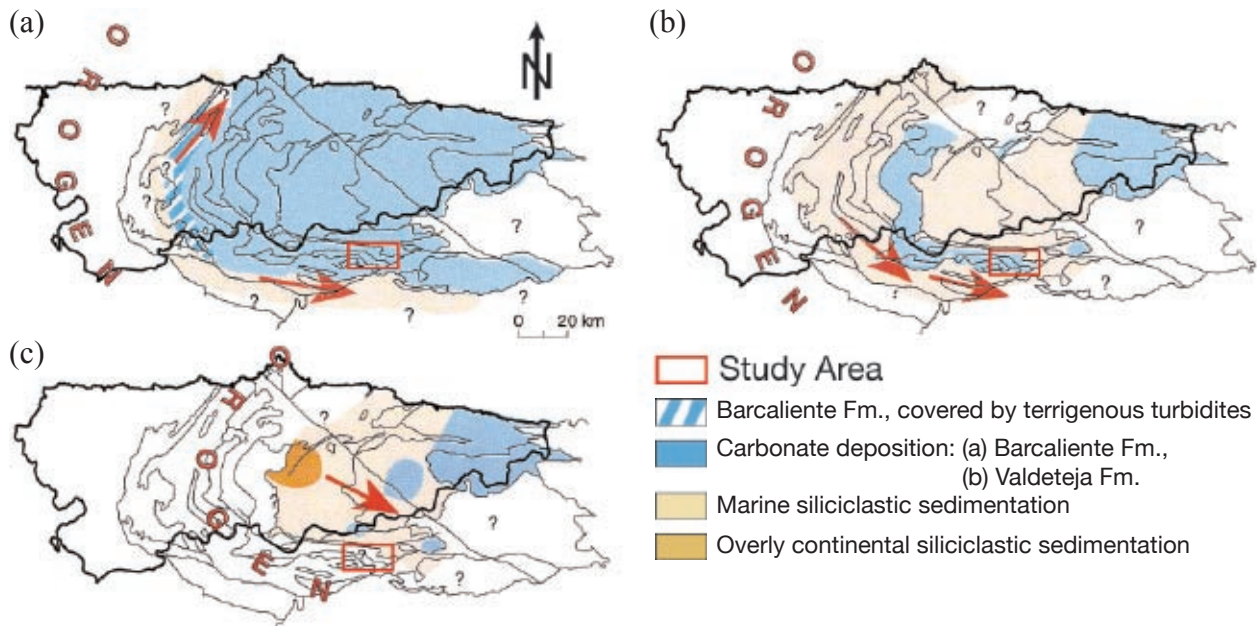


Fig. 2.11: Paleogeography of the Cantabrian Basin during (a) Namurian A, (b) Westphalian A, (c) Westphalian D (Aramburu & Bastida 1995). Note the migration of the Variscan Orogen. Red arrows indicate direction of paleocurrents.

Llopis Lladó (1965) suggested a landmass called Ebroia, Carls (1983, 1988) termed it Cantabro-Ebroian Massif. Despite the well-preserved depositional record indicating the existence of a landmass in the north, Robardet & Gutiérrez-Marco (2002) proposed an overall south-to-north deepening trend being related to the position on the North Gondwanan shelf. They suggested a more complex, regionally

differentiated topography in order to explain a northern uplifted zone.

### Devonian

During the Devonian, the northern landmass did not supply sufficient siliciclastic sediments for distribution over the whole Cantabrian Basin (Aramburu 1995). This allowed for

the development of carbonates of the La Vid Group, Santa Lucía Fm., and Portilla Fm. during early and middle Devonian. During late Devonian, siliciclastic input increased due to uplift of the northern landmass resulting in deposition of the Nocedo and Fueyo Formations. However, due to the uplift of a northern landmass, Devonian successions are diminishing and even vanishing from the southern to the northern part of the field area (Fig. 2.7b, c)

### *Carboniferous*

After deposition of the shallow-water siliciclastics of the Ermita Formation, the basin successively deepened during deposition of the Baleas, Vegamián and Alba Formations. The structural setting became increasingly unstable during deposition of the regionally widespread Barcaliente Fm. (Fig. 2.10a & 2.11a) during the Namurian A and B. Contemporaneously to deposition of the Barcaliente Fm., the Variscan foredeep was established west of the study area, recorded by siliciclastic turbidites of the Olleros Fm. (Fig. 2.10a) being present in the Alba Syncline. Differentiation continued in front of the migrating Variscan Orogen, the initiation of the carbonate platform marked the beginning of the Valdeteja Fm. (Fig. 2.10b, 2.11b). Basin deposits surrounded the platform carbonates (Fig. 2.11b) to the west/southwest (Variscan foredeep) and to the north/east/southeast (starved basin setting of the Forcoso Zone). The diachronously following and interfingering San Emiliano Fm. represents the Variscan foredeep deposits present in the study area. The orogen approached from the south to west according to today's coordinates (Bowman 1983, 1982, Wagner & Bowman 1983), as shown by migration of

facies belts. Input of siliciclastics from the Variscan Orogen continued and successively terminated carbonate platform deposition. Due to their distal position from the siliciclastic source area, platforms of the Picos de Europa Unit in the Northern Cantabrian Basin existed until Westphalian D (Eichmüller & Seibert 1984). In the Southern CZ, the sedimentary record concludes with Westphalian C deposits (Fig. 2.11c). Stephanian basins (Fig. 2.11c) overlie the Westphalian deposits with an angular unconformity.





### CHAPTER 3: CANTABRIAN BASIN FILL

Stratigraphic information is the basis for later quantitative basin analysis. Reverse modeling is calculated along time lines and therefore does not require as much stratigraphic detail as forward modeling that also considers facies changes between the time lines. Since the Herrería to Huergas Fm. were included in reverse modeling only, these formations are described only briefly. For further information, the reader is referred to e.g. Aramburu & Bastida (1995), Evers (1967), Vera (2004) and others.

All thickness values mentioned refer to measurements in the field area, if not otherwise indicated. Recorded profiles are attached in the appendix. Figure A.1 shows the location of the

recorded profiles within the field area.

During the Cambrian, sediments were deposited uniformly across the study area and the Southern Cantabrian Basin (Fig. 3.1). During the time of the Barrios Fm. and later, various erosional hiatus were reported (Aramburu et al. 1992, Aramburu & García Ramos 1993). In the Southern Cantabrian Zone, sedimentary deposits show an east- and northward thinning trend. Within the northern and eastern part of the study area, a long-lasting hiatus occurred from the Ordovician to Devonian (Chapter 6.2; Tab. A.2-4). Sedimentary record is most complete preserved in the southwestern part of the study area (Correcilla Unit), onlapping on an uplifted area in the north and east.

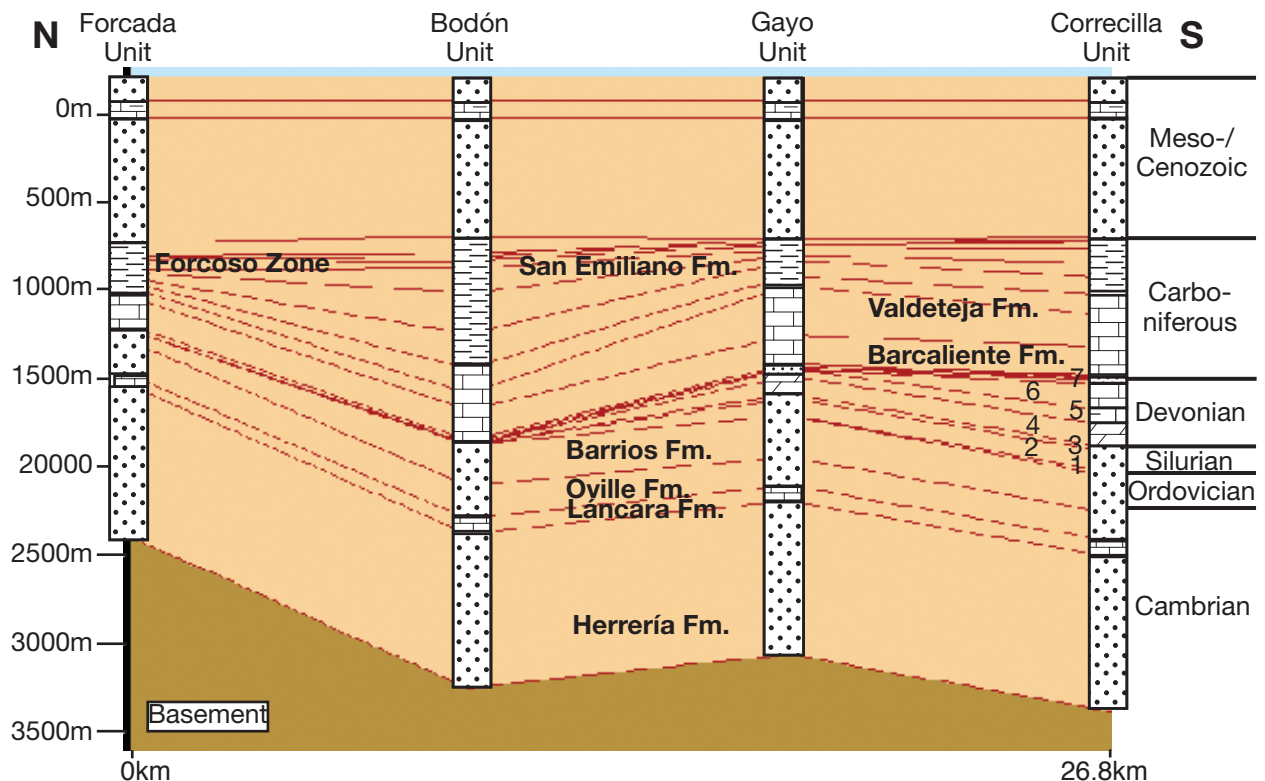


Fig. 3.1: Synthetic overview of basin architecture along the Torio Transect. Graphic output of the reverse modeling program. Stratigraphic columns were added as an overview over the lithology of the formations. Red lines represent time lines, which mostly coincide with formation boundaries. See text for more detailed description of the formations and spatial relationships. Table A.2 lists the quantified input values used to model the transect. 1: Capas de Getino, 2: Formigoso Fm., 3: San Pedro Fm., 4: Abelgas Fm., 5: Esla Fm., 6: Santa Lucía Fm., 7: from base to top: Huergas Fm., Ermita Fm., Vegamián Fm., Alba Fm.

### 3.1 Cambrian to Upper Devonian Deposits

#### *Herrería Formation*

Age: Base: Vendian to Tommotian (trilobites; Sdzuy 1961, Truyols et al. 1990), Precambrian/Cambrian as stated by Liñán et al. (1993), Ediacaran according to Aramburu et al. (1992).

Top: Lower Cambrian (Atdabanian) according to Truyols et al. (trilobites; 1990), in accordance with Meer Mohr (1969) and Vidal et al. (1999).

Thickness: A detachment fault at the base obscures the original thickness, but the measurable sediments amount to a thickness of 700m (Evers 1967).

Lithofacies: Subdivision into three members was established (Aramburu et al. 1992, Aramburu & García-Ramos 1993, Evers 1967, Oele 1964, Staaldunin 1973). In the study area, lithology starts with conglomerates, followed by an alternation of sandstones and shale. Its distribution is uniform across the field area.

Depositional environment: The deposits were interpreted belonging to a deltaic to shallow marine environment by Bosch (1969), Comte (1959), Evers (1967), Oele (1964), Rupke (1965), Savage & Boschma (1980).

#### *Láncara Formation*

Age: Upper Lower Cambrian - lower Middle Cambrian (Liñán et al. 1993, 2002, Meer Mohr 1969, Sdzuy 1961). The top is diachronous; deposits are younger to the east and south within the Cantabrian Zone: Upper Lower Cambrian for the western part of the Bodón Unit (near Lena de Gordón) and upper Middle Cambrian for the eastern part (Liñán et al. 1993, 2002, Sdzuy 1961).

Thickness: 70 - 100m

Lithofacies: This formation was divided into two and three members (see Barba & Fernández 1991, 1990, Zamarreño 1972). In the field area, deposits start with dolomites showing stromatolites and birds-eye structures, followed by gray limestones containing glauconite and birds-eye structures, and red, nodular, argillaceous limestone in “griotte” facies. In the field area, the “griotte” facies deposits decrease in thickness from the south to the north (Braun 1981, Evers 1967, Hinsch 1997, Potent 2000). Depositional environment: The dolomites indicate intertidal environment, whereas the nodular, argillaceous limestones were deposited in slightly deeper marine conditions (Álvaro et al. 2000, Aramburu et al. 1992, Oele 1964).

#### *Oville Formation*

Age: Uppermost Middle Cambrian to lowermost Ordovician (trilobites and palynomorphs; Liñán et al. 1993, Lotze 1961, Sdzuy 1961, Truyols et al. 1990, Zamarreño & Julivert 1967).

Thickness: 140 - 300m

Lithofacies: Aramburu & García-Ramos (1993) proposed a subdivision into three members, Gietelink (1973) into four members. The formation consists of alternating trilobite-rich shales and silt-/sandstones containing glauconite. Towards the top, the fraction of quartzitic sandstone increases (Gietelink 1973, Seibert 1980, Truyols et al. 1990).

Depositional environment: Various authors agreed on a gradual transition from a shallow platform environment to deltaic conditions (Aramburu & García Ramos 1993, Gietelink 1973, Sánchez de Posada et al. 1998, Seibert 1980, Truyols et al. 1990). An overall southward deepening trend was recognized (Aramburu & García Ramos 1993, Gietelink 1973).



Fig. 3.2: Quartzitic, red sandstones of the Barrios Fm. (northwest of Montuerto, Curueño Valley, Pozo Unit).

### *Barrios Formation*

Age: Middle Cambrian to upper Arenigian (Aramburu & García-Ramos 1993, Baldwin 1978, Crimes & Marcos 1976). The top is highly diachronous, with increasingly older top of the preserved record to the northeast.

Thickness: 0 - 330m

Lithofacies: Aramburu & García Ramos (1993) divided the formation into three members. It consists mainly of white, subordinately red, quartzitic sandstones (Fig. 3.2) and interbedded shales (Aramburu & García-Ramos 1993, Gietelink 1973, Oele 1964, Sánchez de Posada et al. 1998). Erosional unconformities are situated between the members and at the top of the formation (Aramburu & García-Ramos 1993, Gietelink 1973, Potent 2000).

Depositional environment: Aramburu et al. (1992), Aramburu & García-Ramos (1993), Fernández-Suárez et al. (2002), Gietelink (1973), and Oele (1964) interpreted a littoral to subaerial environment of a braid-plain delta.

### *Capas de Getino*

Age: Arenigian to Llandoveryan (Aramburu et al. 1992, Aramburu & García Ramos 1993)

Thickness: 0 - 20m

Lithofacies: The formation is bounded by unconformities. Thickness and lithology vary greatly (Aramburu et al. 1992). In the study area, dolomites, limonites and shales can be found (Aramburu et al. 1992).

Depositional environment: The deposits accumulated in a shallow marine environment.

### *Formigoso Formation*

Age: Upper Llandoveryan to lower Ludlovian according to Truyols et al. (1990), to uppermost Llandoveryan/lowermost Wenlockian according to Aramburu et al. (1992), Sánchez de Posada et al. (1998), Cramer (1964) (graptolites, palynomorphs)

Thickness: 30 - 60m (Potent 2000)

Lithofacies: The lower member (Bernesga Mb.) consists of black graptolite-rich shales and minor amounts of alternating siltstones and sandstones; the upper member (Villasimpliz Mb.) consists of iron-rich sandstones and green-gray siltstones (Sánchez de Posada et al. 1998). Sand content increases to the top.

Depositional environment: The lower member was deposited in a euxinic, shallow neritic environment (Truyols et al. 1990) on an external platform (Aramburu et al. 1992) whereas the upper member was deposited in a littoral setting (Aramburu et al. 1992). An overall

shallowing upward trend is recorded by the increasing terrestrial influence (Aramburu et al. 1992, Rodríguez 1983, Truyols et al. 1990).

#### *San Pedro Formation*

Age: Lower Ludlovian to Lower Gedinian (Truyols et al. 1990)

Thickness: 0 - 20m (Vilas Minondo 1971)

Lithofacies: In the lower part of the formation, red and green, iron-rich, often-oolithic sandstones were deposited. The iron originated from subaerially weathered volcanics (Suárez de Centi et al. 1989, Van den Bosch 1969). To the top, light-colored quartzitic sandstones and shales prevail.

Depositional environment: Sediments were deposited on a very shallow epicontinental platform located close to the coast (Evers 1967, Suárez de Centi et al. 1989, Vilas Minondo 1971).

#### *La Vid Group*

Age: Base: Lower/middle Gedinian to Emsian (Keller 1997, 1988, Rupke 1965)

Thickness: 0 - 200m (Keller 1988, present work, Vilas Minondo 1971)

Lithofacies: The La Vid Group is subdivided into the Abelgas Fm. and the Esla Fm. Sedimentation starts with dolomites and an alternation of limestones and marls. In the upper part, the shale content increases (Braun 1981, Keller 1988, present work, Vilas Minondo 1971).

Depositional environment: Dolomites are interpreted belonging to subtidal to intertidal and sabkha conditions (Keller 1988, Kullmann & Schöenberg 1980). Water depth increased toward the upper part of the La Vid Group. Euxinic conditions were established for a short

time period, indicated by black shales (Keller 1988, Kullmann & Schöenberg 1980).

#### *Santa Lucía Formation*

Age: Base: Uppermost Emsian to lower Eifelian (brachiopods; García Alcalde et al. 2000, Reijers 1984)

Thickness: 0 - 190m

Lithofacies: In the study area, argillaceous, laminated, peloidal limestones with birds-eye structures prevail. Fossil content includes brachiopods, corals, echinoderms, bryozoans, bivalves etc.

Depositional environment: For the research area, an intertidal to supratidal environment, shallowing toward the north, was proposed by Buggisch et al. (1980), De Coe et al. 1971 (1971), Reijers (1980).

#### *Huergas Formation*

Age: Upper Eifelian to lower Givetian (Wagner 1971). Frankenfeld (1981) determined conodonts at the top near Valporquero (Torío Valley) belonging to Givetian to Frasnian.

Thickness: 0 - 30m (Vilas Minondo 1971)

Lithofacies: Iron-rich sandstones and euxinic, argillaceous shales containing pelagic fauna (Evers 1967, Truyols et al. 1990).

Depositional environment: García Alcalde (2002) and Reijers (1973) proposed pro-delta and delta slope settings.

### **3.2 Upper Devonian to Carboniferous Deposits**

A time scale was assembled out of literature data for the Carboniferous of the Cantabrian Basin. Ages within the following text will refer to this scale (see Fig. 3.3 for details).









Fig. 3.4: Sandstones of the upper part of the Ermita Fm. (Arroyo de Barcaliente, Curueño Valley, Bodón Unit).

### *Ermita Formation*

Type locality: Bernesga Valley, opposite the “Ermita del Buen Suceso” near the village of Nacedo (Comte 1959), IGME Map 103 “La Pola de Gordón” (Alónso et al. 1991).

Age: Upper Famennian to lower Tournaisian (brachiopods, condonts; Comte 1959, García Alcalde et al. 2000, Higgins et al. 1964, Van Adrichem Boogaert 1967, Wagner 1971, Winkler Prins 1968)

Contacts: In the Bodón Unit of the study area, the Ermita Fm. unconformably overlies the Barrios Fm. (Buggisch et al. 1980, IGME Map 104 “Bonar”, Potent 2000, present work, Truyols et al. 1984, Wagner 1971 etc.). Buggisch et al. (1980) reported karstification

at this contact in the Arroyo de Barcaliente. In the Correcilla Unit and the southern limb of the Montuerto Syncline (Gayo Unit), the formation unconformably follows the Santa Lucía Formation, whereas in the northern limb of the Montuerto Syncline (Gayo Unit), it postdates La Vid Group deposits.

Thickness: 0 - 10m (Potent 2000, present work, Seibert 1980, Vilas Minondo 1971). Further to the SW, thickness increases to 65m (measured north of Piedrasecha by Veselovsky 2004).

Lithofacies: Well-sorted, fine to medium grained, ferruginous sandstones of brownish to dark-red color (Fig. 3.4), often exhibiting cross-stratification. Locally, abundant brachiopod moulds reach sizes of up to 5cm (e.g. Arroyo de Barcaliente). Lower parts of the formation, which are not present in the study area, were recorded to consist mainly of siltstones and some intercalated sandstone beds. The upper part may contain polymict conglomerates and thin intercalations of shale and siltstone (Veselovsky 2004).

Depositional environment: The distribution of sediments suggests a basal transgression from the SW into the working area. The sandstones were deposited in a littoral, high-energy environment (Raven 1983, Reijers 1973). Evers (1967) attributed the deposits to sand bars parallel to the coast. Evers (1967) suspected that the Sancenas High influenced the deposition, resulting in a low thickness of the sandstones.

### *Baleas Formation*

Type locality: Baleas quarry north of La Pola de Gordón (Alónso et al. 1991, Wagner 1971), IGME Map 103 “La Pola de Gordón” (Alónso et al. 1991).

Age: Base: South of Montuerto, Menéndez-

Álvarez (1991) determined conodonts indicating upper Famennian in agreement with results published by Gandl (1973), Higgins (1971), Higgins et al. (1964) and Higgins & Wagner-Gentis (1982). At Genicera, Truyols Santonya & Sánchez de Posada (1983) reported an age of Tn1a (Lower Tournaisian).

Top: Near Aviados, conodonts belonging to the *anchoralis-latus* zone indicate upper Tournaisian (Tn3c according to Higgins et al. 1964, Menéndez-Álvarez 1991). At Genicera, Truyols Santonya & Sánchez de Posada (1983) dated the top as Tn1a - b (lower Tournaisian).

Contacts/discontinuities: Base and top of the formation are diachronous (Sánchez de Posada et al. 1998). Only locally does the top show a gradual transition to the overlying Alba Fm. (Seibert 1988). The Baleas Fm. can locally replace the Vegamián Fm. (see below) but both can occur together as well (e.g. at Genicera), which causes a strong variation of the ages for the top of the formation.

Thickness: 0 - 10m (present work; Truyols & Sánchez de Posada 1983)

Lithofacies: Light-colored, crinoidal grainstones and grayish, arenitic biosparites. Veselovsky (2004) reported current ripple marks in the crinoidal grainstones. The Baleas Fm. has often been described as the upper part of the Ermita Fm. (Bosch 1969, Evers 1967, Loevezijn 1986, Raven 1983).

Depositional environment: Loevezijn (1986) interpreted the limestones as crinoidal shoal deposits. In the study area, the Baleas Fm. occurs only in the Gayo Unit (present work, Winkler Prins 1968). Sánchez de la Torre et al. (1983) proposed a carbonate platform with high-energy bars and shoals (Baleas Fm.) and laterally deeper settings represented by the Vegamián Fm.

### *Vegamián Formation*

Type locality: South of the village of Vegamián de Porma, which is inundated today by the artificial Porma Lake (IGME Map 104 “Boñar”, Truyols et al. 1984).

Age: Base: The age is well constrained by conodont determination belonging to the *Siphonodella crenulata* to *anchoralis* zone indicating lower Tournaisian (Gandl 1973, Higgins et al. 1964, Higgins & Wagner Gentis 1982, Wagner 1963, Wagner et al. 1971, Winkler Prins 1968).

Top: Conodonts belong to the *anchoralis* zone indicating uppermost Tournaisian (Gandl 1973, Higgins et al. 1964, Higgins & Wagner Gentis 1982, Sánchez de Posada et al. 1990, Wagner 1963, Wagner et al. 1971, Winkler Prins 1968).



Fig. 3.5: Contact between black shales of the Vegamián Fm. and limestones of the Alba Fm. (Arroyo de Barcaliente, Curueño Valley, Bodón Unit).



Radiolarians of a section north of Llamazares belong to the upper *Albaillella indensis*-Zone confirming the conodont age (Braun 1981).

Contacts/discontinuities: Winkler Prins (1968) and Bialk (1989) noted a disconformable contact to the underlying Ermita Fm. Bialk (1989), Evers (1967) and Frankenfeld (1981) reported discontinuities during deposition of the formation.

Thickness: 1 - 7m (Braun 1981, present work, Reuther 1977)

Lithofacies: Locally (e.g. south of Genicera), deposition starts with a sandy, transgressional interval (Higgins 1971). Black, poorly fossiliferous shales are found predominantly (Fig. 3.5). Phosphorous nodules, chert layers, manganese, thin calcareous lentils, and thin beds (up to 2cm thick) of silt to fine grained sandstone occur.

Depositional environment: Deposition took place on an euxinic shelf area, water depth was 50 - 200m according to Boden (1982), Raven (1983), and Seibert (1986). A deepening upward environment is indicated by fewer occurrences of silt-/sandstone layers toward the top (e.g. Arroyo de Barcaliente). Frankenfeld (1981) proposed a locally uplifted area located in the area of the Sancenas Syncline. Bialk (1989) found terrestrial plant remains in the study area, which would point to the proximity of the coast (max. 15km according to Bialk 1989).

#### *Alba Formation*

Type locality: South of Puente de Alba in the Bernesga Valley (Comte 1959, Ginkel 1965), IGME Map 103 "La Pola de Gordón" (Alónso et al. 1991). Wagner et al. (1971) changed its name to Genicera Fm. and proposed a type

locality south of Genicera (IGME Map 104 "Boñar", Lobato et al. 1984).

Age: Numerous authors (e.g. Becker et al. 1975, Higgins et al. 1964, Kullmann 1976, 1965, 1963, 1961, Menéndez-Álvarez 1991, Raven 1983, Savage & Boschma 1980, Seibert 1988, Van der Ark 1982, Wagner et al. 1971) carried out investigations on conodonts, goniatites, and radiolarians and agreed on a duration from lower Viséan to lower Namurian A. However, locally, the top of the formation reaches upper Namurian A, e.g. at La Braña (Bodón Unit) of the study area (Balthasar 2001). Locally, the base belongs to the upper Tournaisian as measured in Aviados by Raven (1983), Seibert (1988) and Van der Ark (1982).

Contacts/discontinuities: Gradual transition

Thickness: 18 - 41m (Braun 1981, present work, Reuther 1977, Seibert 1988)

Lithofacies: Various authors established different subdivisions of the Alba Fm.: Winkler Prins (1968) described the Gete Mb., Valdehuesa Mb., and La Venta Mb., Balthasar (2001), Sánchez de la Torre et al. (1983) and Wagner et al. (1971) used a subdivision into Gorgera Mb., Lavandera Mb., and Canalón Mb., whereas Seibert (1988) named Members A to E. Balthasar (2001) described the lithology as follows: (i) Gorgera Mb.: reddish shale with calcareous concretions, (ii) Lavandera Mb.: reddish to greenish chert, radiolarites, and shales, (iii) Canalón Mb.: grayish, reddish, wavy nodular limestones (Fig. 3.6). At the top, the thin Adrián Mb. is described by Kullmann (1980) and Reuther (1977) and interpreted as distal carbonatic turbidites, being a transition to the overlying Barcaliente Fm. that shows a similar facies.

Depositional environment: Balthasar (2001) proposed a facies variation of swell, slope,



Fig. 3.6: Typical succession of the Alba Fm. along the roadcut close to Mirador de Vegamián at the southeastern shore of the artificial Porma Lake (Forcada Unit).

basinal, and steeper foreslope facies in relation to its paleogeographic position. In the study area, predominantly basinal facies is found in the Gayo and Bodón Units, whereas the Alba Fm. of the Forcada Unit was deposited on a slope (Balthasar 2001). Bialk (1989) and Evers (1967) noted a local high in the area where the Valdeteja platform nucleated during the Bashkirian.

#### *Barcaliente Formation*

In earlier literature, the Barcaliente and the succeeding Valdeteja Fm. were described as one formation and named Caliza de Montaña Fm. (Comte 1959, Ezquerro del Bayo 1844, and others). Evers (1967) subdivided the formation into the Lower Micrite Member and the Upper Biosparite Member. Wagner et al. (1971) established a formation status for both members and named the older one Barcaliente



Fig. 3.7: View into the Arroyo de Barcaliente, type section of the Barcaliente Fm., located in the northern part of the Curueño Valley.



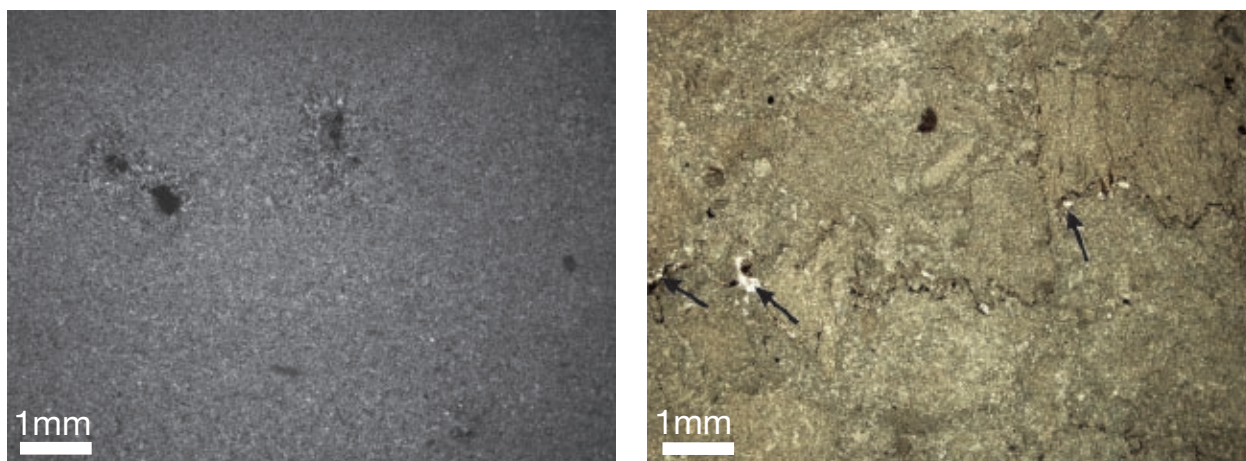


Fig. 3.8: Thin sections of the Barcaliente Fm. (a) Monotonous mudstone is characteristic for the lower part of the formation (sample BT3-2, profile “Arroyo de Barcaliente”). (b) Lower part of the Porma Breccia (sample BAR 5-3, profile “Arroyo de Barcaliente”): subangular components in a micritic matrix. Note the irregular, anastomosing sutured seam (microstylolite) with dark insoluble residue along the pressure-solution surfaces. White spots within the matrix may represent leached evaporitic minerals (marked by black arrows).



Fig. 3.9: Characteristic regular bedding of the lower part of the Barcaliente Fm. Bed thickness ranges between 5 to 15cm (type section at the Arroyo de Barcaliente, Bodón Unit).

Fm. and the younger one Valdeteja Fm.

Type locality: Arroyo de Barcaliente (Wagner et al. 1971), a valley diverging from the Curueño Valley near the road intersection to

Valdeteja (Fig. 3.7). IGME Map 104 “Boñar” (Lobato et al. 1984).

Age: Serpukhovian to lowermost Bashkirian. Table A.1 lists biostratigraphic data as available from literature.

Contacts/discontinuities: Age determinations of base and top indicate isochronous ages (see Tab. A.1). Reuther (1977) and Braun (1981) reported local erosive surfaces from the base and from the top.

Thickness: 93m (North of Llamazares) - 190m (Las Hoces de Vegacervera, Coto Calvo), up to 400m as reported by Reuther (1977), 0 - 250m according to Evers (1967)

Lithofacies: For the Southern Cantabrian Zone, Reuther (1977) distinguished a lower part, followed by what is known as the Porma Breccia and a transitional member (Señaras Mb. according to Frankenfeld 1976) at the top of the formation.

The lower part consists of dark-gray, bituminous, micritic, often laminated limestones (Fig. 3.8) with frequent calcite veins. The limestones show excellent stratification. The beds have a mostly platy character, but may be wavy (Fig. 3.9). Their average thickness



ranges between 10 - 15cm. Lateral variations were observed, from well-layered beds to sections of massive appearance. Macroscopically, the massive sections reveal no lithologic differences from its lateral, well-layered continuations. The nature of those sections could not be investigated as it would exceed the scope of this project and is not reported in available literature yet.

Normal gradation, parallel lamination and bioturbation are frequent features.

As observed during fieldwork and reported by Hemleben & Reuther (1980) and Reuther (1977) from the upper part, minor erosional contacts, cross-bedding and sedimentary channels diversify the otherwise monotonous appearance of the limestones indicating a shallowing upward depositional regime. Minor slumping was found close to the overlying Porma Breccia (Appendix, profile "Mirador de Vegamián").

Fossil content is extremely scarce, but several findings have been reported: corals, conodonts, goniatites, foraminifers, microspores, brachiopods, ostracods, and crinoids (Braun 1981, Brouwer & van Ginkel 1964, Kullmann et al. 1977, Martínez-García 1971, Menéndez Álvarez 1991, Moore et al. 1971, Rácz 1964, Reuther 1977). Pyrite concentrations occur frequently. Local, post-depositional recrystallization and dolomitization are present and increasingly found toward the west (Evers 1967, Gasparrini 2003, Reuther 1977).

**Porma Breccia:** Without sharp contact, the well-stratified limestones pass into a limestone breccia zone. The Porma Breccia was named after its type locality at the southwestern edge of the artificial Porma Lake (Reuther 1977). The thickness of the breccia varies between 5m (East of Oville) and 60m (Las Majadas del

Caserio).

Components are mostly sub-angular, mm - m sized and unsorted (Fig. 3.10). The fragments consist of the typical, bituminous, mostly laminated Barcaliente limestone.

The matrix consists of black calcareous and arenaceous mudstones, which are typical for the Barcaliente Fm. (Evers 1967, Kullmann et al. 1977, Reuther 1977), and brecciated material of mm-sized components.

Profile "Arroyo de Barcaliente" (see Appendix) contains small amounts of single evaporitic crystals in the matrix of the lower part of the breccia whereas in profiles "Llamazares" and "Porma Lake" single crystals were found in the horizon below the breccia (see Appendix). According to an S.E.M. analysis by González Lástra (1978), the calcite and quartz crystals grew pseudomorph after gypsum and/or anhydrite.

The top of the breccia zone is in sharp contact to the Señaras Mb. (Reuther 1977).

**Señaras Mb.:** The thickness of the Señaras Mb. ranges in the study area between 3m (Mirador de Vegamián) and 44m (East of Oville). Locally, it is strongly tectonized and shows abundant calcite veins. Well-stratified, often laminated and bioturbated, dark-gray to black limestones alternate with marl, siltstone, and shale. Beds are 5 - 15cm thick.

The fossil content is higher here than in the lower part of the Barcaliente Fm.: radiolarians, remains of algae, gastropodes, thick-walled brachiopods, foraminifers, remains of bryozoans, ostracods, lamellibranchs, and crinoids were reported (Braun 1981, Frankenfeld 1976, Reuther 1977). Most of the fossils are only slightly broken, but heavily micritized. Cm - sized burrows occur (Braun 1981). About 2m below the top of the member, Winkler Prins

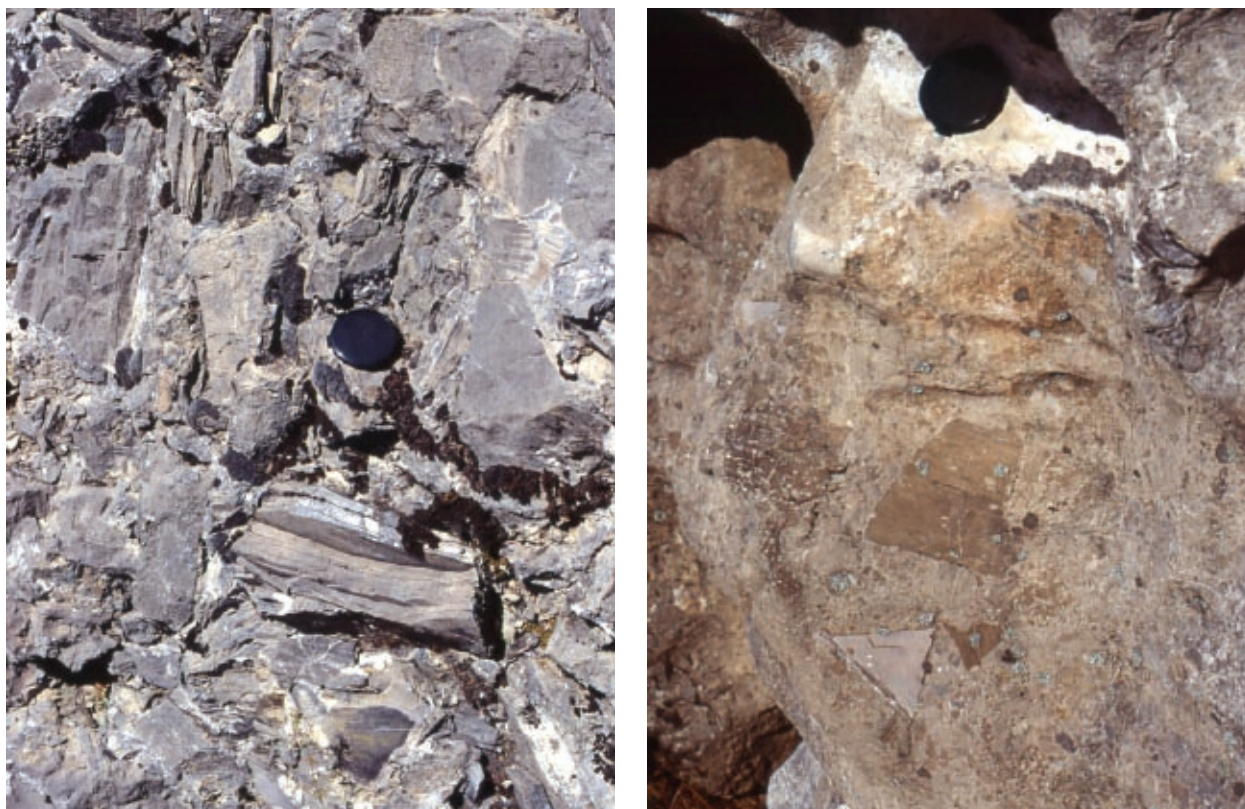


Fig. 3.10: Unsorted, sub-angular components of the Porma Breccia (Arroyo de Barcaliente, Bodón Unit). Lens cap for scale.

(1968) first described the *Martiniopsis* Band, which consists of a slightly calcareous black shale containing reticulariid spirifers and crinoid ossicles. It yields abundant fossils and was used for age-determination (e.g. goniatites by Kullmann 1979, 1963, 1962, and Sjerp 1967, conodonts by Menéndez-Álvarez 1991, foraminifers by Villa 1982). Stromatoliths exist (Reuther 1977). Idiomorph pyrite crystals occur frequently.

0.5 - 8m thick horizons of breccia are present in various locations (e.g. Arroyo de Barcaliente, Caldas de Nocedo). The components are generally cm-sized. The brecciated parts extend laterally only within the scale of tens of meters.

Braun (1981) described oololiths at the top of the Señaras Mb. (Caldas de Nocedo), followed by massive limestones of the Valdeteja Fm.

Depositional environment: Various attempts

have been made to interpret depositional conditions of the lower part. Earlier authors (Evers 1967, Rupke 1965, Van den Bosch 1969, Wagner et al. 1971, Winkler Prins 1968) proposed euxinic conditions with low (Evers 1967, Rupke 1965) / high (Van den Bosch 1969) rates of sedimentation in a restricted, low energy environment. González Lástra (1978) favored shallow marine to lagoonal conditions. Martínez Chacon & Winkler Prins (1993) attributed the fauna to a quiet, relatively shallow environment below wave base.

According to Reuther (1977), a single bed of the lower part corresponds to Meischner's description of allodapic limestones (1964). The occurrence of fossils, trace fossils, the absence of chondrites and abundant bioturbation indicated oxic conditions and he proposed that the high content of bitumen is of post-sedimentary origin. However, north of Cármenes (Bodón

Unit), sub-millimeter sized bituminous laminites exist (pers. com. Bechstädt 2005). Reuther (1977) proposed a water depth of approximately 100 - 300m. Bissell & Barker (1977) described a very similar setting for the Mississippian Great Blue Fm. (Utah, U.S.A.) and concluded bathyal depositional conditions.

In any case, water depth decreased towards the top as indicated by the increasing occurrence of sedimentary structures such as erosional contacts, cross-bedding, sedimentary channels and slumping (Reuther 1977). González Lástra (1978) reported gypsum (see above) from layers directly beneath the Porma Breccia, whereas in the study area, evaporites were also found in the matrix of the lowermost breccia horizon. However, this might be due to reworking of the underlying limestones. González Lástra (1978) attributed the morphology, shape and structure of the evaporitic crystals to deposition in intertidal to supratidal conditions.

The exact position and nature of the source location is not clarified yet, but Braun (1981), Hemleben & Reuther (1980) and Sánchez de la Torre & González Lástra (1978) agreed on a transport direction from the northeast to the southwest, based on distribution in grain size, slumping, cross-bedding and decreasing bed thicknesses.

The Porma Breccia is generally interpreted as a synsedimentary breccia (Hemleben & Reuther 1980, Reuther 1977). Reuther (1977) speculated that strong vertical, tectonic movements were to blame for triggering the generation of the breccia. Yet González Lástra (1978) holds a collapse due to the dissolution of evaporites responsible for causing the breccia.

During deposition of the Señaras Mb., sedimentation continued to take place in shallow water

conditions. Laminated stromatoliths, minor erosional surfaces, cross-bedding and small channels were found by Reuther (1977), which indicate subtidal environment. Additionally, Braun (1981) reported oolites and transverse ripple marks. Furthermore, Braun (1981) concluded that the environment deepened from the west to the east, which is supported by the facies of the formations that follow.

**Distribution:** The Barcaliente Fm. occurs all over the Cantabrian Basin. However, Porma Breccia and Señaras Mb. are present in the southern Cantabrian Basin only.

### *Olleros Formation*

**Type locality:** Arroyo de San Martín north of Olleros de Alba (Wagner et al. 1971), IGME Map 129 “La Robla” (Matas & Rodríguez Fernández 1984).

**Age:** The formation is mainly time-equivalent to the Barcaliente Fm. and the lower part of the Valdeteja Fm. (Colmenero et al. 2002). However, data for the base may indicate diachronous onset. Menéndez-Álvarez (in: Truyols & Sánchez de Posada 1983) determined fauna older than Kinderscoutian (R1) at the type section, whereas Wagner et al. (1971) established an upper Arnsbergian (E2) age south of Barrios de Gordón. Wagner & Fernández García (1971) found plant remains of Namurian B or C close to the top.

**Thickness:** 740m (Wagner et al. 1971), 518m (Sánchez de la Torre et al. 1983). Thickness of the formation can only be an approximation due to heavy tectonic overprint. Additionally, the top has been eroded.

**Lithofacies:** The formation consists predominantly of siliciclastics of grain sizes varying from shale to micro-conglomerate (Fig. 3.11).



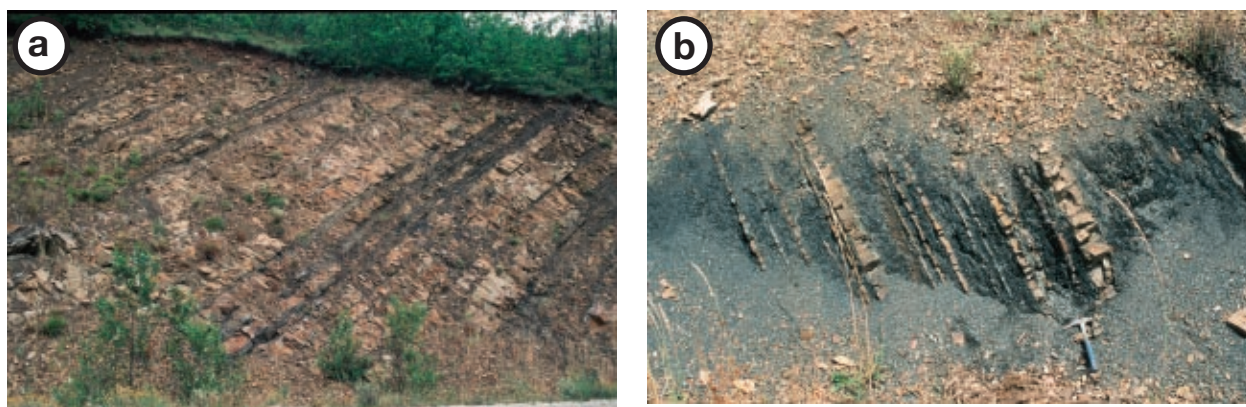


Fig. 3.11: Siliciclastic Turbidites of the Olleros Fm. (a) Road section north of Llombera (Alba Syncline), (b) south of Carbonera (Alba Syncline).

Thick shale successions occur in various levels. Bouma sequences (Tb-e, Tc-e) were reported (Sánchez de la Torre et al. 1983). Fossils are scarce. Tongues of dark-gray to black limestone occur in varying, laterally non-correlatable levels of the succession. Their facies seems to be identical with the typical Barcaliente limestone. The limestones are highly deformed, more so than the surrounding siliciclastics. Contacts to the siliciclastics are generally disturbed.

Depositional environment: Wagner et al. (1971) interpreted that the formation was deposited under basinal conditions in front of the Variscan Orogen. The shales represent slowly deposited muds, whereas the turbidites point to an increase in the rate of sedimentation. The sediment source area was located in the southern hinterland (Wagner et al. 1971).

The tectonic horses of the Barcaliente-like limestone units can have been derived as slides from the Barcaliente Fm., which was deposited on a nearby swell in the north and east of the Olleros Fm.

Distribution: The Olleros Fm. crops out in the Alba Syncline.

### *Valdeteja Formation*

Type locality: Road section east of Valdeteja, northern Curueño Valley (Wagner et al. 1971), IGME Map 104 “Boñar” (Lobato et al. 1984).

Age: Lower Bashkirian to upper Bashkirian, locally reaching lower Moscovian (Tab. A.1).

Contacts/discontinuities: Definition of the basal contact varies. Braun (1981), Eichmüller (1981, 1985), Evers (1967), Winkler Prins (1971), and this work set the boundary where the dark, well-layered limestones end and the first massive, light-gray limestone occurs, showing a gradual, mostly synchronous transition. In the vicinity of the basin margin, the platform progrades into the basin, resulting in sharp contacts between the basin and platform breccia (Fig. 3.12).

Other authors (e.g. Menéndez Álvarez 1991) defined the formation boundary along a local discontinuity located 1.5m below the described contact (Appendix, profile “Arroyo de Barcaliente”).

The top of the formation interfingers with siliciclastics of the San Emiliano Fm. Its upper boundary has been defined by the onset of siliciclastic sedimentation. Generally, the top of the Valdeteja Fm. is clearly visible due to morphological differences: whereas the massive







Fig. 3.14: Massive appearance of carbonates of the Valdeteja Fm. (Las Hoces de Vegacervera, Torío Valley, Correcilla Unit).

limestones build ridges (Fig. 3.13 & 3.14), the predominantly fine grained siliciclastics form morphological depressions (Fig. 3.13). The top is highly diachronous (Fig. 3.33).

Thickness: 0m (East of Oville, Nocado de Curueño, and Forcada Unit) - 677m (Las Majadas del Caserio)

Lithofacies: The formation consists mainly of light gray limestones with a massive appearance. The overall fossil content is relatively scarce. Nevertheless, local accumulation, mainly of crinoids, occurs. In general, brachiopods, crinoids, corals, calcareous algae, foraminifers, goniatites, gastropods, stromatopores, ostracods, and bivalves can be found.

Based on aerial photographs, field studies and

thin section analysis, depositional environments were specified and are described below. Recorded stratigraphic profiles are attached in the appendix.

### Slope

Geometries of slope deposits are recognized in air photographs northwest of Nocado de Curueño, at Coto Cabañas (Fig. 4.1 & 4.2) and in the field at the top of the Valdeteja Formation north of Valdorria (Fig. 3.15) and south of Coto Cabañas (3.16).

The thickness of the slope deposits amounts to up to 190m (see Appendix, West of Oville). Based on lateral correlation of the profiles Las Majadas del Caserio, Valdeteja and Valdorria as well as on the analysis of aerial photographs, slope deposits are laterally traceable up to 8km. They interfinger with siliciclastic basin deposits from the time-equivalent Forcoso Formation (Fig. 3.12) and the younger San Emiliano Formation (Fig. 3.16; and below).

The lithological composition indicates increasing depositional depth of the slope deposits. Monomict breccias exist in wide areas at the platform-to-basin transition. Component sizes range between 0.5cm on the lower slope (e.g. West of Oville) and 3m on the upper slope (e.g. Valdeteja, Fig. 3.17a). The components are subangular and consist of platform-margin derived material. The matrix is composed of mudstone, frequently recrystallized. Lateral extension of breccia deposits reaches up to 3km (e.g. at Montuerto, Oville), their thickness amounts to more than 100m (Appendix, profile "West of Oville").

Furthermore, a well-layered alternation of silty shale, (marly) mudstone, (marly) wackestone, packstone and grainstone characterizes





Fig. 3.15: Slope deposits at the top of the Valdeteja Fm. northwest of Valdorria (Gayo Unit). Deposits derived from the platform margin east of the shown photo.

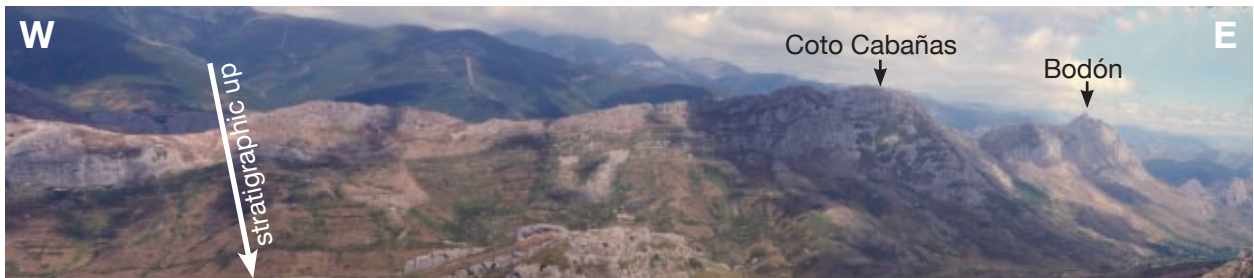


Fig. 3.16: Lateral interfingering of the ridge-building deposits of the Valdeteja Fm. with siliciclastics of the San Emiliano Fm. within the valley, viewed along strike of the Bodón Valley (Bodón Unit).

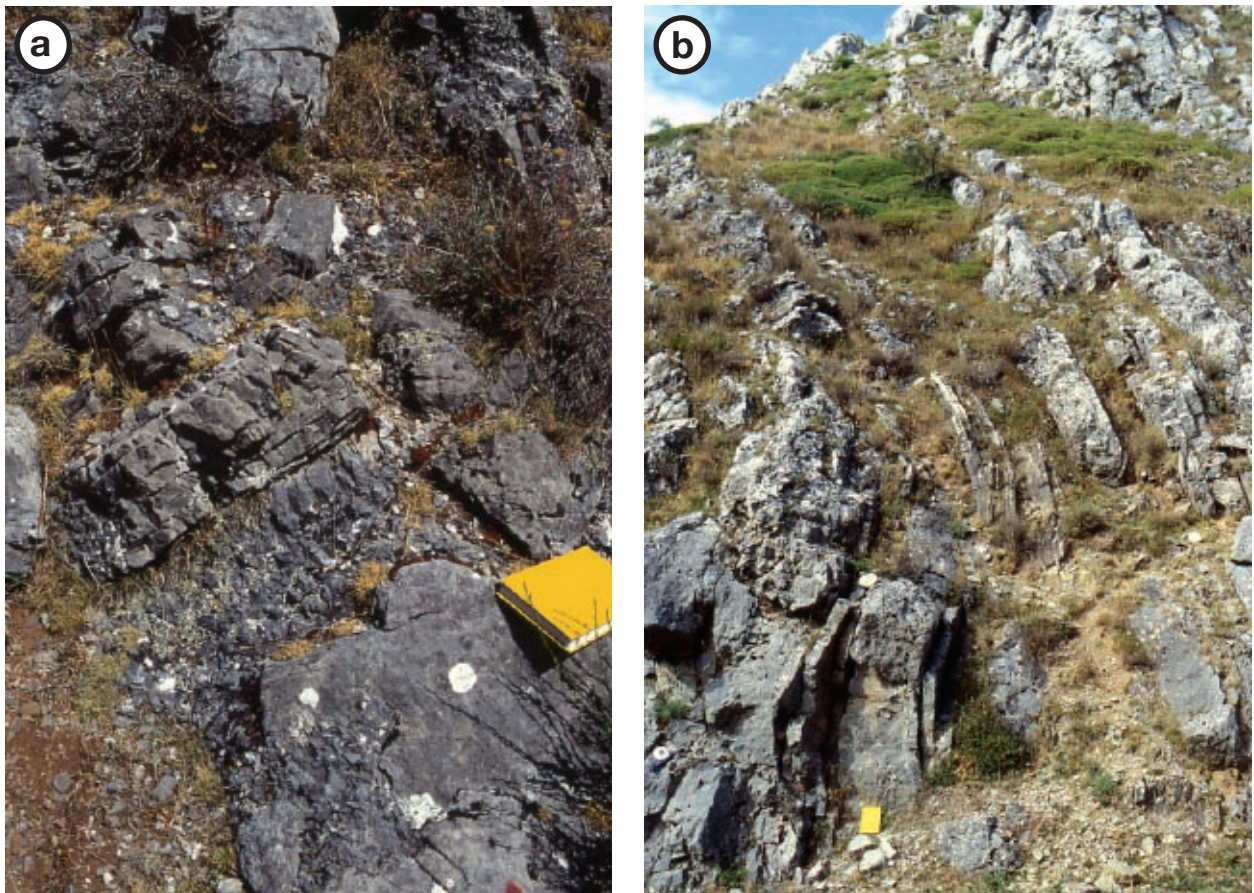


Fig. 3.17: Slope deposits of the Valdeteja Fm. (a) Breccia of the upper slope. The location corresponds to the area “C” of Figure 3.18. (b) Typical alternation of shaly mudstone to grainstone (lower part of the type section of the Valdeteja Fm., Curueño Valley, Bodón Unit).



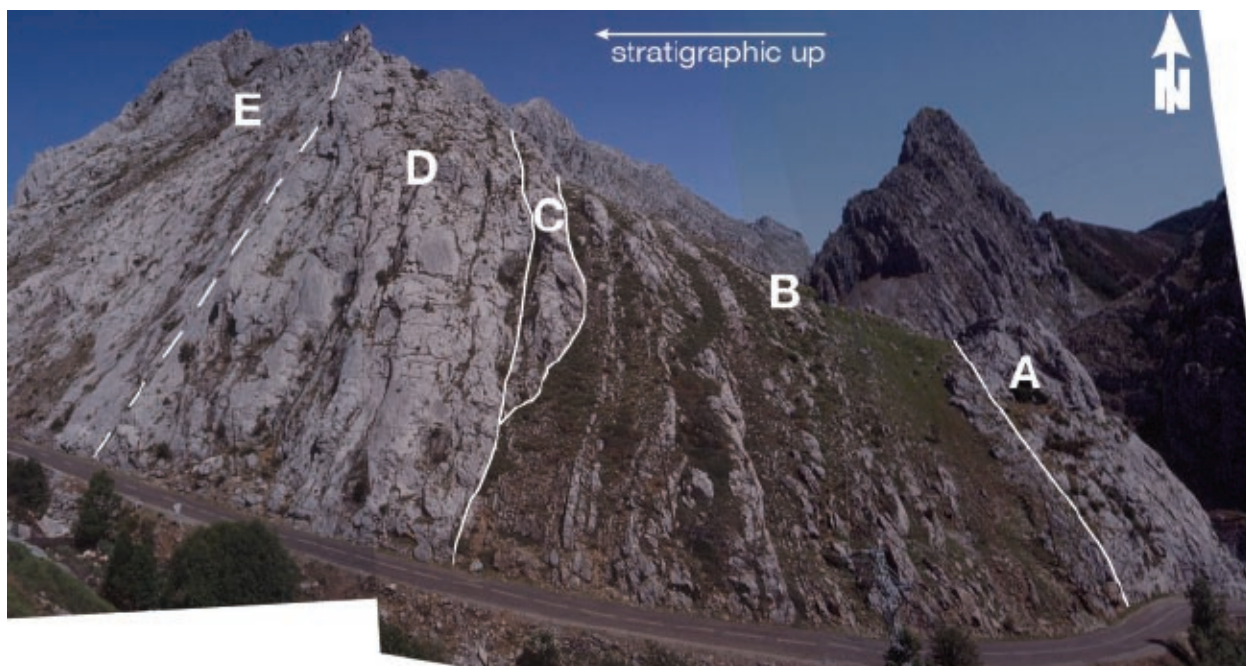


Fig. 3.18: Depositional environments in the lower part of the type section of the Valdeteja Fm. The mountain in the background to the right belongs to the type section of the underlying, well-stratified Barcaliente Fm. (Arroyo de Barcaliente). From base toward the top: A: platform margin, B: deepening upward slope, C: upper slope breccia, D: platform margin, E: platform interior. See text for further explanation.

the slope environment (Fig. 3.17b & 3.18). (Marly) mudstones account for the largest portion. Bedding ranges from 0.3m to 1.1m and 0.01m to 0.05m, respectively. Thin beds of 0.01m thickness of shedded crinoidal grainstone intercalate. The marly mudstone contains scarce skeletal components such as crinoids, small shell fragments, scarce cal-

careous algae and (silicified) solitary corals. Locally, the dark-gray mudstone shows load



Fig. 3.19: Macroscopic fossils within the slope deposits of the Valdeteja Fm. (a) Bioturbation (lower part of the type section of the Valdeteja Fm., Bodón Unit), (b) abundant skeletal components. The crinoid stem is exceptionally long for the Valdeteja Fm. within the field area (Northeast of Valdorra, Gayo Unit).



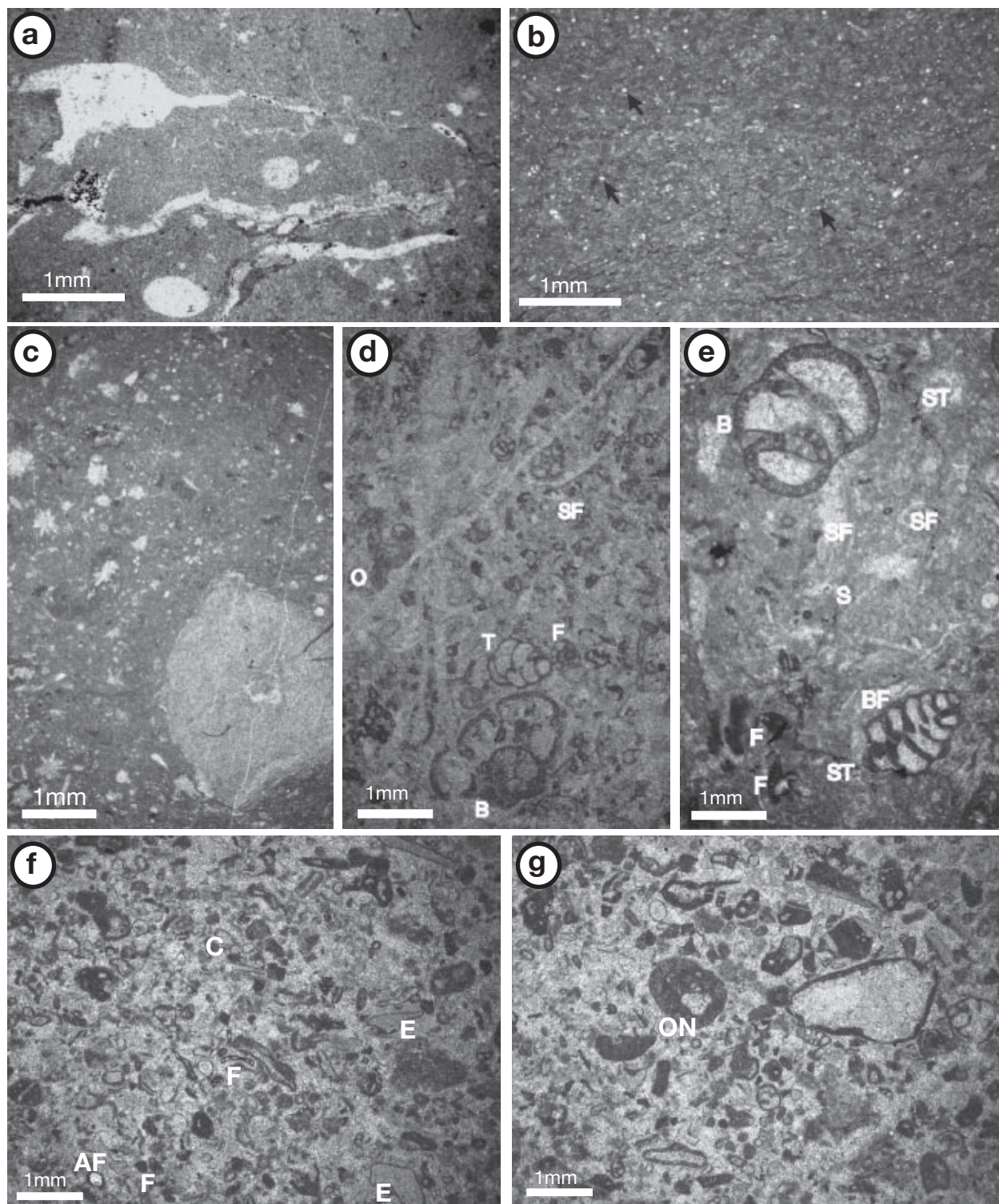


Fig. 3.20: Thin sections of slope deposits of the Valdeteja Fm. (a) Mud-/wackestone. Bioclastic components are mostly replaced by calcite (sample LM64-2, profile “Las Majadas del Caserio”). (b) Radiolaria-bearing biogenic packstone with few peloids and broken, small shell fragments. Small circular structures are cross-sections of radiolarians (arrow). Black seams represent microstylolites (sample BV7-2, profile “Valdeteja”). (c) Spiculite mud-/wackestone. Asterisks are spiculites, crinoidal stem in the lower right (sample VV7-2, profile “Valdorria”). (d) bioclastic pack-/wackestone with few, small ostracods (O), shell fragments (SF) and diverse foraminifera: *Bradyina* (B), multichambered biserial paleotextulariid (T), tangential section of a fusulinid (F) (VV3-2, profile “Valdorria”). (e) Bioclastic wackestone. Foraminifera comprise e.g.: fusulinids (F), *Bradyina* with typical inner perforated calcareous wall (B), multichambered biserial form (BF); shell fragments (SF) and a sponge fragment (S) are present, as well as stylolites (ST) (sample VV5-2, profile “Valdorria”). (f) Well-cemented biogenic pack-/grainstone. Components are relatively small and broken. They comprise foraminifera (F), a coral (C), fragments of echinoderms with a micritic envelope (E), and algal fragments (AF) (sample WO 16-2, profile “West of Oville”). (g) Bioclastic pack-/grainstone with similar composition as (f), containing an oncoid (ON) with several biogenic nuclei (sample WO 17-2, profile “West of Oville”).



casts at its base and beds pinch out laterally. It contains small amounts of pyrite. On top of the mudstone, either grainstone and packstone or wackestone follow, which may contain small amounts of shale as well. Bioturbation is present (Fig. 3.19a). Bedding thickness ranges from 5 to 15cm. Peloids, coated grains and scarce aggregate grains were found (Fig. 3.20). Some wackestone beds show normal gradation. Skeletal components comprise abundant crinoids, foraminifers and shell fragments (Fig. 3.19b). Larger components are generally broken.

Lower slope deposits show an increasing amount of bituminous material, decreasing fraction of shedded skeletal components, and an increasing bed thickness of autochthonous sediments. Additionally, thin sections contain abundant radiolarians (Fig. 3.20b; see Appendix, profiles “Valdeteja”, “Las Majadas del Caserio”).

### Platform Margin

Because of the faunal crisis at the Frasnian/Famennian boundary, reef-building organisms did not exist worldwide during the Carboniferous as known from other periods of the earth history (James 1978, 1983, Longman 1981, Wilson 1975). In the Valdeteja Fm., the platform margin facies consists of small mounds, which lie off ooid-sand bars (Eichmüller 1985).

At the base of the formation, margin deposits reach thicknesses of only a few meters (Fig. 3.18), followed by distinct slope deposits with a sharp contact (e.g. profile “Valdeteja”). The contact with the underlying Señaras Mb. was observed as being gradational (“Valdeteja”, “Las Majadas del Caserio”; Braun 1981), which was also the case for the transition from



Fig. 3.21: Inter-mound beds within massive platform margin deposits (lowermost part of the type section of the Valdeteja Fm., Bodón Unit).

platform interior deposits to platform margin. At the top of platform margin facies, transition to platform interior facies is gradational (“Valdeteja”).

The highest thickness of platform margin deposits measured amounts to 99m.

Predominantly, the platform margin deposits are made up of light gray, massive limestones, which represent stacked, small mounds. The lithology shows a wide spectrum ranging from bioclastic mudstone to grainstone, rarely containing minor amounts of shale (Fig. 3.22). The frequent vertical change of lithologies is characteristic for this depositional environment. The components are poorly sorted. Skeletal components comprise crinoids, lo-



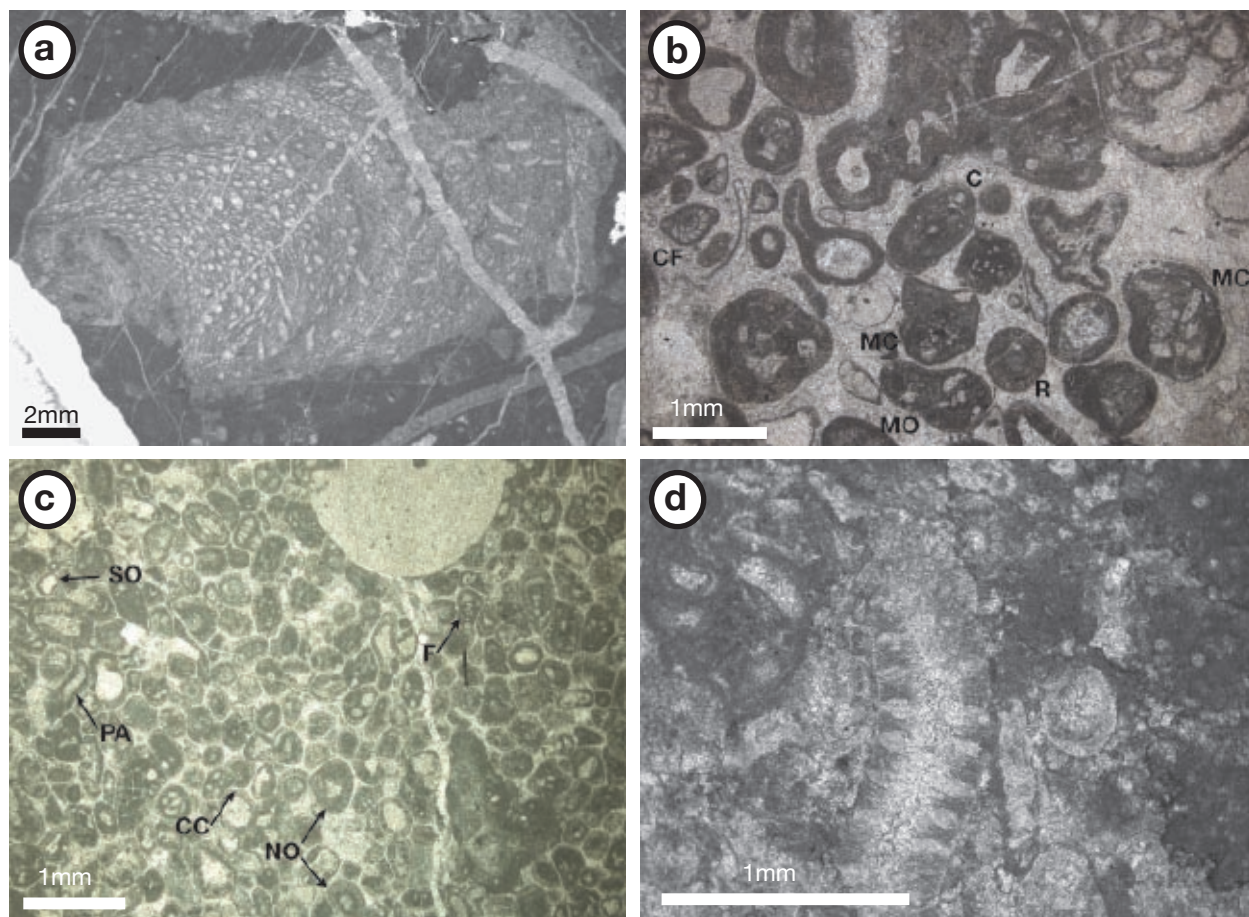


Fig. 3.22: Thin sections of platform margin deposits of the Valdeteja Fm. (a) Rugose coral (pers. com. E. Villa 2005) embedded in peloidal wackestone (sample BV 1-2, profile “Valdeteja”). (b) Ooid grainstone. Normal ooids are radial (R) and concentric (C), they reach sizes up to 2mm. Laminae are well defined. Multiple ooids (Ooidviellings) occur (MO). Nuclei are mostly bioclastic. Often, multiple components are present within the nuclei (MC). Coated foraminifers can be found (CF). The matrix consists of cement (sample LM101-2, profile “Las Majadas del Caserio”). (c) Bioclastic ooid-grainstone containing mostly normal ooids with several laminae (NO) and scarce superficial ooids with a single lamina (SO). The ooids are partly broken due to reworking. Pressure solution caused concavo-convex boundaries (CC). The nuclei are composed of skeletal components, mostly foraminifers (F). Phylloid algal components (PA) are encrusted with micrite (sample BV 16-1, profile “Valdeteja”). (d) Enlargement of the dasyclad green algae *Donezella*, which acted as sediment baffle within the mounds of the Valdeteja Fm. (sample LM77-2, profile “Las Majadas del Caserio”).

cally abundant solitary corals (*Cladochonus* Band at the base of the formation according to Winkler Prins 1968, 1971), abundant calcareous algae, calcareous sponges, foraminifers, bryozoa, extremely scarce brachiopods, and scarce gastropods (Fig. 3.22a). Intraclasts are common.

Interbeds of 10 - 20cm thickness occur, which pinch out after a few meters laterally (Fig. 3.21). They represent inter-mound facies.

An oolitic horizon was recognized at the type locality and laterally in the “Las Majadas del

Caserio” profile. Eichmüller (1981) traced this horizon laterally over 1.8km, correlating it between the type locality and the section south of Las Majadas del Caserio. Its thickness is 5.5m at the type section, 2.5m at Las Majadas del Caserio (see reference profile in the Appendix) whereas Eichmüller (1985) reported thicknesses of up to 100m. The bioclastic oolitic grainstone comprises predominantly normal ooids with several laminae; some superficial ooids with only one lamina can be found. The identifiable nuclei of the ooids are



Fig. 3.23: Spatial relationship between intra-platform basin and platform interior deposits (upper part of section “Las Majadas del Caserio”, Bodón Unit, see Appendix for profile).

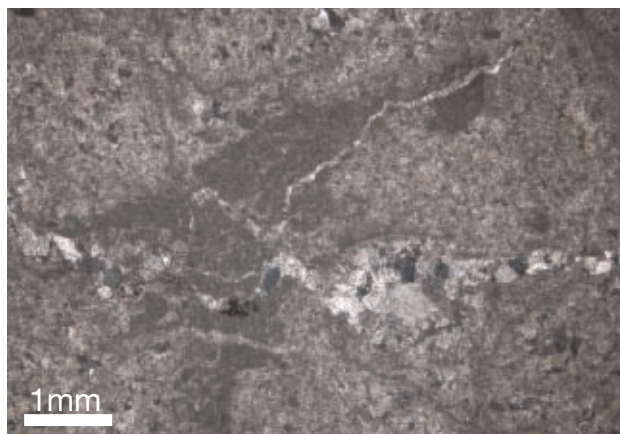


Fig. 3.24: Thin section of the platform interior environment. Peloidal wacke-/packstone with bioturbation (HV 26-2, Correcilla Unit; profile “Las Hoces de Vegacervera”). Unfortunately, sediments of this environment show extremely often recrystallization.



Fig. 3.25: Irregularly distributed, isolated bubble-like, mm-sized, spar-filled voids: Birds-eye structures within dismicrite (after Folk 1959) of the platform interior at the top of profile “Las Majadas del Caserio” (Bodón Unit; see Appendix for profile). Coin for scale.

of skeletal origin (Fig. 3.22b, c). Locally, the ooids are reworked and laminae are indented due to pressure solution (concavo-convex boundaries, Fig. 3.22c).

#### Platform Interior

The platform interior deposits are mostly massive, locally well-bedded, light gray limestones, which possess no large-scale geometries. These massive carbonates reach thicknesses of up to 203m (see Appendix, profile “Valdeteja”).



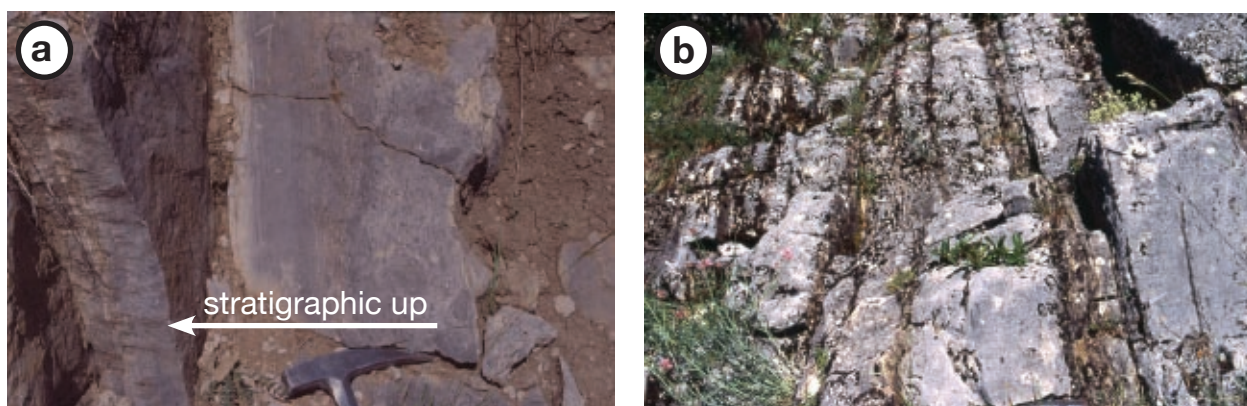


Fig. 3.26: Bedding within intra-platform basin deposits. (a) Single, turbiditic bed showing normal gradation in the lower and middle part and fine-grained, laminated top, (b) turbiditic succession, (c) irregular bedding (Las Majadas del Caserio, Bodón Unit).

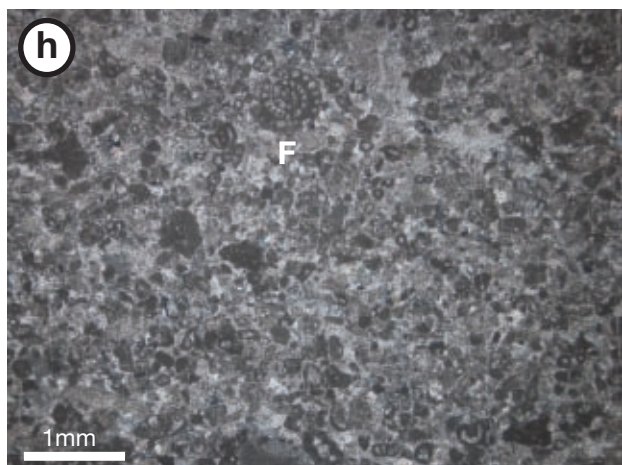
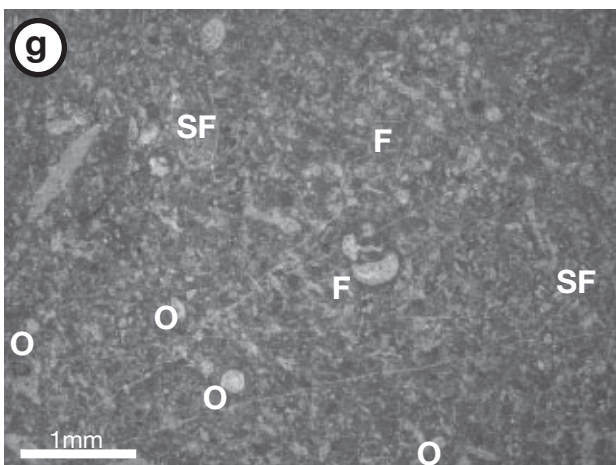
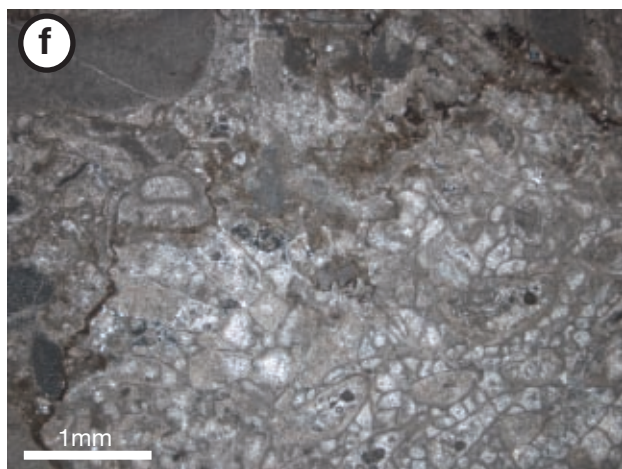
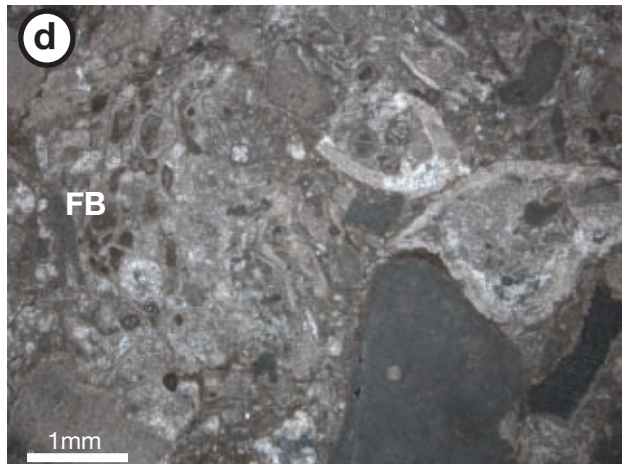
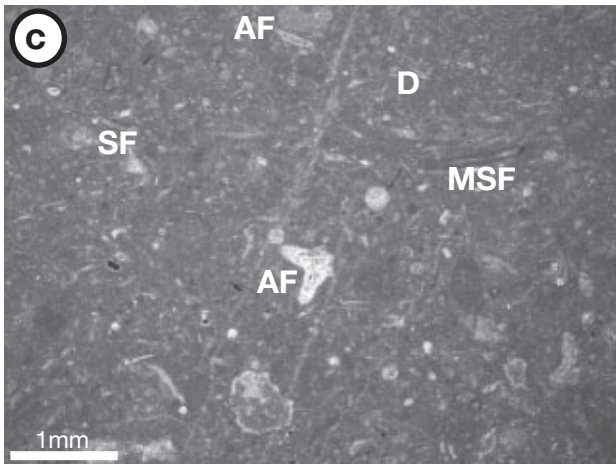
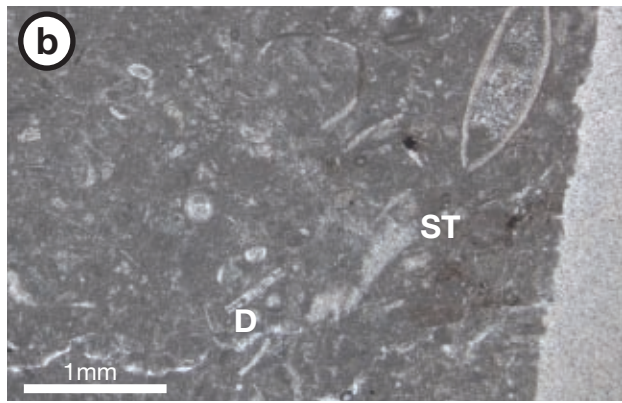
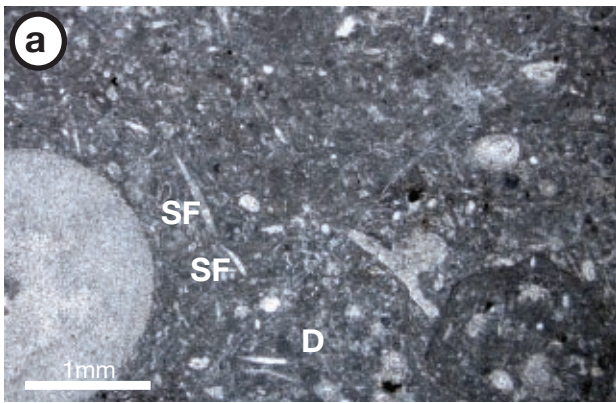
Laterally, platform interior environments are correlated between the “Valdeteja” and “Las Majadas del Caserio” profiles, decreasing to half the thickness from the west to the east. Eichmüller (1985) traced this facies up to 10km along strike. Lateral interfingering with intra-platform basinal deposits is shown in Figure 3.23. Vertical transition from and into platform margin deposits is always gradational, whereas the contact to overlying intra-platform basin deposits is sharp.

Platform morphology is determined by small mounds and morphological lows in-between. On this shallow marine to inter-tidal platform (Bosch 1969, Eichmüller 1985, Evers 1967), even little morphological differences are displayed by the change from mound facies to inter-mound facies. Eichmüller (1985, 1981) described the mounds in detail. Their thickness varies from 5 to 15m, sometimes up to 50m. The lateral extension is 50 - 100m. Eichmüller (1981) defines the mounds as “algal dismicrite mounds”. Biogenic composition of the mounds varies. The green alga *Donezella* is predominant, but red algae such as *Komia*, *Ungdarella* and *Petschoria* make up a varying amount of



the organisms. Generally, peloids are abundant (Fig. 3.24). Laterally, the mounds pass into well-layered, locally irregularly bedded, bioturbated, bioclastic packstones and grainstones. Furthermore, crinoids, brachiopods, foraminifers, and scarce solitary corals occur. Terrigenous components are generally absent. Birds-eye structures can be found (Fig. 3.25), Eichmüller (1981) reported stromatactis.





### Intra-Platform Basin

Thicknesses vary between 5m (“Valdeteja”) to 174m (“Las Majadas del Caserio”; Fig. 3.23). Generally, intra-platform basins make up an increasing portion of the succession toward the top of the Valdeteja Fm. Its lateral extent ranges from between 3 to 10km (Eichmüller 1985).

The basal contact to platform interior deposits is normally sharp whereas the top shows a gradual transition to the overlying platform interior facies (profiles “Valdeteja”, “Las Majadas del Caserio”).

The dark-gray, poorly sorted biogenic mudstone to grainstone is generally well-layered, but often irregularly bedded (Fig. 3.26c). The shale content increases toward the upper part of the Valdeteja Fm. Single beds are 5 - 50cm thick (Fig. 3.26a, b). Turbiditic beds show normal gradation and laminaton (Fig. 3.26a). Some beds pinch out over a distance of tens of meters.

Components occur chaotically within the thin sections. Fossil diversity is relatively high: spicula, shell fragments, foraminifers, crinoids, abundant brachiopods (0.5 - 3cm), bivalves (up to 4cm), scarce solitary corals, scarce gastropods, bryozoa, and ostracods (Fig. 3.27). Non-skeletal components comprise intraclasts, extraclasts, peloids, locally oncoids, coated and aggregated grains. Bioturbation is common. Pyrite bearings occur. Eichmüller (1985) reported slumping.

Distribution: The Valdeteja Fm. crops out in the Somiedo-Correcilla Unit, Sobia-Bodón Unit, northern part of the Central Asturian Coalfield and Picos de Europa (Fig. 2.4). In the northern Ponga Unit, it is time-equivalent with the lower part of the Cuera Formation.

### Forcoso Zone

Type locality: Reuther (1977) described the clastic turbidites north and east of the thinning out Valdeteja Fm. as “Forcoso Zone”. Lobato et al. (1984) did not distinguish between the sedimentation of the Forcoso Zone and the San Emiliano Fm. on the IGME Map 104 “Boñar”. Evers (1967) referred to the turbidites as “flysch facies in the Forcada Unit”. Figure 5.1a shows the distribution as described in this work. Outcrop conditions are mostly poor due to strong vegetation on top of the overly fine-grained siliciclastics (Fig. 3.28, 3.29). A good outcrop along a road-cut exists north of Llamazares, but due to large scale folding, only a succession of 93m in the lower part of the zone was recorded (see Appendix). Outcrop conditions east of Oville are reasonably good (Fig. 3.29), but the section is heavily deformed.

Age: Base: Lowermost Bashkirian (Kinderscoutian) (ammonites; Reuther 1977). Thrusting generally obscures the top. The age of the top is within the upper Bashkirian, locally reaching lower Moscovian (e.g. at “Las Majadas del Caserio”).

Fig. 3.27 (previous page): Thin sections of the intra-platform environment. (a) - (c) Biogenic pack-/grainstone of sample BV 36-1 (profile “Valdeteja”) with (a) fragile shell fragments (SF), crinoid stem (lower left), scarce foraminifers, *Donezella* (D), intraclast (lower right). Some of the bioclasts were substituted by calcite. (b) Stromatactis (ST), (c) shell fragment with micritic envelope (MSF), algal fragments (AF). (d) - (f) Crinoidal grainstone of sample BV13-2 (profile “Valdeteja”) containing (d) fenestrate bryozoa (FB), (e) fragment of dasyclad green algae (DGA), crinoidal fragments with indented borders (C), (f) colony of bryozoa. (g) Bioclastic packstone with abundant ostracods (O), shell fragments (SF), foraminifers (F) and some peloids (sample LM 52-2, profile “Las Majadas del Caserio”). (h) Peloidal grainstone with fusulinids (F) (sample BV 17-1, profile “Valdeteja”).





Fig. 3.28: The well-weathering fine-grained siliciclastics of the Forcoso Zone build morphological valleys, outcrops are rare (northern Curueño Valley, Forcada Unit).



Fig. 3.29: Dark-colored, silty shales of the Forcoso Zone (East of Oville, Bodón Unit).



Fig. 3.30: Typical fining-upward cycle within the basinal part of the Forcoso Zone (Llamazares, Forcada Unit).

**Contacts/discontinuities:** The base shows a gradual transition from the underlying Señas Mb. Locally, sediments of the Forcoso Zone onlap on platform carbonates of the Valdeteja Fm. (profiles “West of Oville”, “East of Montuerto”). The top is generally sheared off. **Lithofacies:** At the base, lithology varies with a distinct pattern. In the Gayo Unit, Bodón Unit, and in the eastern part of the Forcada Unit (see Appendix, profiles “Quarry Porma Lake”, “Mirador de Vegamián”), biogenic, (marly) wackestone to grainstone beds alternate with silty shale and siltstone. In the profile Mirador

de Vegamián, frequent graywacke beds occur as well. The highest portion of limestones was found east of Oville. Frankenfeld (1976) referred to this part of the formation as “Lower and Upper Marl Member” and measured a thickness of 100m. Lithology in the western part of the Forcada Unit shows hardly any calcareous content. Thin and rare beds (5 - 10cm) of detrital limestone (Fig. 3.31b, c) alternate with a turbiditic succession of silty shale, silt (1 - 10cm thick beds), and fine to medium grained, often normally graded, poorly sorted sandstones (6 - 20cm thick beds; Fig. 3.30),

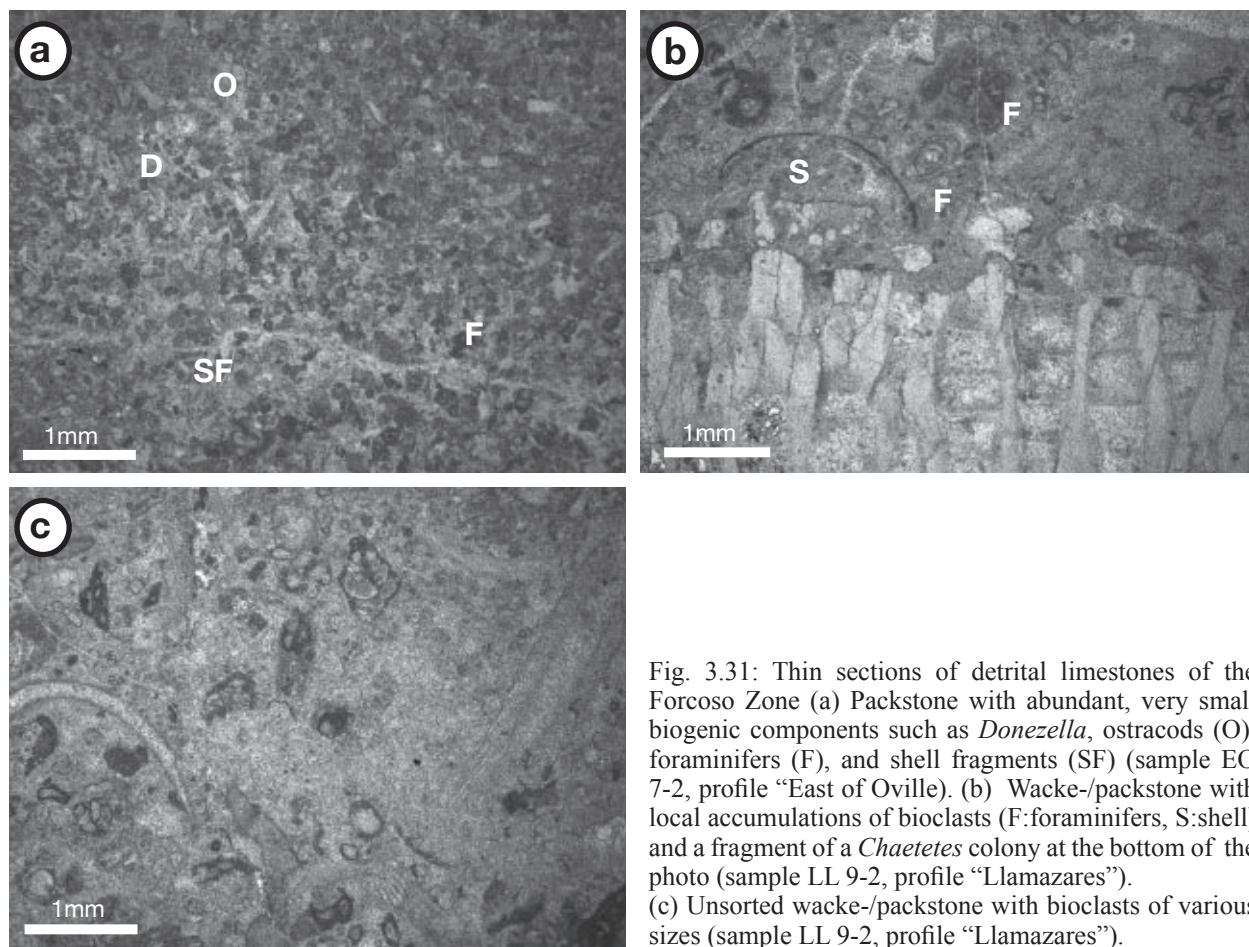


Fig. 3.31: Thin sections of detrital limestones of the Forcoso Zone (a) Packstone with abundant, very small biogenic components such as *Donezella*, ostracods (O), foraminifers (F), and shell fragments (SF) (sample EO 7-2, profile “East of Oville”). (b) Wacke-/packstone with local accumulations of bioclasts (F:foraminifers, S:shell) and a fragment of a *Chaetetes* colony at the bottom of the photo (sample LL 9-2, profile “Llamazares”). (c) Unsorted wacke-/packstone with bioclasts of various sizes (sample LL 9-2, profile “Llamazares”).

which locally show sole marks (see Appendix, profile “Llamazares”). North of Llamazares, a small number of calcareous lentils was found. Following the basal, locally calcareous part of the succession, an alternation of predominantly silty shale with fine to medium grained sandstone and siltstone follows. East of Oville, on top of what is known as the “Upper Marl Member”, Frankenfeld (1976) reported up to 1m thick beds of calcareous breccia, obviously platform-derived debris.

Thickness: Reuther (1977) estimated a thickness of 350m at Llamazares. Evers (1967) measured 400m at Tolibia de Arriba and proposed that the succession is thicker in the Bodón Unit than in the Forcada Unit. The highest measured thickness amounts to 280m (see Appendix, profile “East of Oville”). The real

thickness is obscured due to severe folding and the top being sheared off.

Depositional environment: The starved basin deposits of the Forcoso Zone surround the carbonate platform of the mostly time-equivalent Valdeteja Fm. from the north, east, and south. Following the Barcaliente Fm., the depositional environment changed abruptly. The underlying Señaras Mb. of the Barcaliente Fm. represents a shallow marine environment, whereas the following deposits show deep-water basinal facies (Eichmüller 1985). The depositional gradient between the platform and the basin was high, as shown by breccias and limestone beds, derived from the nearby Valdeteja platform as carbonate debris flows. The siliciclastic deposits represent turbidites, with an overall deepening trend. The source area for the siliciclastic sediments is unclear. The poor sorting



of the sandstones and the distinct character of the turbidites point to a proximal position of the source area. The Gayo Unit in the south-east has the lowest portion of sandstones, the amount of sandstones in the Bodón Unit near Oville is low. The highest amount can be found north of Llamazares. Measured current marks (Reuther 1977) indicate a NW-SE direction (120 - 135°). Therefore, the source area was probably located in the NW of the study area. Distribution: Forcada Unit and in the eastern part of the Bodón and Gayo Units (Fig. 5.1a).

### *San Emiliano Formation*

Type locality: North of the village San Emiliano de Luna (Brouwer & van Ginkel 1964), IGME Map 102 “Los Barrios de Luna” (Suárez Rodríguez et al. 1990)

Age: Lower Bashkirian to lower Moscovian (Boll 1985, Eichmüller 1985, Rácz 1966, and others: see Tab. A.1). Only at Gete (Gayo Unit), the base is determined with Namurian B (Eichmüller 1985, Fernández González 1990), whereas the onset within the Bodón Unit occurred within the Namurian C.

Contacts/discontinuities: The base is highly diachronous, interfingering with the Valdeteja Fm. (Fig. 3.16). Progressive onset of the San Emiliano Fm. from the west to the east is displayed in Fig. 3.33. The top is cut by thrusts.

Lithofacies: Various authors (e.g. Bowman 1982, Brouwer & van Ginkel 1964, Wagner & Bowman 1983) described the San Emiliano Fm. at its type locality. It is subdivided into three members (from base to top): (i) Pinos Mb.: shale dominated succession alternating with thin sandstone beds towards the top, (ii) La Majua Mb.: eight cycles of terrigenous

clastics, detrital and mound limestones, (iii) Candemuela Mb.: terrigenous clastic cycles with coals and isolated, thin limestones (Bowman 1982).

East of the type section, various authors used differing nomenclature (Fig. 3.33). Based on age determination of fusulinids by van Ginkel (1965) and strong lithological similarities to the type locality, Rácz (1966) and Evers (1967) correlated the Bernesga Valley succession with the type locality. Controversely, based on age determination of miospores, Moore et al. (1971) determined an extremely reduced thickness of the San Emiliano Fm. and called the time-equivalent deposits “Villanueva Beds”. On top of it, the “caliza masiva” is positioned (Julivert 1960, Sjerp 1967), which Bowman (1982) and Wagner & Bowman (1983) defined as the basal

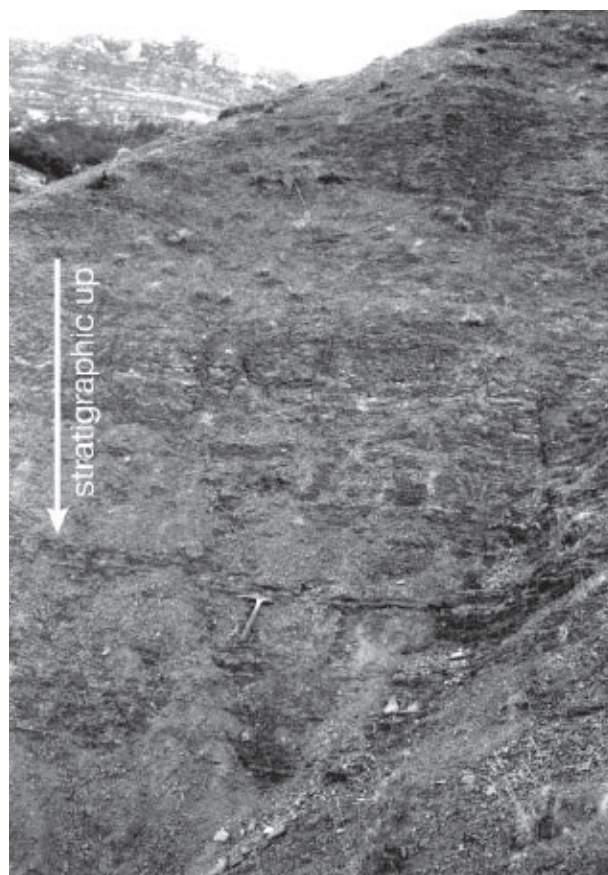


Fig. 3.32: Alternation of silty shale and siltstone within the San Emiliano Fm. (North of Valverde, Bodón Unit; see Appendix for profile).

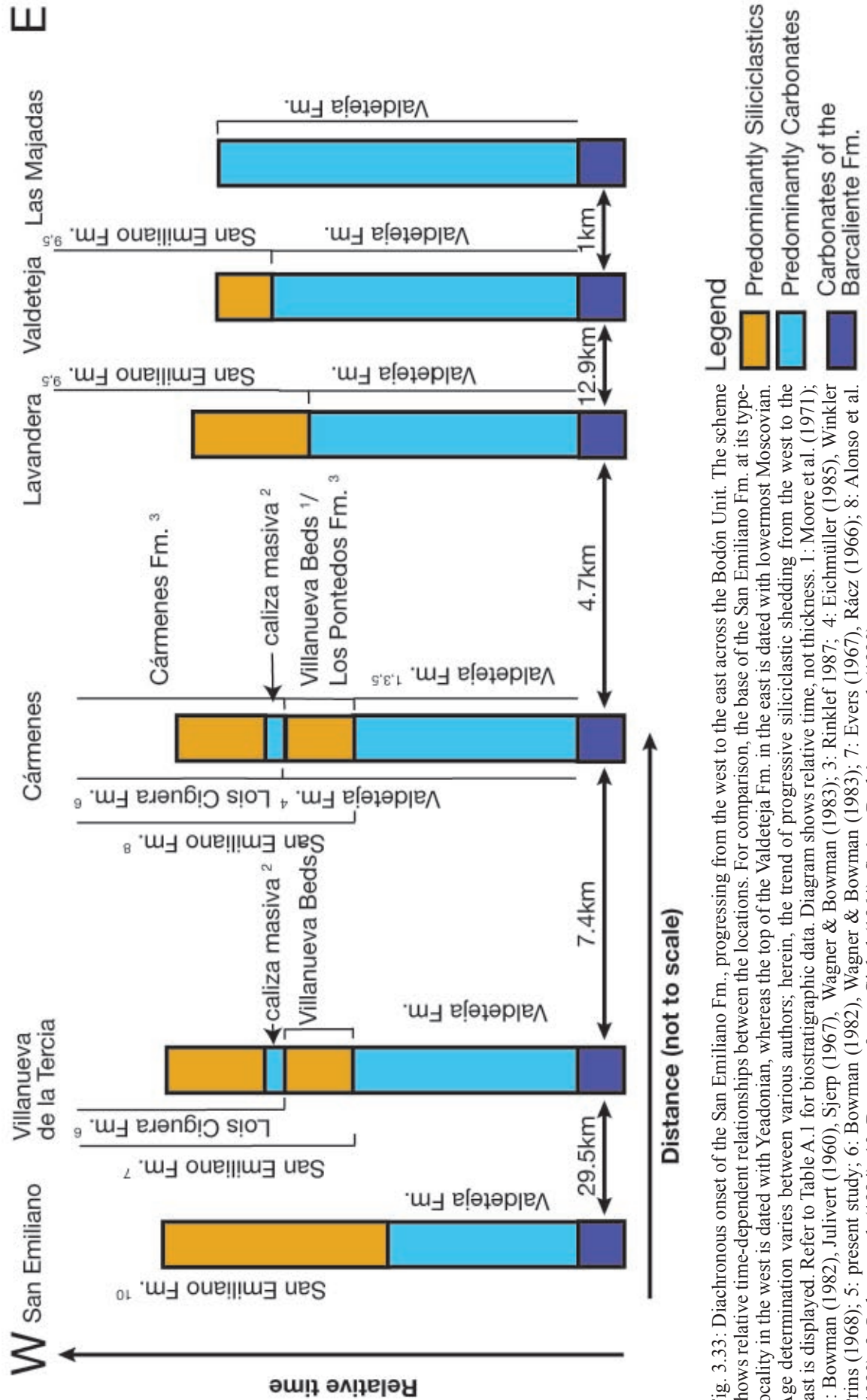


Fig. 3.33: Diachronous onset of the San Emiliano Fm., progressing from the west to the east across the Bodón Unit. The scheme shows relative time-dependent relationships between the locations. For comparison, the base of the San Emiliano Fm. at its type-locality in the west is dated with Yeadonian, whereas the top of the Valdeteja Fm. in the east is dated with lowermost Moscovian. Age determination varies between various authors; herein, the trend of progressive siliciclastic shedding from the west to the east is displayed. Refer to Table A.1 for biostratigraphic data. Diagram shows relative time, not thickness. 1: Moore et al. (1971); 2: Bowman (1982), Julivert (1960), Sjøerp (1967), Wagner & Bowman (1983); 3: Rinklef (1987; 4: Eichmüller (1985), Winkler Prins (1968); 5: present study; 6: Bowman (1982), Wagner & Bowman (1983); 7: Evers (1967), Rácz (1966); 8: Alonso et al. (1990); 9: Lobato et al. (1984); 10: Brouwer & van Ginkel (1964), Suárez Rodríguez et al. (1990).





Fig. 3.34: Characteristic succession of the San Emiliano Fm.: (a) Fine-grained siliciclastics at the base, being followed by alternating limestone units and siliciclastics. Viewed to the west from Coto Cabañas, along the Bodón Unit. (b) Close-up of a succession of alternating limestones - siliciclastics - limestones (West of Coto Cabañas, Bodón Unit).

part of the Lois-Ciguera Fm. (Brouwer & van Ginkel 1964). The “caliza masiva” is traced to the east until the Torío Valley. Winkler Prins (1968) and Eichmüller (1985) ascribed the terrigenously influenced part below the “caliza masiva” near Cármenes/Torío Valley to the Valdeteja Fm.

The varying use of these terms within the literature may locally be useful, but is also confusing. In this study, siliciclastic deposits, which follow and interfinger with the limestones of the Valdeteja Fm., and which may contain intervals of limestones, are called San Emiliano Fm. (Fig. 3.34).

The basal part of the formation within the

Bodón Unit is dominated by dark-gray, locally colored silty shale, which partly shows carbonate cementation. Scarce laminated siltstone and fine to medium grained sandstone beds can be interlayered (Fig. 3.32). Their thickness varies from 5cm to 2m. Cross-bedding and normal gradation occur. The base of a single bed is typically sharp. Channel deposits consist of sandstone and pinch out laterally. Locally, shale ellipsoids were found at the base of thick sandstone beds. Following the Valdeteja Fm., the ratio of siltstone-/sandstone to shale is initially higher than in the upper part of the basal siliciclastic succession but decreases toward the first limestone unit of



Fig. 3.35: Well-rounded chert nodules at the base of the San Emiliano Fm. (west of Nocado de Curueño, Gayo Unit).

the San Emiliano Fm. Following the first limestone unit, the overall sand content increases again (Appendix, profile “Lavandera”).

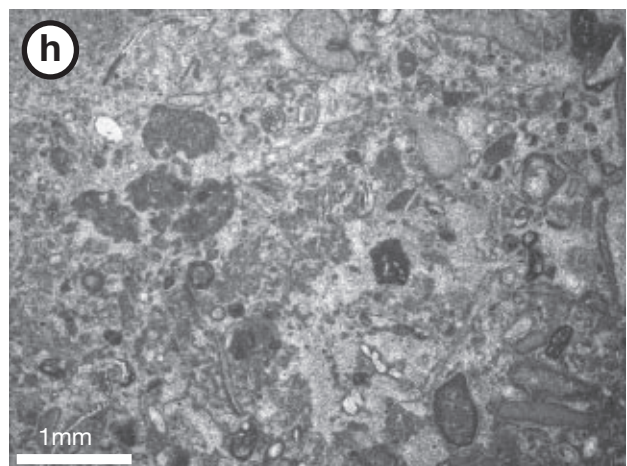
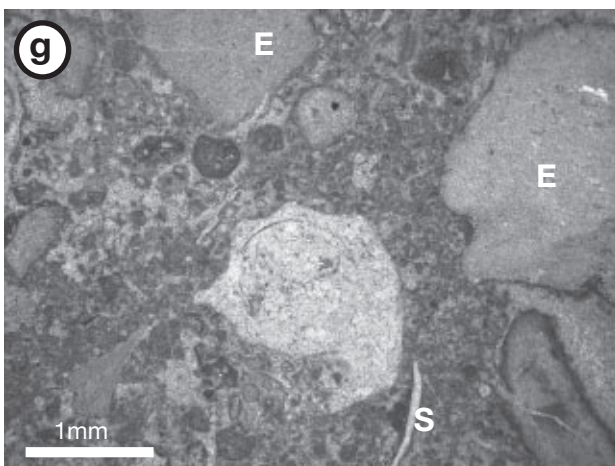
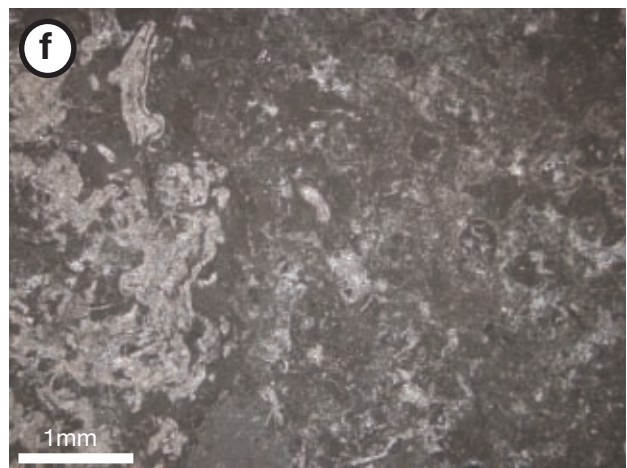
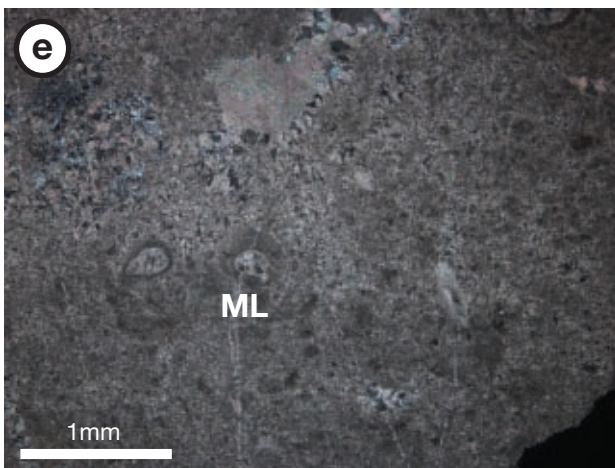
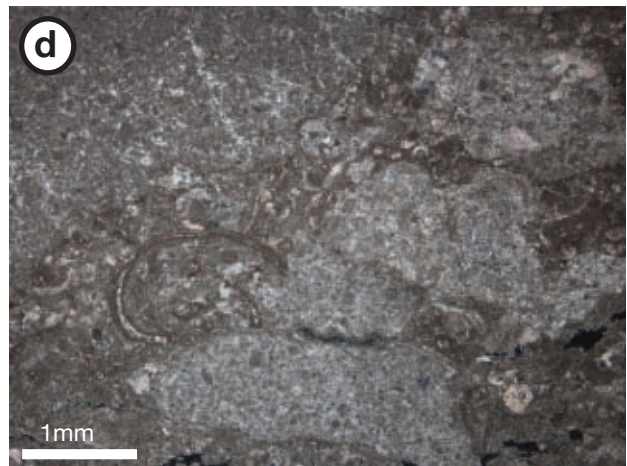
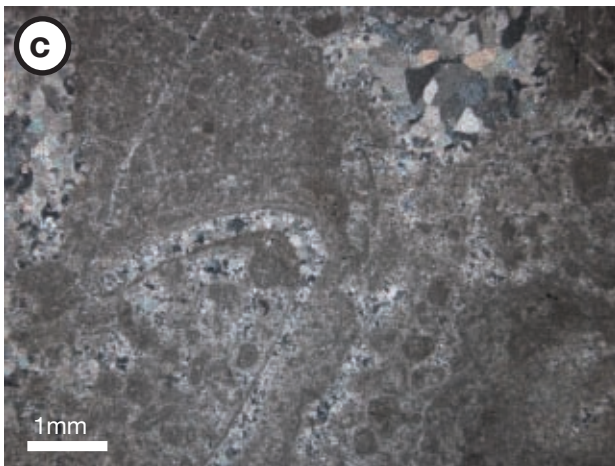
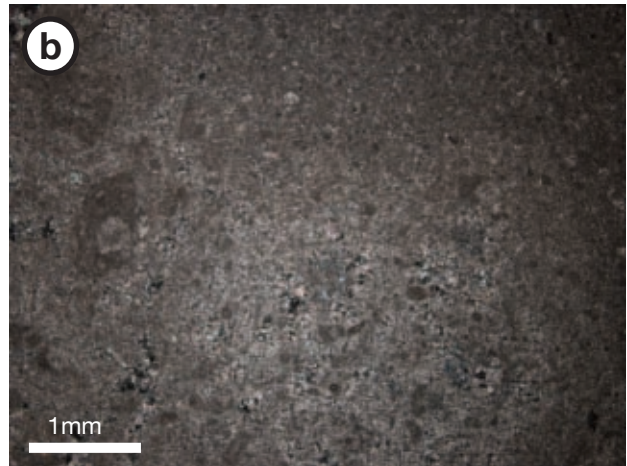
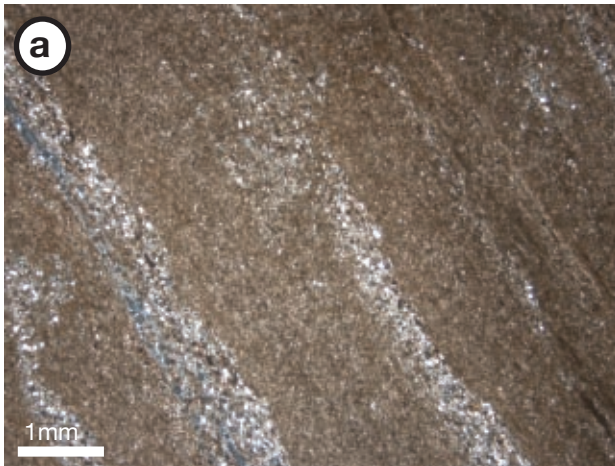
Mica is often present on bedding planes. Plant remains were found; Rinklef (1987) reported parts of calamites. Few detrital limestone beds appear in-between the shales. The dark-gray limestone beds are packstones to grainstones and contain skeletal fragments of crinoids, brachiopods, and bryozoa. The occurrence points to the proximity of the Valdeteja Fm. (north of Valverde and in the Gayo Unit).

Within the Gayo Unit, occasional well-rounded chert nodules, sized up to 15cm, were found in the basal shales west of Nocado de Curueño (Fig. 3.35). North of Gete, paraconglomerates

occur, as described by Evers (1967). In-between the siliciclastics, no in-situ limestone units exist but only single limestone beds consisting of platform-derived debris (Fig. 3.36g, h). The shale-to-sandstone ratio varies; the basal part in the eastern area (profile “Valdorria”) is predominantly made up of shale in the basal part, whereas the basal part in the western study area (profile “Gete”) shows a higher sandstone content and paraconglomerates. Manganese was found north of Gete.

In-situ limestone units are characteristic of the San Emiliano Fm. of the Bodón Unit (Fig. 3.34). In the study area, the limestone units reach thicknesses of up to 24m. In some cases, they are laterally traceable for a number of kilometers. Profile “North of Lavandera” (Appendix) contains three such units. The lowermost unit starts at its base with dark-gray, 5 - 15cm thick, well bedded mudstone to wackestone beds. They contain many small intraclasts, small, broken shell fragments, irregularly shaped, up to 2mm large extraclasts and many recrystallized components, which show poor sorting in a micritic matrix (Fig. 3.36b). Skeletal-microbial boundstones with a massive appearance follow on top. This mound facies is characterized by the existence of *Donetzites milleporoides* Dampel (Boll 1983, Bowman 1982, Dingle et al. 1993, Rácz 1966, Samankassou 2001). Calcsponges and agglutinated worm tubes occur frequently (Samankassou 2001). Subordinately, foraminifers, gastropods, and brachiopods are present. The matrix is typically peloidal-clotted (Fig. 3.36c, d, g, h). Laterally, the inter-mound facies consists of well bedded, skeletal wackestone/packstone. The dark-gray, 5 - 20 cm beds of wackestone/packstone at the top of the lime-







stone unit contain abundant fossils: crinoid stems, shell fragments, abundant brachiopods, and foraminifers. It occasionally contains quartz indicating the influence of a terrigenous depositional environment. The contact between the limestones and the siliciclastic deposits is sharp. Sand content increases towards the top of the formation. Thin fine-grained sandstone beds alternate with silty shale in a higher frequency than at the base of the formation. Thick, fine to medium grained sandstone beds occur as well. North of Valverde, abundant, up to 10cm thick calcareous concretions were found in a matrix of silty shale.

Thickness: 0 - 570m (North of Lavandera). At its type section, Barba & Fernández (1990) reported 1,250m - 1,800m, Bowman (1982, 1980) 2,000m. The top is generally cut by thrusts.

Depositional environment: Bowman (1982) and Wagner & Bowman (1983) described for the type section, that the sediments accumulated in a rapidly subsiding, highly mobile and apparently quite narrow basin, which was probably less than a hundred kilometers wide. However, the field area is positioned in a distal position to the approaching orogen and therefore shows lower subsidence and consequently lower accumulation.

At its type section, three phases were recognized within the San Emiliano Formation: (i) early basin initiation (Pinos Mb.), (ii) alter-

nating, mainly deltaic clastics and carbonates (La Majua Mb.), (iii) predominantly deltaic sedimentation (Candemuela Mb.; Wagner & Bowman 1983). This reflects an overall shallowing trend within the formation, which was found in the Bodón Unit of the study area as well.

In front of the rising hinterland, the facies belt progressively migrated towards the study area.

Bowman (1982) and Wagner & Bowman (1983) assumed that the source area was located in the south and west. Across the Bodón Unit, the onset of the San Emiliano Fm. subsequently progressed from the west to the east (Fig. 3.33).

The lowermost San Emiliano Fm. in the study area (profile "Lavandera") corresponds to the lower part of the La Majua Mb. in the type section (San Emiliano). The siliciclastic deposits in the study area represent a pro-delta environment. Generally, a higher paleo-bathymetry is interpreted for the deposition of the siliciclastics than for the limestone units (Dingle et al. 1993, Fernández González 1990, Samankassou 2001, pers.com. 2003). The distribution of sand-to-shale ratio indicates a progressively deepening environment. This part of the section is interpreted as representing the highest water depth within the preserved succession of the study area. Afterwards, an overall shallowing trend prevails. However,

Fig. 3.36 (previous page): Thin sections of the San Emiliano Fm. (a) Fine-laminated shale and siltstone, cut oblique to bedding (NL 10-2). (b) Mudstone at the base of the lowermost limestone unit (sample NL 13-2). (c) Pack-/wackestone with peloidal-clotted matrix (sample NL3-3). (d) Bioturbated pack-/wackestone with peloidal-clotted matrix. Bioclasts are poorly sorted (sample NL 1-3). (e) Packstone with asymmetrical growth of micritic laminae around a clast (sample NL 2-3). (f) Packstone with an accumulation of phylloid algae (?) on the left side of the photograph (sample NL 21-2). (g) Peloidal-clotted packstone with large fragments of echinoderms (E) and shells (S) (sample WG3-2). (h) Poorly sorted peloidal-clotted packstone with abundant and diverse bioclasts (sample WG3-2). Samples (a) - (f) were collected north of Lavandera (Bodón Unit), (b) - (f) within limestone units, (g) and (h) west of Gete (Gayo) within detrital beds.

water depth changes, which is represented by the alternation of carbonate and siliciclastic intervals.

The carbonate units were deposited on local high zones (Samankassou 2001), e.g. between channels (Dingle et al. 1993). Laterally, they pass into shale. Some limestone units are traceable for kilometers along the Bodón Unit.

Rácz (1966) and Winkler Prins (1968) proposed that the oldest limestone unit was generated in a shallow, quiet water environment in a calm, undisturbed sea. Samankassou (2001) described an initial phase of stabilization of ooid shoals, being followed by mound nucleation in a quiet environment below wave base. However, younger limestone units within the San Emiliano Fm. indicate a higher energy index (Rácz 1966).

The controlling factors for the changes of the depositional environment remain unclear to date. Samankassou (2001) proposed that sea-level fluctuations and siliciclastic input were the primary factors. The latter depends on the topographic relief of the hinterland as well as the amount of erosion. In turn, the amount of siliciclastic input influences regional sea-level fluctuations.

No limestone units are present in the Gayo Unit. On the one hand, the sedimentary record of the San Emiliano Fm. is very limited due to the thrust top. Maximum thickness is approximately 150m. The dark-gray to black colored shales, presence of manganese and the absence of in-situ carbonates indicate a deeper basin environment. The conglomerates and quartzitic pebbles point to a higher proximity to the hinterland than the Bodón Unit, which would be expected for the Gayo Unit due to its tectonic position closer to the hinterland.

Distribution: The San Emiliano Fm. occurs in the western part of the Bodón Unit and the Gayo Unit of the field area (Fig. 5.1a).

### 3.3 Post-Westphalian Deposits

In the studied area, no cover rocks younger than the Westphalian C are preserved. In the CZ, inter-montane coal basins of Stephanian age such as the Ciñera-Matallana Coal Basin, Sabero Coal Basin, and Central Coal Basin overlie the Westphalian deposits with an angular unconformity. The preserved sedimentary thicknesses extend from 1,500m to 3,000m (Colmenero et al. 1996, Heward 1978). According to Agueda et al. (1991), the today-isolated Stephanian coal basins were interconnected, forming a single foreland basin during the Stephanian, which was deformed in front of the approaching orogen. Earlier authors, e.g. Evers (1967), proposed single basins without any connection to each other.

In the area of the Southern Cantabrian Basin, no indication of Permian deposits has been found. Due to an exhumation phase, they may be completely eroded.

To the south, the Cretaceous and Tertiary basin fill of the Duero Basin amounts to 1,100m thickness (Barba & Fernández 1991, Evers 1967). Hiati are reported and included in Tables A.2-A.4.

However, it is unclear whether or not these sediments covered the study area at all and if so, up to which thickness. Frings et al. (2004) estimated approximately 1,000m of sedimentary cover on top of the Stephanian Ciñera-Matallana Coal Basin based on vitrinite reflectance measurements and thermal modeling. The authors attributed this to overlying Stephanian to Permian rocks, which had been eroded subsequently. Bastida et al.

(1999) determined anchizonal conditions in the lower part of the Somiedo Unit by conodont color alteration index (CAI) and illite crystallinity (IC) measurements. CAI data for pre-Stephanian Carboniferous rocks of the Somiedo Unit indicate a maximum temperature of 50-60°C, which corresponds to an overburden of approximately 1,700m (assuming a geothermal gradient of 35°C/km; Raven & Van der Pluijm 1986). Slightly higher values were reported for siliciclastic rocks in the La Sobia Unit (Bastida et al. 1999).

Unpublished CAI measurements in the upper part of the San Emiliano Fm. north of Villamanin (Bernesga Valley) gave values of 1.5 to 2 (pers.com. Mulhall 2003). This corresponds to an overburden of 1,400 - 2,100m (Raven & Van der Pluijm 1986), assuming an average thermal gradient of 35°/km as did García López et al. (1997) in the northern CZ. Raven & Van der Pluijm (1986) determined a mean CAI value of 1.6 (1,700m burial depth) for the Famennian-Viséan succession in the Bodón and Forcada Units of the study area that points to an even smaller amount of sedimentary rocks on top of the youngest preserved deposits.

Marschik (1992) measured Kübler indices in the area between the Curueño and Bernesga Valley. Following his interpretation, the uniform distribution pattern of values implied that the tectonic stacking of units did not significantly influence the thermal evolution in the area. Across the Bodón Unit, measured values indicated a higher load between Cármenes and Valverde (values range between  $0.38^{\circ}\Delta 2\Theta$  to  $0.5^{\circ}\Delta 2\Theta$ , mean:  $0.44^{\circ}\Delta 2\Theta$ ; within the San Emiliano Fm.) than at Valdeteja, where the lowermost part of the San Emiliano Fm. was measured with values of  $0.62^{\circ}\Delta 2\Theta$  and

$0.61^{\circ}\Delta 2\Theta$ .

Additionally, comparing values within the Gayo Unit of the Torío and Curueño Rivers with the pattern of the Bodón Unit, values point to a slightly lower load within the Gayo Unit (Gete/San Emiliano Fm.:  $0.51^{\circ}\Delta 2\Theta$ ; Montuerto/Forcoso Zone:  $0.53^{\circ}\Delta 2\Theta$  and  $0.50^{\circ}\Delta 2\Theta$ ) than in the western Bodón Unit. This results in a sedimentary load with a wedge-shaped geometry, having a maximum thickness in the western Bodón Unit and a minimum thickness at Valdeteja (eastern Bodón Unit). Values cited were not measured in the proximity of major fault systems. Kisch (1980) defined  $0.38^{\circ}\Delta 2\Theta$  as the boundary between the diagenetic and anchizone. A correlation of IC data with mineral facies by Warr (1996) and Frey et al. (1991) assigned a temperature of 175°C and pressure of 0.5 - 4.5kbar to this boundary. Calculation of the thickness of the sedimentary load results in a thickness of 5,000m of cover rocks, which is significantly higher than CAI values indicated (see above).

It is unclear whether the wedge-shaped cover may be assigned to the missing sheared-off parts of the San Emiliano Fm. or to post-Westphalian sedimentation.





## CHAPTER 4: INTEGRATED TECTONO-SEDIMENTARY AND SEQUENCE STRATIGRAPHIC MODEL FOR THE SERPUKHOVIAN TO MOSCOVIAN

### 4.1 Tectono-Sedimentary Model

Essentially, two models exist to explain the tectono-sedimentary setting of the late Namurian and Westphalian.

#### 4.1.1 Fault-bounded Basin

Evers (1967) introduced the model of a syn-orogenic, asymmetric marginal basin, bounded by faults. This theory was further employed and refined by various authors to explain the Carboniferous sedimentary setting.

Arthaud & Matte (1977) proposed that after an initial Variscan phase, which included subduction, a dextral mega-shear zone developed between the American-European Plate and the African Plate. The authors related the deposition of the Upper Carboniferous deposits within the Cantabrian Zone to smaller regions within the strike-slip setting, which are dominated by conjugate wrench faults, thrusts and folds.

Based on the work by Arthaud & Matte (1977), Heward & Reading (1980) related the differentiation of the post-Namurian B depositional environments of the Cantabrian area to a system of normal faults. The assumed tectonic style comprised a general transpressive regime, and combined vertical and horizontal movements, which formed rapidly subsiding small basins. However, they stated that those normal faults were hardly to prove within the basin fill due to later movements. According to Eichmüller (1985), no proof of major synsedimentary normal faults was found.

Heward & Reading (1980) proposed that the Namurian and Westphalian basin fill was deposited in several small, fault-bounded basins that were not interconnected and partly of differing age. However, according to Fernández González (1990), these conclusions were based on incorrect biostratigraphic data. The author concluded that the Namurian and Westphalian deposits belonged to a common sedimentary basin, which was subdivided into several smaller segments.

Spatially stationary, not migrating subsidence curves would be expected in case of a fault-bounded sedimentary basin. However, the following discussion and the results of this study show the existent migration pattern within the Cantabrian Basin.

#### 4.1.2 Orogenic Foreland Basin

The history and theoretical considerations regarding foreland basins are outlined in Chapter 1.1.2.

The following factors support the existence of a foreland basin:

The presence of a fold-and-thrust belt in the hinterland of the assumed foredeep is proven by seismic investigations (Pérez-Estaún et al. 1995, 1994, Pulgar et al. 1996).

The sediment source of the Bashkirian and Moscovian sediments of the Southern CZ was located within a rising orogen in the south and west (according to today's coordinates; e.g. Bowman 1983).

High accumulation of Serpukhovian to Moscovian sedimentary deposits in the vicinity of the orogen and decreasing sedimentary thicknesses in distal positions created a sedimentary basin with a wedge-shaped cross-section.

Lateral and vertical development of the sedimentary succession from the Serpukhovian to Moscovian reflects the migration of the depocenter in front of the advancing orogen (see Chapter 8.2).

Progressive segmentation of the depositional environment during the Bashkirian is indicated by vertical facies changes from the regionally distributed Barcaliente Fm. to the laterally co-existing San Emiliano Fm., Valdeteja Fm. and Forcoso Zone.

Agueda et al. (1991) published convex-up subsidence profiles for the Westphalian A to D at Teverga (Sobia Unit) and Quiros (Aramo Unit) within the western part of the Cantabrian Zone. The authors proved the progressive migration of the depocenter in front of the approaching orogen from the west to the east. Additionally, deposits indicate an overall shallowing upward trend within the Namurian and Westphalian deposits. The age of the coal-bearing sequences was proven to be younger in the east than in the west.

Successive filling of the basin from the Serpukhovian to Stephanian corresponds to the progressive development from an initial underfilled basin state to filled foreland basin state.

Hence, the foreland basin model is adopted

within this study. Serpukhovian to Moscovian sediments within the field area overly belong to the distal area within the foreland basin system. During the early foreland basin stage, the Barcaliente Fm. mostly was deposited uniformly. The deep-water deposits of the Olleros Fm. occurred in the proximity of the orogen. Later siliciclastic deposits show an overall shallowing trend. The initiation of the Valdeteja platform, which is in an initially sub-parallel position to the orogenic front, and the adjacent basin deposits of the cratonward positioned Forcoso Zone show the differentiation of the foreland basin system. The shallow-water carbonate platform of the Valdeteja Fm. is interpreted to reflect the position of the forebulge, whereas the lateral basin deposits of the Forcoso Zone represent the back-bulge region between the forebulge and the craton. The subsidence pattern matches this interpretation and will be discussed in Chapter 6. Generally, deposits of ancient forebulge zones are not preserved within the sedimentary record due to erosion. However, if the foredeep zone is not entirely filled, carbonate platforms may evolve in the forebulge depozone and can connect the foredeep and the back-bulge depozone to each other (Dorobek 1995, Pigram et al. 1989, Wuellner et al. 1986). Moreover, axial transport of terrigenous detritus parallel to the orogen can reduce the amount of detrital input on the carbonate platform.

The width of each depozone within the foreland basin of the Southern CZ can only be approximated since only single slices are exposed within the tectonic units. Based on structural balancing carried out within this study (see Chapter 5), the width of the carbonate platform was 19km from the Bodón Unit to the Correcilla Unit. However, this is based on



minimum shortening rates. Therefore, the real width of the platform was higher. Additionally, the time-equivalent deposits of the tectonic units south of the Correcilla Unit are not preserved. Only within the Pedroso and the Alba Synclines further to the south, deposits of the Barcaliente and Olleros Fm. are cropping out. According to Veselovsky (2004), the minimum distance between the Correcilla Unit and the Pedroso Syncline amounts to 31km. The distance to the orogen is unknown, and so is the extension of the Forcoso Zone.

Although the distances will be considerably higher considering internal deformation during structural balancing, distances between the depozones within the foreland basin system are low in comparison with values as cited in literature (see Chapter 1.1.2), yet still within reasonable range. Structural elements influencing the sedimentary depositional setting of the field area cannot be excluded. However, a blind thrust being responsible for the uplift of the area covered by the Valdeteja platform as suggested by Fernández González (1990) is rejected. The wide extension of the platform would require a prominent thrust. The early Bashkirian age of this thrust would predate all so-far known thrust movements and represent an early out-of-sequence thrust within an otherwise forward-breaking in-sequence thrust system, which is highly improbable.

## 4.2 Bashkirian and Moscovian Sequence Stratigraphy

Correlation along the transects was accomplished using biostratigraphic data (Tab. A.1), facies interpretation (Chapter 3.2) and sequence stratigraphy (see below).

In this chapter, the Serpukhovian to Moscovian

development of the field area will be explained in chronological order based on sequences and systems tracts as a means to describe the depositional system.

Large-scale geometries enhance the understanding of spatial and genetic relationships within the succession. They are present in aerial photographs of the area (Fig. 4.1 & 4.2). Most geometries exist at the platform margin (Valdeteja Fm.) to basin (Forcoso Zone) transition.

The discussion focuses on third-order sequences, systems tracts, and bounding surfaces if recognizable. T-R sequences of deposits older than described here were evaluated by Veselovsky (2004). Parasequences (i.e. fourth-order cycles) and parasequence sets are not addressed in the context of this study.

Sequences were named by the name of the referring stage according to international standards. For example, the first sequence during the Bashkirian is named Bas 1.

Further definitions of the applied sequence stratigraphy are outlined in Chapter 1.2.

### *Pre-Bas 1 (Barcaliente Fm.)*

During the preceding Serpukhovian, shedding of the basinwide distributed carbonatic turbidites of the lower part of the Barcaliente Fm. took place during sea-level highstand. An overall shallowing upward trend is recognizable. The exact position of the sequence boundary at the top of the highstand systems tract could not be determined.

### *Bas 1 (ca. 321Ma - 317.5Ma, Barcaliente Fm. - Valdeteja Fm.)*

The upper part of the Barcaliente Fm. exhibits a shallowing upward trend (Chapter 3.2),

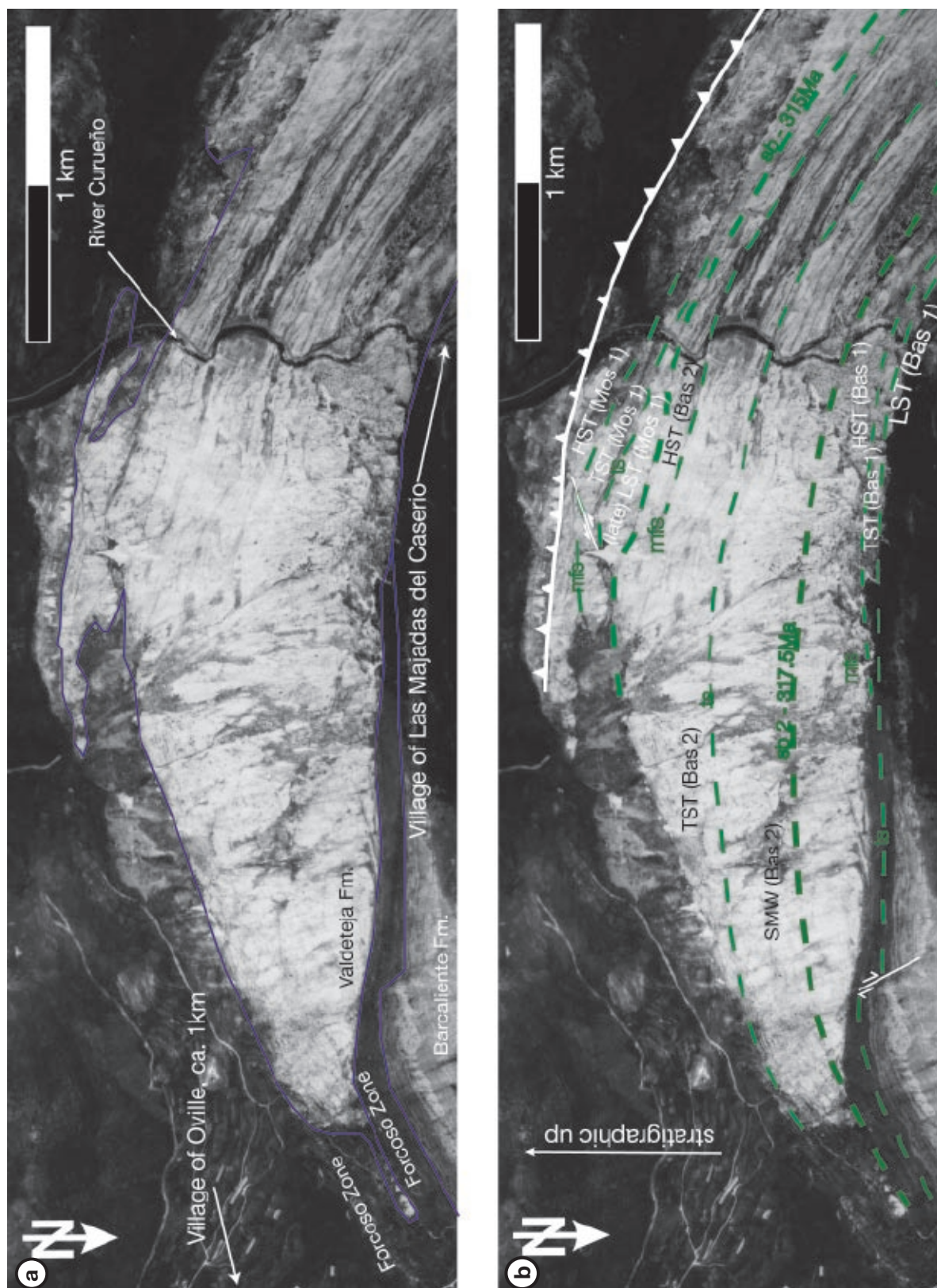


Fig. 4.1: Aerial photograph of the eastern Bodón Unit. Due to subvertical dip of the bedding planes, the depositional geometry is exposed in a cross-sectional view on the air photograph. (a) Blue lines schematically follow formation boundaries. At the top of the Valdeteja Fm., scree slopes obscure the transition from the platform to the onlapping basin deposits of the Forcoso Zone. (b) Superimposed sequence stratigraphic interpretation. The north-south directed cut of the meandering River Curueño through the Valdeteja Fm. corresponds to the stratigraphic profile “Las Majadas del Caserio” (see Appendix). The interfingering of the massive carbonates of the Valdeteja Fm. (whitish colors) with basinal deposits of the Forcoso Zone in the left part of the image is enlarged in Figure 3.12. LST: lowstand systems tract, SMW: shelf-margin wedge, TST: transgressive systems tract, HST: highstand systems tract, ts: transgressive surface, mfs: maximum flooding surface, sb: sequence boundary, sb 2: type 2 sequence boundary. White lines: faults/thrust.



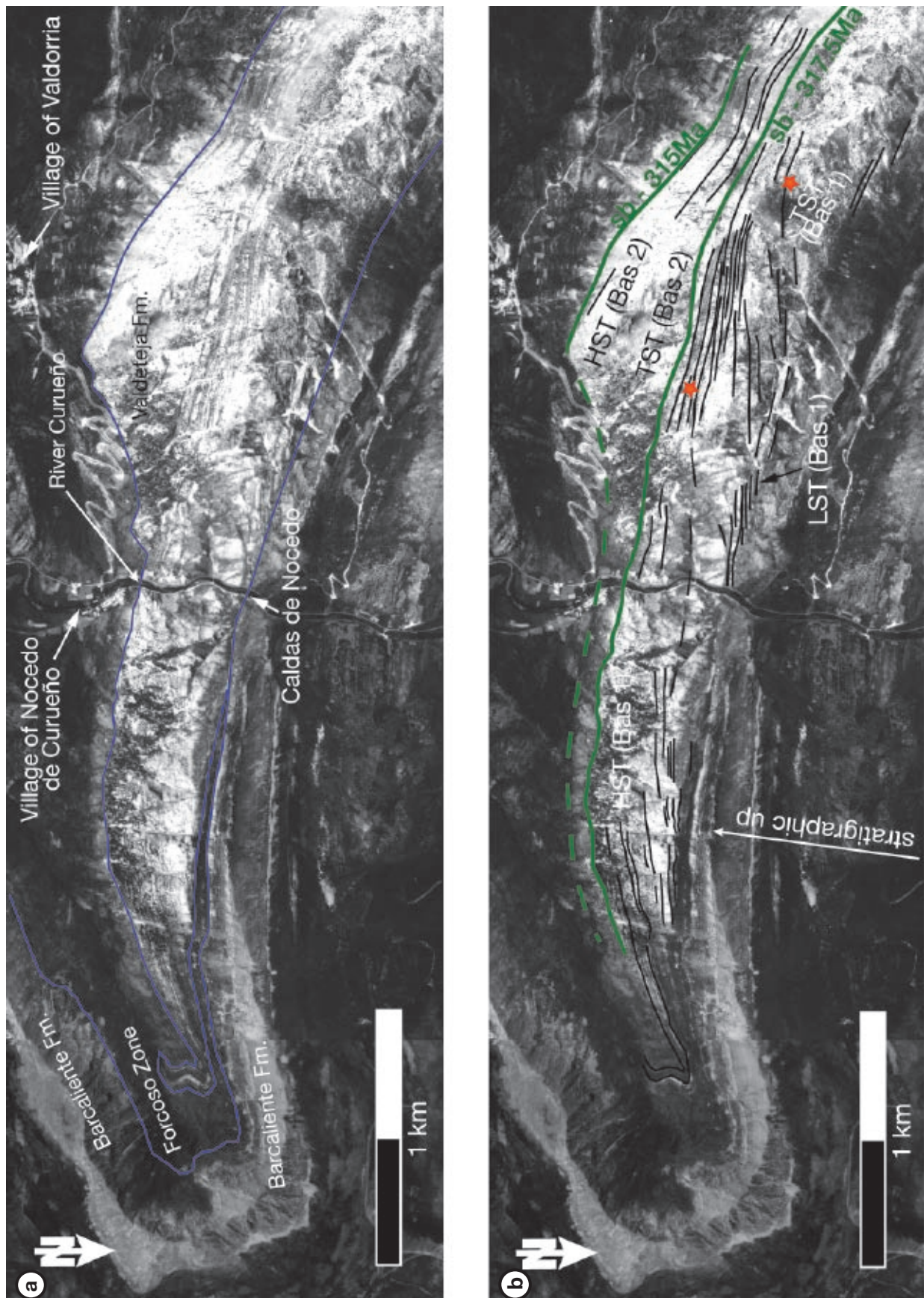
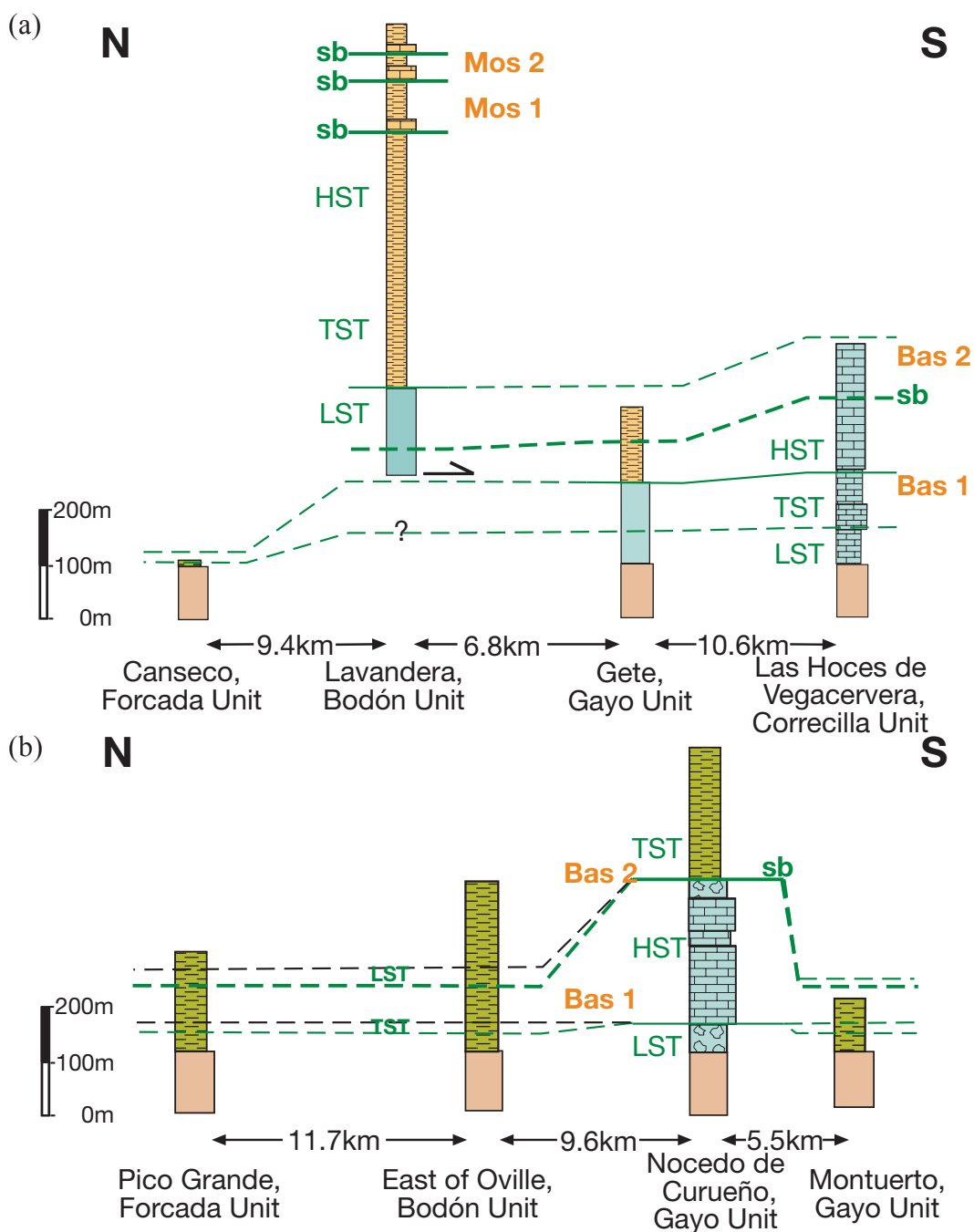


Fig. 4.2: Aerial photograph of the eastern Gayo Unit. Bedding planes have subvertical orientation. (a) Blue lines schematically follow formation boundaries. On the left side of the image, the curvature of the blue line outlines the Montuerto Syncline. (b) Superimposed sequence stratigraphic interpretation. Green lines represent sequence boundaries. Black lines mark stratal patterns within the Valdeteja Fm. The red star to the right denotes the position of offlap break 1, the star to the left indicates the position of offlap break 2. Abbreviations as in Fig. 4.1.



**Formations**

San Emiliano Fm.

Forcoso Zone

Valdeteja Fm.

Barcaliente Fm.

?

No preserved record

**Bas 1,**  
**Mos 1**
**sb**
**sb2**
**HST**
**TST**
**LST**
**Depositional Environment**

Limestone units within the San Emiliano Fm.

Basin (Forcoso Fm.)/prodelta (San Emiliano Fm.)

Slope

Platform margin

Platform interior

Intra-platform basin



Fig. 4.3: Correlation of measured and interpreted stratigraphic profiles along (a) Torio Transect, (b) Curueño Transect (both previous page), and (c) Bodón Transect (see Fig. 5.1 for position of transects within the study area). Boxes without signature represent measured sections where no stratigraphic column was recorded either due to poor outcrop conditions or dolomitization. The Barcaliente Fm. was also not further subdivided. For detailed profiles, see Appendix. For legend, see Fig. 4.3a, b, previous page.

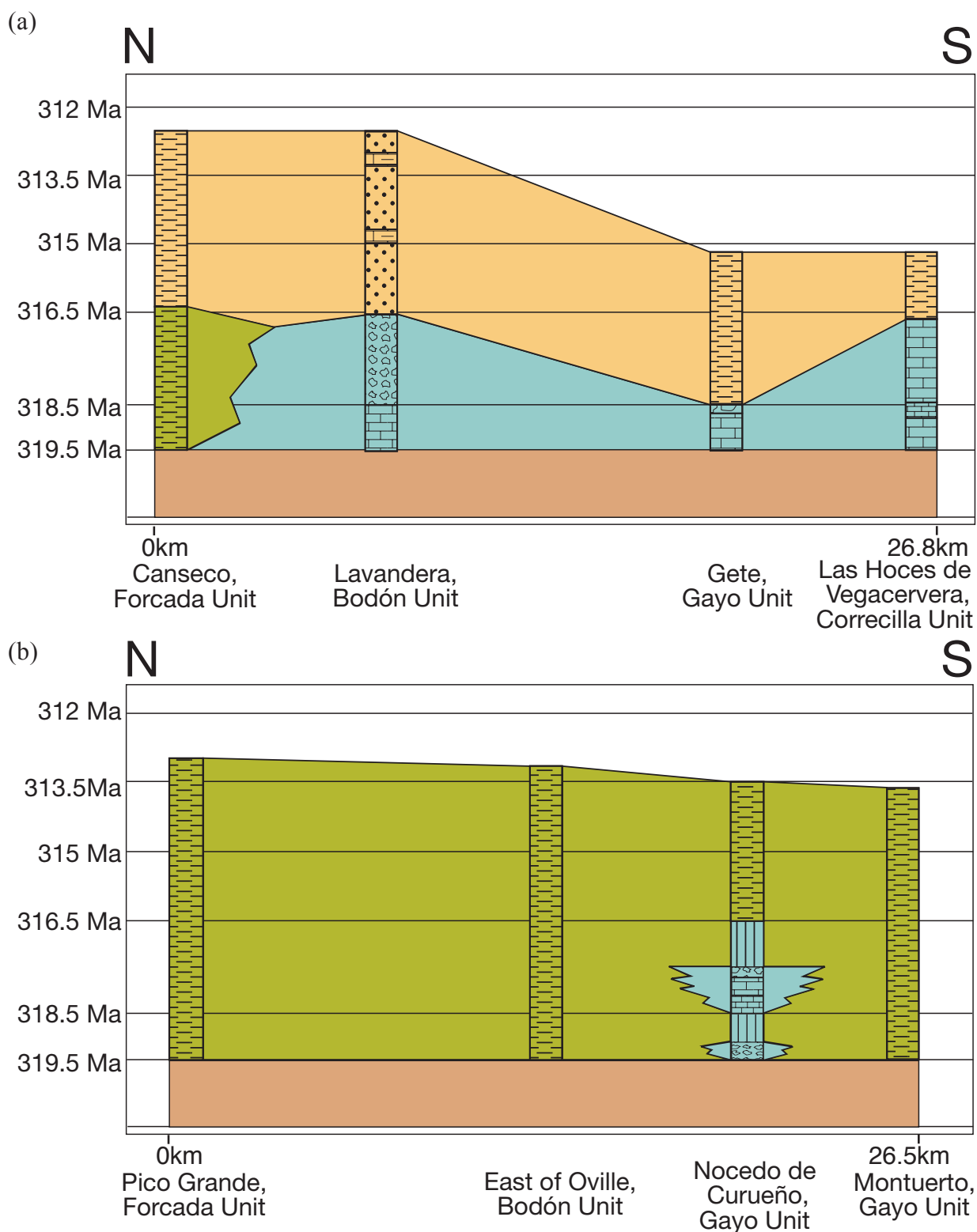


Fig. 4.4: Time-distance plots (Wheeler plots) of (a) Torío Transect, (b) Curueño Transect, (c) Bodón Transect (next page). Stratigraphic columns shown are based on recorded profiles as attached in the appendix. The position of profiles is shown in Fig. A.1. Lateral correlation was done using the recorded profiles, biostratigraphic data and sequence stratigraphic analysis. Lateral relationships are shown schematically only. The termination of the San Emiliano Fm. and the Forcoso Zone, respectively, is visualized as interpreted for reverse basin modeling (Chapter 6). The stratigraphic record as available in the field is shown in Figure. 4.3. Colors indicate different formations. Due to scarce biostratigraphic data, the Barcaliente Fm. was not further differentiated. For legend, please refer to the following page.



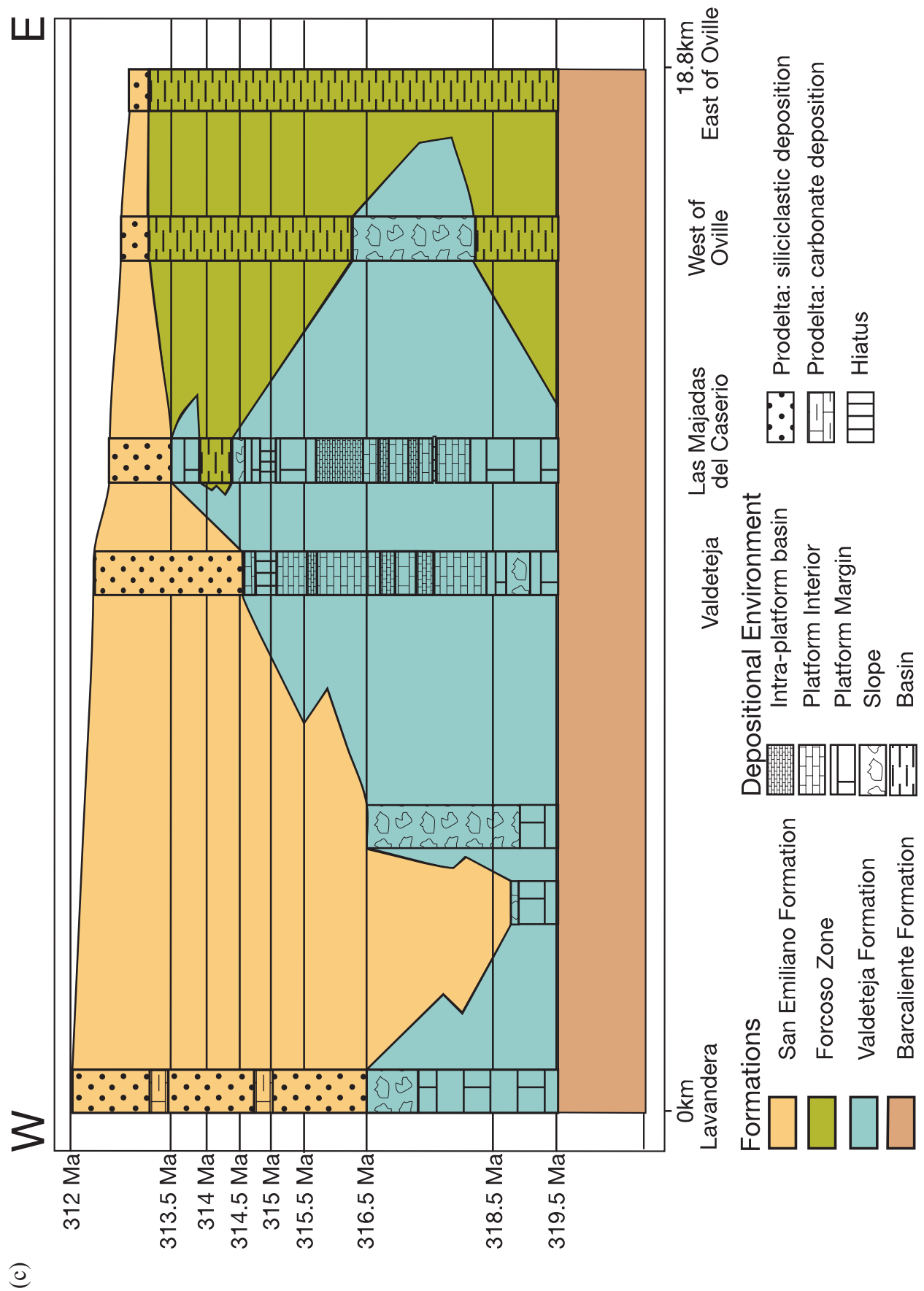




Fig. 4.5: Disconformity in the uppermost part of the Señaras Mb. (Barcaliente Fm.) at the roadcut east of Valdeteja (Bodón Unit). Whitish weathering rocks in the upper left and background belong to the succeeding Valdeteja Fm.

which is contemporaneous with a strong drop of the eustatic sea-level (Fig. 6.2). Deposits of the Señaras Mb. belong to the shallow marine to intertidal realm. These are interpreted to belong to the LST of Bas 1. Although the Barcaliente Fm. has a regional extension up to the Asturian coast, the lowstand deposits of the Porma Breccia and Señaras Mb. occur in the Southern Cantabrian Basin only. Close to the top of the Señaras Mb. in the Arroyo de Barcaliente, an erosional unconformity exists (Fig. 4.5). It could not be found laterally in the referring level, neither in distal nor in proximal position. Therefore, it is considered to be of local importance.

During deposition of the Señaras Mb., a differentiation of the paleobathymetry occurs within the field area (Chapter 3.2); in the eastern area, deposits reflect higher water depth than in the western area (Tab. A.2 & A.4). The shallow water-depth of the Señaras Mb. enables the nucleation of the Valdeteja platform carbonates on top of a local high in most parts of the study area (Fig. 5.1). This high existed at least since deposition of the Vegamián Fm. (see Chapter 3.2). At the type locality of the Valdeteja Fm., deposits start with small *Donezella*-mounds in a platform margin environment reaching a thickness of 47m (Fig. 4.3c). Deposits of the LST in the eastern Gayo Unit similarly possess a very small thickness (Fig. 4.2). The shingles of the lowstand fan are visible in the aerial photographs and indicate a slightly progradational pattern (Fig. 4.1 & 4.2).

Contemporaneously to platform initiation in the western part of the field area, high subsidence rates in the east created an initially shallow basin. East of Oville (see Appendix for profile), basin deposits consist at the base of fine-grained siliciclastics and beds of carbonate detritus and breccia, which derived from the nearby platform during lowstand deposition. Frankenfeld (1985) traced the basinal carbonate horizons from Oville to Las Majadas del Caserio.

At the type section of the Valdeteja Fm., slope deposits of the following TST succeed the platform margin setting of the prior LST, indicating deepening of the environment. The slope deposits show several breaks, which may represent parasequence boundaries within the retrogradational stacking pattern of the TST. The facies belt shifts toward the platform,

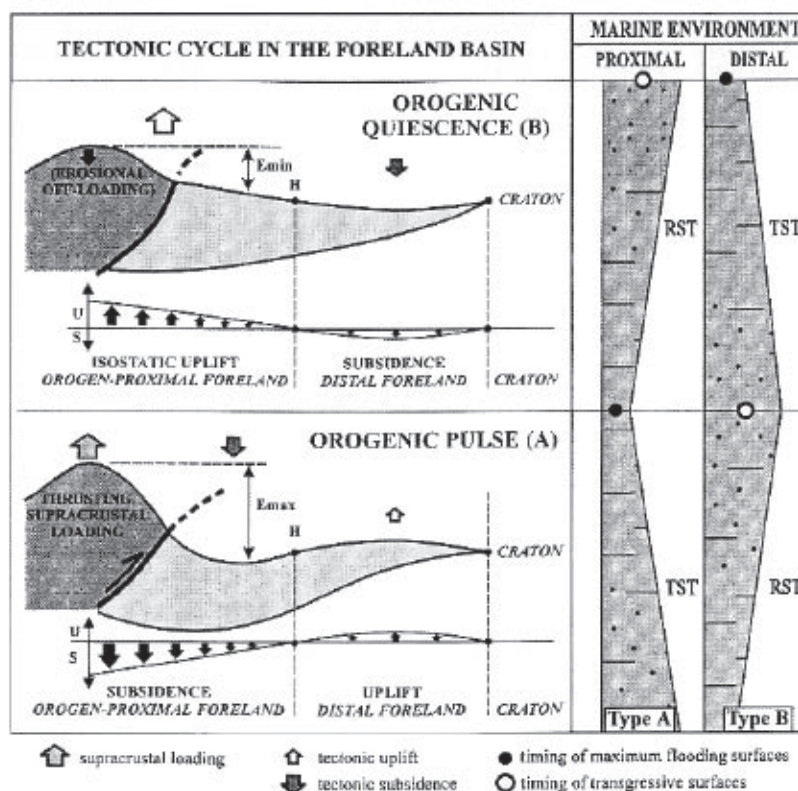


Fig. 4.6: Reciprocal sedimentation model for foreland basins by Catuneanu et al. (1997). (a) Proximal transgression is coeval with peripheral bulge regression, and (b) vice versa. TST: transgressive systems tract, RST: regressive systems tract,  $L_S$ : effect of static tectonic load,  $L_D$ : effect of dynamic tectonic load.

the slope deposits show an overall deepening pattern. Thicknesses of the TST deposits at the type locality of the Valdeteja Fm. and at the section south of Las Majadas del Caserio (both Bodón Unit) are small. Slope deposits at the type section of the Valdeteja Fm. have the highest water depth at their top, which is concluded to represent the maximum flooding surface (318.5Ma). The following sedimentation shows a shift of the facies belts toward the basin, which is expressed by transition from lower slope deposits to upper slope breccia, succeeded by platform margin and platform interior deposits (see Appendix, profile “Valdeteja”).

In the eastern Gayo Unit, transgression of the sea and higher subsidence caused a significantly higher retrogradation of the platform than within the Bodón Unit (Fig. 4.2). The recorded

stratigraphic profile along the Curueño River shows a hiatus during the TST (Fig. 4.4c). In Figure 4.8a, the panorama view displays the changing stratification pattern at the contact of the LST and the HST, visualizing the hiatus during the intermediate TST. However, at locations of preserved TST deposits, aggradation is higher within the Gayo Unit than within the Bodón Unit, due to higher creation of accommodation space.

Contrastingly, within the Gayo Unit of the Torío Valley, biostratigraphy points to an age of 318.5Ma for the top of the Valdeteja Fm. Additionally, Fernández González (1990) correlated the top of the Valdeteja Fm. with a stratigraphic level within the San Emiliano Fm., which belongs to the Namurian B (R2). The Valdeteja Fm. is followed by fine-grained siliciclastics of the San Emiliano Fm. Time





Fig. 4.7: Type section of the Valdeteja Fm., viewed from the east of Las Majadas del Caserio (Bodón Unit). The photo shows a part of the Bodón Unit that is strongly bended. Strike changes within the photo from north-south at the right side to west-east directed in the left foreground. See text for sequence stratigraphic interpretation. SMW: shelf-margin wedge, TST: transgressive systems tract, HST: highstand systems tract, mfs: maximum flooding surface, sb 2: type 2 sequence boundary. The green line marks the position of the type section of the Valdeteja Fm. along the roadcut east of Valdeteja.

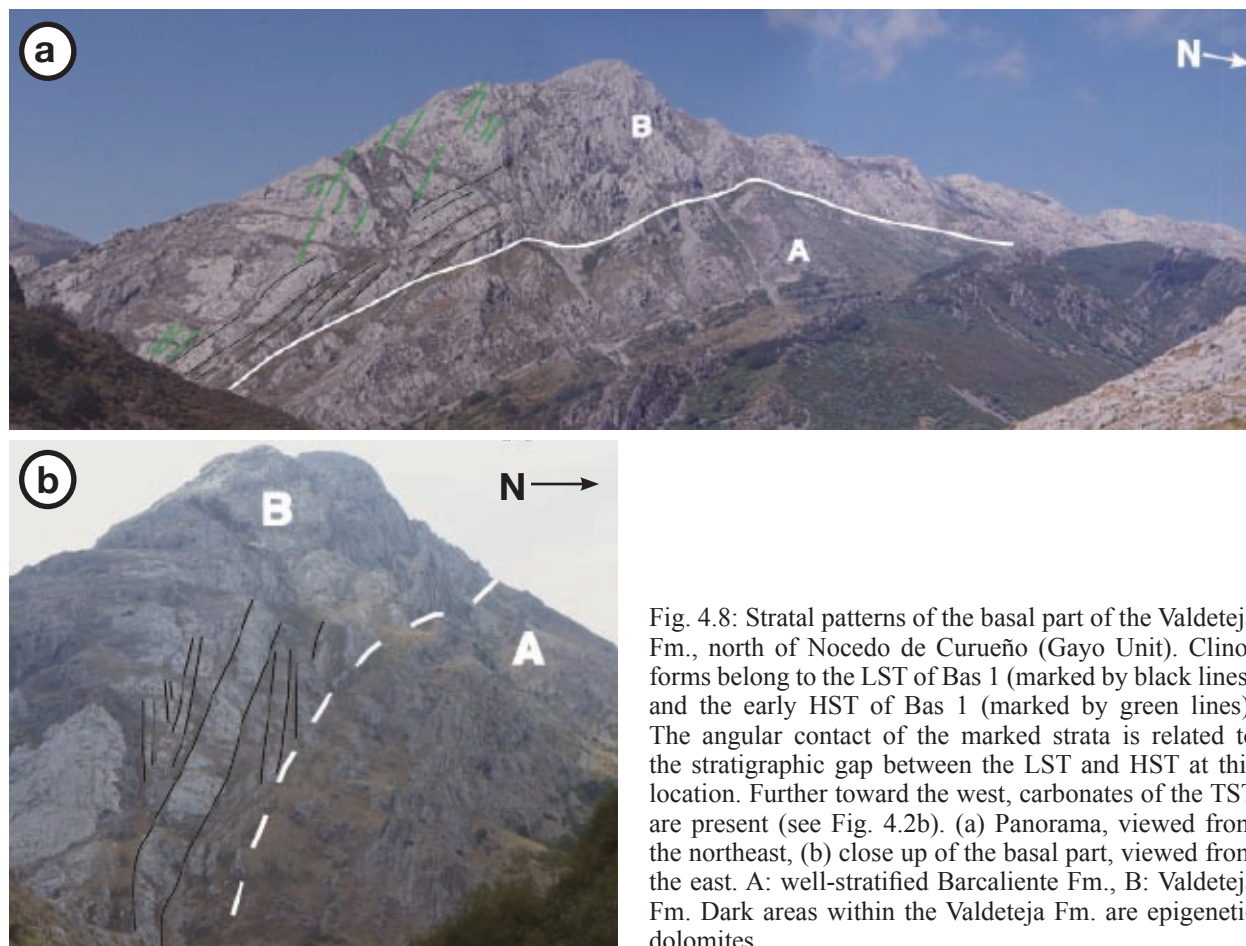


Fig. 4.8: Stratal patterns of the basal part of the Valdeteja Fm., north of Nocado de Curueño (Gayo Unit). Clinoforms belong to the LST of Bas 1 (marked by black lines) and the early HST of Bas 1 (marked by green lines). The angular contact of the marked strata is related to the stratigraphic gap between the LST and HST at this location. Further toward the west, carbonates of the TST are present (see Fig. 4.2b). (a) Panorama, viewed from the northeast, (b) close up of the basal part, viewed from the east. A: well-stratified Barcaliente Fm., B: Valdeteja Fm. Dark areas within the Valdeteja Fm. are epigenetic dolomites.



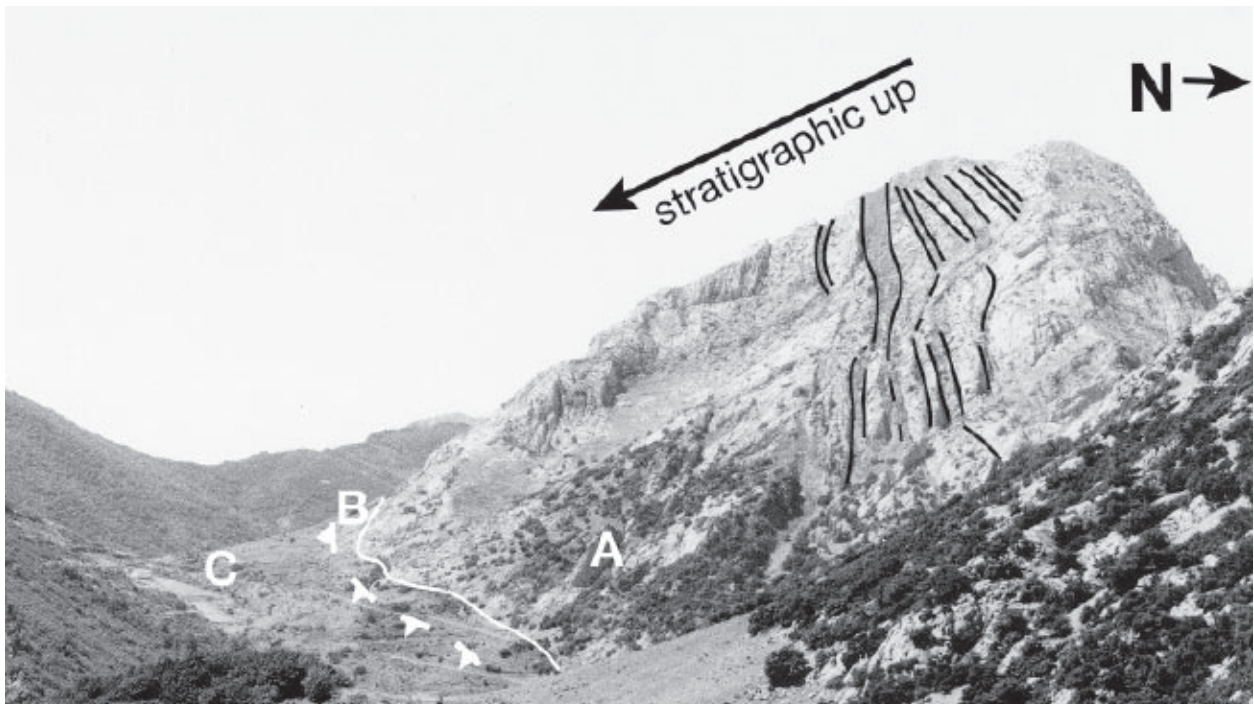


Fig 4.9: Clinoforms of the late HST of Bas 1 (see text for discussion), west of Nocedo de Curueño (Gayo Unit), viewed from northeast of Montuerto. A: Valdeteja Fm., B: San Emiliano Fm., C: Cambrian sediments of the overlying Pozo Unit. Triangles show the position of the thrust separating the Gayo Unit (to the right) and the Pozo Unit (to the left). White lines limit formations, black lines highlight geometries.



Fig. 4.10: Erosional surfaces at the top of the Valdeteja Fm. (a) south of Las Majadas del Caserio (Bodón Unit), viewed toward the east, (b) east of Nocedo de Curueño, viewed into the Montuerto Syncline (Gayo Unit).

line 318.5 represents a transgressive surface within the Gayo Unit of the Torío Valley. The facies indicates a higher water depth than deduced for the younger, basal part of the San Emiliano Fm. within the Bodón Unit. Unfortunately, biostratigraphic constraints are poor and need further investigation. However, the overall subsidence pattern in front of the orogen approaching from the west/southwest, may have caused higher subsidence within the foredeep (i.e. Gayo Unit) due to supracrustal loading applied during an orogenic pulse. Jordan (1995) stated that for tectonically controlled stratigraphic sequences, cycles of the proximal and the distal margin were 180° out of phase. In concordance with Jordan, Catuneanu et al. (1997) presented a tectonic model of reciprocal sedimentation in foreland basins by carrying out detailed sequence stratigraphy in the Alberta Basin. They proposed that when the proximal foreland (i.e. proximal foredeep according to the classification by Horton & DeCelles 1997) subsided, the distal foreland (i.e. distal foredeep/forebulge according to the classification by Horton & DeCelles 1997) uplifted whereas during isostatic uplift of the foredeep, the forebulge subsided. Consequently, the development of accommodation space of the foredeep is opposed to that of the forebulge, resulting in a reciprocal stratigraphy. Transgressive deposits within the foredeep would correlate in time with regressive deposits of the forebulge (Fig. 4.6). Accordingly, the western Gayo Unit would be part of the proximal foreland at 318.5Ma as indicated by the onset of the San Emiliano Fm. Contemporaneous deposits of the study area belong to the forebulge and back-bulge depozone showing an progradational pattern of the platform. However, later foredeep deposits of the

San Emiliano Fm. belonged to distal parts of the foredeep and are directly correlatable with the platform development.

Within the eastern part of the Bodón and Gayo Units, stratal patterns indicate considerable progradation and heavy shedding during the following HST (Fig. 4.1, 4.2, 4.8, 4.9). Compared to younger highstand systems tracts within the study area, this HST possesses the highest rate of progradation of the platform carbonates into the basin, i.e. creation of accommodation space within the platform was low. Carbonate production rates were high, as indicated by voluminous sheddings into the basin. Figure 3.12 shows the Valdeteja Fm. advancing into the basin in the eastern Bodón Unit. West of Oville (Bodón Unit), the carbonates were shedded into the basin approximately 2km, whereas east of Nocado de Curueño (Gayo Unit), progradation width reaches approximately 3.5km (Fig. 4.1 & Fig. 4.2). The excellent stratal pattern visible in the aerial photograph of the eastern Gayo Unit (Fig. 4.2) permits distinction between an early and a late HST and the referring offlap breaks could be determined. The topmost surface shows erosional features east of Nocado de Curueño (Fig. 4.10b). Eichmüller (1985) described karstification in this location, which is indicated by filled vuggy porosity.

At the top of the HST of the Bodón Unit, an erosional unconformity truncates the clinoforms (Fig. 4.7). Laterally, the erosional unconformity is hardly traceable. However, Fernández González (1990) reported a hiatus in this stratigraphic level. The duration of the hiatus is not sufficiently constrained by biostratigraphy. The geometry of the HST deposits proves heavy highstand shedding into the ad-



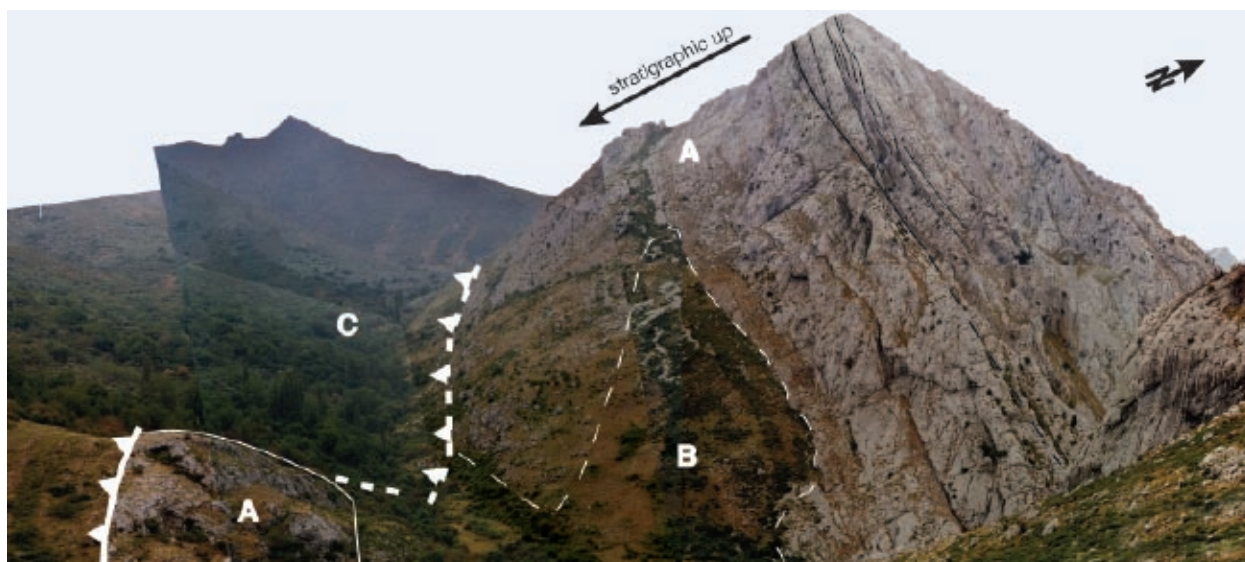


Fig. 4.11: Truncation of clinoforms at the top of the HST of Bas 2, south of Las Majadas del Caserio (Bodón Unit). A: Valdeteja Fm., B: Forcoso Zone (both Bodón Unit), C: Cambrian Láncara Fm. (Gayo Unit). Triangles show the position of the thrust separating the Bodón Unit (to the right) and the Gayo Unit (to the left).

jacent basin due to a lack of accommodation space in proximal areas and high carbonate production rates. Therefore, the erosional unconformity is interpreted as caused by a short period of subaerial exposure during the late HST. The duration of the hiatus was probably short (Fig. 4.4c).

*Bas 2 (317.5Ma - 315Ma, Valdeteja Fm., Forcoso Zone, San Emiliano Fm.)*

At the base, the sequence is bounded by a type 2 sequence boundary in the eastern Bodón Unit, whereas no indication for a type 2 but type 1 boundary is found in the eastern Gayo Unit. The change from progradation within the underlying HST to accumulation of slope deposits within the SMW (shelf-margin wedge) and the pattern of the HST of Bas 1 as described above, point to a type 2 sequence boundary and a succeeding SMW. However, in the Gayo Unit, no lowstand sedimentation is apparent within the platform and is not distinguishable in the basin. Erosion caused an undulating appearance of the top surface of the carbonates

of the HST of Bas 1, visible east of Nocedo de Curueño (Fig. 4.10b).

Above the transgressive surface (316.5Ma), the overall stacking pattern changes to retrogradation (Fig. 4.1) west of Oville (Bodón Unit). The depositional environment within the profile “Las Majadas del Caserio” shows a strong deepening upward trend. Due to this transgressive event, platform growth is terminated in the western part of the Bodón Unit (see Appendix, profile “Lavandera”). Contemporaneously, siliciclastic material is derived from the approaching orogen from the west. It is proposed in this study, that high creation of accommodation space caused by subsidence is the main reason for termination of the platform depositional environment. At the eastern platform-to-basin transition, the sedimentary record shows no influence of siliciclastic material derived from the west. Yet, east of Oville, the platform exhibits a strong retrogradational pattern without any siliciclastic influence.

Within the Gayo Unit, platform growth suc-



Fig. 4.12: Cyclic pattern within the lowstand wedge of Mos 1 in the uppermost part of the section south of Las Majadas del Caserio (Bodón Unit).

ceeded only west of Nocado de Curueño within a small area (Fig. 4.2b), but was terminated east of Nocado de Curueño where basin facies of the Forcoso Zone was established. The “Nocado Escarpment” must have experienced high subsidence (see Chapter 6) to establish the basinal environment after preceding sub-aerial exposure.

The maximum flooding surface (mfs) is positioned at the top of the deep intra-platform basin in the upper part of section “Las Majadas del Caserio” (Bodón Unit; see Appendix). The following HST shows an overall aggradational

pattern. Within the siliciclastics of the San Emiliano Fm., the transition from the TST to the HST is deduced from changes in the shale-to-sand ratio (Fig. 4.3c; profile “Lavandera” in the Appendix).

West of Nocado de Curueño (Gayo Unit), HST deposits reach relatively high thicknesses. Subsidence was higher than in the Bodón Unit, where the HST reaches only minor thickness (Fig. 4.1).

The condensed basinal deposits of the Forcoso Zone do not allow exact determination of the location of the mfs due to poor exposure.

South of Las Majadas, truncation of clino-

forms occurs at the top of the HST as can be seen in the field (Fig. 4.11). Laterally, Figure 4.12 shows an erosive contact between HST deposits and the following LST of Mos 1.

Biostratigraphic data by Villa (1982) indicated that the Bashkirian-Moscovian boundary coincides with the bounding unconformity. The boundary between *Profusulinella* subzone A and B is located at this age (315Ma, see Fig. 3.3). Aitken et al. (2002) reported third-order cycle boundaries often associated with marine biostratigraphic boundaries, which fits well in this case. Further to the west, a correlatable conformity defines the sequence boundary (Fig. 4.3c).

*Mos 1 (315Ma - 313.5Ma, Valdeteja Fm., Forcoso Zone, San Emiliano Fm.)*

Carbonate sedimentation of the Valdeteja Fm. continues only within a lowstand wedge in the eastern Bodón Unit. The small, isolated platform is surrounded by basinal clastic deposition. The aerial photograph (Fig. 4.1) exhibits the wedge-shaped geometry, having an increasing thickness towards the basin. The remaining platform shows a cyclic pattern as apparent in Figure 4.12.

North of Lavandera, the limestone units within the clastic succession are interpreted as representing lowstand deposition. The lowermost limestone unit may be correlatable with the “caliza masiva” (Julivert 1960), which occurs further to the west of the study area (Fig. 3.33).

Following the LST, the environment shows a sudden deepening (see profiles in the Appendix; Fig. 4.3c). Basin deposits onlap on the platform carbonates. This TST has a minor thickness only.

During the following HST, shallow water carbonates accumulate on top of the previous carbonates in the section of Las Majadas del Caserio. There is only minor progradation into the basin, possibly due to the limited extension of the underlying LST wedge. The extent of the LST wedge is assumed to constrain the areal extent of the subsequent carbonate deposition. At the top, a thrust plane cuts the succession south of Las Majadas del Caserio and sedimentary record ends.

*Mos 2 (<313.5, San Emiliano Fm.)*

Deposits of this sequence occur only north of Lavandera (Fig. 4.3c), thrusting and erosion erased the sedimentary record everywhere else in the study area. Within the siliciclastics of the San Emiliano Fm. at Lavandera, the sequence boundary is determined by a change in the depositional environment from fine-grained, distal prodelta siliciclastics to the topmost limestone unit of the cross-section recorded (see Appendix, profile “Lavandera”). The latter are interpreted as lowstand deposits. The subsequent transgression deposited siliciclastics on top. The stratigraphic record ends within the core of the syncline of the Bodón Unit (Fig. 5.8).





## CHAPTER 5: STRUCTURAL BALANCING

Two transects positioned subparallel to the thrust transport direction were balanced (Fig. 5.1) to calculate initial distances between stratigraphic columns.

### 5.1 Constraints

As a guideline for constructing cross-sections, the regional structural style was compiled and subsequently applied. The structural style of an area can be seen in outcrops and road-cuts. Using this, the constructed cross-section will be admissible (Elliott 1983).

Dahlstrom (1969) proposed a “family” of structures for the Canadian Foothills of the Rocky Mountains and these can be partly applied to the fold-and-thrust belt of the Cantabrian Mountains. As basic structural forms he proposed décollement, thrusts, tear faults, concentric folding and late normal faults.

The family of structures applied to the cross-sections A-B and E-F consists of:

- (i) Features commonly associated with thin-skinned tectonics:
  - Detachment horizon (décollement)
  - Thrusts, frontal ramps, fault-bend folds
  - Tear faults, lateral ramps
  - Concentric folding
- (ii) Regional features:
  - Forward-breaking thrust sequence (= piggy-back thrust sequence)
  - Staircase-trajectory thrusts
  - Steep dipping, sometimes overturned thrust faults with associated longitudinal folding
  - Out-of-sequence deformation

The existence of a basal detachment horizon in a fold-and-thrust belt is nowadays widely accepted (e.g. Chapple 1978, Dahlstrom 1970, Elliott 1976, Fermor & Moffat 1992, Roeder et al. 1978, Woodward et al. 1989). The detachment horizon is a bedding plane parallel fault along which a stratigraphic package was transported from the hinterland to the undeformed foreland.

The average detachment dip is remarkably uniform (Woodward et al. 1989). According to investigations using reflection seismics in various fold-and-thrust belts e.g. of the Canadian Foothills, the Appalachians, and Jura Mountains, values for the detachment dip range between 2° and 3° (e.g. Dahlstrom 1970, Elliott 1976, Fermor & Moffat 1992, Roeder et al. 1978). This is consistent with regional seismic investigations carried out in the western part of the fold-and-thrust belt of the Asturian Arc. The seismic reflection profile ESCI-N2 (Pérez-Estaún et al. 1994, 1995, Pulgar 1996) reveals a detachment dip of 3°. Due to significant sedimentary changes between the western part of the Asturian Arc and the working area, other data derived from the seismic profile, such as depth-to-detachment distances cannot be applied to this work.

Thrust faults step up-section along what are known as frontal ramps, which consist of a footwall and a hanging wall part (Fig 5.2a). Thrusts generally follow a staircase or stair-step trajectory (McClay 1992, Rich 1934) made up of ramps and flats (Butler 1982, Douglas 1950, McClay 1992, Fig. 5.2a). Staircase trajectories were commonly described for high-level fold-and-thrust belts (McClay 1992,

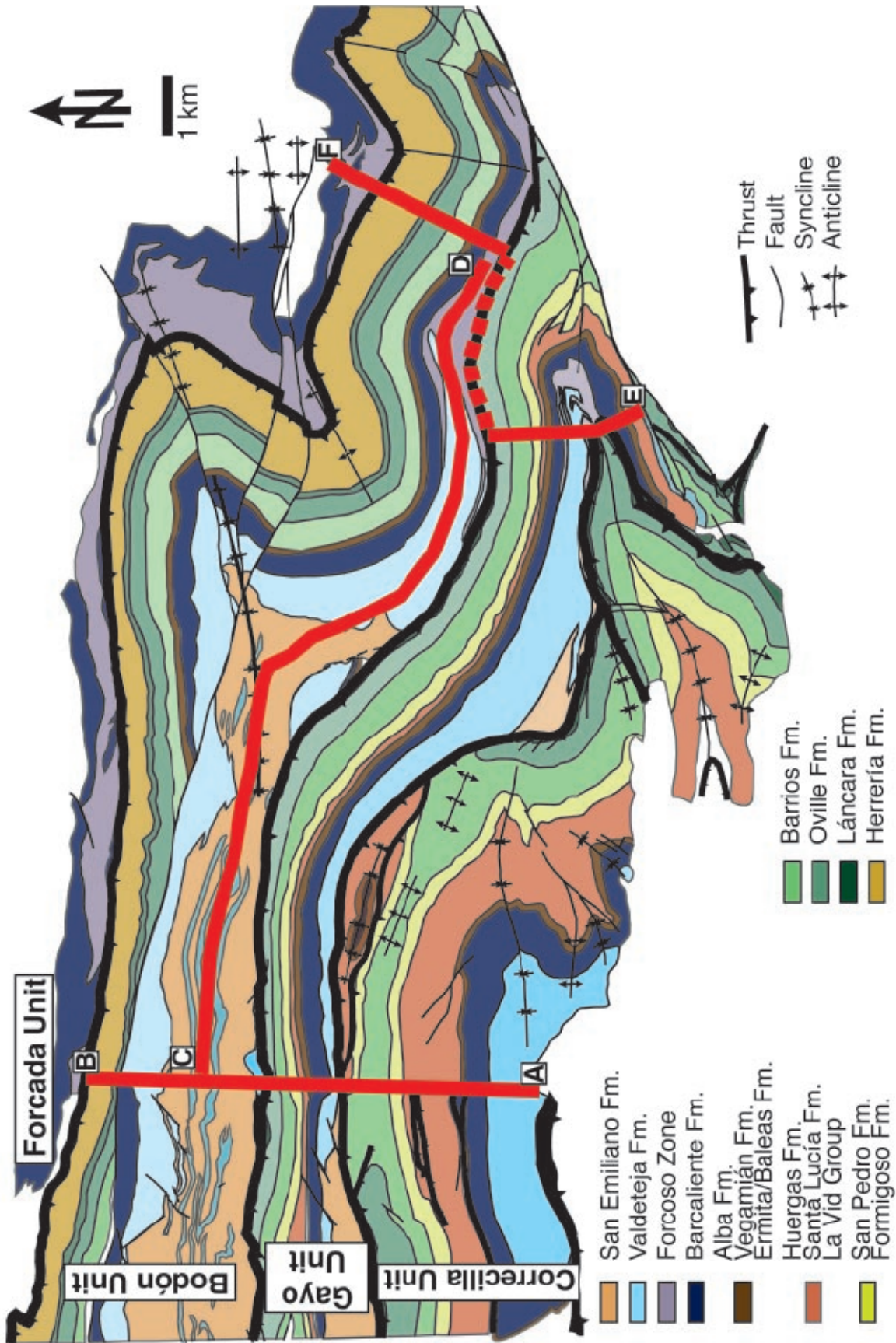


Fig. 5.1a: Geological map of the study area, modified after IGME Map 103 “La Pola de Gordón” (Alonso et al. 1991) and IGME Map 104 “Boñar” (Lobato et al. 1984). The position of the transects is marked by red lines. Transect A-B: Torío Transect, transect C-D: Bodón Transect, transect E-F: Curueño Transect.



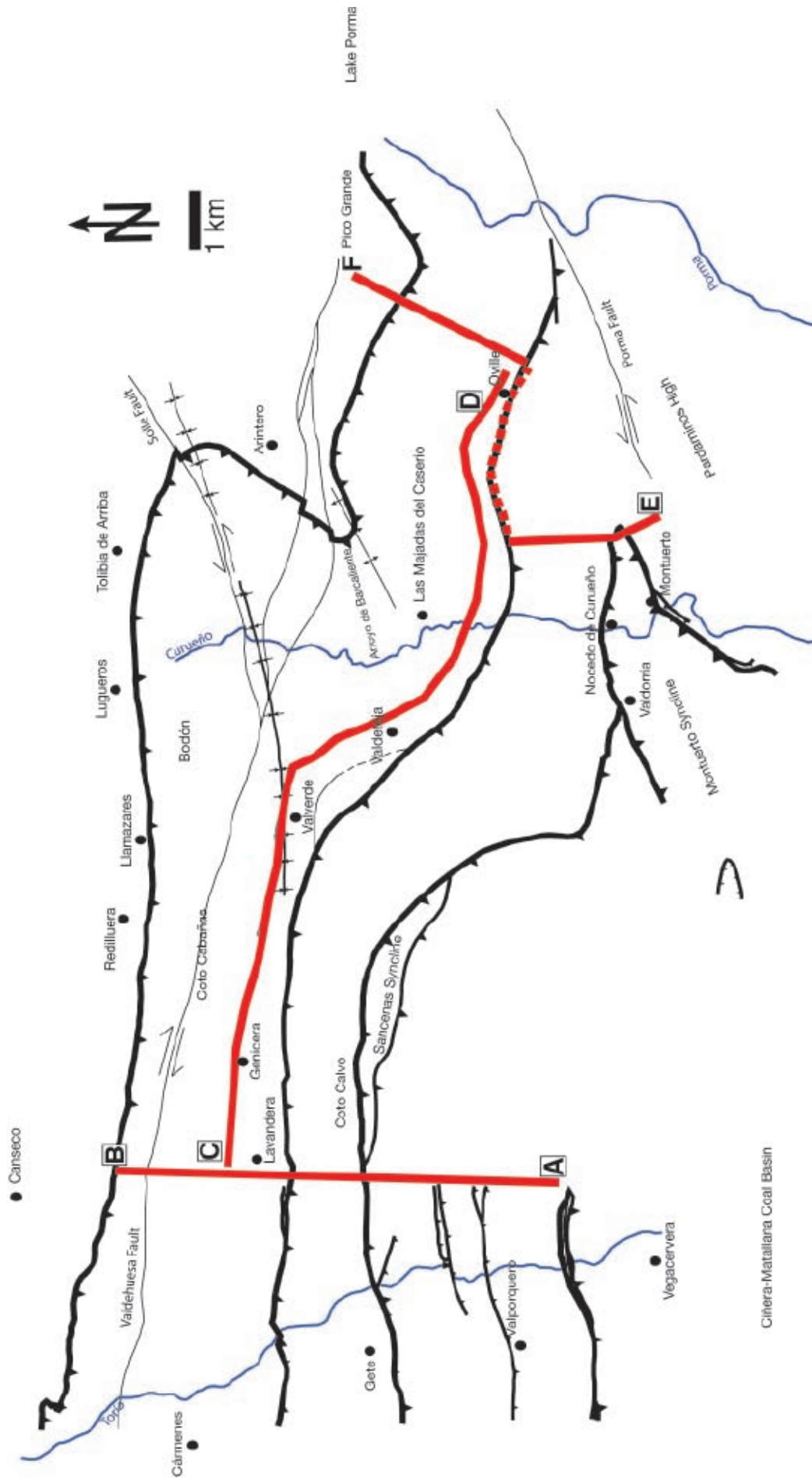


Fig. 5.1b: Schematic overview of terminology of structural elements and of the geological map and geographical locations as used in the text.

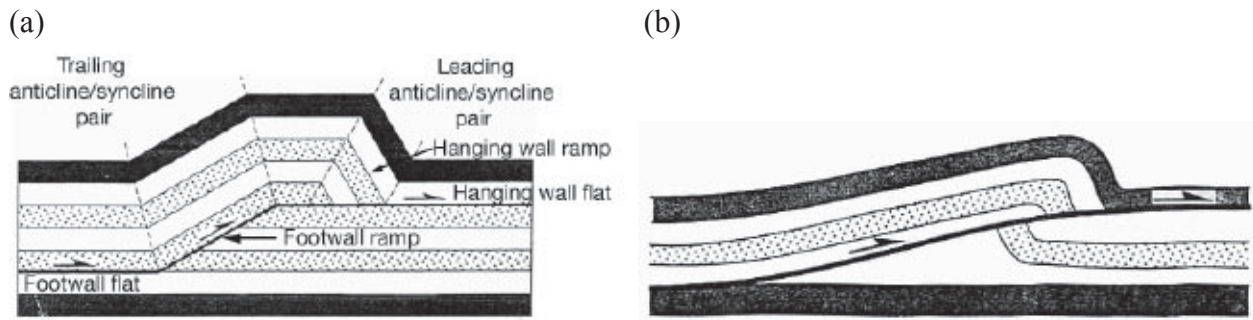


Fig. 5.2a: Staircase trajectory thrust based on the classic model by Rich (1934), after Cooper & Trayner (1986). Terminology of the resulting fault-bend fold after McClay (1992). (b) Smooth-trajectory thrust (Cooper & Trayner 1986).

Pérez-Estaún et al. 1988), whereas smooth trajectory thrusts (Fig. 5.2b) were found in higher-grade metamorphic rocks where ductile penetrative strains are developed within the thrust sheet (Cooper & Trayner 1986, McClay 1987). Julivert & Arboleya (1984) reported for the southern Cantabrian Mountains that beds below the footwall ramp were normally not bent in a syncline. In the study area, staircase trajectories were observed in small-scale structures (Arroyo de Barcaliente).

Thrusts cutting up-section create cut-off lines at the intersection between the thrust surface and a stratigraphic horizon (Fig. 5.3). In a 2D cross-section, the equivalent is the cut-off point. The thrust fault may often be concave showing an increasing dip to the upper section of the fault ("listric thrust fault"). Several thrust faults are generated in a thrust belt; to-

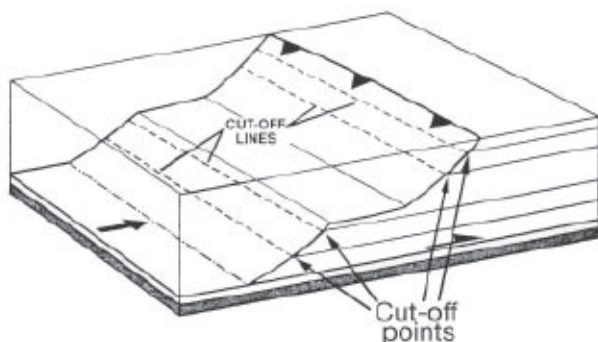


Fig. 5.3: Footwall cut-off lines and points after McClay (1992). Note the thrust plane changing stratigraphic level resulting in a splitting of the ramp into two sections.

gether they constitute the thrust system.

The thrust sheet is transported above steps in the thrust surface and this generates geometrically necessary folds in the hanging wall, known as fault-bend folds (Fig. 5.4). Kink band style folding creates a leading and a trailing anticline/syncline pair, whereas the footwall shows no deformation (Fig. 5.2a; McClay 1992). In the southern Cantabrian thrust belt, the leading anticline/syncline pair of comparable fault-bend folds was usually eroded. Only two localities were preserved: one situated in the Correcilla Unit east of Getino (cross-section A-B) and the other in the frontal part of the Esla nappe further to the east of the study area (Julivert & Arboleya 1984).

If a thrust changed stratigraphic level along strike, a lateral or oblique ramp was probably involved. A lateral ramp strikes perpendicular to the strike of the thrust sheet. A vertical lateral ramp is called a tear fault. Oblique ramps strike obliquely to the transport direction (McClay 1992) (Fig. 5.5).

Since no thinning or thickening of beds was recorded or observed in the Cantabrian fold-and-thrust belt, folding was considered to be concentric (Dahlstrom 1969). Deformation was obtained by flexural slip, which occurred paral-

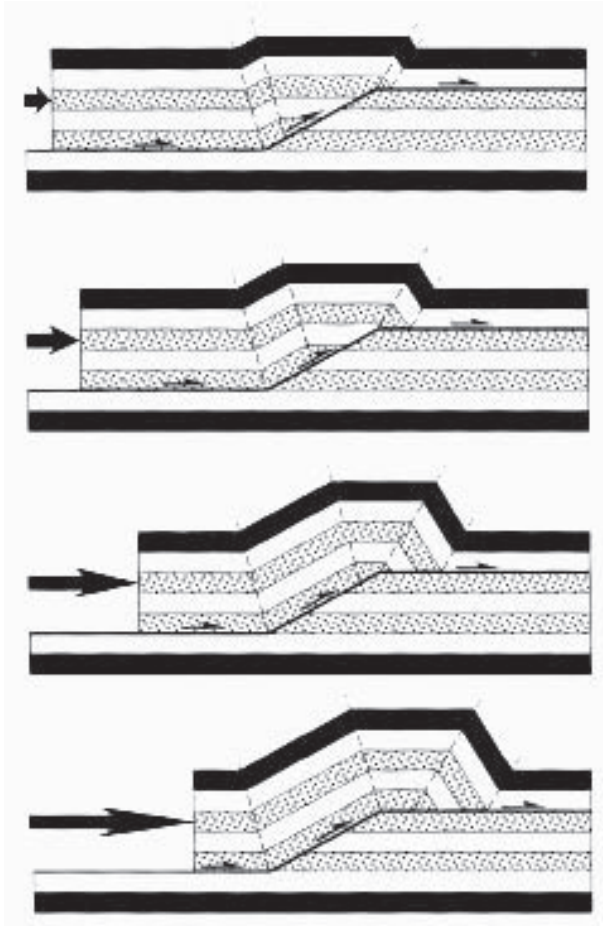


Fig. 5.4: Progressive geometrical development of a fault-bend fold (in: McClay 1992, after Suppe 1983).

lel to bedding (Suppe 1983). It is the prevalent deformation mode for rather competent rocks with mechanical bedding continuities (Ramsay 1967). Woodward et al. (1989) stated that non-parallel folding may occur in fold-and-thrust belts, but they did not consider it to be significant in areas without penetrative strain, which is the case in the field area.

#### *Deformation Mechanism*

The deformation in thrust belts may advance from the hinterland to the foreland (break-forward thrusting or piggy-back thrusting) or a sole thrust propagates out into the foreland and major structures form above the sole thrust, propagating from the foreland to the hinterland (break-back thrusting) (Morley 1988).

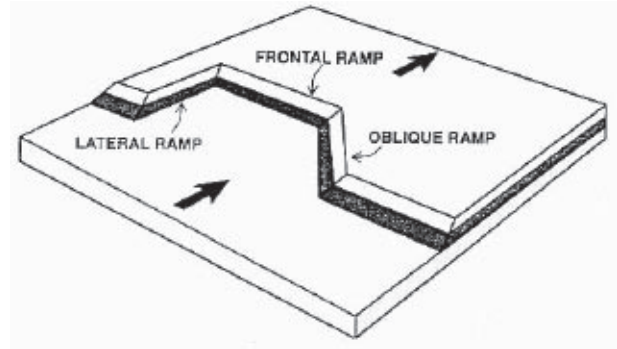


Fig. 5.5: 3D-diagram of the footwall of a thrust fault, illustrating different kinds of thrust ramps (McClay 1992). A vertical lateral ramp is referred to as a tear fault. Heavy arrows give transport direction.

Generally, the break-forward thrusting model is nowadays accepted as a common model for the deformation sequence in fold-and-thrust belts (Morley 1988). Identifying the sequence of development of thrust faults is essential for the interpretation of the geometry and the kinematic evolution and the construction of balanced and restored sections (Boyer 1991, Boyer & Elliott 1982, Butler 1987, McClay 1992, Morley 1988, Suppe 1985, Woodward et al. 1989).

Pérez-Estaún et al. (1988) and Alonso et al. (1992) proved a forward propagating thrust sequence in the Cantabrian fold-and-thrust belt, advancing from the hinterland in the west to the foreland in the east. Although locally out-of-sequence thrusting is reported in the nappe units of the Southern Cantabrian Mountains (Alonso et al. 1992), it is reasonable to expect overall in-sequence thrusting.

The high dip-angle of the thrust faults is a special feature of the Cantabrian structural style. As outlined in Chapter 2, the fold-and-thrust belt experienced a multiphase deformation. After the emplacement of the thrust nappes, a later deformation phase occurred (Marcos 1968) which further deformed the thrust sheets. In



some nappes transverse folds prevail, but in the studied area longitudinal folding is dominant. It caused steepening and local overturning of the thrust surfaces (De Sitter 1962, Julivert 1971, Pérez-Estaún et al. 1988, Pérez-Estaún & Bastida 1990, Potent & Reuther 2000). Alpine deformation further compressed the area and steepened and reactivated pre-existing thrusts and faults.

Dip data collected during fieldwork provided the basis for the construction of the dips of the thrust faults used in the cross-sections.

#### *Out-of-Sequence Deformation*

Although out-of-sequence thrusting can reasonably be excluded for the study area (see above), out-of-sequence faulting clearly exists. West-east trending faults and shear zones such as the León Line, Porma Fault and Valdehuesa Fault (Fig. 5.1b) show post-thrusting displacement (Chapter 2). Pre- and post-Variscan activity along some of these out-of-sequence faults is probable. The exact timing of activity along these zones is still to be investigated.

A vast amount of literature exists about fold-and-thrust belts and their structural style. For further reading, reference can be made to e.g. Butler (1982), McClay (1992), Mitra (1986), Ramsay & Huber (1987).

## **5.2 Construction of Cross-Sections**

### *Choice of Line*

The cross-sections were positioned parallel to the direction of the horizontal component of the maximal stress in compression, i.e. the overall thrust transport direction. This was determined by the average regional strike of the emergent thrusts and stratigraphic layers. According to

today's-coordinates, the thrust sheets were transported from the south to the north.

Since 2D cross-sections passing lateral ramps will not balance and cannot be restored (Hossack 1983), it was necessary to minimize the possibility of lateral material transport oblique to the cross-sections. Woodward et al. (1989) stated that the line of the cross-section should not deviate more than 5° from the thrust transport direction. Cross-section A-B is positioned parallel to the N-S striking Torío Valley (southern end: N 42°54.170', W 005°31.185'; northern end: N 42°59.081', W 005°31.222'). Cross-section E-F starts in the south (N 42°52.811') perpendicular to the southern limb of the Montuerto Syncline of the Gayo Unit. As it continues, its direction shifts slightly in order to stay perpendicular to the overall strike in the northern limb of the Montuerto Syncline. Between the Gayo and Bodón Units, cross-section E-F is offset along strike of the thrust fault (from N42°54.459', W 005°22.962' to N 42°54.324', W 005°20.759'; Fig. 5.1a). In the northern part of the Curueño Valley, the Bodón Unit is deformed in a z-shaped structure, which is indicative of the underlying complex system consisting of various lateral and frontal ramps (Hinsch 1997). To avoid this area, where transport of material oblique to the cross-section is certain, the northern part of the cross-section E-F is offset along a thrust plane and continues further to the east (northern end of the transect: N 42°55.946', W 005°19.463'). The northernmost Forcada Unit was not structurally balanced in this study. Its complicated polyphase deformational history exceeds the scope of this study. Hinsch (1997) constructed a balanced and restored cross-section of the Forcada Unit which is positioned only about 2.5 km to the west of cross-section E-F. The

investigated minimum shortening rate of 40-50 % was used in this study to calculate the distance between the stratigraphic columns of the Bodón and Forcada Units.

The Pozo Unit, which is indicated in the deformed cross-section E-F (Fig. 5.10), is not relevant for the stratigraphic modeling procedure and therefore has not been restored.

#### *Sedimentary Thickness Changes*

Due to a long-lasting hiatus in the north, sediments onlap on progressively older sediments in the north (Chapter 3). Thicknesses of the Ordovician Barrios Fm., the Silurian Formigoso and San Pedro Formations, the Devonian La Vid Group, Santa Lucía, Huergas, Portilla, Nocado, Ermita, and Baleas Formations decrease significantly to the north and northeast. Most of them are not preserved in the northernmost part of the cross-sections.

The Carboniferous Valdeteja Fm. comprises mainly platform carbonates, which show quick lateral changes (Chapter 3). Its thickness varies along the transect due to changes in the depositional environmental setting. In the Forcada Unit, the lateral time-equivalent Forcoso Zone was deposited with a significantly lower thickness. The San Emiliano Fm. diachronically overlies the Valdeteja Fm. Due to migration of the depocenter, its thickness changes along the transect.

#### *Internal Deformation*

A mechanism for internal deformation in thrust sheets is layer parallel shortening. For the Cantabrian thrust belt, layer parallel shortening has not been reported by available literature and not been observed in the field area.

A significant factor is the occurrence of

small-scale folding and faulting (Fig. 5.6). Unfortunately, it could not be taken into account in this study. An extensive and comprehensive tectonic study would be required to evaluate small-scale structures and their effects on the shortening rate within the field area. Therefore, only minimum shortening rates were calculated in this study.

#### *Detachment*

The detachment was constructed with a dip angle of 3° (see above). The position of the detachment horizon was concluded from surface data. In the Bodón and Forcada Units it is located within the Herrería Fm., whereas in the Gayo and Correcilla Units it is located at the base of the Láncara Fm. (Fig. 5.1).

The sedimentary thicknesses of the formations, which comprise the thrust sheets, were measured at the surface. Therefore, the sum of the stratigraphic thicknesses of all formations provided the relevant depth-to-detachment.

The dip of the emergent thrust surfaces was measured in the field.

#### *Duplexes and Imbricate Thrust System*

In the basal Herrería Fm., hinterland-dipping duplexes were constructed due to the local necessity of structural elevation.

Mitra (1986) revised the duplex classification proposed by Boyer & Elliott (1982). His classification is based on the relative displacements on adjacent thrusts, final spacing between ramps, ramp angles, and ramp lengths. The system, which is shown in Figures 5.8 & 5.10, fits into class III, which comprises foreland sloping duplexes with partly overlapping crests of the ramp anticlines. Subclass 1 further refines the given definition. It requires the following



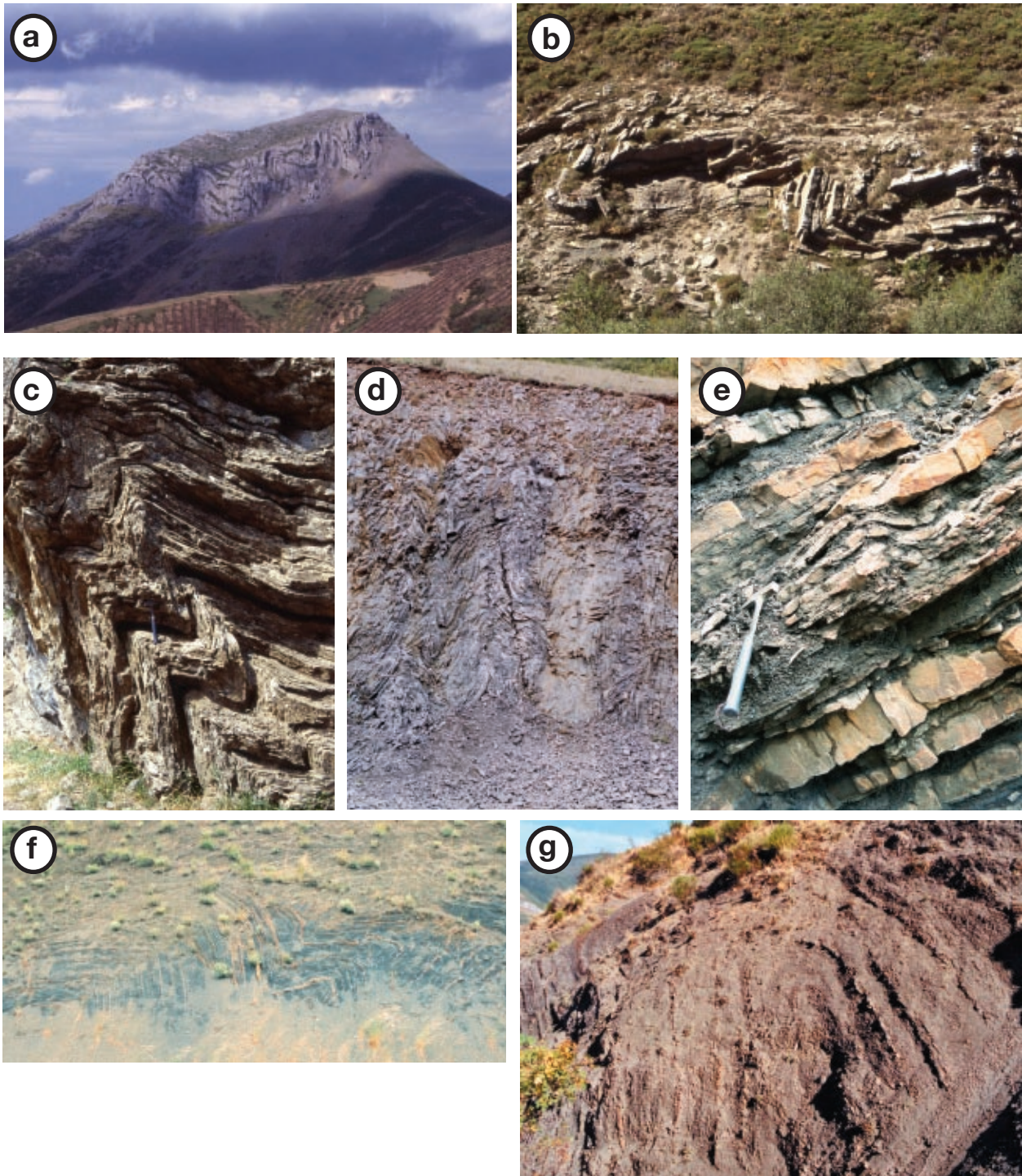


Fig. 5.6: Outcrop photos demonstrating examples of deformational style within the Southern Cantabrian Mountains. (a) Folding within the core of the Alba Syncline, (b) asymmetric third-order folding within San Emiliano Fm. north of Cármenes (Bodón Unit), (c) chevron folds generated in finely laminated limestone of the Barcaliente Fm. north of Piedrasecha, located at the southern limb of the Alba Syncline, (d) chevron folds within limestones of the Olleros Fm. at the road-cut north of Llombera, (e) small-scale fault within the Olleros Fm. along the road-cut north of Llombera, (f) concentric folding within the fine-grained siliciclastics of the Olleros Fm., along the road-cut north of Llombera, (g) symmetric, concentric folding within the Forcoso Zone north of Arintero (Forcada Unit).



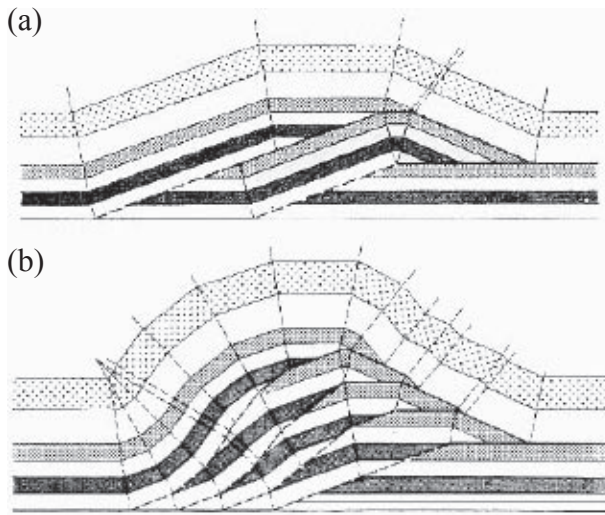


Fig. 5.7: Duplexes were classified following Mitra (1986). This classification is based on the relative displacements on adjacent thrusts, final ramp spacing and ramp lengths. (a) The system of partly overlapping anticlines within the cross-sections was assigned to class III, subclass A. (b) System of stacked, partly overlapping anticlines. Note the variation in dip of the thrust faults. Ramp angles of the upper and lower ramp of the modeled cross-sections correspond to this.

setting (Fig. 5.7a):

$$a' > h_r * \operatorname{cosec} \partial,$$

$a'$  : final spacing between the thrusts

$h_r$  : ramp height

$\partial$  : ramp angle.

Figure 5.7 shows a system of partly overlapping anticlines. The ramp angles vary from the lowermost to the uppermost thrust sheet, resulting in sigmoidal thrusts. In cross-section A-B, the thrust sheets of the Bodón, Gayo, and Correcilla Units partly overlap each other. As displayed in Table 5.1, the ramp angles of the upper and lower ramp follow this geometry.

### 5.2.1 Cross-Section A-B

Figure 5.8 shows the constructed cross section. Cross-section A-B is bounded to the north by the south-vergent out-of-sequence Valdehuesa Fault, which cuts through the complete thrust

sheet. Strata north of the Valdehuesa Fault are denoted in shaded colors and are not part of the balanced section. To the south, surface data for the cross-section could only be measured as far as the northern limit of the Stephanian Matallana Coal Basin, which overlies the Westphalian formations in a high-angle discordance. Surface data were acquired along the erosional surface displayed in Fig. 5.8 between points A and B. South of point A, the further extension of the transect was a necessary geometric construction for restoration.

During the process of thrust emplacement and oversteepening of the thrust planes, erosion occurred that was not accounted for in the construction above the today-erosional profile. Therefore, the bulk thickness of the stacked tectonic units on top of the Bodón Unit is a geometrical construction. It is not assumed that this erosional profile as shown in Figure 5.8 existed but that the structural style applied corresponds to the deformation history, which created the today-visible deformation style at the surface. According to Marschik (1992), the tectonic stacking did not significantly influence the thermal evolution. Further thermal data (see Chapter 3.3) indicate relatively low thicknesses of sedimentary cover rocks on top of the preserved record.

The thickness of the La Vid Group is tectonically induced in the Correcilla Unit. Various bedding parallel faults obscure the initial sedimentary thickness. For the stratigraphic modeling process, the thickness was estimated by information gained by its lateral continuation. In the cross-section, tectonically induced thicknesses were maintained at the erosional surface but adjusted along the constructed plane with respect to the initial sedi-

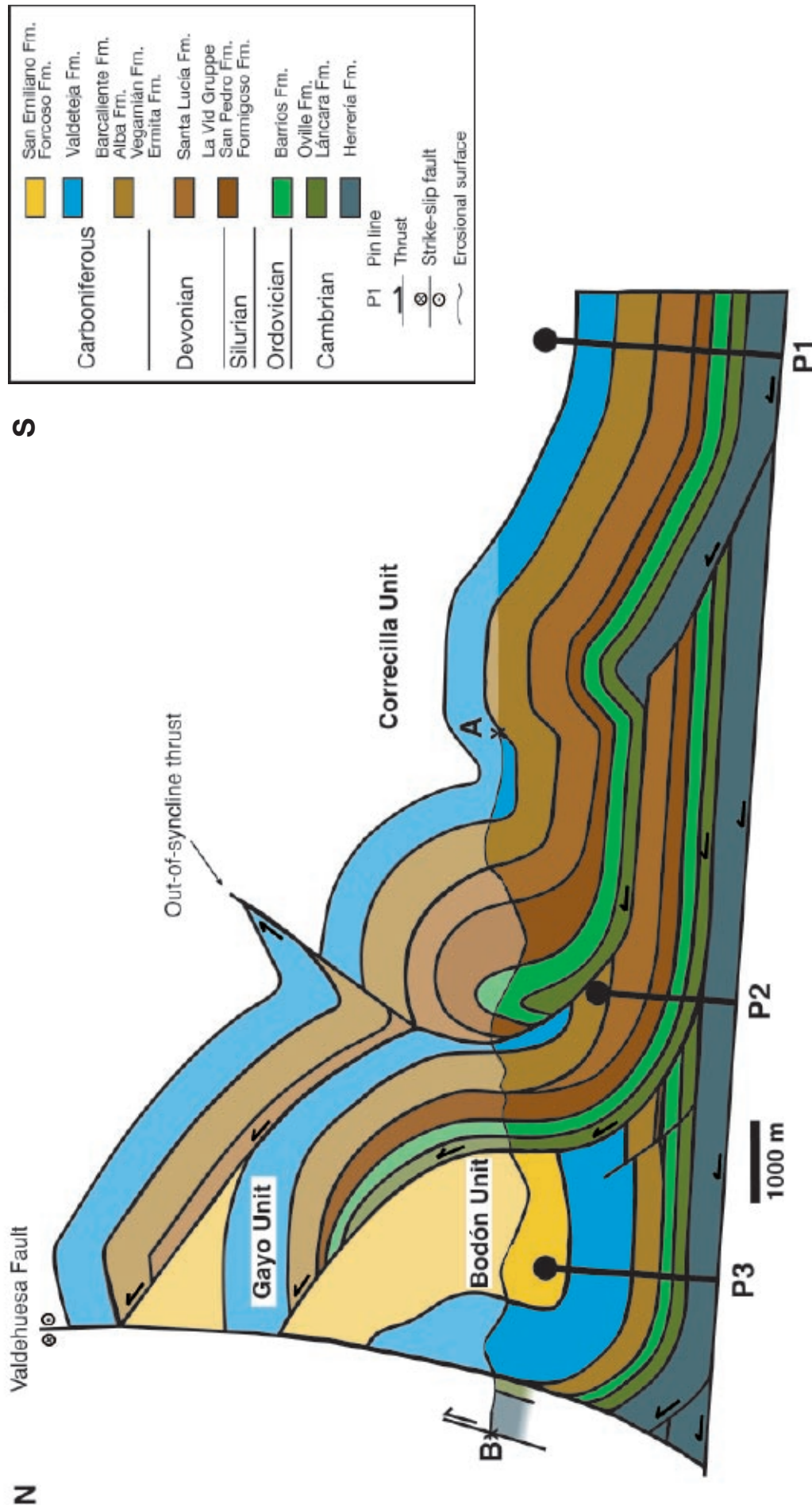
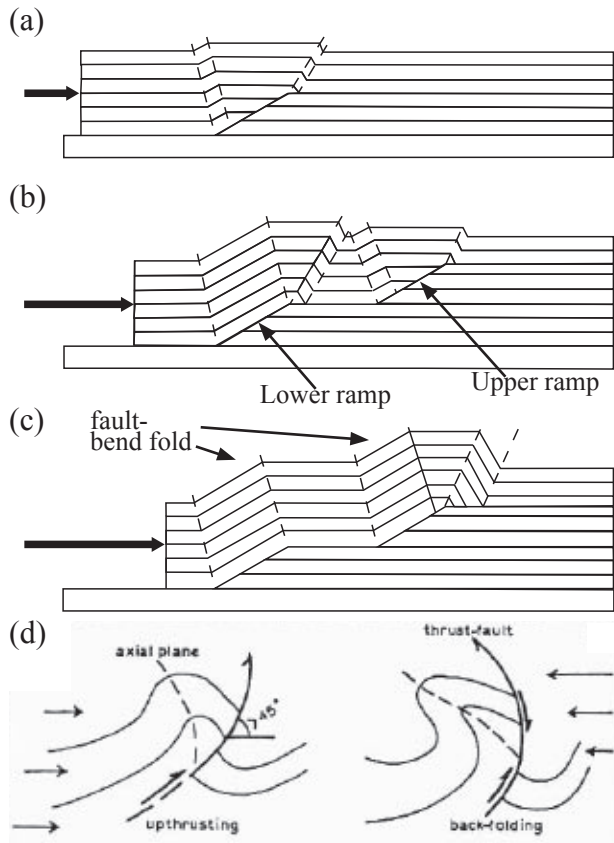


Fig. 5.8: Re-constructed cross-section A-B of the Torío Transect. Figure 5.1a shows the position of the cross-section within the study area. Some formations were grouped for better visualization (see legend). The recent erosional surface is shown by the black line connecting points A and B. Constructed parts above the erosional surface are shown in transparent colors, geometries below the erosional surface are shown in saturated colors. Not balanced areas north of the Valdehuesa Fault and the Forcada Unit are displayed only schematically. Note, that the reconstruction is based on surface data along the displayed erosional surface and geometrical constraints derived from the regional structural style. Erosion acting contemporaneously to deformation could not be considered within this work. Hence, the stack of tectonic units on top of the Bodón Unit is a geometrical construction.



mentary thickness as recorded throughout field work.

According to Julivert & Arboleya (1984), footwall ramp angles in the Cantabrian fold-and-thrust belt can reach values of up to  $32.5^\circ$ . The steepest angle of the constructed frontal ramps reaches  $27^\circ$  in the lower part of the footwall ramp of the Gayo Unit (Fig. 5.12a). This specific case shows the thrust cutting up-section from the base of the Herrería Fm. to the Santa Lucía Fm., wherein marly horizons enable the thrust to continue parallel to the bedding for about 2.8 km before cutting further up-section along the upper part of the footwall ramp.

Fig. 5.9 shows an interpretation of the possible origin of the deformation of the Correcilla

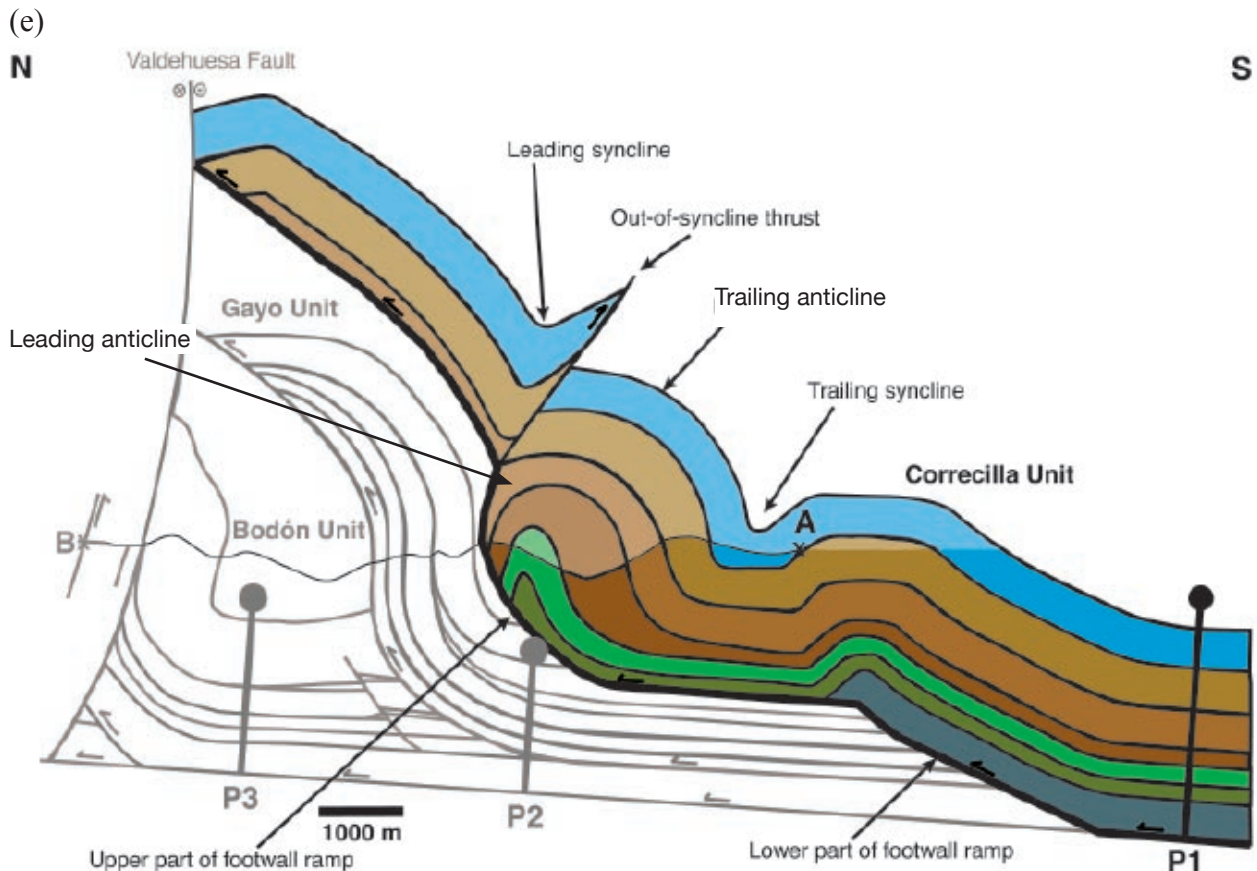


Fig. 5.9: (a)-(c) Genetical model showing the progressive development of the Correcilla Thrust Sheet climbing up a partitioned ramp. Based on the fault-bend fold model by Suppe (1983). (d) Later compression resulted in tightening of the folds (Evers 1967) and initiation of the out-of-syncline thrust as shown in Figure 5.8. (e) Explanation of structural elements of the Correcilla Unit. Elements of the Bodón and Gayo Units are shown in gray. The footwall ramp of the Gayo Unit is highlighted by a thick black line on top of the Gayo Unit and at the base of the Correcilla Unit, respectively. See text for explanation of the genetic model of the Correcilla Unit.



Thrust Sheet climbing up the lower and upper footwall ramp of the Gayo Unit. After initiation of the lower footwall ramp, due to climbing up the ramp, the thrust sheet is deformed in a ramp anticline. Increasing displacement moves the thrust sheet further to the north and above the upper frontal ramp. In today's state, the leading and trailing anticlines above the upper part of the ramp are present in the field area. In the core of the anticline, the quartzitic sandstones of the Barrios Fm. are tightly folded. The synclinal structure north of Vegacervera represents the trailing syncline of the upper part of the frontal ramp. In this case, it coincides with the leading syncline of the fault-bend fold, which formed above the lower part of the frontal ramp. Due to later compressional deformation, the leading ramp anticline is relatively tight. The late compressional event created a lack of space in the leading syncline of the northern fault-bend fold. It was solved by the creation of an

out-of-syncline thrust. Out-of-syncline thrusts nucleate and propagate out from the core of a syncline and are normally generated by a lack of space in the cores of tight synclines (McClay 1992). Genetically, they are not necessarily related to other thrusts.

In the Bodón Unit, a blind thrust was implemented to elevate the stratigraphic level to do justice to the north dipping strata of the southern limb of the syncline.

### 5.2.2 Cross-Section E-F

Cross-section E-F is bounded to the north by the basal thrust plane of the Bodón Unit. As outlined above, the Forcada Unit was not restored. Therefore, the strata north of the Bodón Unit are shown in shaded colors. To the south, the south-verging out-of-sequence Porma Fault limits the cross-section. Restoration was accomplished between the northern termination

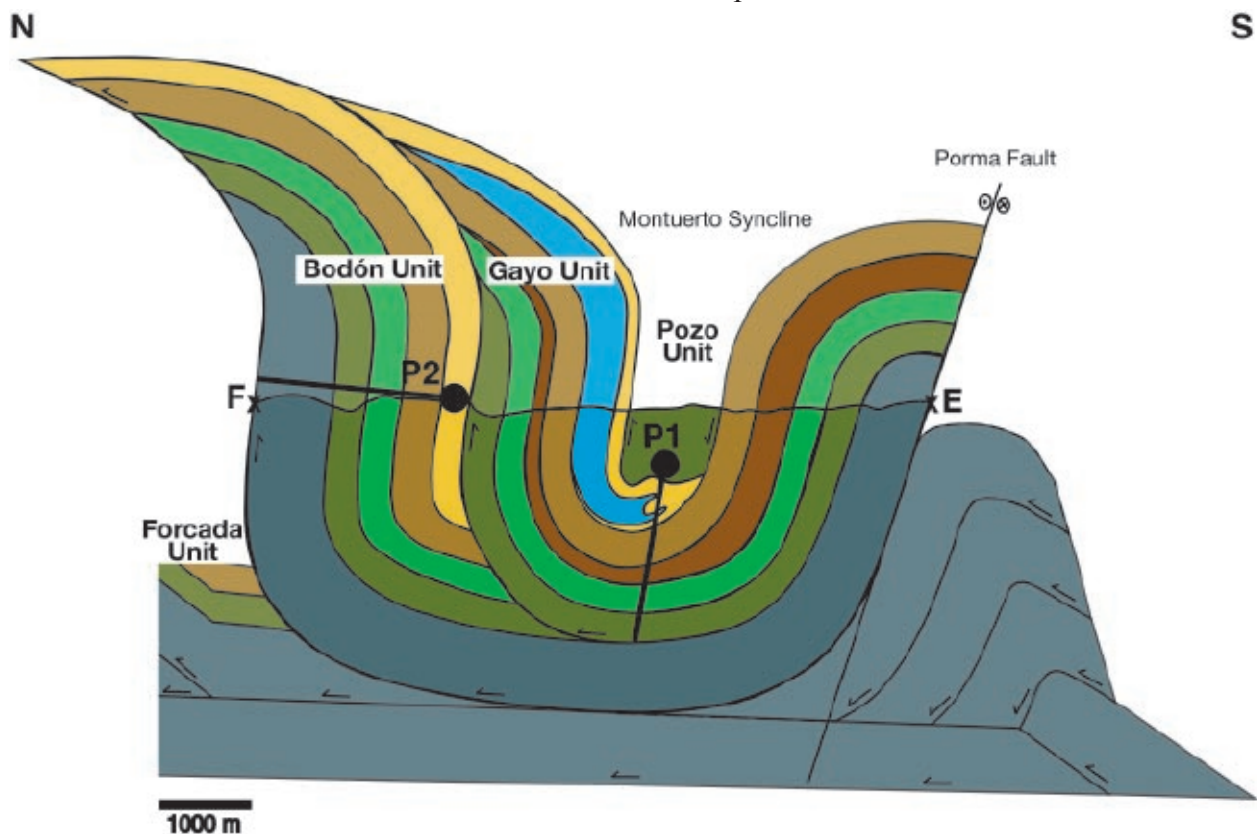


Fig. 5.10: Re-constructed cross-section E-F of the Curueño Transect (based on Potent 2000). Please refer to Figure 5.8 for legend and notes.

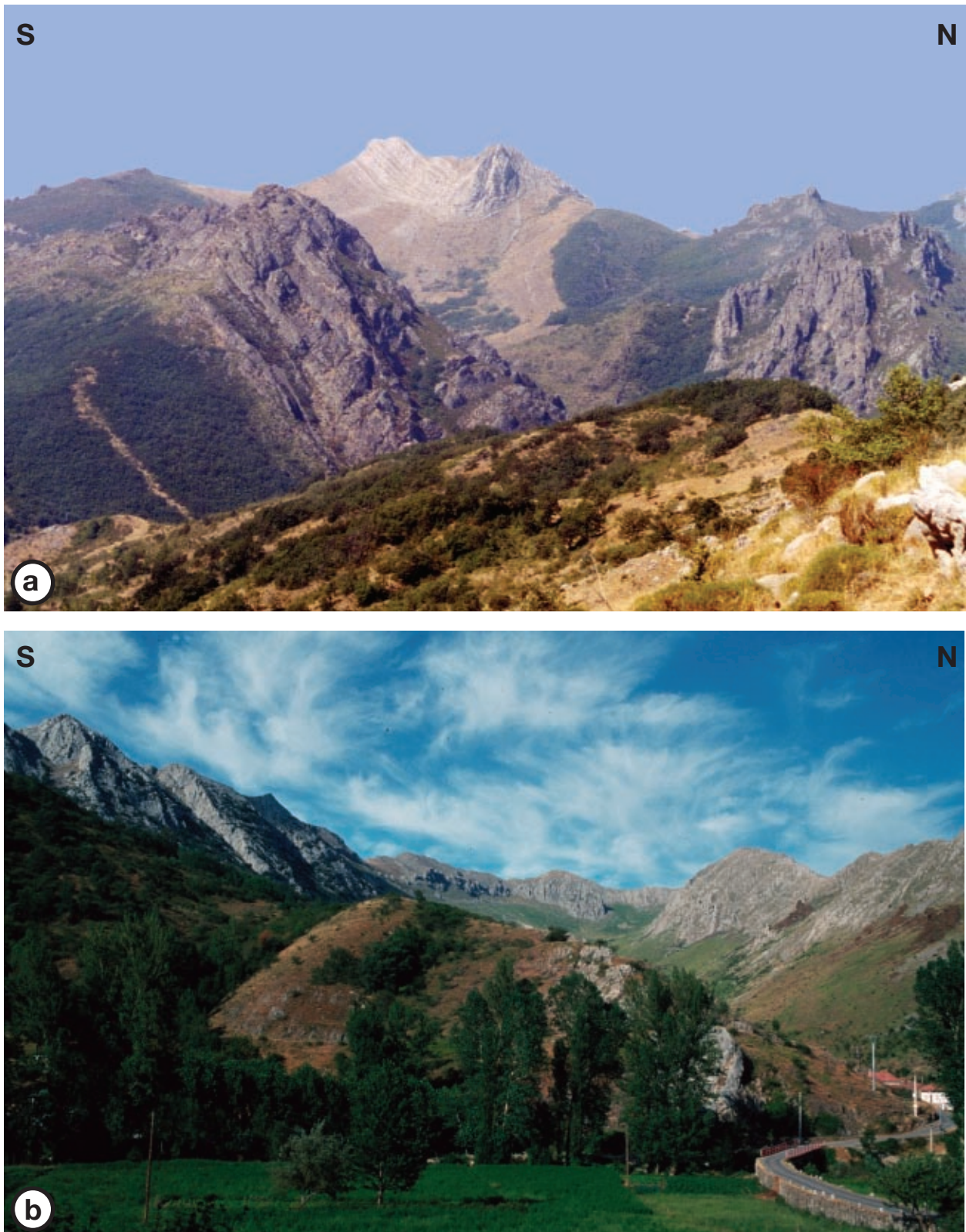


Fig. 5.11: View along the axial surface of the south-vergent, upright and gently to the west plunging Montuerto Syncline (see Fig. 5.10). (a) View to the west. Massive, brownish colored rocks in the foreground belong to the Barrios Fm., light-colored rocks in the background to the Santa Lucía Fm. of the Pozo Unit. (b) Opposed view to the east. Carbonatic ridges of the Gayo Unit highlight the centroclinal strike at the eastern termination of the Montuerto Syncline. The small ridge in the center consists of the Oville Fm. of the Pozo Unit, overlying the Gayo Unit (see Fig. 5.10).

of the Bodón Unit and pin line 1 (Fig. 5.10).

The Montuerto Syncline of the Gayo Unit is remarkably tight (Fig. 5.10 & 5.11). Its genesis may be explained by multiphase deformation. As proposed by Potent & Reuther (2000), the first deformation phase occurred in Westphalian B. Thrusting took place along the base of the Cambrian Láncara Fm., duplexes and fault-bend folds developed. During the second deformation phase in Westphalian B/C, the level of the detachment horizon shifted to the older Herrería Fm. An antiformal stack developed at the southern end of the cross-section, which is responsible for the steep dip of the southern limb of the Montuerto Syncline. Later deformation events further tightened the syncline (Potent & Reuther 2000).

### 5.3 Restoration of Cross-Sections

Due to the regional extent of the Barcaliente Fm. and the synchronicity of its base, its base was chosen as the reference horizon along which the stratigraphic package of the restored sections was re-constructed (Fig. 5.12).

As outlined above, pin lines are used as fix points to straighten out the deformed beds. In the Correcilla Unit of cross-section A-B, it was possible to place pin 1 (P1) vertically in the re-constructed, undeformed layer-cake sedimentary stack representing an approximation of an undeformed hinterland. P2 and P3 of cross-section A-B as well as P2 of cross-section E-F are local pin lines placed in the trailing edge of the thrust sheets. P1 of cross-section E-F is located parallel to the fold axis of the Montuerto Syncline.

Thrust sheets were restored in isolated blocks. Afterwards, the undeformed thrust sheets

were assembled along the common ramps. Figure 5.12 shows the undeformed sedimentary stack of both restored cross-sections. Sedimentary thickness variations as observed on the surface are taken into account when constructing the restored sedimentary package.

### 5.4 Results and Discussion

Calculated minimum shortening rates within each single thrust sheet ( $MSR_{TS}$ ) range between 19% and 54% (Tab. 5.1). The value for the Bodón Unit of cross-section A-B is not taken into account since the Bodón Unit has not been restored completely but only between the foot-wall ramp and P3. This is sufficient to calculate the distance between the stratigraphic columns of the Bodón and Gayo Units.

Overall minimum shortening rates were calculated between pin lines ( $MSR_{PL}$ ). They comprise large-scale deformation within the thrust sheet but additionally consider the amount of offset along the referring thrusts. As to be expected, the resulting values are higher than the  $MSR_{TS}$ .  $MSR_{PL}$  values range between 44.5% and 64.4% (Tab. 5.1). The value relating to the Correcilla Unit increases significantly when the amount of transport above the frontal ramp is taken into account: its offset is higher than that of the other units.

The value for the Gayo Unit of cross-section E-F is relatively high compared to the value within cross-section A-B. The structure within cross-section E-F differs strongly as expressed by the tightly folded Montuerto Syncline (see above; Fig. 5.10). Although Dahlstrom (1969) stated that in adjacent cross-sections the amount of shortening at a specific horizon between comparable reference lines must be nearly the same, he further outlined that this



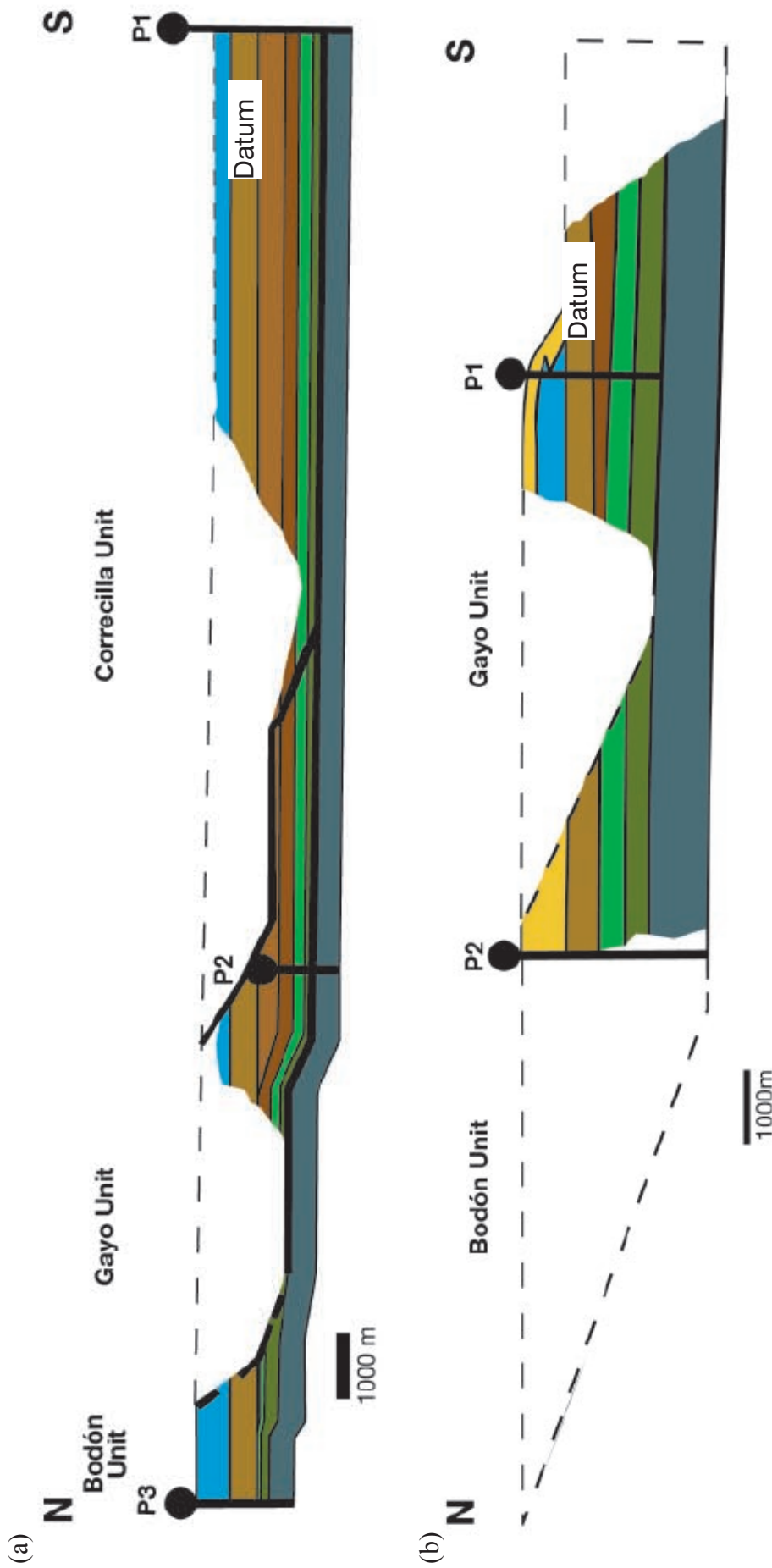


Fig. 5.12: Restored sections of cross-sections (a) A-B along the Torío Transect, and (b) E-F along the Curueño Transect. Sedimentary thickness changes are included in the illustration. Dashed lines bound the area missing due to erosion. Note the pin lines being vertical and parallel to each other and the initial ramp angles. Datum horizon is the top of the Barcaliente Fm.

Tab. 5.1: Results of the balanced cross-sections A-B and E-F.  $MSR_{TS}$ : minimum shortening rates within each single thrust sheet,  $MSR_{PL}$ : minimum shortening rates between pin lines.

Location	Minimum shortening rate	Initial hanging wall ramp angles	Horizontal separation distance between footwall and hanging wall cut offs	Calculated cumulative distances between stratigraphic columns along transects
----------	-------------------------	----------------------------------	---	---

**Cross-section A-B:**

**Shortening as calculated within each single thrust sheet ( $MSR_{TS}$ ):**

Forcada Unit				0m
Bodón Unit	7.5% *			9,360m
Gayo Unit	37,70%	20°	5,200m	16,200m
Correcilla Unit	19,10%	27° and 21°, resp. **	5,800m	26,800m

**Shortening as calculated between pin lines ( $MSR_{PL}$ ):**

P1 - P2	44,50%
P2 - P3	57,90%

**Cross-section E-F:**

**Shortening as calculated within each single thrust sheet ( $MSR_{TS}$ ):**

Forcada Unit	40 - 50 %***			0m
Bodón Unit	42%	19°	5,600m	11,730m
Gayo Unit	54,20%	20°	3,500m	21,000m and 26,455m, resp. ****

**Shortening as calculated between pin lines ( $MSR_{PL}$ ):**

P1 - P2	64,40%
---------	--------

\* measured only between footwall ramp and referring pin line (see Fig. 5.12a)

\*\* first value refers to the upper part of the ramp, second to the lower part (see Fig. 5.8)

\*\*\* Hinsch (1997)

\*\*\*\* first value refers to the northern limb of the syncline, second to the southern limb of the syncline (see Fig. 5.10)

does not apply if a tear fault exists in-between. A tear fault is a geometrically special case of a lateral ramp (Fig. 5.5) and therefore an indicator for out-of-plane movement. As outlined above, a lateral ramp is present in the Bodón Unit of the northern part of the Curueño Valley. Additionally, the antiformal stack in the south of the Montuerto Syncline further tightened and therefore shortened the Gayo Unit. Julivert & Arboleya (1986, 1984) proposed values of 40-50% for north-south directed shortening, whereas Dallmeyer et al. (1997) estimated shortening values of between 50% and 75%. Potent (2000) calculated a 60% minimum shortening rate for the Gayo Unit of a cross-section, which roughly coincides with the position of cross-section E-F.

This study and the one by Potent (2000) consider minimum shortening only. Consequently, shortening rates, which would include internal

deformation, would be even higher. Values as proposed by Julivert & Arboleya (1986, 1984) seem to be too low.

Cutoff angles of frontal ramps are commonly between 10° and 30° (Fermor 1999, McClay 1992, Suppe 1983). Generally, values for ramp angles come to about 20° (Fermor 1999, Suppe 1983). Julivert & Arboleya (1984) reported footwall ramp angles of up to 32.5° in the Cantabrian thrust belt.

The restored cross-sections show initial hanging wall ramp angles of about 20°. Only the upper part of the hanging wall ramp of the Correcilla Unit is restored to an angle of 27°. However, thrust planes often listrically increase dip toward their upper part.

Based on the line length of the balanced cross-sections and the calculated minimum

shortening rates, cumulative distances between the measured stratigraphic columns along the transects are calculated and used as input parameters for reverse and forward modeling. Table 5.1 provides an overview of all results.

The length of the restored cross-section A-B totals 26.8km. Cross-section E-F, which in the recent deformed state is significantly shorter than the other section, initially had a length of 26.5km.

Finally, it should be noted that due to the scope of this study, influencing factors such as tectonic compaction (Hossack 1979), pressure solution (Woodward et al. 1989) and internal deformation, were not integrated. The resulting values are to be understood as an approximation.





## CHAPTER 6: SUBSIDENCE ANALYSIS

Reverse modeling was carried out for all three transects (see Fig. 5.1 for position of transects). Analysis of the north-south directed Torío and Curueño Transects incorporates the full Paleozoic basin succession from the Cambrian Herrería Fm. (560Ma) up to the San Emiliano Fm. (312Ma).

Quantified subsidence values were acquired by stratigraphic 2D-reverse modeling using PHIL<sup>TM</sup> software (PetroDynamics Inc.).

Results are compared to subsidence studies, which were carried out by Veselovsky (2004) along the north-south directed Bernesga Transect, located west of this field area along the Bernesga Valley.

Time increments will be cited by the time line, which is located at the top of the increment. For example, increment 319.5Ma refers to the time increment from 322Ma to 319.5Ma. To refer to the basal time line of an increment, compare with Tables A.2 - A4.

Negative subsidence values indicate uplift, positive values indicate subsidence.

### 6.1 Database

#### *Time Lines*

Time lines were established using biostratigraphic data, stratigraphic correlation and sequencestratigraphic interpretation. All available biostratigraphic data for the Carboniferous have been calibrated to the absolute time scale as displayed in Figure 3.3. For older formations, literature sources were used as cited in Chapter 3.

A total of 37 time layers have been used for

backstripping of the western and west-east directed transects, 34 time layers were used for the eastern transect.

#### *Sedimentary Thickness*

Values of thicknesses of Lower Paleozoic formations are mostly derived from the extensive literature whereas Carboniferous data are a synthesis of information gathered from field work and from literature. The thicknesses of Mesozoic rocks were projected from the south and southeast into the study area. The overall thickness of the eroded sedimentary cover younger than Westphalian C is unclear (see Chapter 3.3 for discussion). Estimations are based on CAI and IC values. However, existing studies (Chapter 3.3) constrain the possible thickness of eroded cover rocks insufficiently. Calculations range between 1,000 and 5,000m in thickness, although most authors agree on a thickness between 1,000 and 2,100m. Fig. 6.1 shows subsidence curves calculated for 1,000 and 2,000m in thickness of cover rocks, respectively. On average, differences between the curves are in the range of 0 - 5m/Ma. Only for increments 316Ma to 315Ma does the differing amount range between 12 - 20m/Ma. These increments were calculated with highly compactable fine-grained siliciclastics, which show a higher impact of the thickness of the overlying rocks. Nevertheless, using 1,000 or 2,000m thickness of cover rocks, does not significantly affect the resulting subsidence values, which will be further discussed below. Within this study, a thickness of 1,000m was used for the sedimentary cover younger than Westphalian C. Tables A.2 - A.4 list all input

data used for reverse modeling.

### *Paleobathymetry and Sea-Level Curve*

A composite eustatic sea-level curve (Fig. 6.2) was assembled using the following literature sources (modified based on Veselovsky 2004):

0-70Ma	Haq et al. 1987, Mitchum et al. 1991
70-160Ma	Haq et al. 1987, Kendall et al. 1992
160-256Ma	Haq et al. 1987
256-355Ma	Heckel 1986, Ross & Ross 1988, 1987
355-410Ma	Dennison 1985, Johnson et al. 1985
410-438Ma	Ross & Ross 1996
438-540Ma	Ross & Ross 1988
540-560Ma	Vail et al. 1977

Additionally, paleo-water depth along the time lines was determined using facies analysis (Chapter 3.2) for the Upper Carboniferous formations and literature values if available (Tab. A.2 - A.4). Rapid lateral facies changes occur within the unstable platform environment of the Valdeteja Fm. due to its vicinity to the basin margin toward the north and also to the east.

### *Flexural Parameters*

Veselovsky (2004) gave an overview of flexural parameters of the lithosphere in general and also for the Southern Cantabrian Basin. Only some major facts are outlined below.

The common model for describing the flexural response of the lithosphere to applied loads is the assumption of a visco-elastic plate overlying a viscous fluid (asthenosphere) (Cloetingh &

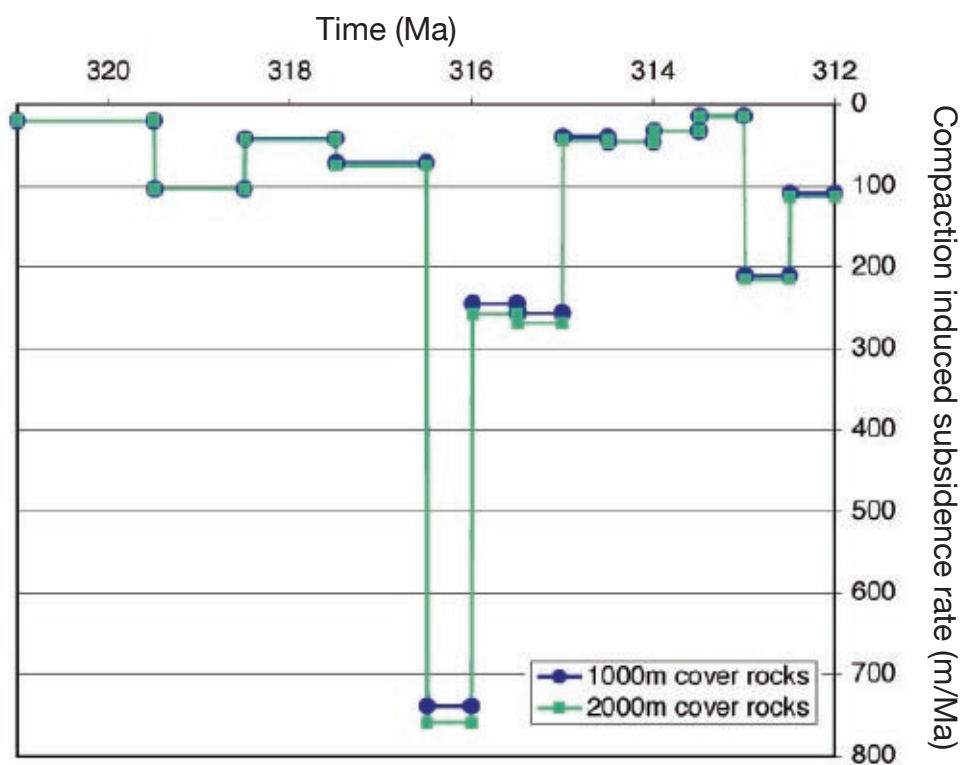


Fig. 6.1: 1D-curves of compaction induced subsidence rates (y-axis) comparing the effect of varying thickness of cover rocks younger than the Westphalian C on subsidence of increments 319.5Ma - 312Ma (x-axis). No other input data were varied other than the thickness of the cover rocks. Differences between the curves are suspiciously low. Calculated at location Lavandera (Bodón Unit).



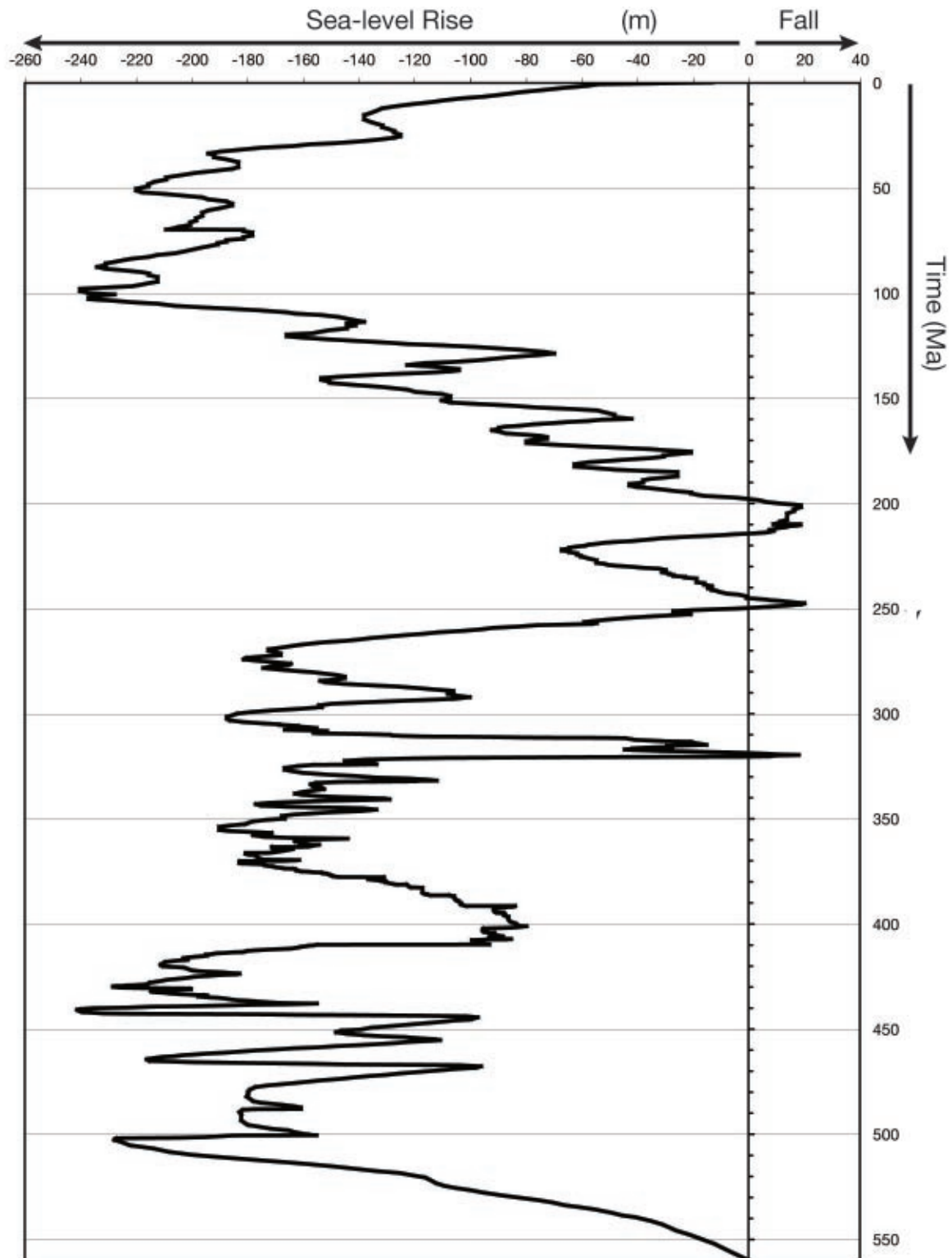


Fig. 6.2: Composite eustatic sea-level curve assembled from literature data (see text).

Burov 1996, Einsele 2000, Turcotte & Schubert 2002, Waschbusch & Royden 1992, Watts 1992, 2001). The effective or equivalent elastic thickness  $T_e$  characterizes the apparent strength of the lithosphere (Burov & Diament

1995, Cloetingh & Burov 1996, Einsele 2000, Stüwe 2000; mathematical derivations can be found therein).

Oceanic and continental lithosphere show widely differing geological history and there-

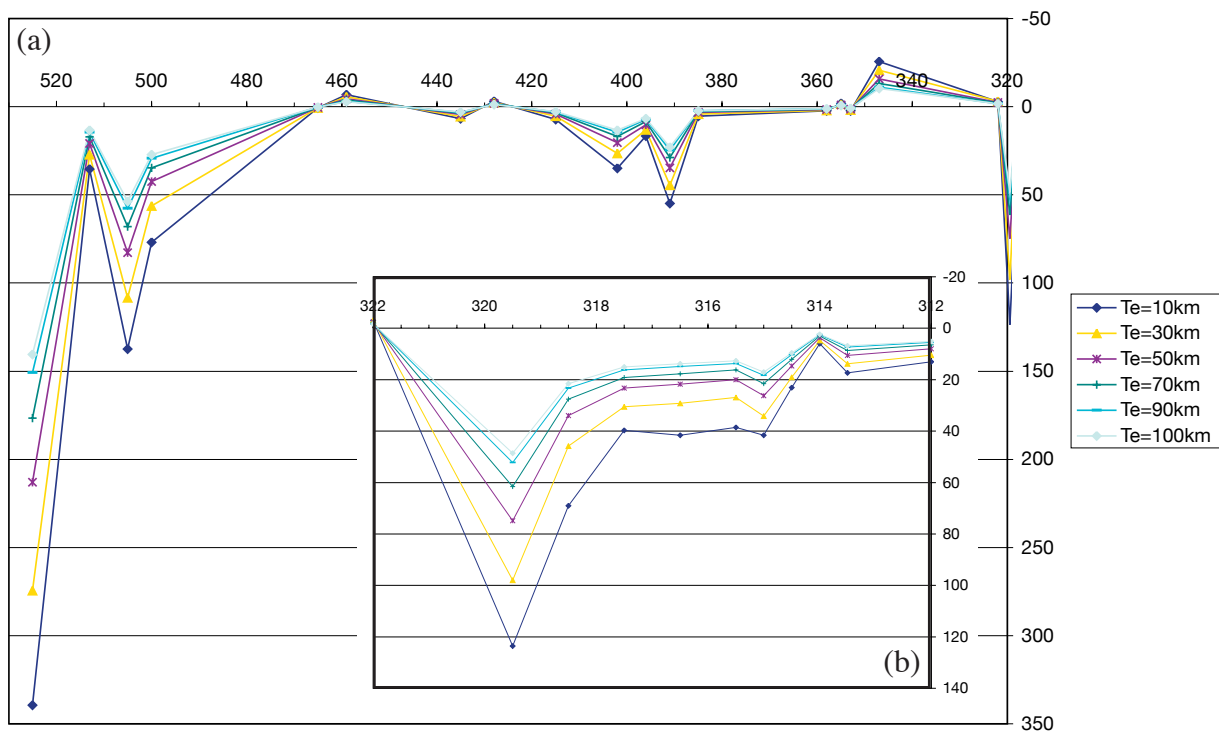


Fig. 6.3: Comparison of the effect of varying  $T_e$ -values on the flexural-induced subsidence rates, calculated at location Las Hoces de Correcilla (Correcilla Unit) at the southernmost termination of the Torío Transect. (a) Paleozoic basin fill, (b) Carboniferous basin fill. Y-axis: flexural-induced subsidence rate (m/Ma), x-axis: time (Ma).

fore  $T_e$  values vary strongly. Continental  $T_e$  values are up to 4-5 times higher than those for the oceanic realm.  $T_e$  of the oceanic lithosphere is determined by the isotherm at the base of the mechanical lithosphere (wet/dry olivine rheology; Turcotte & Schubert 2002). Values between 400°C and 900°C are in discussion for the position of this isotherm (Burov & Diament 1996, Cloetingh & Burov 1996, Einsele 2000, McKenzie & Fairhead 1997, Ranalli 1994, Stockmal et al. 1986, Watts 1992).

Continental lithosphere shows a more complex geological evolution than the oceanic lithosphere. Loads may have existed for a far longer period; (tectonic) erosion, denudation, and orogenesis obscure the geological evidence and determination of  $T_e$  values during time (Watts 2001). If the crust thickens significantly (>35km) and if high temperatures are reached at the Moho depth, mechanical decoupling between the crust and mantle lithosphere may

occur, resulting in a significant reduction of  $T_e$  (Burov & Diament 1996, Burov et al. 1998, Cloetingh & Burov 1996). Gutiérrez Alonso et al. (2004) proposed mechanical decoupling to have occurred below the Asturian Arc during the Permian (see Fig. 2.6).

Together, the age of the lithosphere and its relation to plate configuration at any time as well as the depth of the Moho are important factors for determining  $T_e$ .

The Cantabrian Zone has a complex history of tectonic realms. From late Precambrian until Silurian, an extensional regime prevailed, followed by inversion of the tectonic regime resulting in the Variscan Orogenesis.

Cloetingh & Burov (1996) proposed a  $T_e$  of 15km for the Lower Paleozoic, increasing to 60 km for the Upper Paleozoic of the Cantabrian Zone. Zoetemeijer (pers.com. 2003 in Veselovsky 2004) suggested a value of 50-100km, comparing it to a North American

type of lithosphere. To quantify the influence of the  $T_e$ -value on the resulting subsidence rates, flexural subsidence rates were calculated with  $T_e$ -values varying between 10km and 100km at the location “Las Hoces de Vegacervera” (Torío Transect, Correcilla Unit), which shows the most complete stratigraphic record within the modeled transects. Results vary significantly depending on the  $T_e$ -value used (Fig. 6.3). Comparing the flexural subsidence values calculated with  $T_e=50$ km with the flexural subsidence values calculated with  $T_e=10$ km and 100km, the former resulted in up to 60% higher values, whereas the latter resulted in up to 70% lower values.

However, it has to be considered that flexural subsidence rates are only a part of the total subsidence rates (i.e. 9-14%, see below), as shown in Figure 6.6a,c.

The reverse modeling software employed allows only one mean  $T_e$  value for the whole succession modeled. The primary aim of this subsidence analysis is to compare and analyze the subsidence curves of the whole Paleozoic succession with the study of Veselovsky (2004) and additionally to analyze the Carboniferous setting in more detail. Veselovsky (2004) used an average value of  $T_e=35$ km, which was adopted for the modeling of the Paleozoic basin fill. However, during the Carboniferous, the lithosphere was thickened due to the orogenesis. The assumed delamination occurred within the Permian (see Chapter 2.1.2; Gutiérrez Alonso et al. 2004). Therefore, the subsidence results of the Carboniferous succession were calculated with  $T_e=60$ km.

Flexural calculations of the software follow studies of Bowman & Vail (1999), Dickinson et al. (1987) and Turcotte & Schubert (1982, 2002).

### *Lithologies and Compaction*

PHIL<sup>TM</sup> software provides predefined parameters for 11 siliciclastic and 8 carbonate/evaporitic lithologies (Bowman & Vail 1999). Compaction is calculated as a function of burial depth, using the following algorithm:

$$\Phi(z) = \frac{\Phi_0}{1 + (z * r_c)}$$

$\Phi$ : porosity;  $z$ : depth (m);  $\Phi_0$ : initial porosity;  $r_c$ : compaction coefficient (Bowman & Vail 1999).

The program includes average values for initial porosities, bulk rock densities, and compaction rate, which were adopted in this study. However, the comparison of compaction induced subsidence rates as a function of the thickness of the cover rocks as shown in Figure 6.1 resulted in very small differences of the subsidence rates. Apart from the thickness of the cover rocks, the input data were not varied within the modeling runs used to produce the curves as shown in Figure 6.1. Therefore, it should be taken into account that the software may be underrating the effects of compaction within its algorithm for compaction induced subsidence rates.

The software is not capable of considering lateral, but only vertical changes to lithological parameters in reverse basin modeling. This is considered to be critical for the Bashkirian-Moscovian platform-to-basin transitional setting along the Bodón Transect, since the compaction curve for basin mudstones and platform limestones differs greatly (Fig. 6.4). Therefore, the critical locations and time increments were modeled separately in various steps in a pseudo-1D approach. The results were later assembled and incorporated into the original west-east directed Bodón Transect.



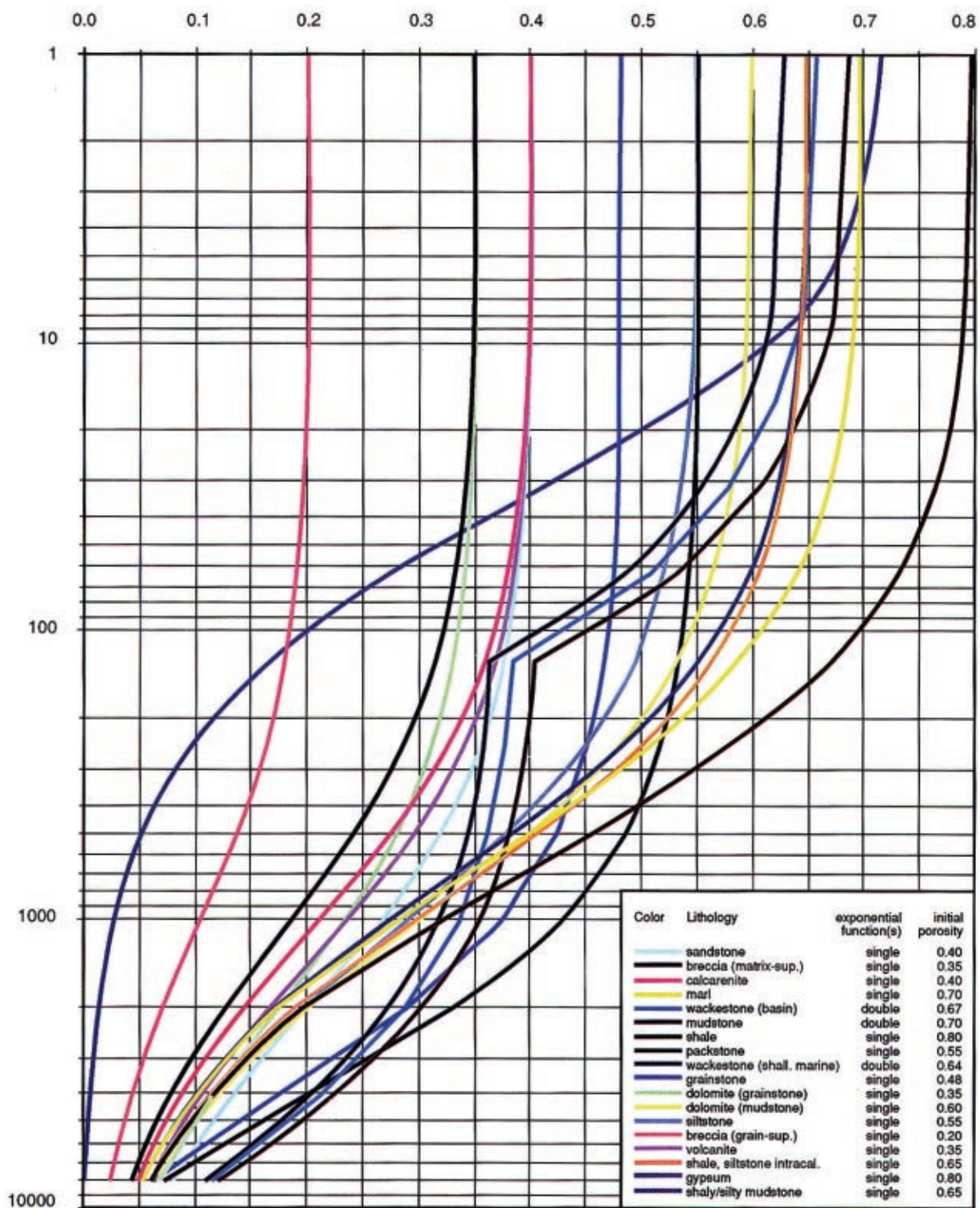


Fig. 6.4: Logarithmic plot of initial porosities (x-axis) versus burial depth (y-axis). Data were assembled by Veselovsky (2004) from Goldhammer (1997) and Welte et al. (1997).

## 6.2 Pre-Carboniferous Basin Fill

### 6.2.1 Results

Figure 6.5 displays the graphic output of the reverse modeling program for the Torío Transect. It shows significant stages within

the development of the Southern Cantabrian Basin during the Paleozoic as recorded by the sedimentary deposits available. The stages are further outlined below (Chapter 6.2.2) and marked in Figure 6.8. The positions of the

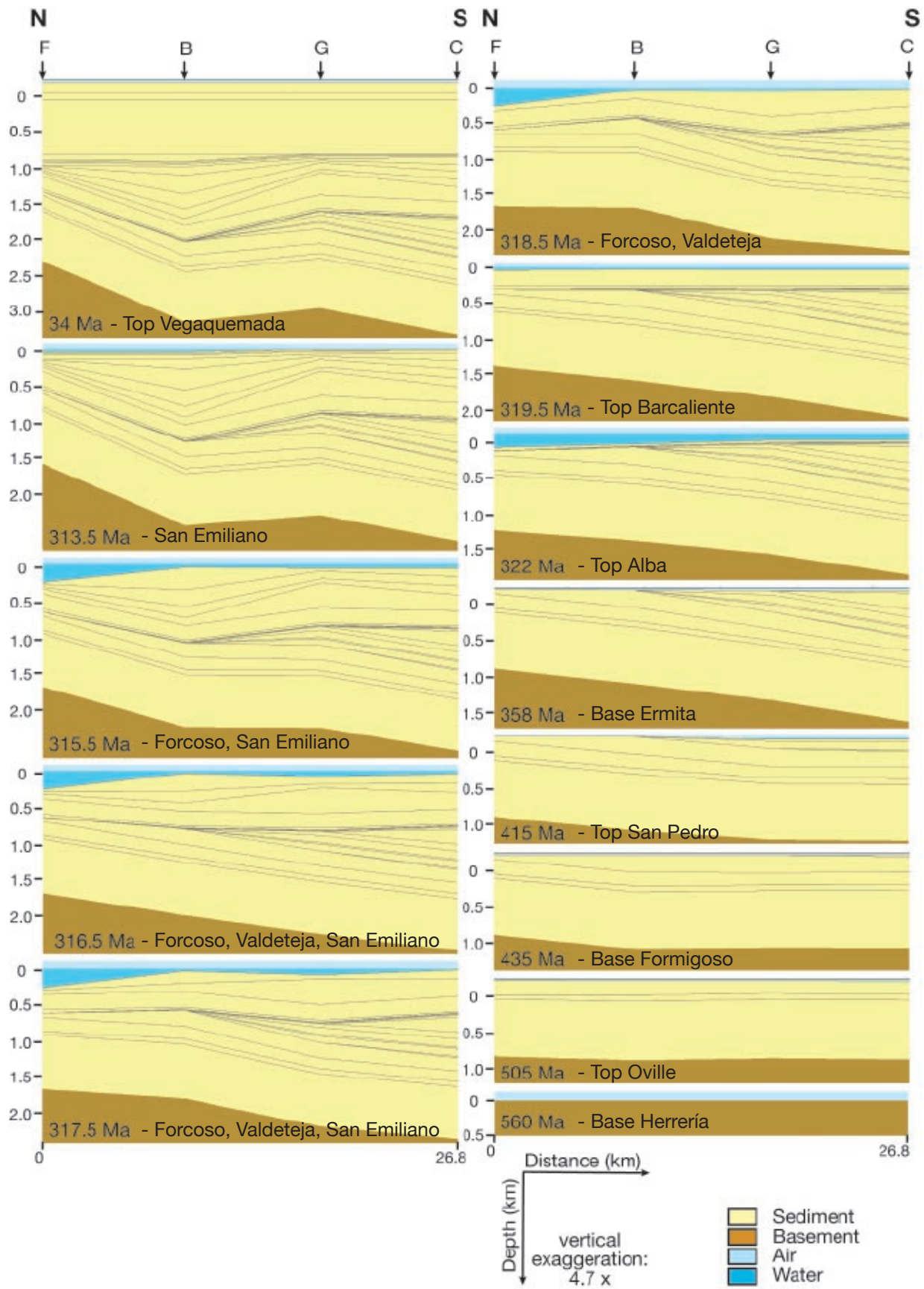


Fig. 6.5: Graphic output of PHIL™ of the north-south directed Torio Transect. Black lines represent time lines. The modeling program calculates the subsidence rates at the specified locations and interpolates along the transect, which generates a rather “edgy” appearance of the time lines. For each increment, the referring formation is cited. The position of the transects and the referring stratigraphic profiles is shown in Fig. 5.1b and A.1. Indices on top of the figure refer to stratigraphic profiles measured in the referring tectonic unit; F: Forcada Unit, B: Bodón Unit, G: Gayo Unit, C: Correcilla Unit.

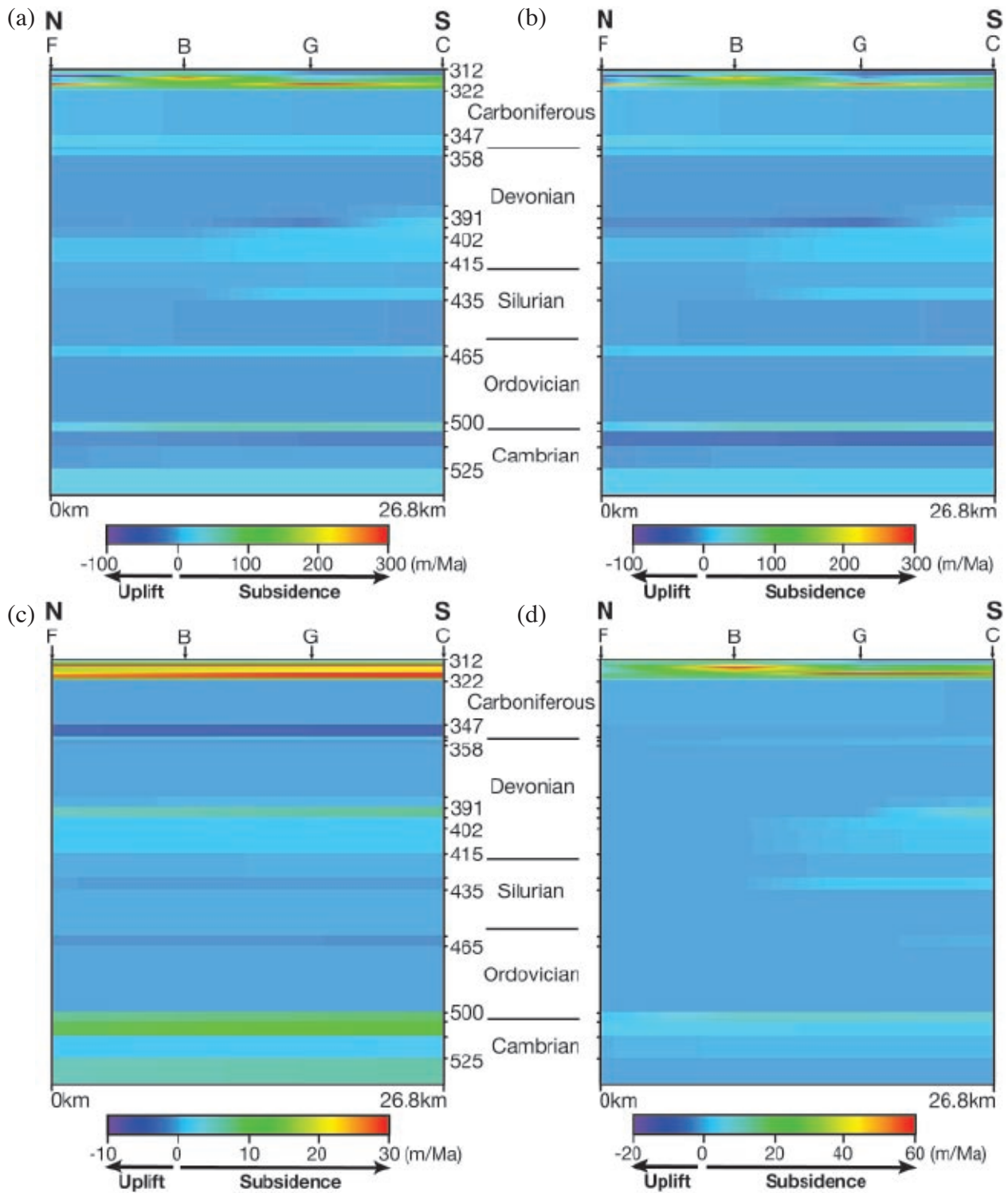


Fig. 6.6: Spectral plots of subsidence rates of the Torío Transect, calculated with PHIL<sup>TM</sup> version 1.5. The y-axis shows the time in Ma, the x-axis displays distance along transect. Subsidence rates are visualized by colors. The range of shown subsidence rates varies in order to visualize high and low values. For quantified input values, compare with Table A.2. (a) Total subsidence rates, (b) thermo-tectonic subsidence rates, (c) flexure-induced subsidence rates, (d) compaction induced subsidence rates. Indices on top of the figure refer to stratigraphic profiles measured in the referring tectonic unit; F: Forcada Unit, B: Bodón Unit, G: Gayo Unit, C: Correcilla Unit.



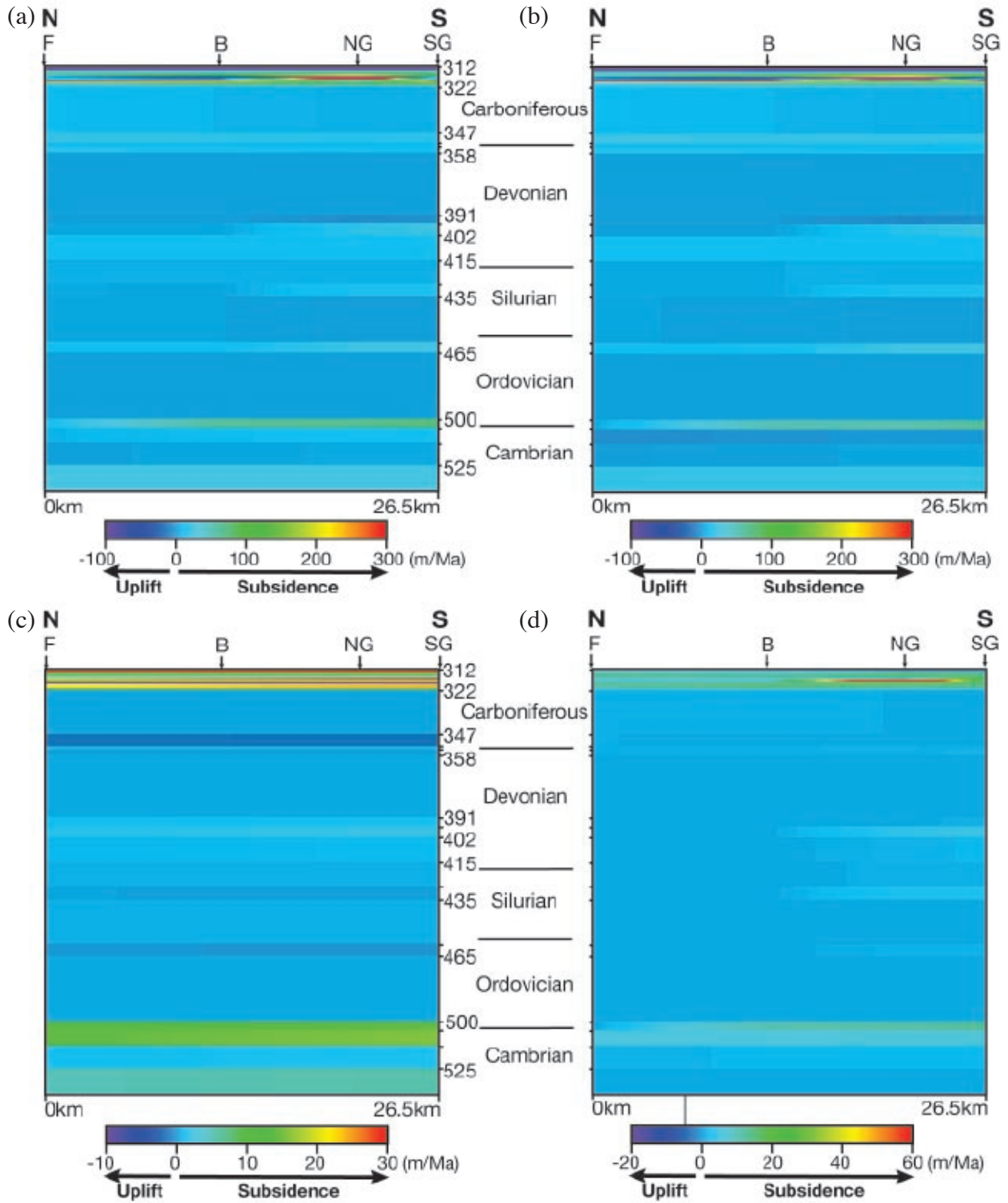


Fig. 6.7: Spectral plots of subsidence rates of the Curueño Transect, calculated with PHIL™ version 1.5. The y-axis shows the time in Ma, the x-axis displays distance along transect. Subsidence rates are visualized by colors. The range of shown subsidence rates varies in order to visualize high and low values. For quantified input values, compare with Table A.4. (a) Total subsidence rates, (b) thermo-tectonic subsidence rates, (c) flexure-induced subsidence rates, (d) compaction induced subsidence rates. Indices on top of the figure refer to stratigraphic profiles measured in the referring tectonic unit; F: Forcada Unit, B: Bodón Unit, NG: northern Gayo Unit, SG: southern Gayo Unit.

recorded stratigraphic columns are marked within the transect. Movies of the graphic output of all transects are attached in the appendix on CD-ROM media.

Up until 505Ma, sedimentary distribution was uniform across the transects. Subsequently, uplifting of the northern and northeastern area caused hiatus. Until 435Ma, very little sedimentation occurred. The overall geometry prior to 358Ma shows a northern, uplifted zone with little to no sedimentation whereas the southernmost Correcilla Unit is an area of subsidence. Units located in distal parts in the south of the transect accumulated significantly higher amounts of sediments than proximal parts in the north of the transect (Fig. 2.9 and Bernesga Transect of Veselovsky 2004). Following increment 358Ma, a transgression to the northeast terminated the hiatus in the northern part of the transects. A local uplift developed within the transects. The Torío Transect cuts only the northern part of the uplift, as reflected by the higher water depth of the northern Forcada Unit in increment 322Ma. The subsequent Barcaliente Fm. (319.5Ma) shows an increasing influence of the Variscan Orogeny, a foredeep developed in front of the approaching orogen. Increments 322Ma to 312Ma will be discussed in detail in Chapter 6.3.

The spectral plots of Figures 6.6 and 6.7 show the distribution of total ( $S_{tot}$ ), thermo-tectonic ( $S_{tect}$ ), flexure ( $S_{flex}$ ) and compaction ( $S_{comp}$ ) induced subsidence rates during time along the Torío and Curueño Transects. Logically, total subsidence rates reach the highest values. Thermo-tectonic subsidence rates represent the major portion of the total. The average percentage of the flexure induced subsidence

component is 14% of  $S_{tot}$  (Torío Transect) and 9% of  $S_{tot}$  (Curueño Transect), respectively. Compaction induced subsidence rates are slightly higher; the maximum percentage of  $S_{tot}$  is 23% within the Torío Transect and 20% within the Curueño Transect. The spatial pattern of all components is similar. However, some features may be more distinct in one component compared to others, as will be outlined below.

During the pre-Carboniferous modeled period,  $S_{tot}$  values range between -13m/Ma and 54m/Ma for the Torío Transect, and -11m/Ma and 81m/Ma for the Curueño Transect.  $S_{tect}$  reaches values between -22m/Ma and 46m/Ma (Torío Transect) and -12m/Ma to 67m/Ma (Curueño Transect). Values for  $S_{flex}$  are very low due to the distal position of the transect: up to 10m/Ma (Torío Transect) and up to 16m/Ma (Curueño Transect). For  $S_{comp}$ , a maximum of 9m/Ma is reached for the Torío Transect and 14m/Ma for the Curueño Transect.

$S_{tect}$  accounts for the highest portion of  $S_{tot}$ . Hence, further evaluation will be based on  $S_{tect}$  values.

### 6.2.2 Discussion

In general, the calculated subsidence rates are very low for the time before the Carboniferous as cited above. The transects cover the transition from the predominantly uplifted Cantabrian-Iberian High into proximal parts of the Southern Cantabrian Basin. Higher subsidence rates occur in the central part of the Cantabrian Basin. However, certain trends in time can be identified within the Paleozoic succession (Fig. 6.8).

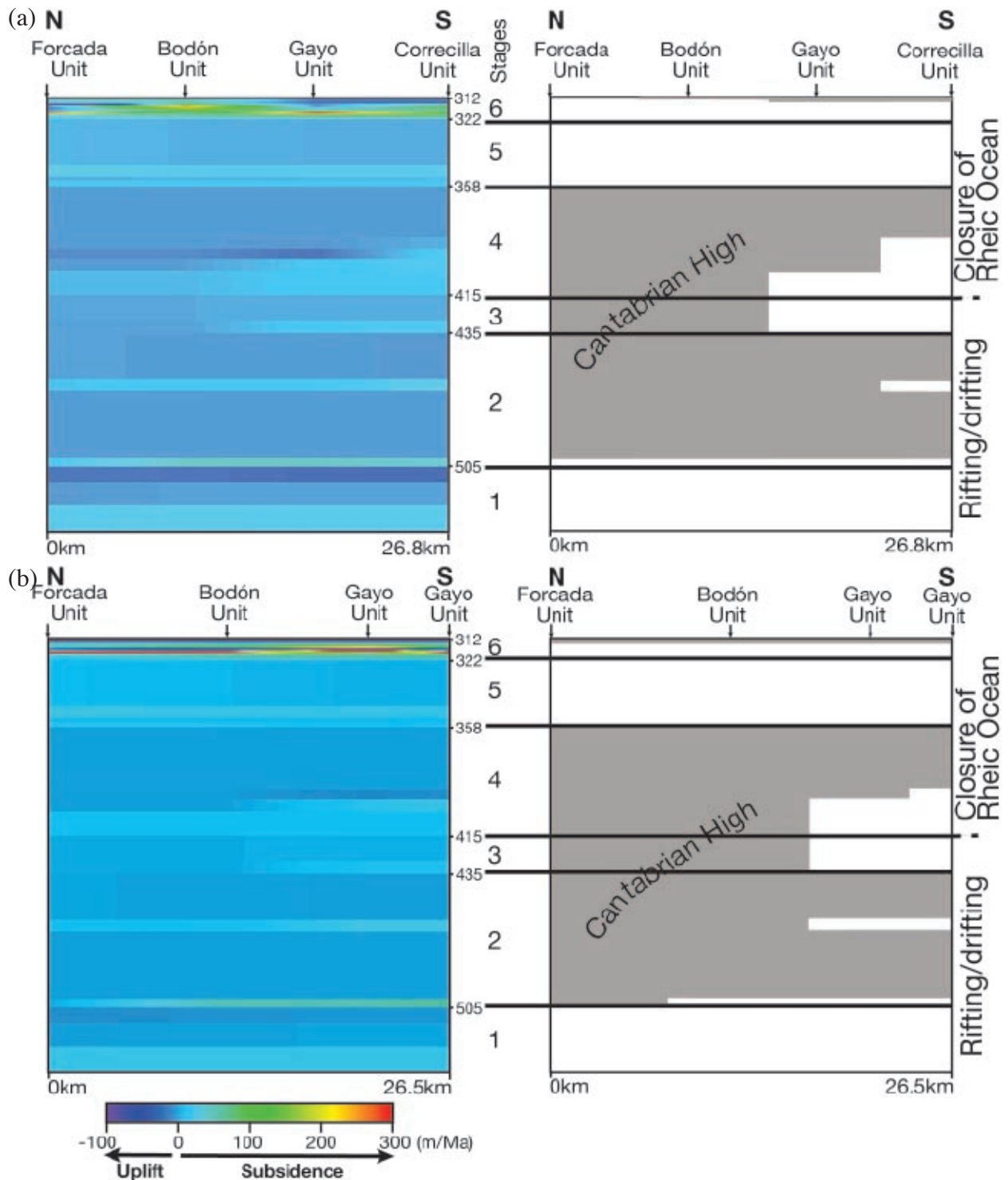


Fig. 6.8: Distinguished stages of the Paleozoic basin fill in relation to the geodynamic setting. To the right, the distribution of hiati (shaded area) versus sedimentation (white area) and division into basin stages following Veselovsky (2004) is shown. To the left, the referring spectral plots of thermo-tectonic subsidence rates are displayed (see also Fig. 6.6b and 6.7b). (a) Torío Transect, (b) Curueño Transect.

Stages 1 and 2 took place during an overall rifting/drift regime, which finally created the Rheic Ocean. Then, the tectonic regime was inverted and the Rheic Ocean successively closed during stages 4-6. The last stage displays the setting of the foreland basin system in front of the approaching Variscan Orogen. Figures 6.12 & 6.13 show an enlarged and refined spectral plot of the last stage.



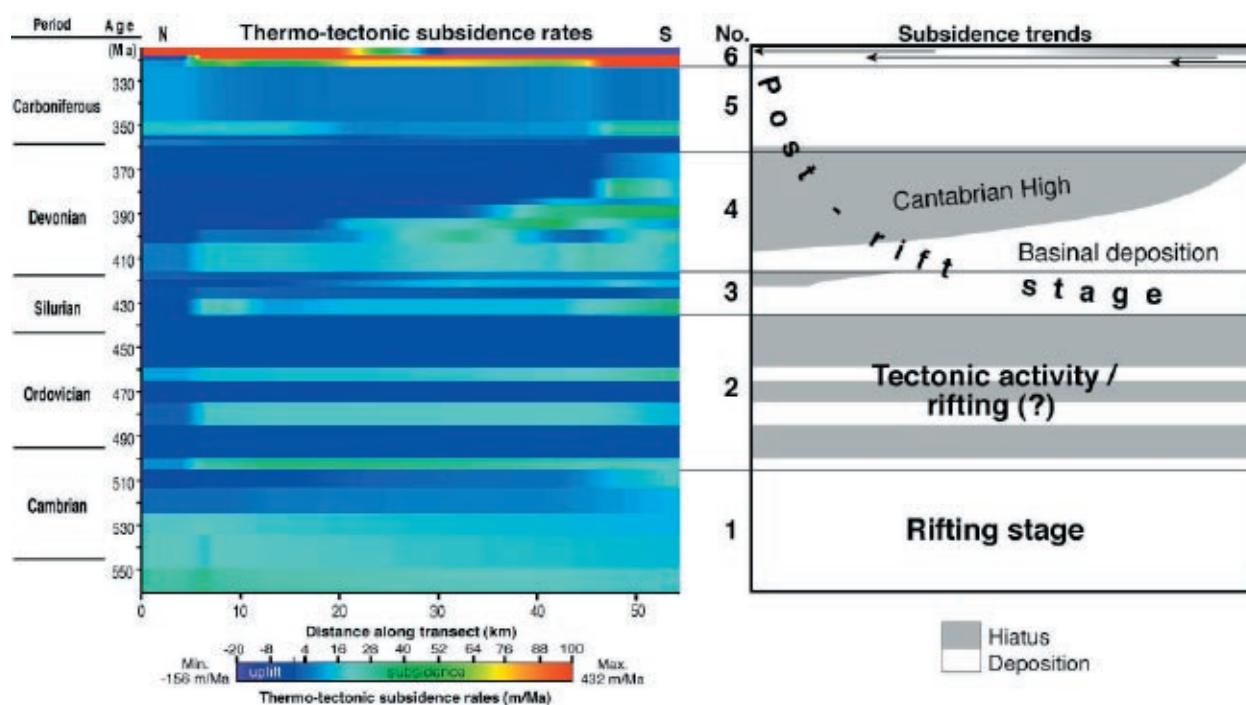


Fig. 6.9: For comparison, thermo-tectonic subsidence rates and interpretation of stages of the Bernesga-Transect by Veselovsky (2004).

Veselovsky (2004) carried out subsidence analysis for the Bernesga Transect, which is located one valley further to the west and parallel to the transects investigated here. Six trends were established within the Paleozoic succession (Fig. 6.8 & 6.9). Although the transects in this study do not extend as far to the south as the Bernesga Transect (Bernesga Transect: 54km, Torío Transect: 26.8km, Curueño Transect: 26.5km), essentially the same trends are apparent (Fig. 6.8) as described by Veselovsky (Fig. 6.9). However, due to the paleogeographic and sedimentological situation, some modifications apply.

The boundary between stage 1 (560Ma - 505Ma) and 2 (505Ma - 435Ma) is set within the uppermost part of the Oville Fm. Veselovsky (2004) interpreted this as the turn-over point from rising to falling relative sea-level. The subsequent Barrios Fm. represents a regressive state; its top is highly diachronous.

Within the Bernesga Transect, the Tanes Mb. is present, whereas in the Torío Transect only the older La Matosa Mb. is preserved (Vilas Minondo 1971), followed by a long hiatus. In the Forcada Unit of the Curueño Transect, no Barrios Fm. is recorded at all. Due to sea-level fall, the proximal areas are increasingly influenced by the Cantabrian-Iberian High (see Chapter 2.2). Based on distribution of the preserved record, the uplifted area must have been positioned in the north and (north-) east of the transects.

In contrast to the Bernesga Transect, the Forcada and Bodón Units of the Torío and Curueño Transects show a continuous hiatus starting at the top of the Barrios Fm. (lowermost Ordovician, 500Ma and 505Ma, respectively) until the base of the transgressive Famennian Ermita Fm. (358Ma). Consequently, stage 2 has hardly any sedimentation in the Torío and Curueño Transects. Only a few meters of the Capas de Getino can be found in the field area

(Vilas Minondo 1971). The duration of this long hiatus decreases successively to the west and south.

With the beginning of stage 3 (435Ma - 358Ma), Silurian basinal deposits onlap on the Ordovician Barrios Fm. After a rapid ingression of the sea, a regressional cycle was established (Veselovsky 2004). Within the Bernesga Transect, this trend was ended by the overall flooding during deposition of the La Vid Group. In the Torío and Curueño Transects, this pattern cannot be confirmed by available data. Uplifted areas were obviously situated in the northeast of the study area, being more proximal to the Torío and Curueño Transects than the Bernesga Transect. Additionally, in the southeast, the Pardamino High restricted the available accommodation space (Keller 1988).

A basinward shift of coastal onlap dominates the following stage 4, resulting in a hiatus across the complete length of the Torío and Curueño Transects from 385Ma to 358Ma, which matches the pattern within the Bernesga Transect.

The onset of stage 5 (358Ma - 322Ma) is characterized by transgression from the SW across the whole field area. Deposition occurred throughout all transects. The field area was tectonically relatively stable at this time. During stage 6, Variscan deformation affected the large-scale geometry of the depositional environments. Stage 6 is elaborated in detail below.

### 6.3 Carboniferous Basin Fill

The development of the sedimentary system within the Upper Carboniferous can be better understood by modeling two parallel, north-

south directed transects (Torío and Curueño Transects, as above) and additionally a west-east directed transect connecting across the Bodón Unit (Bodón Transect).

The preserved sedimentary record ends within increment 312Ma at Lavandera (Bodón Unit). Due to deformation, sedimentary record ends earlier within the other parts of the field area (see Fig. 4.3). For modeling, a hypothetical sedimentary wedge was superimposed on the area for the duration of the missing increments until increment 312Ma in order to include the complete stratigraphic record of location Lavandera into the modeling process. The shape of the sedimentary wedge was deducted from the results of the Kübler indices measurements of Marschik (1992; Chapter 3.3). Values referring to this hypothetical cover will not be included into the discussion.

#### 6.3.1 Results

Figures 6.5 and 6.10 show the graphic output of the reverse modeling program. Locations of recorded stratigraphic columns are marked by arrows and indices.

The lower part of the Barcaliente Fm. (increment 319.5Ma) was deposited within a relatively undifferentiated, stable environment. Within the graphic overview of the transects, increment 318.5Ma shows the first stage of differentiation into a shallow platform area (Valdeteja Fm.) and the adjacent basin of the Forcoso Zone to the east, shown within the figures by the increased water depth. The Curueño Transect consisted entirely of basin deposits at this stage (Fig. 6.10b). Increments 316.5Ma and 315Ma visualize the overall aggradation pattern of the platform by increased thicknesses of the layers. However, the onset

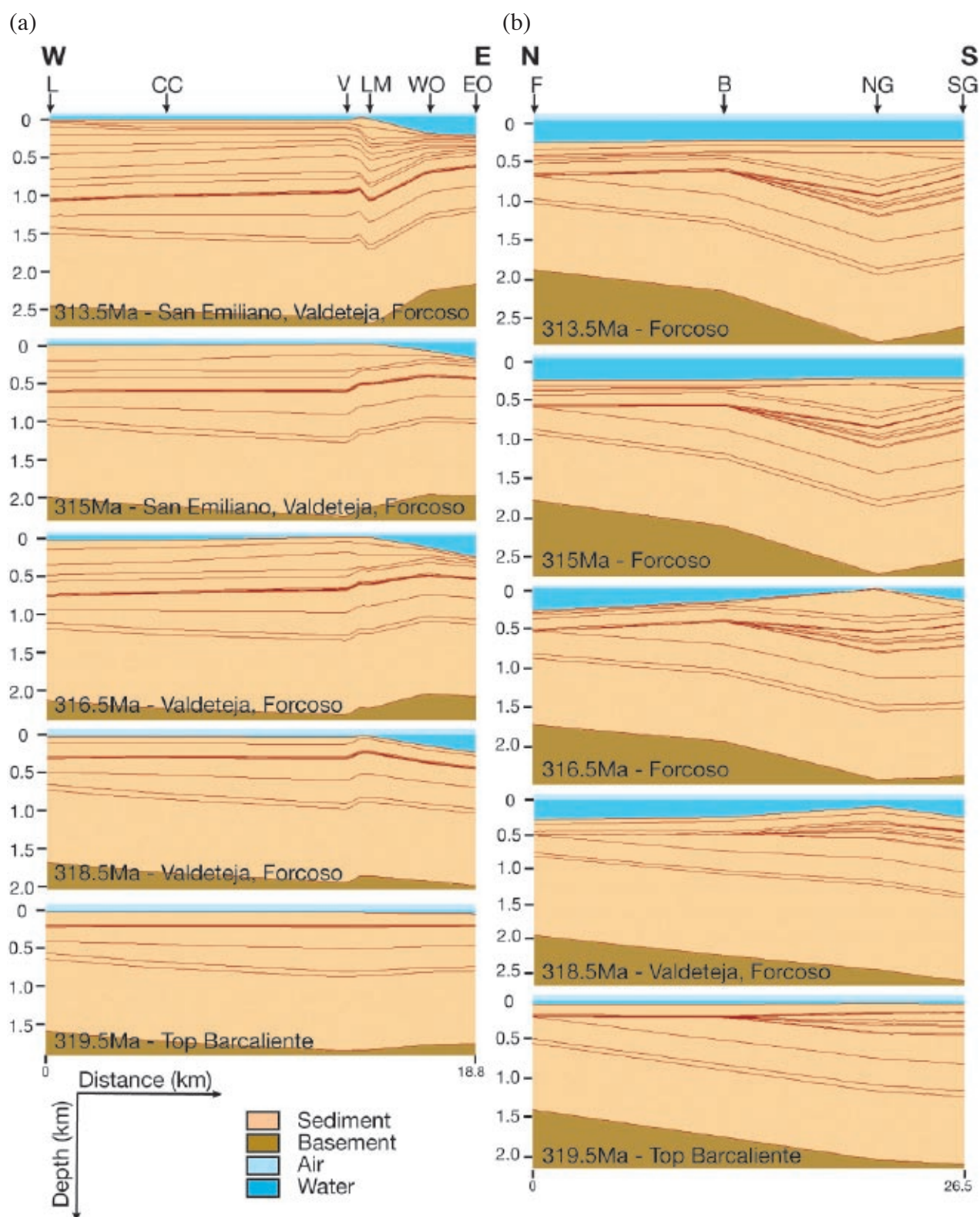


Fig. 6.10: Graphic output of PHIL™ version 5.5.4. (a) West-east directed Bodón Transect, vertical exaggeration factor is 3.3. (b) North-south directed Curueño Transect, vertical exaggeration factor is 4.7. Red lines represent time lines. For each increment, the referring formation is cited. The position of measured stratigraphic profiles is marked by arrows and indices on top of the figure. L: Lavandera, CC: Coto Cabañas, V: Valdeteja, LM: Las Majadas, WO: west of Oville, EO: east of Oville; F: Forcada Unit, B: Bodón Unit, NG: northern Gayo Unit, SG: southern Gayo Unit. The stratigraphic profiles are attached in the appendix. The position of the transects and the referring stratigraphic profiles is shown in Figures 5.1b and A.1.



of the siliciclastics of the San Emiliano Fm. after increment 316.5Ma is not to distinguish within the graphics of Figures 6.5 and 6.10. The sedimentary thickness of this increment varies only slightly along the Bodón Transect. In the east, higher water depths relate to the continuing basin conditions. Finally, increment 313.5Ma records the last stage of the Valdeteja platform within the study area. Only at location Las Majadas del Caserio (Fig. 6.10a) did the platform still exist with a small extension completely surrounded by basin deposits. As outlined previously (Chapter 3), the top of the succession is sheared off within the whole area.

Generally, the platform development mirrors the 1D-curves (Fig. 6.11) of thermo-tectonic subsidence rates. Nonetheless, subsidence of increment 319.5Ma, which corresponds to the Barcaliente Fm., is extremely low, considering the initially deepening conditions of the formation (Chapter 3.2) and its bulk sedimentary thickness (Tab. A.2 - A.4). This example shows clearly the consequence of a low-resolution data input; the data used were confined to the lower and upper formation boundary, not reflecting vertical facies changes in-between. Unfortunately, biostratigraphic constraints are poor within the Barcaliente Formation; therefore no further time lines could be determined. The mostly monotonous character of the deposits requires further investigation in order to establish a proper high-resolution correlation across the study area.

However, available data and the data investigated here allow a higher resolution for the following increments. The sequence stratigraphic model as outlined in Chapter 4.2 is used to explain the Bashkirian and Moscovian

subsidence trends and their influence on the development of the study area.

#### *Bas 1 (ca.321Ma - 317.5Ma)*

Increment 318.5Ma covers the younger part of the LST of Bas 1 and the subsequent TST. Subsidence values are generally low (Fig. 6.11): 71m/Ma at Las Majadas del Caserio, 104m/Ma at Valdeteja and Lavandera. Nonetheless, values for the Gayo Unit are considerably higher: 174m/Ma at Gete (Torío Transect), 269m/Ma at Nocado de Curueño (Curueño Transect), which refers to an initially basinal setting of the Forcoso Zone. Likewise, subsidence rates for increment 317.5Ma (HST) are low, values within the Bodón Unit range between 60m/Ma and 110m/Ma. Subsidence totals 253m/Ma at Nocado de Curueño (Gayo Unit), where a high accumulation of slope deposits and progradation of the platform into the basin occurred.

#### *Bas 2 (317.5Ma - 315Ma)*

During the LST, which is assigned to increment 316.5Ma, subsidence rates are low, locally even negative. The platform was already terminated in the locations of the Gayo Unit, which are cut within the transects. East of Nocado, erosional structures at the top of the platform (Chapter 4.2) prove subaerial exposure of a large part of the platform. Subsidence rates of -120m/Ma indicate strong uplift. Probably, a “Nocado Escarpment” existed.

Furthermore, during the LST, the Bodón Unit shows low subsidence rates (increment 316.5Ma) ranging between 27m/Ma (Valdeteja) and 44m/Ma (Lavandera).

A rising sea-level initiated the subsequent TST of increment 316Ma and flooded the platform and the Nocado Escarpment. Within

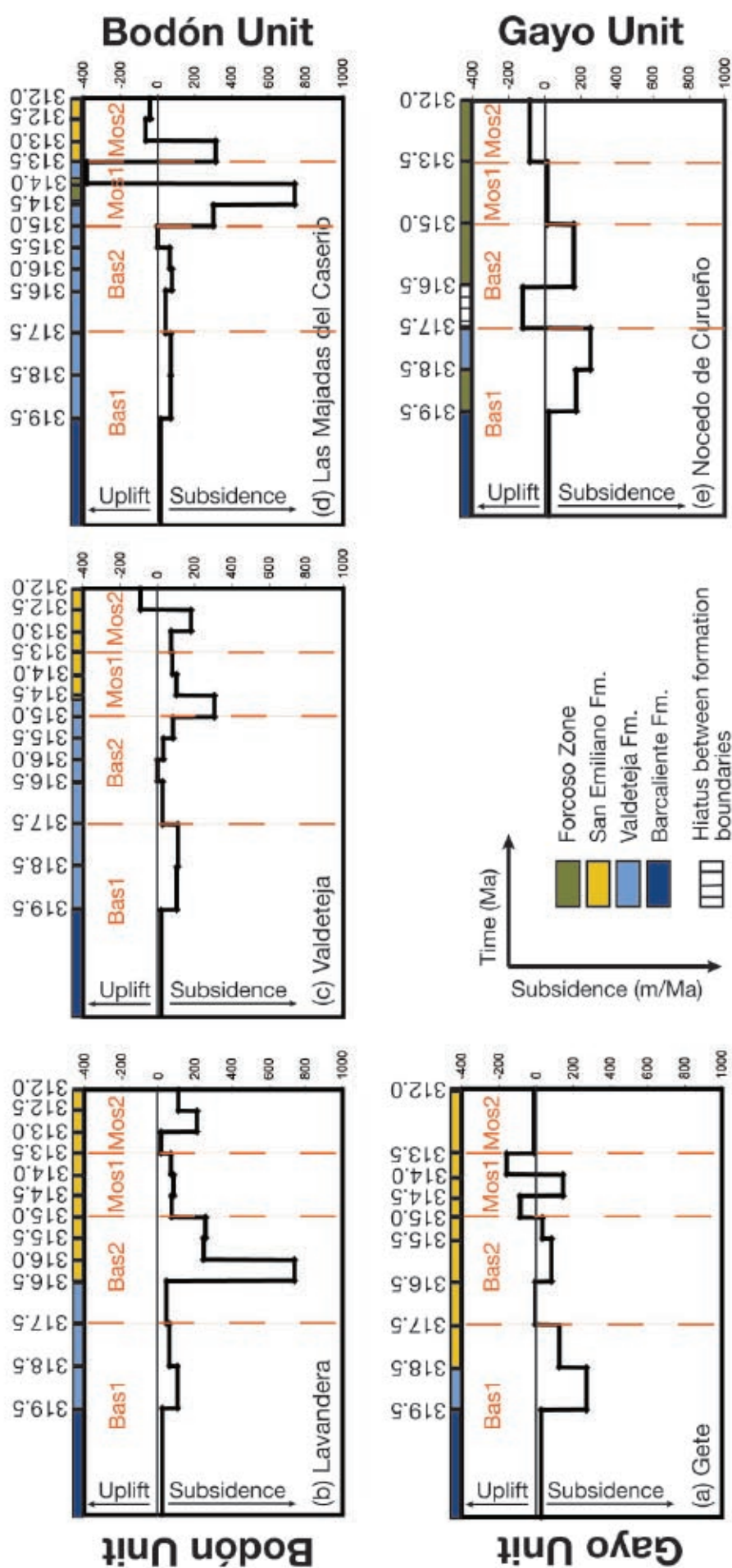


Fig. 6.11: 1D-curves of thermo-tectonic subsidence rates at selected locations. The x-axis displays time (Ma), the y-axis shows thermo-tectonic subsidence rates (m/Ma). Colors at the x-axis highlight the referring formation (see legend). (a) Gete (Gayo Unit, Torío Transect), (b) Lavandera (Bodón Unit, connecting location between Torío Transect and Bodón Transect), (c) Valdeteja (Bodón Unit, Bodón Transect), (d) Las Majadas del Caserio (Bodón Unit, Bodón Transect), (e) Nocado de Curueño (Gayo Unit, Curueño Transect). Dashed orange lines: interpreted sequence boundaries (see text for further explanation and Chapter 4). Bas 1 - Mos 2: sequences (see text).

the platform, subsidence values remain low. Contrastingly, subsidence is 739m/Ma at Lavandera. Increment 316Ma marks the onset of siliciclastic sheddings intruding into the transect. Values within the eastern Gayo Unit are also relatively high, expressed by re-establishing the basinal setting of the Forcoso Zone above the platform area of the former “Nocedo Escarpment”.

The subsequent HST (316Ma - 315Ma) exhibits little progradation or aggradation, subsidence rates are generally low within the platform area (84m/Ma at Valdeteja and at Las Majadas del Caserio). In the siliciclastics-dominated environment of the San Emiliano Fm. at Lavandera, subsidence reached about 256m/Ma, whereas in the basin of the Forcoso Zone, 162m/Ma were determined at Nocedo de Curueño.

#### *Mos 1 (315Ma - 313.5Ma)*

Within this sequence, subsidence rates exhibit a changing pattern in comparison to the earlier sequence. Additionally, values vary between locations. Subsidence rates within the San Emiliano Fm. at Lavandera are surprisingly low within Mos 1. During the LST, the lower limestone unit is deposited. However, values increase only slightly for the subsequent TST and HST.

At Valdeteja (Bodón Unit), increment 314.5Ma has exceptionally high values of 306m/Ma, considering that all other subsidence values within the platform are generally lower. However, the upper time line of the increment is located within the basal part of the succeeding San Emiliano Fm., whose high subsidence rates are reflected by the increasing water depth.

The HST (increment 313.5Ma) possesses low values of 81m/Ma at Valdeteja.

At Las Majadas del Caserio (Bodón Unit), values within this sequence differ greatly. Deposits show that the uppermost Valdeteja platform carbonates interfinger with basin deposits of the Forcoso Zone. During the TST, an ingression of the adjacent basin deposits of the Forcoso Zone starts, without being able to completely terminate platform growth. This is shown clearly by the HST deposits, which again consist of platform carbonates. The change in water depths between the basin and platform deposits mimics the subsidence rates.

Subsidence rates indicate strong vertical movements in the eastern part of the study area (see discussion), whereas the pattern is stable in the western area at Lavandera.

In the eastern part of the Gayo Unit, time lines of Mos 1 could not be defined within the Forcoso Zone since outcrop quality is low and biostratigraphic data are extremely scarce.

#### *Mos 2 (<313.5Ma)*

At Las Majadas del Caserio, stratigraphic record ends at the top of the preceding sequence. However, interpreting the overall pattern, an ingression of the San Emiliano Fm. from the west onto this last platform area is assumed. Therefore, subsidence rates within this sequence are hypothetical at Las Majadas del Caserio. The same applies to the rates at Gete and Valdeteja. At Nocedo de Curueño, deposits exist, but outcrop quality is poor as are biostratigraphic data. Only at Lavandera does sedimentary record allow a proper determination of subsidence rates. A second limestone unit corresponds to LST deposition (14m/Ma). Subsidence rates of 210m/Ma



cause a deepening of the environment, which is reflected by the sand to shale ratio of the siliciclastics of the TST. The youngest basin fill exposed possesses decreasing subsidence values of 109m/Ma.

### 6.3.2 Discussion

#### *Spatial and Temporal Patterns*

Throughout Bas 1, subsidence rates within the Gayo Unit are generally higher than within the Bodón Unit, which can be ascribed to the more proximal position of the Gayo Unit toward the approaching Variscan Orogen. During the HST, local differentiation in front of the approaching orogen occurred. Within the western Gayo Unit, the platform setting had already terminated and fine-grained siliciclastics had entered the area. On the cratonward margin of the platform, the Forcoso basin subsided and created accommodation space for the strongly prograding Valdeteja carbonates (Fig. 4.2), which could not significantly aggrade during this increment due to very low subsidence rates within the platform area.

The western Gayo Unit within this stage resembles (distal?) foredeep deposits, the Valdeteja platform is positioned on the forebulge, and the Forcoso basin corresponds to the back-bulge (Fig. 1.4 for comparison). Therefore, subsidence rates for the foredeep and the back-bulge are relatively high during Bas 1 whereas rates are low for the forebulge zone. The increasing load inflicted by the orogen in the hinterland causes high subsidence within the foredeep and the back-bulge. The forebulge remains in an almost steady vertical position. During Bas 1, the change from a simple foreland basin, which was resembled by the Barcaliente and Olleros Fm., into the

segmented four-component modern foreland basin system (Horton & DeCelles 1997; see Chapter 1.1.2) occurred. This is indicated by the differentiation of the area into the foredeep, forebulge and back-bulge depozone and requires higher subsidence rates within the foredeep and the position of the back-bulge depozone. Figure 6.11 displays the quantified subsidence pattern at this transitional stage. Locations Gete and Nocado de Curueño (Gayo Unit) refer to the foredeep and back-bulge depozone, respectively, whereas during this sequence, all locations across the Bodón Unit show low values at the position of the forebulge. Between locations Gete and Nocado de Curueño, the Valdeteja platform also existed but subsidence rates were not quantified due to extremely poor biostratigraphic constraints, heavy recrystallization within the carbonates and few stratal patterns. The distribution pattern of the depozones indicates non-linear zonation of the four components of the foreland basin system, which will be further discussed in Chapter 8.2.

Interestingly, the forebulge does not migrate toward the hinterland as presumed within the visco-elastic model (see Chapter 1.1).

Subsidence rates were low during the LST of Bas 2. The subsequent TST shows a distinct pattern. Values are high for the western Bodón Unit, expressed by the onset of siliciclastics of the San Emiliano Fm. at Lavandera, and also for the eastern Gayo Unit, where the “Nocado Escarpment” is flooded by the Forcoso Zone, whereas the other graphs (Fig. 6.11) show low subsidence. This pattern is assumed to be related to a deviation of the ideal linear geometry of the depositional zones in front of the approaching orogen (Fig. 1.3), which will

be discussed in detail in Chapter 8.

Within Mos 1, subsidence is relatively low for the San Emiliano Fm. at Lavandera and also for the platform carbonates at Valdeteja. Subtle subsidence changes were sufficient to create topographic differentiation in order to generate a mixed siliciclastic-carbonate succession within the distal part of the foreland basin deposits, represented by the San Emiliano Fm. at Lavandera.

Strong vertical movements at Las Majadas del Caserio resulted in ingression and subsequent regression of basin deposits on top of the platform carbonates. The overall backstepping pattern of the carbonate platform points to an oblique geometry between the platform and the approaching orogen (see Chapter 8).

The complicated, locally differentiated distribution pattern is the reflection of superposed syn-depositional 3D-tectonics in front of the obliquely, probably not linearly positioned orogen.

#### The Bodón Unit

Spectral plots of Figures 6.12 and 6.13 display spatial and temporal changes of the thermo-tectonic subsidence rates across the Bodón Transect as used for stratigraphic forward modeling (Chapter 7). Compared to Figures 6.6 and 6.7, input data were refined for the Upper Carboniferous and time lines were added based on sequence stratigraphic analysis and correlation. Lateral and vertical resolution is higher than within the plots of the complete Paleozoic succession.

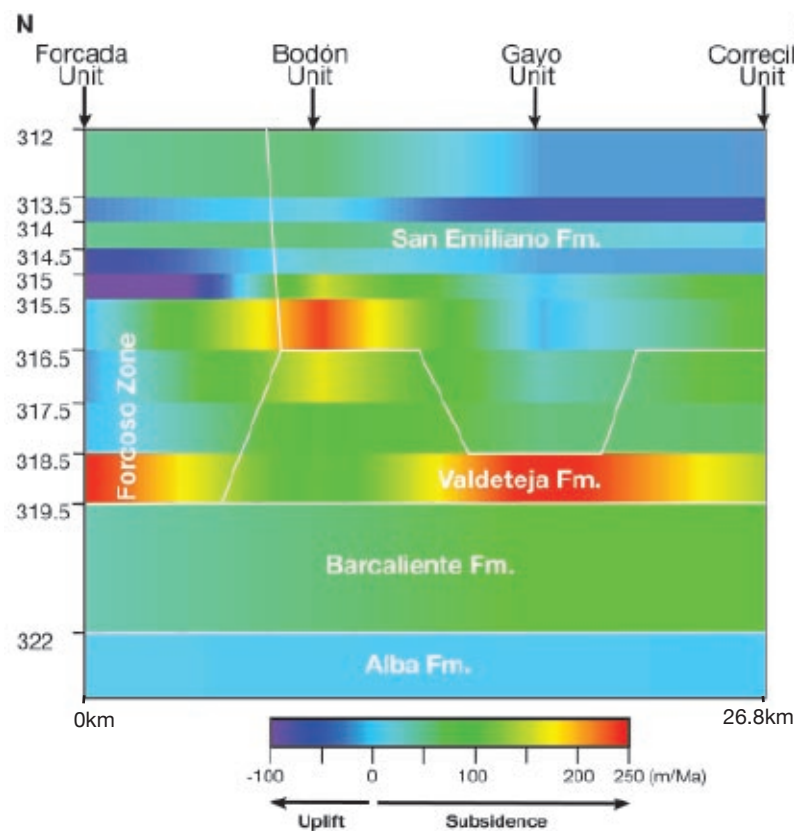


Fig. 6.12: Spectral plot of the Upper Carboniferous thermo-tectonic subsidence rates of the north-south directed Torio Transect. Thermo-tectonic subsidence rates are calculated along marked time lines only. Y-axis: time (Ma), x-axis: distance (km), colors indicate thermo-tectonic subsidence rates. White lines: schematic outline of formation boundaries. Note the early onset of the San Emiliano Fm. within the Gayo Unit during continued growth of the Valdeteja Fm. in the south and the north.

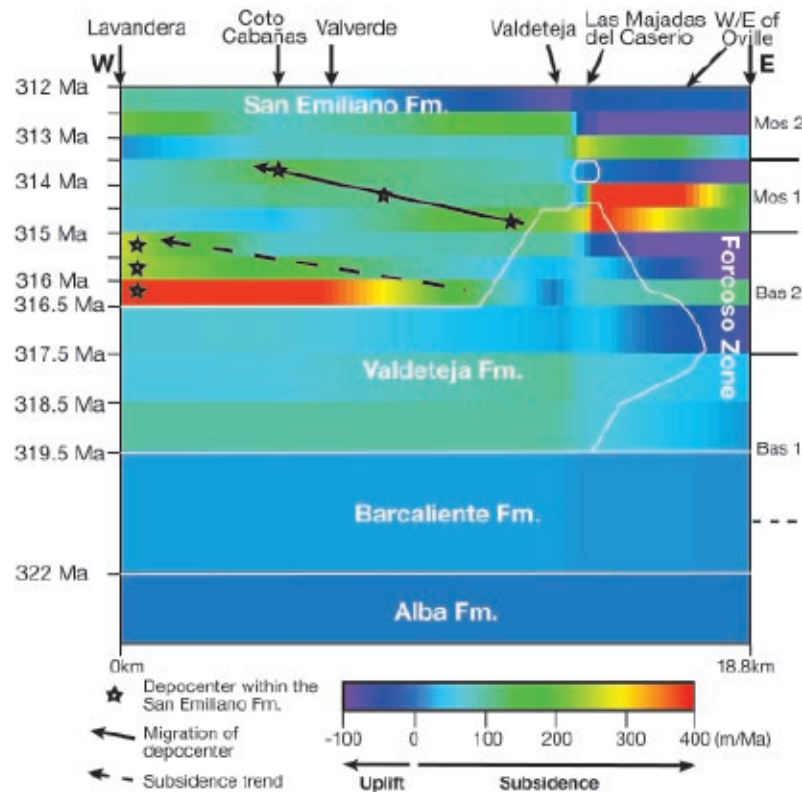


Fig. 6.13: Spectral plot of the Upper Carboniferous thermo-tectonic subsidence rates of the west-east directed Bodón Transect. Out-of-plane geometries influence the platform-to-basin transition (i.e. Valdeteja Fm.-to-Forcoso Zone), which generated the single patch of Valdeteja Fm. at location Las Majadas del Caserio. Bas 1 to Mos 2: sequences. Y-axis: time (Ma), x-axis: distance (km), colors indicate thermo-tectonic subsidence rates. White lines: schematic outline of formation boundaries.

The Alba and Barcaliente Fm. show laterally and vertically a very uniform distribution of subsidence. Development within the Valdeteja Fm. is more distinct, but is best shown in the graphs of Fig. 6.11 and is outlined above. Unfortunately, calculation of subsidence rates for the transition of the platform carbonates into the basin deposits of the Forcoso Zone did not result in a clear picture. If sediment loading exists on one side (i.e. Valdeteja Fm.) and the opposing side does not subside enough in the paleowaterdepth model (i.e. Forcoso Zone), the program creates negative subsidence rates (uplift) (pers.com. Bowman 2004). Paleowaterdepth within the Forcoso Zone does not vary strongly, therefore relative uplift is calculated for these deposits as displayed by dark-blue to purple colors within Figures 6.12 and 6.13.

Due to the distal position of the San Emiliano Fm. in relation to the hinterland, subsidence rates are low compared to rates, which were reported for the depocenter of foreland basins (e.g. up to 1,000m/Ma according to Einsele 2000). However, two trends are discernable. The first is located within Bas 2. The depocenter is not in the process of migrating at this time; it remains steady at location Lavandera. Nonetheless, a trend of decreasing values from the east to the west is visible as shown by the dashed-lined arrow in Figure 6.13. The second trend (Mos 1) shows clearly a migration of the depocenter from the east to the west of the transect.



## CHAPTER 7: STRATIGRAPHIC FORWARD MODELING

### 7.1 Modeling Software: Overview

Stratigraphic forward modeling is achieved by process-imitating (process-based) software. Process-based models can be deterministic and/or stochastic, and empirical and/or theoretical. During the last 20 years, various dynamic 2D- and 3D-stratigraphic modeling programs were developed. Some programs focus on few aspects of sedimentary processes and parameters (e.g. FUZZIM, presented by Nordlund 1996, 1999) or are restricted to carbonate or siliciclastic sedimentation (e.g. REPRO, presented by Hüssner et al. 1997). PHIL<sup>TM</sup> (Bowman & Vail 1999), which was used for reverse modeling in this study, comprises a substantial set of parameters within its forward modeling module. It is based on diffusional calculation of transport mechanisms. The transport and deposition of sediment is modeled controlled by the gradient of the preexisting sediment surface. Unfortunately, it does not provide the possibility to include sedimentary input from both sides of the modeled transect as required for this study. DIONISOS is also based on diffusional calculations and includes a comprehensive set of parameters (e.g. Granjeon & Joseph 1999), but was not available for this study. The three-dimensional SEDSIM-software belongs to the group of hydraulic process-response models. It is based on Navier-Stokes equations, which describe flow in three dimensions (Tetzlaff & Harbaugh 1989). It also incorporates a large set of parameters (e.g. Griffiths et al. 2001, Tetzlaff & Harbaugh 1989).

The joined basin modeling and computer science group of the University of South

Carolina, headed by C. Kendall and P. Moore, developed SEDPAK, which is a geometrical model software. In contrast to the diffusional models, geometrical models do not describe the process itself, but the result of the process, which is the (partially) filling of the accommodation space (Griffiths 2001). SEDPAK is able to model a mixed clastic and carbonate depositional system in a 2D-basin, which can be filled from both sides (Eberli et al. 1994, Ross et al. 1994, Strobel et al. 1989). It calculates empirical relationships to model basin evolution using linear differential equations.

### 7.2 Software Specifics: SEDPAK

SEDPACK is based on sequence stratigraphic concepts. It considers eustatic sea-level changes and subsidence to be the principal factors responsible for the creation and destruction of accommodation space. A second important step within the modeling process is the introduction and removal of sediments from one or both sides. The available accommodation space is filled by a combination of redeposited siliciclastics and in-situ carbonate growth (Kendall et al. 1991, 1993, Strobel et al. 1989). The program divides the transect into evenly spaced vertical columns, which are filled progressively by the transported and/or produced sediment.

Additionally, out-of-plane deposition can be adjusted.

There are several synopses about the basic assumptions and simulation algorithms that SEDPAK is based on (e.g. Eberli et al. 1994, Helland-Hansen et al. 1988, Kendall et al.

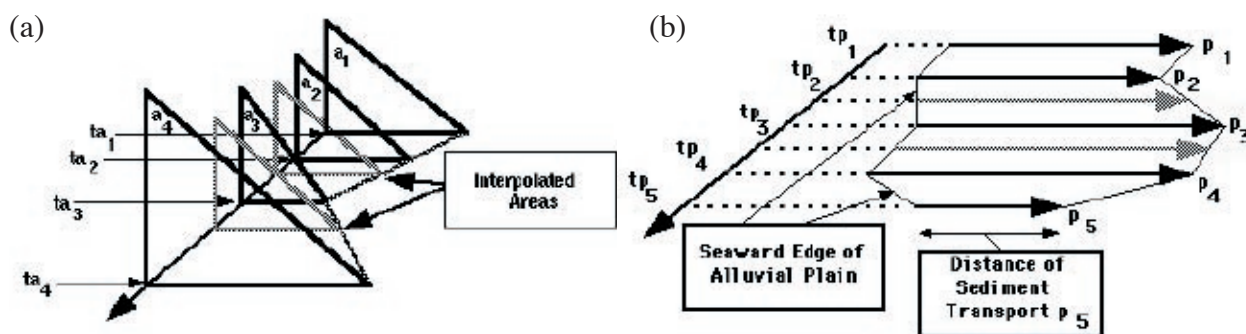


Fig. 7.1: Calculation of the distribution of siliciclastic sediments. (a) Triangles represent the cross-sectional area of sediment available for deposition, which is progressively filled from the left to the right by the user defined rate of sand-to-shale ratio. (b) Calculation of penetration distance from the shoreline into the basin. Shaded arrows point out interpolation between given data points (Kendall & Moore 2004).

1991, Scaturro et al. 1989). Selected components are outlined below.

### 7.2.1 Siliciclastics

#### *Clastic supply*

Clastic geometries are assumed to be primarily derived from the volume of sediments imported and distributed into the basin. The clastic source is considered to be not located within the modeled basin transect (Kendall et al. 1991).

An arbitrary mixture of shale and sand volume can be adjusted for each time step. Interbedded relationships are not reconstructed but the ratio of the total quantity of each grain size is shown. Clastic deposition is calculated column by column from the side of sediment input to the other side of the transect (Strobel et al. 1989).

The transportation distance can be adjusted for each time step. Distance values refer to the distance of transportation from the shoreline into the available area below sea-level.

Since the relief of the hinterland affects the clastic supply, several angles have to be considered when modeling clastic deposition. Subaerially, sediment is eroded down to the

alluvial angle of repose, and distributed into the basin (Fig. 7.2).

For submarine deposition, a shallow and deep depositional angle can be distinguished. The transitional depth defines the boundary between shallow and deep marine deposition. If the surface slope is greater than the corresponding angle, erosion occurs. If it is lower, sediments are deposited (Kendall & Moore 2004).

Erosional effects caused by waves between sea-level and wave-base are calculated by a winnowing curve.

### 7.2.2 Carbonates

In-situ carbonate accumulation and the amount of transported talus are presumed to be the main factors influencing the carbonate deposition and geometry. Therefore, carbonate sources are considered as positioned within the modeled transect, in contrast to the external clastic sediment sources.

Carbonates are modeled to accumulate by biogenic production and pelagic rain out of the water column. Depth-dependent carbonate production curves (Fig. 7.3) can be defined as well as time-dependent pelagic accumulation rates (Eberli et al. 1994). Accumulation of in-situ

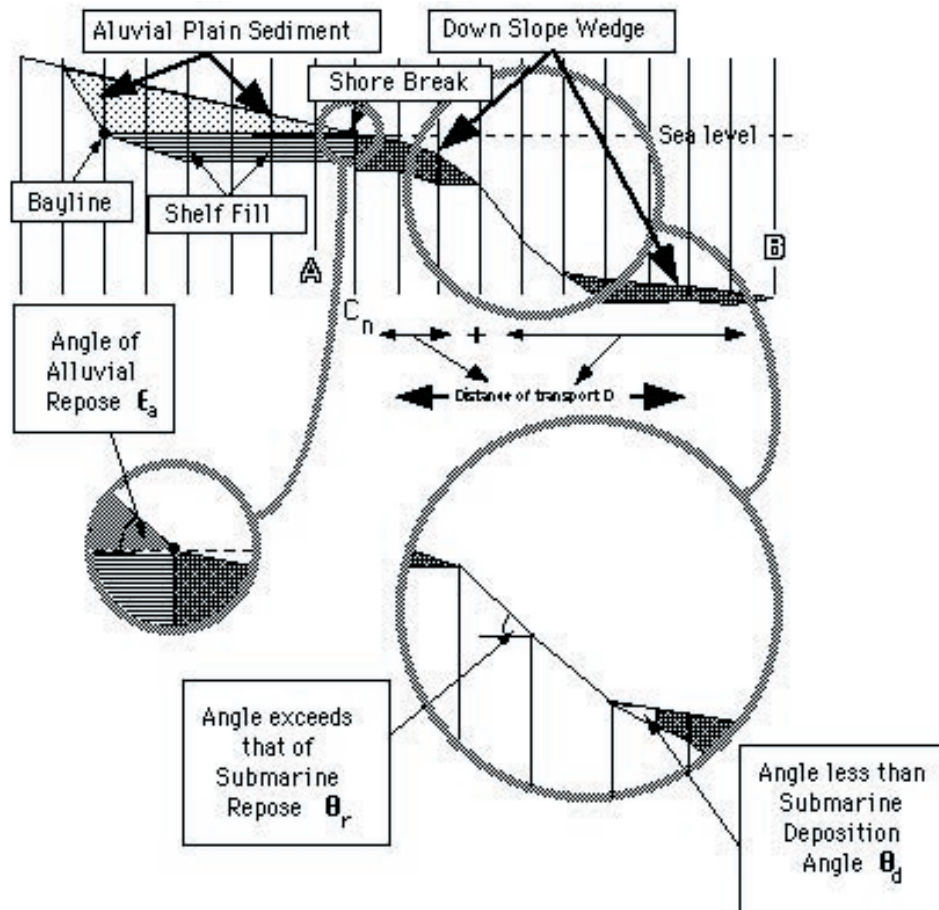


Fig. 7.2: Siliciclastic sediments are deposited observing various factors within the alluvial and submarine siliciclastic depositional system such as the alluvial repose angle and submarine repose angles (Kendall & Moore 2004).

carbonate and carbonate repose angle (Fig. 7.4) predominantly define the slope geometry and are therefore crucial parameters within the modeling process of carbonates. Sediment accumulation exceeding the repose angle will be

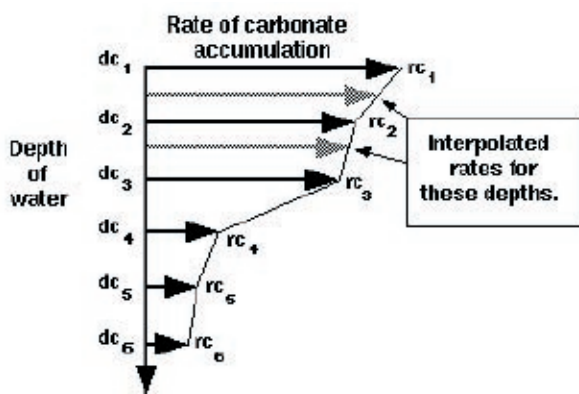


Fig. 7.3: User defined curve for the rate of carbonate accumulation (Kendall & Moore 2004). The y-axis shows the water depth, the x-axis the rate of carbonate accumulation.

eroded and deposited toward the lagoon and/or toward the sea. Slope sedimentation consists of talus deposits and turbidites. For both, penetration distances are adjustable (Fig. 7.4). Accumulation within the lagoon comprises reef-derived debris and in-situ production. Lagoonal damping can reduce the production curve in relation to the distance to the reef crest.

Additionally, the effects of wave energy suppress carbonate accumulation (wave damping). This parameter is specified for the positions at which waves break (Eberli et al. 1994).

### 7.3 Data Input

Within the Bodón Unit, a long hiatus lasted from early Ordovician until late Devonian.



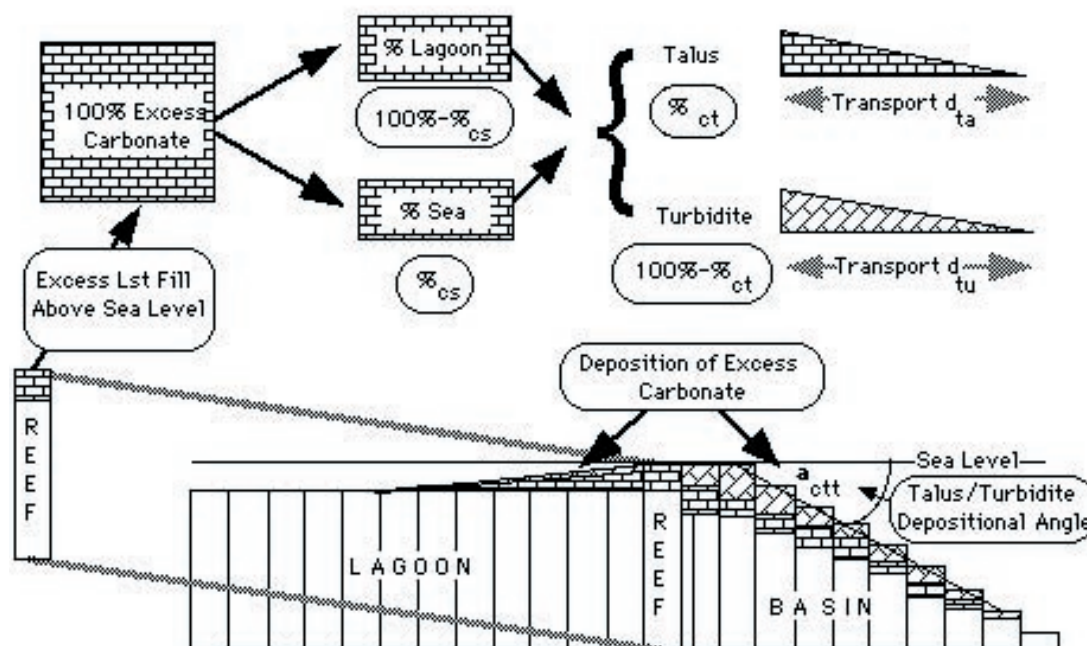


Fig. 7.4: Calculation of carbonate deposition within the forward model by SEDPAK (Eberli et al. 1994). Excess carbonate at the reef is distributed to the lagoon and the basin to a user-defined percentage. The amount of carbonate deposited as talus or turbidite and each transport distance are adjustable. The talus/turbidite depositional angle can only be set to one value for the whole depositional system.

Forward modeling starts with the deposition of the Ermita Fm. over the long-exposed Cantabrian High.

#### *Facies Distribution*

Recorded stratigraphic profiles, facies analysis and lateral relationships as investigated during fieldwork and in aerial photographs (see Chapters 3 and 4) serve as a database to model facies distribution within the Bodón Transect. Forward modeling was carried out from the base of the Ermita Fm. at 358Ma to the San Emiliano and Valdeteja Formations and the Forcoso Zone at 316Ma.

#### *Porosity and Density*

SEDPAK uses pre-defined values for the densities of shale, sand, carbonate, and the mantle (Tab. 7.1). Compaction is calculated using data by Baldwin & Butler (1985; Fig. 7.5).

#### *Eustatic Sea-Level Curve and Subsidence*

The same eustatic sea-level curve used for reverse modeling was employed (Fig. 6.2).

Subsidence rates applied for forward modeling were calculated with PHIL™ version 5.5.4. Forward modeling was carried out between 358Ma and 316Ma. Prior to 358Ma, a long lasting hiatus from the early Ordovician until late Devonian is present within the Bodón Transect. Formations older than early Ordovician show a uniform distribution across the transect with minor facies changes. Therefore, it is assumed that lithological heterogeneities of formations older than 358Ma did not cause significant differential subsidence along the Bodón Transect within the Carboniferous succession.

#### *Resolution*

Modeling resolution through time and space is limited. Horizontally, the amount of vertical columns set by the user is limited. For the

Tab. 7.1: Density values as predefined by SEDPAK.

Substratum	Density [ $\text{g/cm}^3$ ]
Shale	2.65
Sand	2.7
Carbonate	2.65
Mantle	3.3

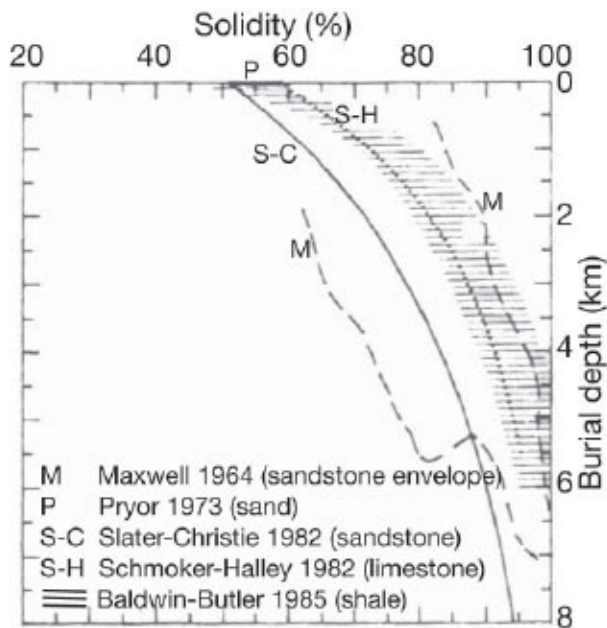


Fig. 7.5: Solidity-depth curves as used by SEDPAK (Kendall et al. 1991). The term “solidity” covers effects of compaction, cementation and pressure solution.

Bodón Transect, a cell-width of 170m was employed.

The amount of modeled time steps is limited by the available computing power and the processing time. Within this work, constant time steps of 0.092Ma were chosen, limited by the resulting computing time. The entire model consists of 456 layers.

#### *Initial Topography*

The model starts at the base of the Ermita Fm. at 358Ma. Initial basin topography hence refers to the paleobathymetry at the base of the Ermita Fm., which was concluded from the

facies of the lowermost preserved record (see Tab. A.3).

#### *Limitations of the Model*

As is the case for all existing modeling software, not all parameters can be considered to achieve a perfect fit with the natural model. First of all, the natural depositional system is not yet understood to a sufficient degree to create such a program. Additionally, programs considering as many parameters as possible may obstruct the modelers view of the major controls of the modeled system.

Within SEDPAK, flexural parameters cannot be included in the model. For flexural subsidence results, refer to Chapter 6.2.

Furthermore, the lithologies considered by the program include only sandstone, shale, and limestone. Therefore, porosity, density and compaction values refer to a mean value defined for sandstone, shale, and limestone as listed above.

Although the program accepts every possible combination of the above lithologies, graphical output does not consider interbedding relationships. Only the rate of lithologies per time step is shown.

As with every model, the quality of the results strongly depends on the quality of the data input. Factors limiting the resolution of the data input are:

**Chronostratigraphy:** Paleozoic successions are not as well constrained in time as younger deposits. Additionally, available biostratigraphic data were limited. The use of varying time scales within literature may have caused an error within the applied ages.

**Tectonics:** Due to the fact that the area was differentiated into tectonic units as a result of deformation, only single slices of information, which represent 2D-sections along the tectonic units, are preserved. This imposes limits on the stratigraphic model of Chapters 3 and 4.

**Stratigraphic record:** The transect is positioned close to the margin of the Valdeteja Fm., where out-of-plane transport of material is certain. Although the software provides the possibility of integrating this into the model, the 2D-record may not always indicate the 3D-origin of the deposits. Lateral interfingering between the San Emiliano and Valdeteja Fm. had to be simplified.

**Quantification of paleobathymetric data** is approached by comparing it with actualistic environments as cited within literature.

## 7.4 Results

The graphic output of the forward modeling program SEDPAK was assembled to Movie A.4 and Movie A.5 (see Appendix on CD-ROM media). The latter contains enlarged pictures of the Bashkirian platform-to-basin transition only.

Due to limited outcrop conditions, the modeled 2D-Bodón Transect is positioned along the strike of a tectonic unit to achieve best constraints on the lateral development of the Valdeteja platform across the transect. However, the transect is located at the outermost edge of the carbonate platform. Subparallel to the transect, the Forcada Unit

in the north is comprised of the basin facies of the Forcoso Zone. Within the Bodón Transect, there is also a platform-to-basin transition in the east (Fig. 5.1a). Therefore, 3D-influences affecting the transect are expected.

The development of the Bashkirian-Moscovian system points to a strong influence of out-of-plane deposition during the Valdeteja and also during the San Emiliano Fm. Within the depositional system of the Valdeteja Fm., out-of-plane sedimentation had to be included into the forward model in order to achieve sedimentary thicknesses as measured in the field across the Bodón Transect. Within the platform interior, the amount of available accommodation space was higher than at the platform margin. This is expressed by the differences of sedimentary thicknesses at location Valdeteja and at location Las Majadas del Caserio. The former mostly corresponds to the platform interior environment, whereas the latter is located close to the platform margin. Higher subsidence within the platform interior is related to the out-of-plane influence at the northern margin of the platform. The resulting 3D-subsidence pattern caused the basal surface below the modeled formations to bend (Fig. 7.7).

The source area of the San Emiliano Fm. was located to the south-to-west (see Chapter 3.2), resulting in a pattern of interfingering with the platform deposits of the Valdeteja Fm., which also reflects out-of-plane deposition (Fig. 3.16, 4.3c & 4.4c).

### 7.4.1 Carbonate Deposition

As outlined in Chapter 6.3.1, due to the low resolution of time lines within the Barcaliente Fm., subsidence rates as calculated by reverse modeling were inaccurate. Since forward



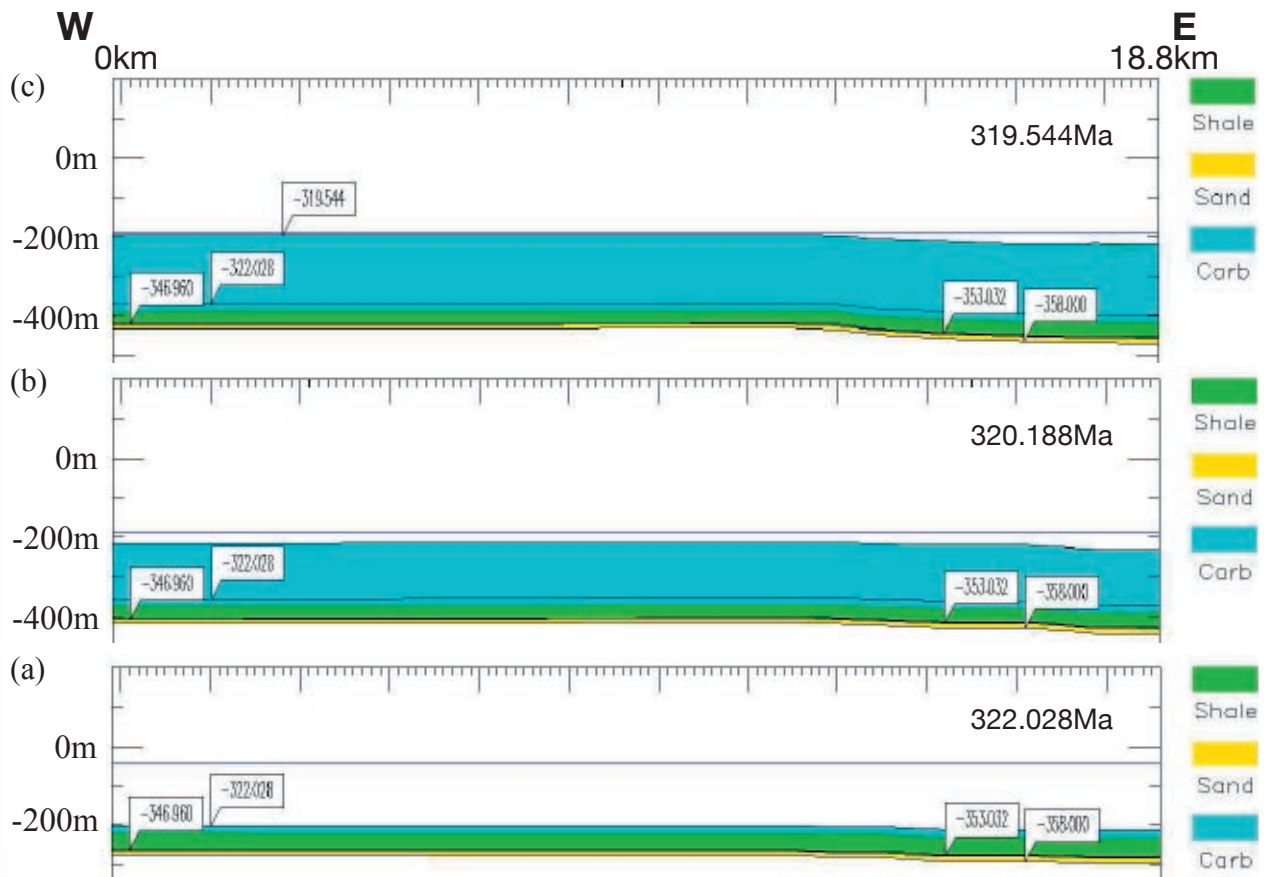


Fig. 7.6: Predicted development within the Barcaliente Fm. of the Bodón Transect. Colors represent the lithology, subdivided into shale, sand and carbonate. The x-axis displays the distance along the transect (km), the y-axis the depth (m). Note the initially deep environment (a), succeeded by shallowing conditions (b), and the differentiation into intertidal conditions at the western side of the transect and the commencing basinal setting at the eastern side of the transect. 358Ma: Base Ermita Fm., 353Ma: Base Vegamián Fm., 347Ma: Base Alba Fm., 322Ma: Base Barcaliente Fm., 319.5Ma: Top Barcaliente Fm. Labels mark formation boundaries. Vertical exaggeration: 10x. Horizontal line: sea-level.

modeling considers the facies development between the time lines, subsidence rates were further differentiated within the formation. Subsidence rates for the lower part of the formation reach 97m/Ma, whereas the shallowing, upper part amounts to up to only 15m/Ma. Figure 7.6 shows the paleobathymetrical development of the Barcaliente Fm. from deep water to shallow conditions. At the top (Fig. 7.6c), a differentiation of the water depth across the transect was modeled as concluded by the facies distribution within the Señas Mb., closely resembling the position of the Sancenas High, which is reported to have existed from the Devonian on (Evers 1967; see

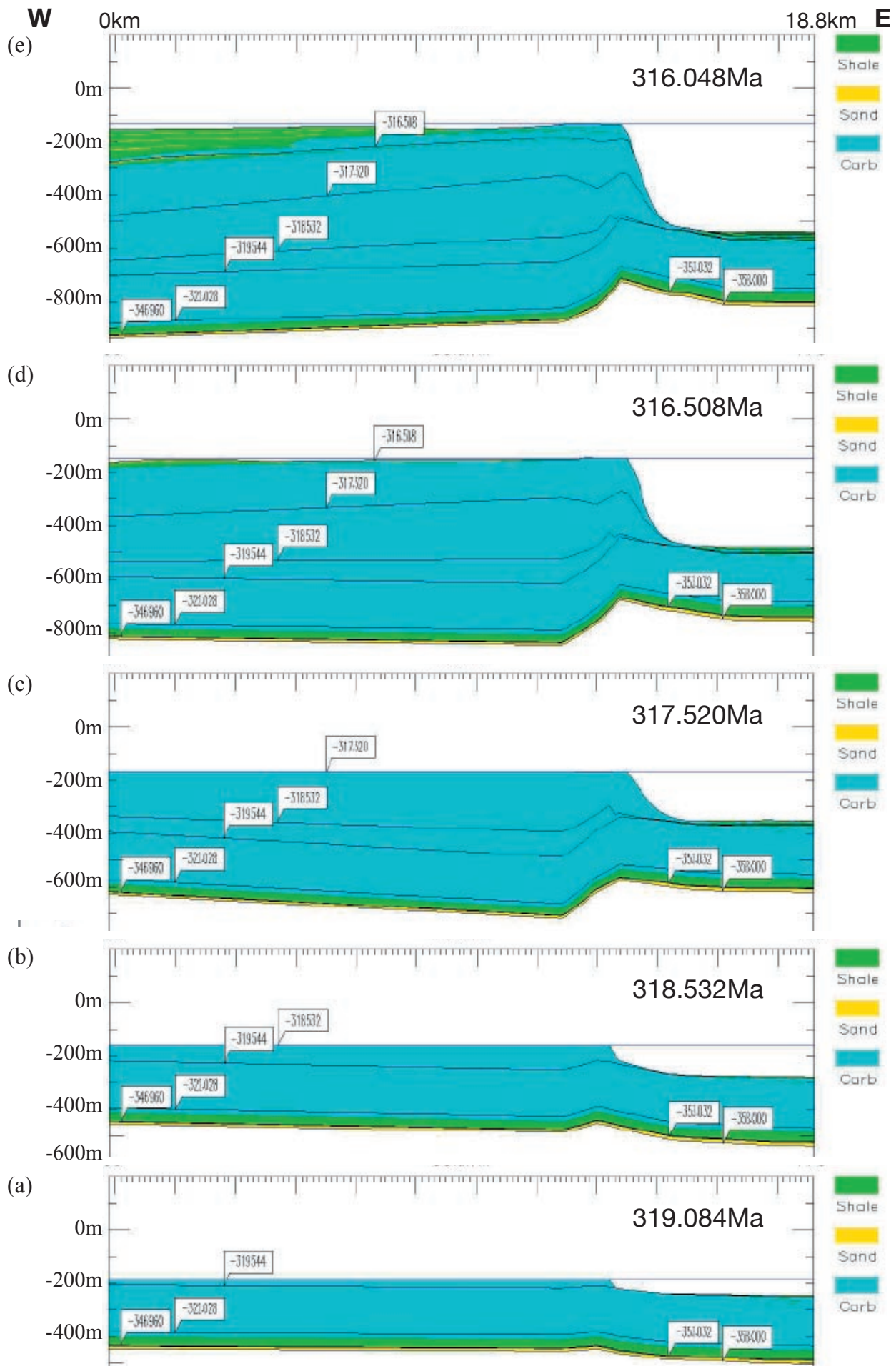
Chapter 2.2). The Sancenas High also influenced the Early Carboniferous sedimentation within the study area.

The Valdeteja platform established on top of the shallow-water deposits (Fig. 7.7a).

#### *Valdeteja Fm.: Platform Patterns*

The modeled stacking patterns follow the sequence stratigraphic interpretation of Chapter 4.2. The stratigraphic prediction of the forward model is mostly in concordance with the sedimentary record as present in the study area.

Aggradational and retrogradational patterns of the platform were modeled by observing given values such as subsidence rates calculated



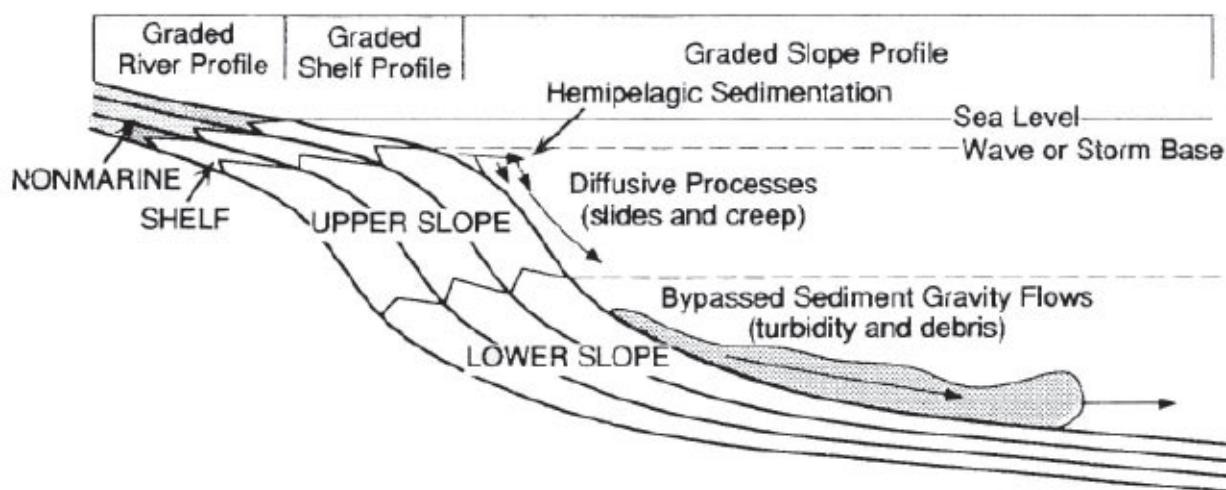


Fig. 7.8: Sketch of a prograding system with depositional processes being in equilibrium (Ross et al. 1994).

by reverse modeling, paleo-water depth (i.e. eustatic sea-level curve, local paleobathymetry) and sediment accumulation. The eustatic sea-level curve was adjusted within the TST of the sequences Bas 1 and 2 (Fig. 7.14) to create a more pronounced retrogradational pattern matching the natural geometries.

During aggradation, the slope angle increased to up to  $45^\circ$  within the upper slope. Della Porta (2003) and Della Porta et al. (2004) reported a steep slope for the Bashkirian-Moscovian Sierra del Cuera platform of the Northern Cantabrian Basin. During aggradation, slope angles varied between  $30^\circ$  to up to  $45^\circ$  at Sierra del Cuera, which was also observed for the Bodón Transect (Fig. 7.7d). This is also comparable to the assumed “Nocedo Escarpment” (see Chapter 4.2) of the eastern Gayo Unit.

However, contrary to the retrogradational and aggradational stacking patterns, progradation of the platform was found to be strongly controlled by geometrical factors, in addition to the factors directly controlling the creation and destruction of accommodation space.

Of major importance are basin and slope physiography. The basin must constantly subside within the model to accommodate the basin deposits and debris derived from the platform in order to not be filled.

As a prerequisite for progradation, the platform needs a foundation across which it can prograde.

Hedberg (1970) introduced the term “graded margin” referring to a progradational margin (Fig. 7.8). Maintenance of the graded state needs an equilibrium state of factors influencing the graded state. Upper slope sedi-

Fig. 7.7 (previous page): Predicted deposition during the Bashkirian of the Bodón Transect. The eye-catching bend of the basal layers near the platform margin is caused by differential subsidence due to out-of-plane influences in the vicinity of the northern basin margin. 319.5Ma: Base Valdeteja Fm. and Forcoso Zone, 319.0Ma: Top LST of Bas 1, 318.5Ma: Top of TST of Bas 1, 317.5Ma: Top of HST of Bas 1 and type-2 sequence boundary, 316.5Ma: Top of SMW of Bas 2 and onset of shedding of siliciclastic sediments of the San Emiliano Fm. from the west into the transect, 316.0Ma: Top of TST of Bas 2. Labels mark significant time lines. Vertical exaggeration: 10x. Mov. A.4 and A.5 show the entire modeled period from the Ermita Fm. to the onset of the San Emiliano Fm. They are attached in the appendix on CD-ROM media.



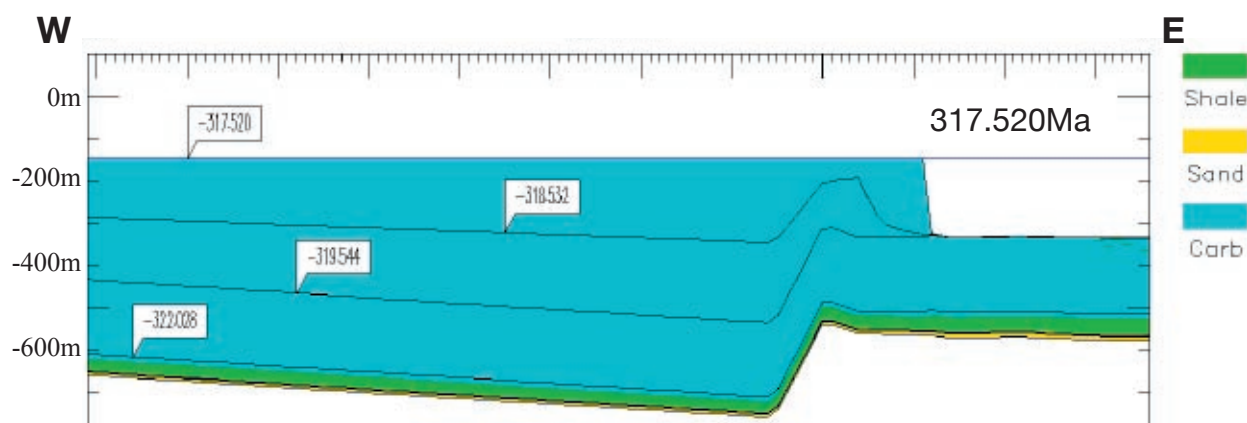


Fig. 7.9: Example of an out-of-grade margin, where erosional and depositional processes are not in equilibrium. Note the oversteepening of the slope. Consequently, no further progradation occurs, the toe-of-slope remains steady. Vertical exaggeration: 10x.

ments consist of material derived by traction and suspension processes, and also by in-situ accumulation, which are reworked down slope (Ross et al. 1994). Turbidity or debris flows transport sediment into a base-of-slope or basin position (Syvitski et al. 1988).

Progradation wedges need a substrate to grow out over (pers. com. Kendall 2005), which in the case of the modeled HST of Bas 1 is provided by a combination of sediment by-pass and the shale deposited within the basin (Mov. A.5). During the early HST, progradation was lower than during the late HST of Bas 1 of the eastern Bodón Unit. This may be related to the amount of debris shedded earlier, which could not provide a considerably sized debris wedge. After expanding this wedge by an increasing amount of turbidites during early highstand sheddings, the platform strongly prograded (Mov. A.4, A.5). Sheddings from the platform into the basin were found to be higher during the HST than during the following LST. This is in accordance with Schlager et al. (1994) who favored the highest amount of carbonates being shedded during the HST and not during the LST.

If the equilibrium of depositional and erosional processes is not given, then the margin changes into an out-of-grade state, where no progradation occurs but the margin oversteepens and sediments are bypassed (Hedberg 1970). In the model of Figure 7.9, depositional and erosional processes were not in concert and resulted in a successive oversteepening of the slope. Once the lower slope oversteepened, the base-of-slope remained steady at its position (Fig. 7.9) and no further progradation was possible.

Progradation width within the HST of Bas 1 and Mos 1 varies significantly at the basin margin of the Bodón Unit. During Bas 1, a substratum was available as the foundation for progradation. During the HST of Mos 1, vertical movements in the eastern part of the study area (see Chapter 6.3.1) resulted in further deepening of the adjacent basin and disturbed the erosional and depositional balance preventing the creation of a foundation for high-progradational width.

#### *Carbonate parameters*

The carbonate production curve used here is plotted in Figure 7.10. Table 7.2 lists the

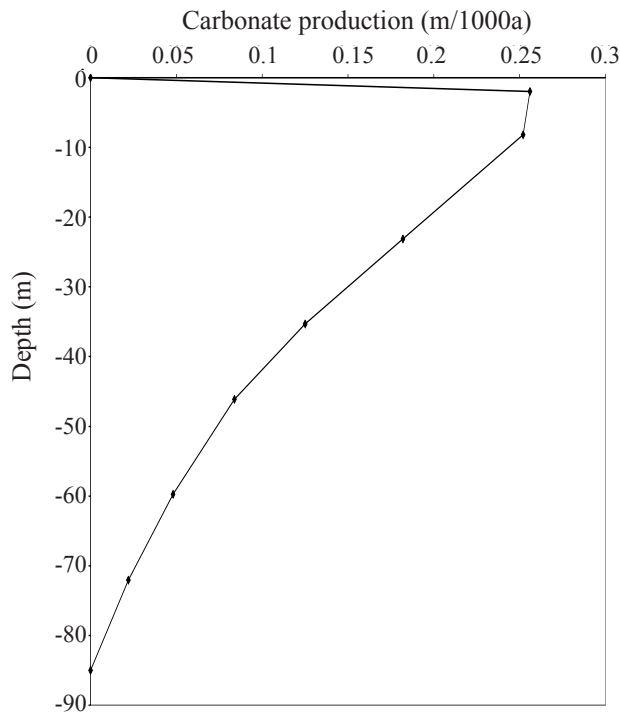


Fig. 7.10: Carbonate production curve for the Valdeteja Fm.

values for carbonate parameters as applied in the forward model. The importance of single parameters was found to vary. Talus and turbidite penetration distances and also the amount distributed between the talus and turbidite do not strongly alter the system. However, changing the carbonate repose angle or changing the amount of material transported towards the sea results in a completely altered system, where the carbonate factory is not able to keep up with the changes of accommodation space (Fig. 7.11).

#### 7.4.2 Siliciclastic Deposition

The predominantly siliciclastic deposits of the Ermita and Vegamián Fm. were distributed uniformly across the transect. The water depth increased constantly. Sediment was supplied from the east into the transect. Table 7.3 lists the alluvial and marine repose angles applied for the whole model. Table 7.4 shows the minimum and maximum values of siliciclastic sediment volumes necessary to model the measured sedimentary thicknesses.

During deposition of the San Emiliano Fm., the interfingering of siliciclastics between locations Lavandera and Valdeteja was modeled exemplified for the deposystem. The platform deposition was progressively terminated from the west to the east (Fig. 3.33) due to increased subsidence rates and the progressive intrusion of siliciclastics. The shale-to-sand ratio of the San Emiliano Fm. increased upward. The interfingering of siliciclastics with carbonates is a delicate system, which reacts quickly to changes. Factors such as the amount of siliciclastics supplied, penetration distance, timing of the interplay of subsidence and sediment input, and the factor of clastic suppression of carbonates have to be carefully adjusted (Fig. 7.12a-b). Minor changes trigger the predominance of carbonate mud mounds

Tab. 7.2: Carbonate parameters as applied in the modeled Bodón Transect.

Carbonate repose angle	< 45°
Percent to talus	95%
Percent to turbidite	5%
Talus penetration distance	1.2km
Turbidite penetration distance	11.0km
Clastic suppression of carbonates	-10.0
Carbonate erosion	15%
Erosion enhancement	0.5%

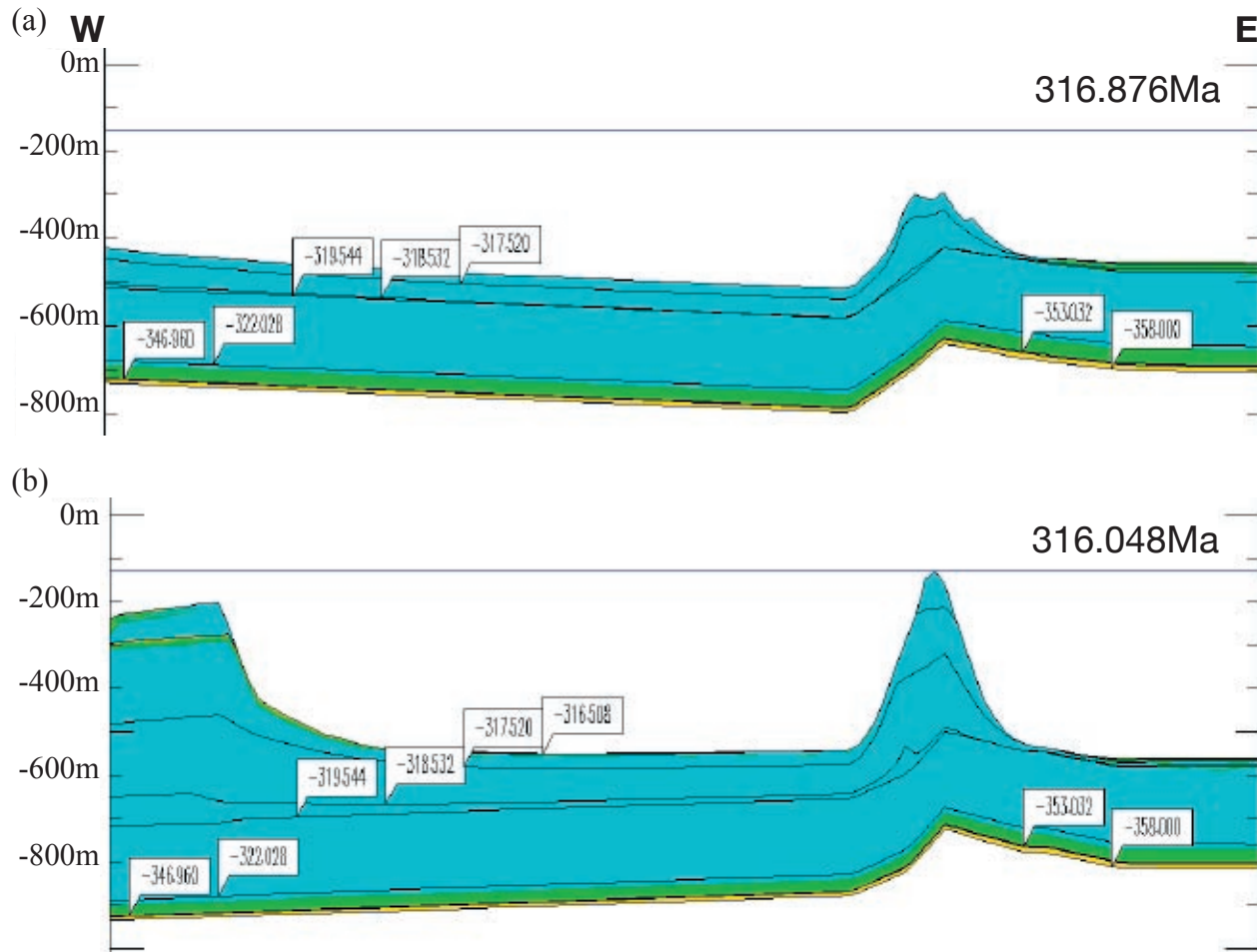


Fig. 7.11: Examples of varying influence of parameters on the model. (a) Modeled with carbonate repose angle =  $25^\circ$ , (b) modeled with 50% of the eroded material being transported towards the sea. Legend as in Fig. 7.9.

Tab. 7.3: Repose angles as applied in this study.

Alluvial repose angle	$0.0052^\circ$
Shallow repose angle	$0.5^\circ$
Deep repose angle	$0.1^\circ$

Tab. 7.4: Minimum and maximum values for siliciclastic volumes.

Formation	Shale supply [ $\text{km}^2/\text{ka}$ ]	Sand supply [ $\text{km}^2/\text{ka}$ ]
San Emiliano	$1.65 \times 10^3 - 4 \times 10^3$	$0.18 \times 10^3 - 0.85 \times 10^3$
Forcoso	$6 \times 10^3 - 15.5 \times 10^3$	$0.0 - 0.02 \times 10^3$
Barcaliente/Señaras Mb.	$0.51 \times 10^3 - 0.81 \times 10^3$	$0.0 - 0.01 \times 10^3$
Alba	$0.0 - 0.52 \times 10^3$	0.0
Vegamián	$0.18 \times 10^3 - 0.25 \times 10^3$	$0.0 - 0.001 \times 10^3$
Ermita	$0.0 - 0.01 \times 10^3$	$0.47 \times 10^3 - 0.94 \times 10^3$



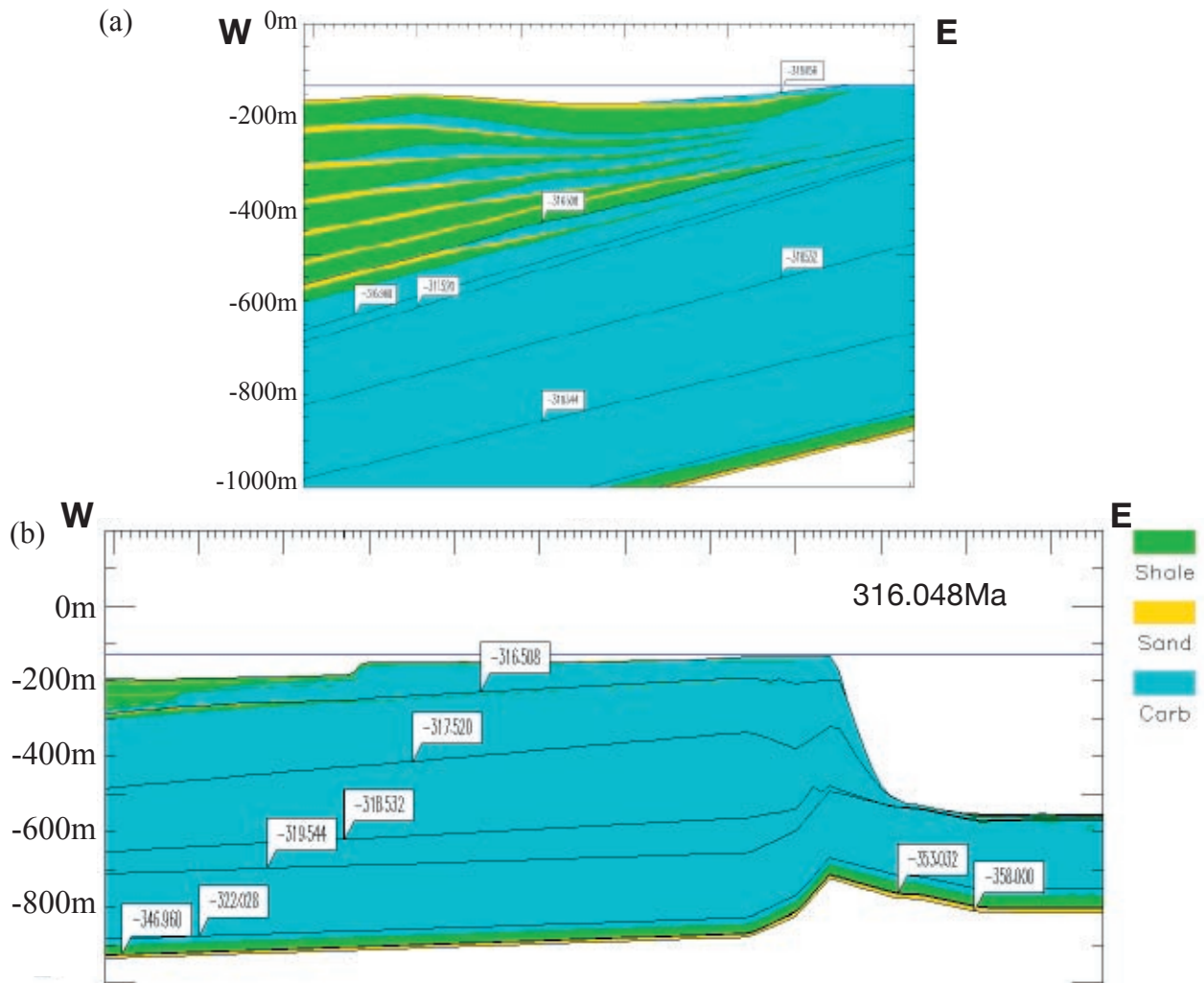


Fig. 7.12: Effect of variations of the depositional factors determining the siliciclastic system. (a) Altered amount of siliciclastics supplied from the west. Enlarged view, vertical exaggeration 10x. (b) Smaller penetration distance of siliciclastics of the San Emiliano Fm. than in the final model of Fig. 7.7e. Vertical exaggeration: 10x.

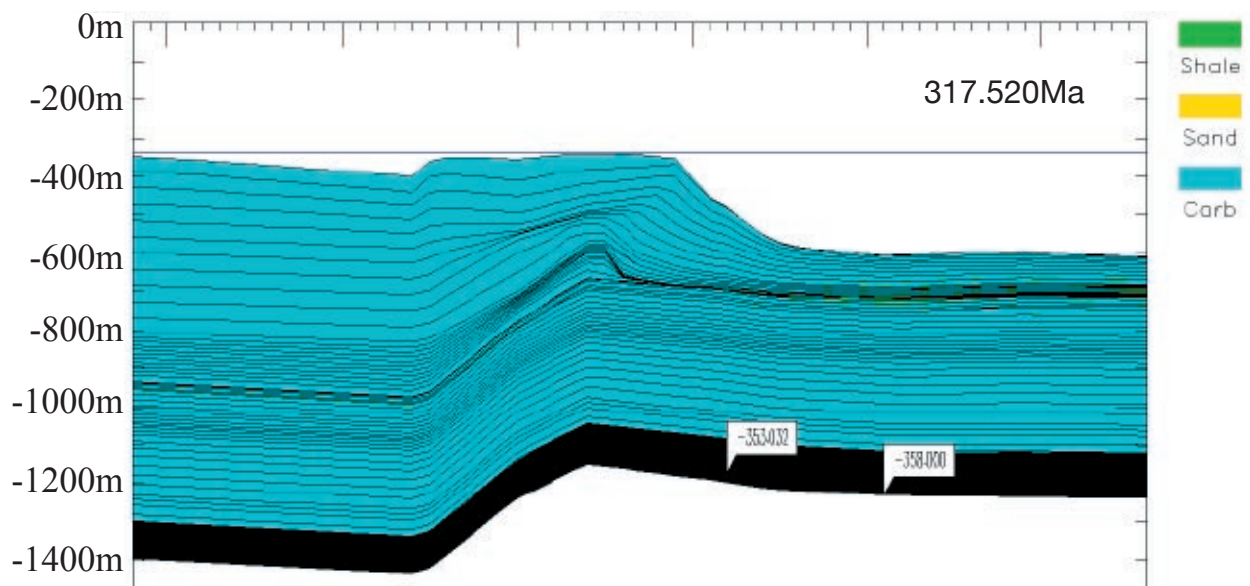


Fig. 7.13: Model run with the unaltered, literature-derived eustatic sea-level curve as shown in Fig. 7.14 (black line). At the top of the HST of sequence 1, the platform interior could not keep up with the rising sea-level, and the basin successively filled with debris from the platform margin. Vertical exaggeration: 10x.

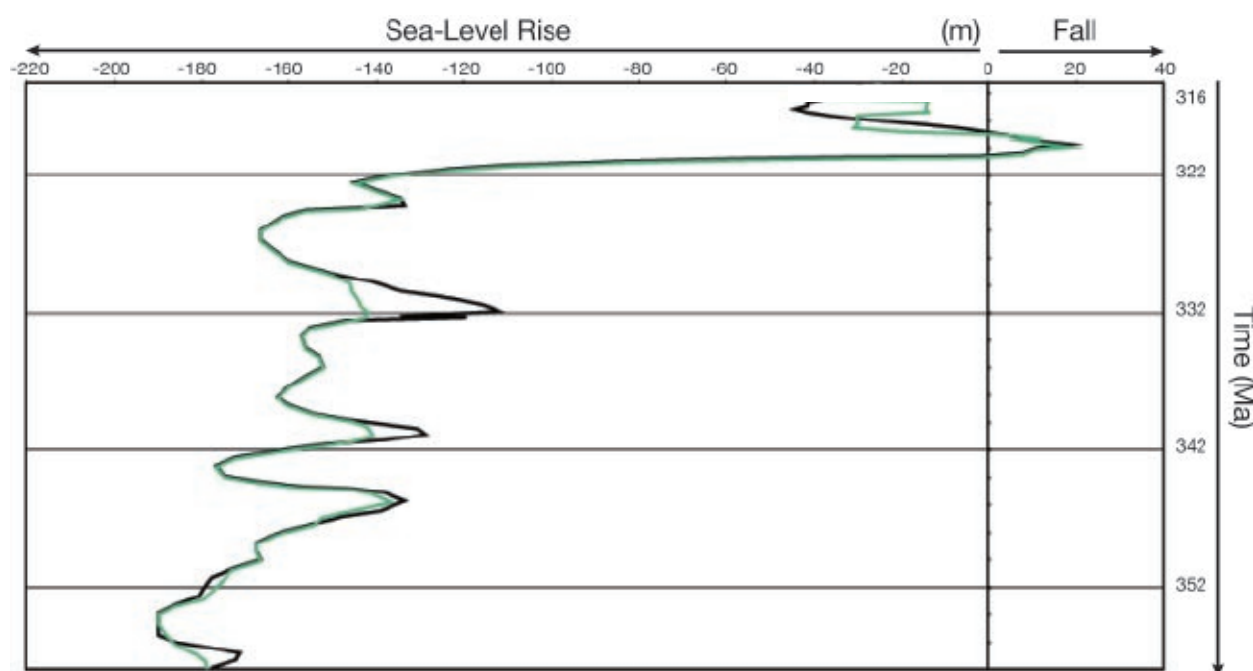


Fig. 7.14: Comparison of the initial eustatic sea-level curve as derived from literature data (black line; see Chapter 6.1) and the curve corrected by forward modeling (green line).

within the rapidly subsiding western part of the Bodón Transect. This mimics the lithologic changes within the San Emiliano Fm., where episodes are dominated by fine-grained siliciclastics and other episodes are dominated by mud-mound generation (see Chapter 3.2).

#### 7.4.3 Eustatic Sea-Level Curve

During the modeling process, it became clear that several values of the eustatic sea-level curve had to be decreased or increased in order to produce the natural stratigraphic patterns. Using the initial sea-level curve, the platform does not prograde far enough within the LST of Bas 1 or within the HST of Bas 1. Figure 7.13 shows the top of the HST of Bas 1 modeled with the initial sea-level curve. Due to the sea-level being too high, more accommodation space was available and the platform reacted with aggradation rather than progradation. Additionally, accommodation space increased within the platform interior, and the carbonate

production was not able to keep up with sea-level rise.

Therefore, some peak values of the sea-level curve were adjusted (Fig. 7.14). The pattern of the curve itself was only changed to the opposing value within the uppermost part of the modeled succession. However, the opposing pattern of rise and fall between 318.5 and 316Ma may reflect a temporal shift of the sea-level curve along the y-axis due to a calibration problem between the absolute time scale used within each literature source and the one used within this study (Fig. 3.3). Figure 7.14 displays a comparison between the initial and the adjusted sea-level curves.

## CHAPTER 8: SYNTHESIS

### 8.1 Southern Cantabrian Basin: The Pre-Carboniferous

The Cantabrian Basin represents a polyhistory basin. From uppermost Precambrian/Cambrian until the Silurian, an extensional regime prevailed. Cantabria was part of the northern passive margin of Gondwana. During the Cambrian, calculated subsidence rates are low within the modeled transects and also within the Bernesga Transect of Veselovsky (2004). At this stage, the depositional environment shows a uniform distribution of the Herrería Fm. (compare with Chapter 6.2.1).

The overall rifting/drifting regime eventually led to the generation of the Rheic Ocean, which separated Avalonia and Armorica. However, within the field area, local paleogeography was dominated by the proximity of the Cantabrian High situated in the north/northeast of the transects. Subsidence values as calculated for this stage are low. Throughout major parts of the transects, hiatus lasted from the uppermost Cambrian until the uppermost Devonian.

The tectonic regime inverted during the Devonian. An overall compressional setting prevailed and led to closure of the Rheic Ocean and subsequent generation of the Variscan Orogen during the Carboniferous. Within the study area, transgression of the sea from the SW during late Devonian re-started sedimentary record and initiated progressive deepening of the environment. This is seen in the changing deposits from the littoral sandbars of the Ermita Fm. to the basinal facies of the Vegamián and Alba Fm. Tectonic activity within the area was still low, the depositional environment was uniform.

### 8.2 The Carboniferous

#### 8.2.1 Serpukhovian - Moscovian: Regional Setting

During the Carboniferous, tectonic activity significantly increased due to the continued convergence and migration of the orogenic front. Flexural subsidence was exerted by the orogen and the sedimentary load and led to a classical differentiation of the foreland area into a foredeep, forebulge and back-bulge zone. During the Serpukhovian, deposits of the Olleros Fm. (see Chapter 3.2) represented deposition of the proximal foredeep, whereas the regionally widespread Barcaliente Fm. was positioned distally (Fig. 2.10a). Succeeding the Barcaliente Fm., subsidence increased significantly. Proximally, the basin center deepened, siliciclastic turbidites of the San Emiliano Fm. followed the Barcaliente Fm.

Distally, subsidence was more moderate resulting in a topographic high representing the forebulge zone, where the carbonate platform of the Valdeteja Fm. was initiated on top of the Barcaliente Fm. Since the foredeep trapped the siliciclastic sediments eroded from the rising orogen, the forebulge zone received little terrigenous input enabling platform development.

The higher sedimentary thicknesses of the Olleros and San Emiliano Fm. in comparison to the Valdeteja Fm. caused the typical wedge-shaped geometry of the foreland basin (see Chapter 1.1.2).

The regional distribution of the Barcaliente, Olleros, San Emiliano and Valdeteja Formations shows the continued convergence and north-/



northeastward migration of the foreland basin.

### 8.2.2 Serpukhovian

Revised subsidence rates of the Barcaliente Fm. (Chapter 7.4) are significantly higher than during the preceding Alba Fm., indicating an increasing influence of the evolving foreland setting. The highest thickness of the Barcaliente Formation accumulated within the lower part of the formation. The uniform and monotonous distribution over a wide region and the sedimentological record indicate a low depositional gradient. The shallowing conditions towards the top (see Chapter 3.2) are related to a significant drop of the eustatic sea-level and decreasing subsidence rates. The occurrence of the Porma Breccia and the following Señaras Mb. is restricted to the southern part of the Cantabrian Basin. Reuther (1977) attributed this to regionally restricted vertical movements of the basin, resulting in shallower conditions within the Southern Cantabrian Basin than in the north. This differentiation is a typical feature throughout partial basin inversion within a compressional setting (Einsele 2000).

### 8.2.3 Bashkirian and Moscovian

Initiation and development of the Valdeteja Fm. mimic the progressive differentiation of the distal foreland in front of the Variscan Orogen.

The development advanced from a low-gradient area during deposition of the Barcaliente Fm. toward the generation of a carbonate platform, which at least at its cratonward margin showed a considerable gradient of up to 45° (Chapter 7.4.1). This matches reportedly high repose angles from the Bashkirian to Moscovian Valdeteja and Picos de Europa Fm.

of the Northern Cantabrian Basin (Della Porta et al. 2004).

Unfortunately, the platform margin toward the foredeep is not accessible by surface-geology either in the Northern Cantabrian Basin or in the Southern Cantabrian Basin due to the subvertical dip of the tectonic units. Therefore, it is not possible to directly observe the platform-to-basin transition toward the foredeep.

The initial depositional sequence (Bas 1) shows an overly progradational pattern at its cratonward margin, whereas the following sequences are dominated by aggradation (see Chapter 4). Initially low subsidence rates enabled the platform to nucleate and triggered strong progradation since little accommodation space was available within the platform area. With increasing flexure and the orogenic front further advancing, subsidence rates increased also within the distal parts of the foreland. Thus, higher accumulation of carbonates was possible. However, due to the continuing rise and migration of the orogenic front, siliciclastic sediment supply increased and eventually, the proximal foredeep was unable to accommodate all the detritus, which led to an encroachment of the siliciclastics onto the distal area, initiating progressive termination of the platform.

During the Bashkirian, siliciclastics of the San Emiliano Fm. intruded from the south-to-west onto the platform area. First deposits occurred within the western Gayo Unit (see below), which probably represented a more proximal foredeep area than the younger siliciclastic deposits within the western Bodón Unit. The Upper Bashkirian San Emiliano Fm. of the Bodón Unit resembled distal foredeep depos-

its within an underfilled basin state. During the Moscovian, the basin was further filled to the west of the study area as indicated by coal beds e.g. north of Villamanin (Bernesga Valley, Bodón Unit).

During initial input of clastics across the Bodón Transect, the depocenter remained located at the western border of the transect. Subsidence trends at this time indicate increasing subsidence in the west. However, during the lower Moscovian, a clear trend of the transport direction from the east toward the west is distinguishable (see Chapter 6.3.2).

Due to the strong deformation of the area, no further conclusions can be drawn regarding the north-south directed evolution of the San Emiliano Fm. However, further information can be gathered from the interplay of the formations within the study area and the subsidence development.

#### **8.2.4 Spatial and Temporal Patterns and their Implications**

To date, the exact direction from which the orogen approached is uncertain. As outlined in Chapter 3.2, sediments of the San Emiliano Fm. are thought to have been transported from the south to west into the field area. The pattern of the highly diachronous base of the formation seems to confirm this. Figure 3.33 shows a schematic overview of the progressive onset from the west to the east across the Bodón Unit, whereas stratigraphic correlation and scarce biostratigraphic data also indicate the existence of a south-north directed diachronous onset.

The spatial distribution and platform backstepping patterns can further constrain the position of the sedimentary source. The shift in facies

belts from the Bashkirian to the Moscovian displays the migration of the depocenter of the foreland basin toward the craton, away from the front of the approaching orogen. Figure 8.1 shows a sketch of the distribution of the Bashkirian to Moscovian formations within the field area, which resembles the setting within the orogenic foreland.

An ideal plane strain orogenesis would create a linear setting with the strike of the orogen being subparallel to the axis of the depocenter of the foredeep, and also subparallel to the orientation of the adjacent platform margin. During migration of the depocenter toward the craton, the entire platform would backstep (Chapter 1.1.2). However, the backstepping pattern of the Valdeteja platform is highly diachronous as outlined in Chapters 3.2, 4 and 6.3.

Within the LST of Bas 1, the Valdeteja platform was surrounded on two sides by the basin facies of the Forcoso Zone. During the HST of Bas 1 (lower Bashkirian), differentiation became more obvious: foredeep deposits of the San Emiliano Fm. intruded into the western Gayo Unit of the field area (Fig. 8.1b). Contemporaneously, platform sedimentation continued to the south, east, and north.

Unfortunately, biostratigraphic constraints are low for the Valdeteja and San Emiliano Fm. in this area. Present data indicate that the top of the Valdeteja Fm. is younger in the Correcilla Unit than in the Gayo Unit (Fig. 8.1b,c; see Fig. 4.3a & 4.4a). Stratigraphic correlation by Fernández González (1990) between the Bodón and Gayo Units in this area confirms the available, but scarce, paleontological data. This implies that while there was carbonate platform growth in the Correcilla Unit in the south and the Bodón Unit in the north, foredeep basin sedimentation was taking place at

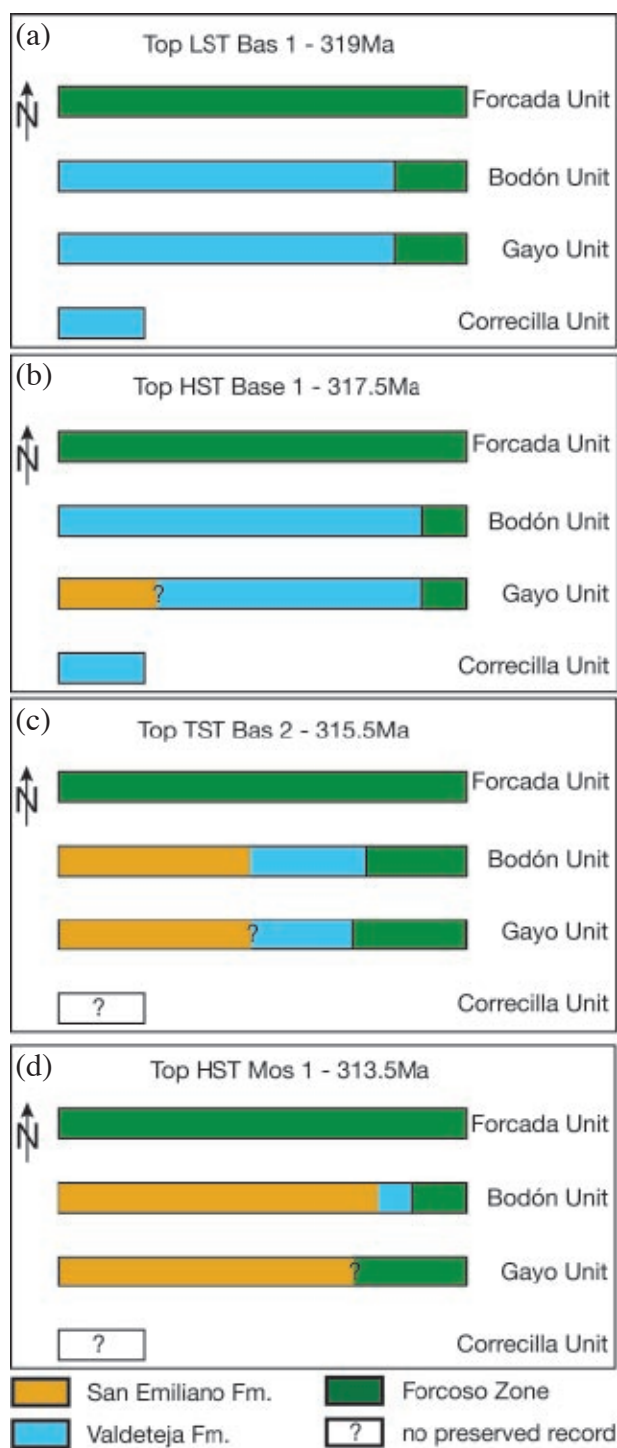


Fig. 8.1: Schematic plan view of the distribution of formations across the tectonic units (x-axis), which are shown as parallel slices according to their pre-deformational depositional setting (not to scale). (a) to (d) display the distribution of the formations from the Bashkirian to Moscovian. Generally, the San Emiliano Fm. represents foredeep deposits, the Valdeteja Fm. the carbonate platform on the forebulge, and the Forcoso Zone represents basin deposits of the back-bulge zone. Note the progressive onset of the foredeep deposits (San Emiliano Fm.) from the south-to-west. Distances are not to scale. Bas 1 - Mos 2: sequences.

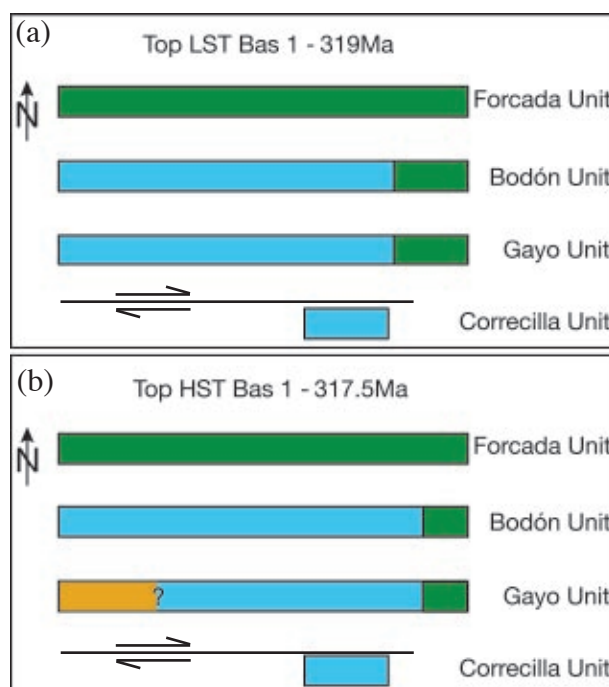


Fig. 8.2: Schematic plan view as in Figure 8.1a&b, but the position of the Correcilla Unit was moved along a dextral fault toward the east. Stratigraphic relationships between the tectonic units could be explained by this spatial, pre-deformational setting. See Fig. 8.1 for legend.

the same time in the Gayo Unit (Fig. 8.1b). It is improbable that the siliciclastics of the Gayo Unit represent an intra-cratonic basin. The surrounding, relatively stable carbonate platform would not leave the possibility of transporting the present conglomerates and coarse-grained siliciclastics into the area. No indication of coarse-grained siliciclastics exists within the platform area.

Another possible solution would be that sediment was transported into the area from the west. However, this would require a sedimentary source, i.e. the orogen, to be located in the west, which does not comply with the regional model.

Therefore, it is assumed that the original paleogeographical relationship of the tectonic units was obscured by a considerably wide, lateral thrust sheet transport of the Correcilla Unit to the east along the basal thrust plane of



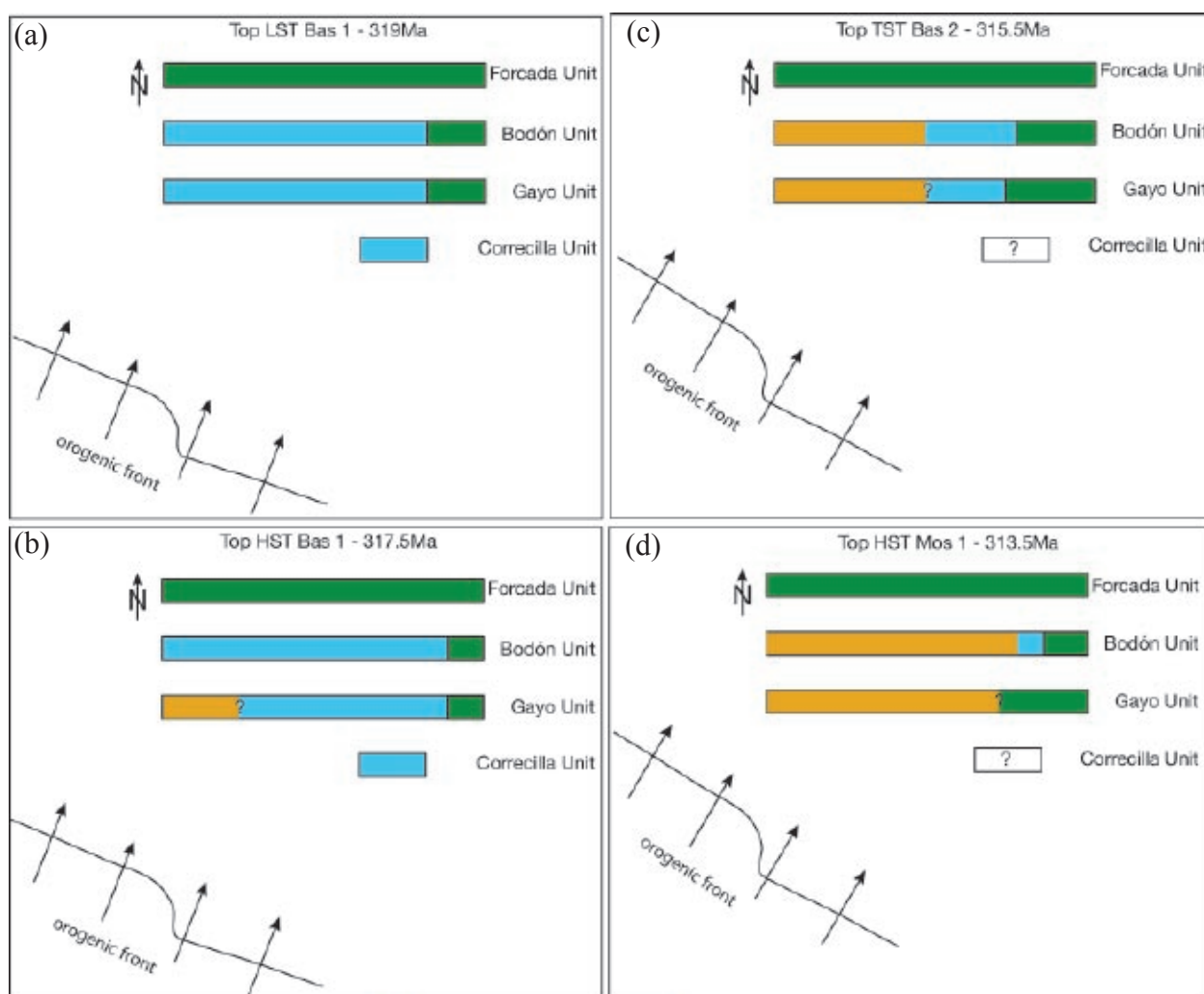


Fig. 8.3: Schematic plan view of the formations across the tectonic units as in Figures 8.1 & 8.2, with the position of the Correcilla Unit moved toward the east. The orogenic front approached from the south-to-west. The sedimentary pattern within the field area indicates the influence of an orogenic recess. Distances are not to scale. Arrows indicate the advancing orogen. For legend, please refer to Figure 8.1.

the Correcilla Unit (Fig. 8.2), which probably occurred during thrust emplacement. This implies a deviation from the generally assumed south-north directed thrust sheet transport direction within this part of the fold-and-thrust belt.

If the position of the Correcilla Unit was located further to the east as shown in Figure 8.2, the local development of the Bashkirian and Moscovian would still be complex in front of the orogen, but explainable.

During Bas 1 (Fig. 8.1a,b), subsidence rates were higher within the Gayo Unit than within

the Bodón Unit. This is related to the fact that the Gayo Unit was in a more proximal position to the orogen than the Bodón Unit. However, the sedimentary record displays a differentiation within the Gayo Unit: in the west, the platform backstepped (see Chapter 6.3), whereas in the east, the platform developed its maximum progradation into the adjacent basin (see Chapters 4.2 and 7.4), indicating low subsidence at the position of the forebulge. The back-bulge zone subsided. A perfectly linear orogen approaching from the south would not have produced such a laterally differentiated subsidence development.

Furthermore, Figure 8.1c shows continuing backstepping of the platform towards the east during Bas 2. At this stage, basinal deposits intrude onto the platform area from the east and also from the west. The last, small remainder of the platform during Mos 1 (Fig. 8.1d) was positioned within the eastern Bodón Unit at Las Majadas del Caserio.

The backstepping pattern of the platform reflects increasing subsidence, caused by the cratonward migration of the foreland basin depocenter. The resulting pattern seems to exclude the possibility of a source area being located south of the field area.

In fact, a more complex pattern is assumed.

Obviously, spatial relationships within the initial depositional system were not linear. Assuming that the Correcilla Unit was originally positioned further to the east (according to today's coordinates; Fig. 8.2), the foredeep may have been narrower in the southeast (i.e. the region of the Correcilla Unit) than in the northwest (i.e. the region of the western Gayo Unit) resulting in an oblique geometrical relationship between the strike of the orogen and the foreland.

Alternatively, the stratigraphic setting may be caused by the influence of an orogenic recess (Fig. 8.3). Thrust belts can deviate from the ideal linear plane strain conditions. Recesses and salients cause sinuous traces of thrust belts (Oriol & Moore 1986, Paulsen & Marshak 1998, Whiting & Thomas 1994). Subsidence patterns within a recess area would be influenced from two sides: (i) the main hinterland, (ii) the salient. The result would be a complex three-dimensional pattern.

Both settings would lead to a complicated interaction, which may have caused the given relationship between the units. Due to the

inconclusive biostratigraphic database in the Gayo and Correcilla Units along the Torío Transect and the regional tectonic model still being keenly discussed, this setting needs more investigation in order to establish a well-constrained 3D-model.

## CHAPTER 9: CONCLUSIONS

This study investigated the sedimentary and tectonic development of the polyhistory Cantabrian Basin. The preserved basin fill consists of Cambrian to Carboniferous deposits, which are deformed in a thin-skinned style due to the overprint of the Variscan and Alpine Orogenies.

### 9.1 Sedimentological Model

The pre-Carboniferous basin fill shows an alternating predominance of carbonate and siliciclastic deposits. Because of the proximal position of the transect, long-lasting hiati occur within the Paleozoic succession.

The Carboniferous sedimentary deposits reflect the progressive differentiation of the foreland of the Variscan Orogen. Field data, facies analysis, aerial photographs and sequence analysis resulted in a time-dependent depositional model of the Serpukhovian to Moscovian mixed carbonate-siliciclastic sedimentation. The foreland basin developed from an early stage during the Serpukhovian (Barcaliente Fm., Olleros Fm.) to a more complex stage, with segmentation of the foreland into foredeep (San Emiliano Fm.), forebulge (Valdeteja Fm.), and back-bulge (Forcoso Zone) depositional zone.

The platform of the Valdeteja Fm. exhibits well-stratified patterns at the cratonward basin margin, which together with the facies analysis and biostratigraphic data enabled a sequence stratigraphic interpretation of the Bashkirian and Moscovian depositional system. Four sequences (Bas 1 - Mos 2) display the development in front of the approaching Variscan Orogen. The platform has its great-

est extension and accumulation during Bas 1. However, already during Bas 1, clastic foredeep deposits were shed into the western Gayo Unit and terminated platform growth at this location. Subsequently, the remaining platform was progressively terminated from the south and west during Bas 2 and Mos 1.

Prominent escarpments existed at the basin margin during the LST of Bas 2, which were subsequently flooded. During Mos 1, remnants of the Valdeteja platform existed only in the eastern Bodón Unit. Accumulation was low at this time and basinal deposits intruded onto the last remaining platform area. Deposits of Mos 2 outcrop only at Lavandera in the western Bodón Unit, where the San Emiliano Fm. has its maximum thickness within the study area.

The sequence stratigraphic model allowed a time-dependent genetic model within the field area to be established, which served as a basis for the quantitative basin modeling.

### 9.2 Structural Balancing

As a prerequisite for reverse basin modeling along the Torío and Curueño Transects, structural balancing was carried out to determine initial distances between the recorded stratigraphic columns.

To construct balanced cross-sections, a family of structures for the fold-and-thrust belt of the Southern Cantabrian Basin was compiled. The cross-sections were restored using the equal-length method. Minimum shortening rates were calculated within each single thrust sheet and between the pin lines. The former vary between 19% - 54%, the highest values occur-



ring within the strongly deformed Montuerto Syncline. The latter includes the amount of offset along the corresponding thrusts. Minimum shortening ranges between 44% and 64%.

### 9.3 Subsidence Analysis

The subsidence analysis is based on results derived by reverse modeling with PHIL<sup>TM</sup> for the north-south oriented Torío and Curueño Transects and the connecting, west-east oriented Bodón Transect.

Subsidence values for the pre-Carboniferous basin fill follow the scheme as introduced by Veselovsky (2004) for the parallel Bernesga Transect. Six stages represent the rifting/drift setting from the Cambrian to the Silurian and the subsequent change of the plate tectonic setting to compression. However, subsidence rates are generally very low for the Cambrian to Devonian basin fill because of the proximal position of the transects and the vicinity of the Cantabrian High in the northeastern part of the field area. Maximum total subsidence rates are 80m/Ma.

Quantification of subsidence rates during Serpukhovian to Moscovian times reveals the progressive segmentation of the Variscan foreland basin within a non-linear setting in front of the approaching orogen. During platform growth at the forebulge, maximum thermo-tectonic subsidence rates equal 270m/Ma during a time of high accumulation in the outer parts of the platform within the HST of Bas 1. Maximum values within the inner part of the forebulge reach 110m/Ma. Maximum values reach 740m/Ma within the time increment containing the onset of the San Emiliano Fm. at Lavandera (Bodón Unit) during Bas 2.

The spatial distribution of the subsidence rates indicates a non-linear geometry within the

foreland. This is related to an orogenic recess that caused a complex three-dimensional pattern during the time of platform growth and its backstepping from the upper Bashkirian to the lower Moscovian. Alternatively, an oblique collision could have created a similar subsidence pattern.

### 9.4 Forward Modeling

Using SEDPAK software, stratigraphic forward modeling was applied to quantify the controlling factors responsible for creating the deposits of the Ermita Fm. (upper Famennian) to San Emiliano Fm. (Westphalian) within the Bodón Transect by using the SEDPAK software. Forward modeling permits the semi-quantitative assessment of the significance of controlling factors influencing the sedimentary system by iterative calibration of the model to the sedimentary record of the field area.

For the sandstone-dominated Ermita Fm., minimum and maximum values for sand supply values ranged over  $0.47 - 0.94 \cdot 10^3 \text{ km}^2/\text{ka}$ . For the more rapidly accumulated siliciclastics of the synorogenic San Emiliano Fm., resembling the distal orogenic foredeep, the shale supply rate reached values of  $1.65 - 4 \cdot 10^3 \text{ km}^2/\text{ka}$ , while the sand supply reached slightly lower rates of  $0.18 - 0.85 \cdot 10^3 \text{ km}^2/\text{ka}$ . During the growth of the Valdeteja Fm. platform carbonates, the carbonate production curve reached a maximum value of 0.26m/ka at the forebulge depozone.

Carbonate repose angles varied between 30 and 45°, steepening during times of aggradation. This corresponds to the results of Della Porta et al. (2004) for the comparable Bashkirian - Moscovian carbonate platform in the Northern Cantabrian Zone.

The modeling process revealed the significance

of a foundation for the platform to prograde across and into the basin. This foundation could consist of sediment by-pass from the margin and/or basin filling. The basin margin physiography had a strong influence on whether the platform prograded into the basin.

Furthermore, facies-dependent modeling further refined the accuracy of the subsidence rates for the Barcaliente Fm., since the lack of sufficient biostratigraphic data meant a good resolution for the input data was not possible in the reverse modeling procedure.

The literature-derived eustatic sea-level curve was corrected during the forward modeling process. Essentially, some peak values were decreased to produce the platform pattern observed in outcrop.





## REFERENCES

- Agueda, J.A., Bahamonde, J.R., Barba, F.J., Barba, P., Colmenero, J.R., Fernández, L.P., Salvador, C.I. & Vera, C. (1991): Depositional environments in Westphalian coal-bearing successions of the Cantabrian Mountains, northwest Spain. *Bull. Soc. géol. France*, 162(2): 325-333.
- Aitken, S.A., Collom, C.J., Henderson, C.M. & Johnston, P.A. (2002): Stratigraphy, paleoecology, and origin of Lower Devonian (Emsian) carbonate mud buildups, Hamar Laghdad, eastern Anti-Atlas, Morocco, Africa. *Bull. Can. Petrol. Geol.*, 50(2): 217-243.
- Allen, P.A., Crampton, S.L. & Sinclair, H.D. (1991): The inception and early evolution of the North Alpine Foreland Basin, Switzerland. *Basin Research*, 4: 143-163.
- Aller, J., Bastida, F., Brime, C. & Pérez-Estaún, A. (1987): Cleavage and its relation with metamorphic grade in the Cantabrian Zone (Hercynian of NW Spain). *Sci. Geol. Bull.*, 40: 1-18.
- Alonso, A., Floquet, M., Mas, J.R., Meléndez, A., Meléndez, N., Salomón, J. & Vadot, J.P. (1987): Modalités de la régression marine sur le détroit ibérique (Espagne) à la fin du Crétacé. *Memoires Geologiques de la Université de Dijon*, 11: 91-112.
- Alonso, J.L. (1987): Sequences of thrusts and displacement transfer in the superposed duplexes of the Esla Nappe Region (Cantabrian Zone, NW Spain). *J. Structural Geology*, 9(8): 969-983.
- Alonso, J.L., Suárez Rodríguez, A., Rodríguez Fernández, L.R., Farias, P. & Villegas, H. (1991): Cartografía del mapa geológico de España, Escala 1:50.000, No.103 (La Pola de Gordón). Madrid, IGME.
- Alonso, J.L., Alvarez Marron, J., Aller, J., Bastida, F., Farias, P., Marcos, A., Marquinez, J., Pérez-Estaún, A. & Pulgar, J.A. (1992): Estructura de la Zona Cantábrica. In: Gutierrez Marco, J.G., Saavedra, J. and Rábano, I., eds., *Paleozoico Inferior de Ibero-América: Universidad de Extremadura*.
- Alvarado, M.M. (1983): Encuadre paleogeográfico y geodinámico de la Península Ibérica. In: Rios, J.M., ed., *Libro Jubilar J. M. Rios. Geología de España*, v. 1: Madrid, Comisión Nacional de Geología, p. 9-55.
- Alvaro, J.J., Vennin, E., Moreno-Eiris, E., Perejón, A. & Bechstädt, T. (2000): Sedimentary patterns across the Lower-Middle Cambrian transition in the Esla nappe (Cantabrian Mountains, northern Spain). *Sedimentary Geology*, 137: 43-61.
- Aramburu, C. & García-Ramos, J.C. (1988): Presencia de la discontinuidad sárdica en la Zona Cantábrica. *Geogaceta*, 5: 11-13.
- Aramburu, C., Truyols, J., Arbizu, M., Méndez-Bedia, I., Zamarreño, I., García-Ramos, J.C., Suarez, d.C.C. & Valenzuela, M. (1992): El Paleozoico Inferior de la Zona Cantábrica. In: Gutierrez Marco, J.G., Saavedra, J. and Rabano, I., eds., *Paleozoico Inferior de Ibero-América: Universidad de Extremadura*.
- Aramburu, C. & García-Ramos, J.C. (1993): La sedimentación cambro-ordovícica en la Zona Cantábrica (NO de España). *Trabajos de Geología*, 19: 45-73.
- Aramburu, C. & Bastida, F., Eds. (1995): *Geología de Asturias*. Gojón, Ediciones Trea, S.L.
- Aramburu, C. (1995): El Precámbrico y el Paleozoico Inferior. In: Aramburu, C. and Bastida, F., eds., *Geología de Asturias: Gojón, Ediciones Trea, S.L.*, p. 35-50.
- Arthaud, F. & Matte, P. (1977): Late Paleozoic strike-slip faulting in southern Europe and northern Africa: result of a right-lateral shear zone between the Appalachians and the Urals. *Bull. geol. Soc. Am.*, 88: 1305-1320.
- Bachtadse, V. & Van der Voo, R. (1986): Palaeomagnetic evidence for crustal and thin-skinned rotations in the European Hercynides. *Geophys. Res. Lett.*, 13: 161-164.
- Badham, J.N.P. (1982): Strike-slip orogens - an explanation for the Hercynides. *Journal of the Geological Society, London*, 139: 493-504.
- Bahamonde Rionda, J.R. (1990): Estratigrafía y sedimentología del Carbonífero Medio y Superior de la Región del Manto de Ponga. Doctoral thesis, University of Oviedo, 215 p.
- Baldwin, C.T. (1978): A comparison of the stratigraphy and depositional processes in the Cambro-Ordovician rocks of the Cantabrian and West-Asturian-Leonese Zones, N.W. Spain. *Cuad. Seminario Est. Cerámicas Sargadelos*, 27: 43-78.
- Baldwin, B. & Butler, C.O. (1985): Compaction Curves. *AAPG Bulletin*, 69(4): 622-626.
- Bally, A.W., Gordy, P.L. & Stewart, G.A. (1966): Structure, seismic data, and orogenic evolution of the southern Canadian Rocky Mountains.

- Bull. Can. Petrol. Geol., 14(3): 337-381.
- Balthasar, U. (2001): Taxonomy and palaeoecology of silicified foraminifera from the Lower Carboniferous Genicera Formation (Cantabrian Mountains, Northern Spain). Diploma thesis, Philipps-Universität, Marburg, 59 p.
- Barba, P. & Fernández, L.P. (1990): Estratigrafía, Memoria del mapa geológico de España, Escala 1:50.000, No.102 (Los Barrios de Luna), 2. Serie (MAGNA): Madrid, ITGE, p. 10-61.
- Barba, P. & Fernández, L.P. (1991): Estratigrafía, Memoria del mapa geológico de España, Escala 1:50.000, No.103 (La Pola de Gordón), 2. Serie (MAGNA): Madrid, IGME, p. 10-73.
- Bastida, F., Brime, C., García López, S. & Sarmiento, G.N. (1999): Tectono-thermal evolution in a region with thin-skinned tectonics: the western nappes in the Cantabrian Zone (Variscan belt of NW Spain). *Int. Journ. Earth Sciences*, 88: 38-48.
- Bauluz, B., Mayayo, M.J., Fernández-Nieto, C. & González López, J.M. (2000): Geochemistry of Precambrian and Paleozoic siliciclastic rocks from the Iberian Range (NE Spain): implications for source-area weathering, sorting, provenance and tectonic setting. *Chemical Geology*, 168: 135-150.
- Beaumont, C. (1981): Foreland basins. *Geophysical Journal of the Royal Astronomical Society*, 65: 291-329.
- Becker, G., Bless, M.J.M. & Kullmann, J. (1975): Oberkarbonische Entomozoen-Schiefer im Kantabrischen Gebirge (Nordspanien). *Neues Jahrbuch fuer Geologie und Palaeontologie, Abhandlungen*, 150(1): 92-110.
- Beetsma, J.J. (1995): The late Proterozoic/Paleozoic and Hercynian crustal evolution of the Iberian Massif, N Portugal: as traced by geochemistry, and Sr-Nd-Pb isotope systematics of pre-Hercynian terrigenous sediments and Hercynian granitoids. PhD thesis, Vrije University, Amsterdam.
- Ben Avraham, Z. & Emery, K.O. (1973): Structural framework of the Sunda Shelf. *Bull. Am. Ass. Petrol. Geol.*, 57: 2323-2366.
- Bergström, S.M. & Massa, D. (1992): Stratigraphic and biogeographic significance of Upper Ordovician conodonts from northwestern Libya. In: Salem, M.J., Hammuda, O.S. and Elia-goubi, B.A., eds., *The Geology of Libya*, v. 4: Amsterdam, Elsevier, p. 1323-1342.
- Bialk, A. (1989): Geologische Kartierung im Paläozoikum des Kantabrischen Gebirges bei Redilluera (Prov. León, NW Spanien) unter besonderer Berücksichtigung der Vegamián-Formation (Tournai), Eberhard-Karls-Universität Tübingen.
- Bissell, H.J. & Barker, H.K. (1977): Deep-water limestones of the Great Blue Formation (Mississippian) in the eastern part of the Cordilleran Miogeosyncline in Utah. *SEPM Special Publications*, 25: 171-186.
- Boden, V. (1982): Fazielle Untersuchungen in der Vegamián-Formation des Tournai (Unter-Karbon) im Kantabrischen Gebirge (Nordspanien). Unveröff. Diploma thesis, Universität Köln, 133 p.
- Boll, F.C. (1983): Der Wandel der rugosen Korallenfauna der Flachwasser-Fazies im Karbon des Kantabrischen Gebirges (Nordspanien). *Dissertation thesis*, Universität Tübingen, 1-275 p.
- Boll, F.-C. (1985): Rugose Korallen der Flachwasser-Fazies im Oberkarbon des Kantabrischen Gebirges (Nordspanien). *Palaeontographica, Abt. A.*, 190: 1-81.
- Bonhommet, N., Cobbold, P.R. & Perroud, H. (1981): Paleomagnetism and cross-folding in a key area of the Asturian arc (Spain). *Journal of Geophysical Research*, 86(B3): 1873-1887.
- Bosch, W.J. (1969): The relationship between orogenesis and sedimentation in the SW part of the Cantabrian Mountains (NW Spain). *Leidse Geol. Meded.*, 44: 227-233.
- Bouroz, A. (1979): IUGS Subcommission on Carboniferous Stratigraphy. In: Meyen, S.V., Menner, V.V., Reytlinger, Y.A., Rotay, A.P. and Solov'yeva, M.N., eds., *Obshchiye problemy stratigrafii kamennougol'nykh otlozheniy: Compte Rendu - International Congress on Carboniferous Stratigraphy and Geology*, 8, v. 3, p. 22-26.
- Bowman, M.B.J. (1980): The sedimentology and stratigraphy of the San Emiliano Formation and associated sequences, Carboniferous, NW Spain. Doctoral thesis, Univ. of Sheffield.
- Bowman, M.B.J. (1982): The stratigraphy of the San Emiliano Formation and its relationship to other Namurian/Westphalian A sequences in the Cantabrian Mts., NW Spain. *Trabajos de Geologia*, 12: 23-35.
- Bowman, M.B.J. (1983): The genesis of algal nodule limestones from the Upper Carboniferous (San Emiliano Formation) of N.W. Spain. In: Peryt, T.M., ed., *Coated Grains*: Berlin, Heidelberg, New York, Springer-Verlag, p. 409-423.
- Bowman, S.A. & Vail, P.R. (1999): Interpreting the stratigraphy of the Baltimore Canyon section,

- offshore New Jersey with PHIL, a stratigraphic simulator. SEPM Special Publications, 62.
- Boyer, S.E. & Elliot, D. (1982): Thrust systems. AAPG Bulletin, 66: 1196-1230.
- Boyer, S.E. (1991): Geometric evidence for synchronous thrusting in the southern Alberta and northwest Montana thrust belts. In: McClay, K.R., ed., Thrust Tectonics.
- Bradley, D.C. (1989): Taconic plate kinematics as revealed by foredeep stratigraphy, Appalachian orogen. Tectonics, 8: 1037-1049.
- Braun, N. (1981): Geologische Kartierung im Paläozoikum des mittleren Curueño-Gebietes (Prov. León, NW-Spanien) und petrographische, sedimentologische sowie fazielle Untersuchungen der Sedimente vom Kambrium bis zum Westfal, unter besonderer Berücksichtigung der Barcaliente-Formation (Namur A, B). Diploma thesis, Eberhard-Karls-Universität, Tübingen.
- Brouwer, A. & van Ginkel, A.C. (1964): La sucesión carbonifera dans la partie méridionale des Montagnes Cantabriques (Espagne du Nord-Ouest). C. R. V. Congr. Strat. Geol. Carb., Paris.
- Brun, J.P. & Burg, J.P. (1982): Combined thrusting and wrenching in the Ibero-Armorican Arc; a corner effect during continental collision. Earth and Planetary Science Letters, 61(2): 319-332.
- Bucher, W.H. (1933): The Deformation of the Earth's Crust, Princeton Univ. Press. 518.
- Buggisch, W., Rabien, A. & Huehner, G. (1980): Das Oberdevon im Rinkenbach-Tal S Oberscheld (Conodonten- und Ostracoden-Stratigraphie, Dillmulde, Rheinisches Schiefergebirge). Geologisches Jahrbuch Hessen, 108: 43-94.
- Burov, E.B. & Diament, M. (1995): The effective elastic thickness ( $T_e$ ) of continental lithosphere: What does it really mean? J. Geophysical Research, 100(B3): 3905-3927.
- Burov, E.B. & Diament, M. (1996): Isostasy, equivalent elastic thickness, and inelastic rheology of continents and oceans. Geology, 24(5): 419-422.
- Burov, E.B., Jaupart, C. & Mareschal, J.C. (1998): Large-scale crustal heterogeneities and lithospheric strength in cratons. Earth and Planetary Science Letters, 164: 205-219.
- Butler, R.W.H. (1982): The terminology of structures in thrust belts. J. Structural Geology, 4(3): 239-245.
- Butler, R.W.H. (1987): Thrust sequences. Journal of the Geological Society, London, 144: 619-634.
- Buxtorf, A. (1907): Zur Tektonik des Kettenjura. Ber. Versammlungen Oberrheinischen Geol. Ver., 40: 29-38.
- Carey, S.W. (1962): Folding. J. Alta. Soc. Petrol. Geol., 10: 95-144.
- Carls, P. (1983): La Zona asturoccidental-leonesa en Aragón y el Macizo del Ebro como prolongación del Macizo cantábrico. In: Comba, J.A., ed., Geología de España, Libro Jubilar J. M. Ríos, v. 3: Madrid, IGME, p. 11-32.
- Carls, P. (1988): The Devonian of Celtiberia (Spain) and Devonian paleogeography of SW Europe. In: McMillan, N.J., Embry, A.F. and Glass, D.J., eds., Devonian of the World, v. 14(1), Canadian Society Petroleum Geologists Calgary, p. 421-466.
- Catuneanu, O., Beaumont, C. & Waschbusch, P. (1997): Interplay of static loads and subduction dynamics in foreland basins: reciprocal stratigraphies and the "missing" peripheral bulge. Geology, 25: 1087-1090.
- Chamberlain, R.T. (1910): The Appalachian folds of Central Pennsylvania. Journal of Geology, 18: 228-251.
- Chamberlain (1919): The building of the Colorado Rockies. Journal of Geology, 27: 225-251.
- Chapple, W.M. (1978): Mechanics of thin-skinned fold-and-thrust belts. Geol. Soc. Am. Bull., 89: 1189-1198.
- Cloetingh, S. & Burov, E.B. (1996): Thermomechanical structure of European continental lithosphere: constraints from rheological profiles and EET estimates. Geophys. J. Int., 124: 695-723.
- Cocks, L.R.M. & Fortey, R.A. (1990): Biogeography of Ordovician and Silurian faunas. In: McKerrow, W.S. and Scotese, C.R., eds., Palaeozoic Palaeogeography and Biogeography: Memoirs, v. 12: London, Geological Society, p. 97-104.
- Cocks, L.R.M. (2000): The Early Palaeozoic geography of Europe. Journal of the Geological Society, London, 157: 1-10.
- Colmenero, J.R., Bahamonde, J.R. & Barba, P. (1996): Las facies aluviales asociadas a los depósitos de carbón en las cuencas estefanienses de León (borde sur de la Cordillera Cantábrica). Cuadernos de Geología Ibérica, 21: 71-92.
- Colmenero, J.R., Fernández, L.P., Moreno, C., Bahamonde, J.R., Barba, P., Heredia, N. & González, F. (2002): Carboniferous. In: Gibbons, W. and Moreno, T., eds., The Geology



- of Spain: London, The Geological Society, p. 93-116.
- Comte, P. (1959): Recherches sur les terrains anciens de la Cordillère Cantabrique. Madrid, IGME.
- Cooper, M.A. & Trayner, P.M. (1986): Thrust-surface geometry: implications for thrust-belt evolution and section-balancing techniques. *J. Structural Geology*, 8(3/4): 305-312.
- Covey, M. (1986): The evolution of foreland basins to steady state: evidence from the western Taiwan foreland basin. In: Allen, P.A. and Home-wood, P., eds., *Foreland Basins*, v. 8, Spec. Publ. Int. Ass. Sed., p. 77-90.
- Cramer, F.H. (1964): Some Acritarchs from the San Pedro Formation (Gedinnien) of the Cantabrian Mountains in Spain. *Bull. Soc. Belge Géol. Paléont. Hydrol.*, 73(1): 33-38.
- Crimes, T.P. & Marcos, A. (1976): Trilobite traces and the age of the lowest part of the Ordovician reference section for N.W. Spain. *Geol. Mag.*, 113: 349-356.
- Dahlstrom, C.D.A. (1969): Balanced cross sections. *Canadian Journal of Earth Sciences*, 6(4, Part 1): 743-757.
- Dahlstrom, C.D.A. (1970): Structural geology in the eastern margin of the Canadian Rocky Mountains. *AAPG Bulletin*, 54(5): 843pp.
- Dallmeyer, R.D., Martínez Catalán, J.R., Arenas, R., Gil Ibarguchi, J.I., Gutiérrez Alonso, G., Farias, P., Bastida, F. & Aller, J. (1997): Diachronous Variscan tectonothermal activity in the NW Iberian Massif: Evidence from  $^{40}\text{Ar}/^{39}\text{Ar}$  dating of regional fabrics. *Tectonophysics*, 277: 307-337.
- Davies, G.R., Richards, B.C., Beauchamp, B. & Nassichuk, W.W. (1989): Carboniferous and Permian reefs in Canada and adjacent areas. In: Geldsetzer, H.J., James, N.P. and Tebbutt, G.E., eds., *Reefs, Canada and Adjacent Areas*, v. 13, Canadian Society of Petroleum Geologists Memoir, p. 565-574.
- DeCelles, P.G. & Burden, E.T. (1992): Non-marine sedimentation in the overfilled part of the Jurassic-Cretaceous Cordilleran foreland basin: Morrison and Cloverly Formations, central Wyoming, USA. *Basin Research*, 4: 291-314.
- DeCelles, P.G. & Currie, B.S. (1996): Long-term sediment accumulation in the Middle Jurassic-early Eocene Cordilleran retroarc foreland-basin system. *Geology*, 24: 591-594.
- DeCelles, P.G. & Giles, K.A. (1996): Foreland basin systems. *Basin Research*, 8: 105-123.
- De Coo, J.C.M., Deelman, J.C. & Van der Baan, D. (1971): Carbonate facies of the Santa Lucía Formation (Emsian-Couvinian) in León and Asturias, Spain. *Geol. en Mijnbouw*, 50(3): 359-366.
- De Sitter, L.U. (1962): The structure of the southern slope of the Cantabrian Mountains. *Leidse Geol. Meded.*, 26: 255-264.
- Della Porta, G. (2003): Depositional anatomy of a Carboniferous high-rising carbonate platform (Cantabrian Mountains, NW Spain). Ph.D. thesis, Vrije Universiteit, Amsterdam, 250 p.
- Della Porta, G., Kenter, J.A.M. & Bahamonde, J.R. (2004): Depositional facies and stratal geometry of an Upper Carboniferous prograding and aggrading high-relief carbonate platform (Cantabrian Mountains, N.Spain). *Sedimentology*, 51(2): 267-295.
- Dennison, J.M. (1985): Devonian eustatic fluctuations in Euramerica: Discussion. *Geol. Soc. of America Bulletin*, 96: 1595-1597.
- Dias, R. & Ribeiro, A. (1995): The Ibero-Armorican Arc: A collision effect against an irregular continent? *Tectonophysics*, 246: 113-128.
- Dickinson, W.R. (1974): Plate tectonics and sedimentation. *Spec. Publ. Soc. Econ. Paleont. Min.*, 22: 1-27.
- Dickinson, W.R., Armin, R.A., Beckvar, T.C., Goodlin, S.U., Janecke, R.A., Mark, R.D., Norris, G., Radel, G. & Wortman, A. (1987): Geohistory analysis of rates of sediment accumulation and subsidence for selected California Basins. In: Ingersoll, V.R. and Ernst, W.G., eds., *Cenozoic basin development of coastal California*, v. 6, p. 1-23.
- Dingle, P.S., Bader, B., Hensen, C., Minten, B. & Schäfer, P. (1993): Sedimentology and Palaeoecology of Upper Carboniferous Shallow-Water Carbonate Complexes of the Carmenes Syncline (Cantabrian Mts., N-Spain). *Z. dt. geol. Ges.*, 144: 370-395.
- Díez Balda, M.A., Vegas, R. & González-Lodeiro, F. (1990): Central-Iberian Zone. Autochthonous sequences. Structure. In: Dallmeyer, R.D. and Martínez-García, E., eds., *Pre-Mesozoic Geology of Iberia*: Berlin, Springer-Verlag, p. 172-188.
- Dorobek, S.L. (1995): Synorogenic carbonate platforms and reefs in foreland basins: controls on stratigraphic evolution and platform/reef morphology. *SEPM Special Publications*, 52: 127-147.
- Douglas, R.J.W. (1950): Callum Creek, Langford Creek, and Gap map areas, Alberta, Geological Survey of Canada 124.

- Duff, P.M.D. (1993): *Holmes' Principles of physical geology*. London, Chapman & Hill 791.
- Eberli, G.P., Kendall, C.G.S.C., Moore, P., Whittle, G.L. & Cannon, R. (1994): Testing a Seismic Interpretation of Great Bahama Bank with a Computer Simulation. *AAPG Bulletin*, 78(6): 981-1004.
- Eichmüller, K. (1981): Geologische Kartierung im Paläozoikum des Kantabrischen Gebirges südlich von Tolibia de Abajo (Curueño-Tal, Provinz León, NW Spanien). Lithofaziesuntersuchung der Valdeteja Formation am Beispiel eines massigen Kalkkörpers am Peña La Verde, Nahe der Typlokalität Valdeteja. Unveröff. Diplomarbeit, Tübingen.
- Eichmüller, K. & Seibert, P. (1984): Faziesentwicklung zwischen Tournai und Westfal D im Kantabrischen Gebirge (NW-Spanien). *Z. dt. geol. Ges.*, 135: 163-191.
- Eichmüller, K. (1985): Die Valdeteja Formation: Aufbau und Geschichte einer oberkarbonischen Karbonatplattform (Kantabrisches Gebirge, Nordspanien). *Fazies*, 13: 45-154.
- Einsele, G. (2000): *Sedimentary basins*, Springer Verlag 792 p.
- Elliott, D. (1976): The energy balance and deformation mechanisms of thrust sheets. *Philosophical Transactions of the Royal Soc. London*, A283: 289-312.
- Elliott, D. (1983): The construction of balanced cross-sections. *J. Structural Geology*, 5(2): 101.
- Emery, D. & Myers, K. (1996): *Sequence Stratigraphy*. London, BP Exploration.
- Emmerich, A. (2004): Controlling Factors of two Middle Triassic Carbonate Platforms: Latemar and Rosengarten (Dolomites, Northern Italy). Doctoral thesis, Ruprecht-Karls-Universität Heidelberg.
- Evers, H.J. (1967): Geology of the Leonides between the Bernesga and Porma Rivers, Cantabrian Mountains (NW Spain). *Leidse Geologische Mededelingen*, 41: 83-151.
- Ezquerro del Bayo, J. (1844): Descripción geognóstica y minera de la provincia de Palencia. *Bol. of Min.*, 14: 160-163.
- Fermor, P.R. & Moffat, I.W. (1992): Tectonics and structure of the Western Canada Foreland Basin. In: Macqueen, R.W. and Leckie, D.A., eds., *Foreland Basins & Fold Belts: AAPG Memoir*, v. 55: Tulsa, p. 81-105.
- Fermor, P.R. (1999): Aspects of the three-dimensional structure of the Alberta Foothills and Front Ranges. *GSA Bulletin*, 3: 317-346.
- Fernández González, L.P. (1990): *Estratigrafía, sedimentología y paleogeografía de la region de Riosa, Quiros y Terverga-San Emiliano*. Doctoral thesis, University of Oviedo, Oviedo, 322 p.
- Fernández Rodríguez-Arango, R., Alonso Reguera, F., Péon Peláez, A. & Rodríguez Suárez, R. (1981): *Prospección general de la Cuenca Carbonífera de Quirós (Asturias, zona S)*. Fondo Documental ITGE.
- Fernández-Suárez, J., Dunning, G.R., Jenner, G.A. & Gutiérrez Alonso, G. (2000): Variscan collisional magmatism and deformation in NW Iberia: constraints from U-Pb geochronology of granitoids. *J. Geological Society*, 157: 565-576.
- Fernández-Suárez, J., Gutiérrez Alonso, G., Jenner, G.A. & Tubrett, M.N. (2000): New ideas on the Proterozoic-Early Paleozoic evolution of NW Iberia: insights from U-Pb detrital zircon ages. *Precambrian Research*, 102: 185-206.
- Fernández-Suárez, J., Gutiérrez Alonso, G., Cox, R. & Jenner, G.A. (2002): Assembly of the Armorica Microplate: A Strike-Slip Terrane Delivery? Evidence from U-Pb Ages of Detrital Zircons. *J. Geology*, 110: 619-626.
- Fernández-Suárez, J., Gutiérrez Alonso, G. & Jeffries, T.E. (2002): The importance of along-margin terrane transport in northern Gondwana: insights from detrital zircon parentage in Neoproterozoic rocks from Iberia and Brittany. *Earth and Planetary Science Letters*, 204: 75-88.
- Flemings, P.B. & Jordan, T.E. (1989): A Synthetic Stratigraphic Model of Foreland Basin Development. *J. Geophysical Research*, 94(B4): 3851-3866.
- Flemings, P.B. & Jordan, T.E. (1990): Stratigraphic modeling of foreland basins: Interpreting thrust deformation and lithosphere rheology. *Geology*, 18: 430-434.
- Folk, R.L. (1959): Practical petrographic classification of limestones. *Bull. Am. Ass. Petrol. Geol.*, 43(1): 1-38.
- Frankenfeld, H. (1976): Verzahnung einer Flachwasserkalk-Fazies mit einer Beckenfazies im Namur/Westfal bei Oville in der Provinz León im Kantabrischen Gebirge, Spanien. Diploma thesis, Universität Tübingen.
- Frankenfeld, H. (1981): Krustenbewegungen und Faziesentwicklung im Kantabrischen Gebirge (Nordspanien) vom Ende der Devonriffe (Givet/Frasne) bis zum Tournai. *Clausthaler Geol. Abh.*, 39: 1-91.

- Frankenfeld, H. (1985): Paleogeographic section through the Lower Carboniferous and Namurian Basin of the Southern Cantabrian Mountains (NW Spain). *Compte Rendu - International Congress on Carboniferous Stratigraphy and Geology*, 3: 523-532.
- Frey, M., De Capitani, C. & Liou, J.G. (1991): A new petrogenetic grid for low-grade metabasites. *J. Metamorphic Geol.*, 9: 497-509.
- Frings, K.H., Lutz, R., de Wall, H. & Wall, L.N. (2004): Coalification history of the Stephanian Ciñera-Matallana pull-apart basin, NW Spain: Combining anisotropy of vitrinite reflectance and thermal modelling. *Int. J. Earth Sci.*, 93: 92-106.
- Füchtbauer, H. (1988): *Sedimente und Sedimentgesteine*. Stuttgart, Schweizerbart 1141.
- Galloway, W.E. (1989): Genetic stratigraphic sequences in basin analysis, I. Architecture and genesis of flooding-surface bounded depositional units. *AAPG Bulletin*, 73: 125-142.
- Gandl, J. (1973): Die Karbon-Trilobiten des Kantabrischen Gebirges (NW-Spanien), 1. Die Trilobiten der Vegamián-Schichten (Ober Tournai). *Senckenb. Lethaea*, 54(1): 21-63.
- Gandl, J. (1985): Trilobites from the Upper Carboniferous of the Cantabrian Mountains (NW-Spain) and their biostratigraphical significance. *Compte Rendu - International Congress on Carboniferous Stratigraphy and Geology*, 2: 501-507.
- García López, S., Brime, C., Bastida, F. & Sarmiento, G.N. (1997): Simultaneous use of thermal indicators to analyse the transition from diagenesis to metamorphism: an example from the Variscan Belt of northwest Spain. *Geol. Mag.*, 134(3): 323-334.
- García-Alcalde, J.L., Truyóls-Massoni, M., Pardo-Alonso, M., Bultynck, P. & Carls, P. (2000): Devonian chronostratigraphy of Spain. *Cour. Forsch.-Inst. Senckenberg*, 225: 131-144.
- García-Alcalde, J.L., Carls, P., Pardo Alonso, M.V., Sanz López, J., Soto, F., Truyóls-Massoni, M. & Valenzuela-Ríos, J.I. (2002): Devonian. In: Gibbons, W. and Moreno, T., eds., *The Geology of Spain*: London, The Geological Society, p. 67-91.
- Gasparrini, M. (2003): Large-scale hydrothermal dolomitisation in the southwestern Cantabrian Zone (NW Spain): causes and controls of the process and origin of the dolomitising fluids. Doctoral thesis, Ruprecht-Karls-Universität Heidelberg, Heidelberg, 203 p.
- Gietelink, G. (1973): Sedimentology of a linear prograding coastline followed by three high-destructive delta-complexes (Cambro-Ordovician, Cantabrian Mountains, NW Spain). *Leidse Geol. Meded.*, 49: 125-144.
- Ginkel, v.A.C. (1965): Carboniferous fusulinids from the Cantabrian mountains (Spain). *Leidse Geol. Meded.*, 34: 1-225.
- Goguel, J. (1952): *Tectonics*. San Francisco, Freeman and Company 384.
- Goldhammer, R.K. (1997): Compaction and decompaction algorithms for sedimentary carbonates. *Journal of Sedimentary Research*, 67(1): 26-35.
- González Lástra, J. (1978): Facies salinas en la Caliza de Montaña (Cordillera Cantabrica). *Trabajos de Geología*, 10: 249-263.
- Granados, L.F., Solovieva, M.N., Reitlinger, E.A. & Martínez-Díaz, C. (1985): The Bashkirian-Moskavian boundary problem in the Asturias (Northwest Spain). *Compte Rendu - International Congress on Carboniferous Stratigraphy and Geology*, 1: 27-34.
- Granjeon, D. & Joseph, P. (1999): Concepts and applications of a 3-D multiple lithology, diffusive model in stratigraphic modeling. *SEPM Special Publications*, 62: 197-210.
- Griffiths, C.M., Dyt, C., Paraschivoiu, E. & Liu, K. (2001): *SedSim in Hydrocarbon Exploration*. In: Merriam, D. and Davis, J.C., eds., *Geologic Modeling and Simulation*: New York, Kluwer Academic.
- Griffiths, C.M. (2001): Brief review of stratigraphic forward modeling. *Short Course Notes. CSIRO Petroleum*: 1-21.
- Groves, J.R. & Sanderson, G.A. (1990): Systematics of the North American species of *Profusulinella* (Middle Pennsylvanian Fusulinidae). *Micropaleontology*, 36(2): 105-140.
- Groves, J.R., Nemyrovska, T.I. & Alekseev, A.S. (1999): Correlation of the type Bashkirian stage (Middle Carboniferous, South Urals) with the Morrowan and Atokan series of the midcontinental and western United States. *J. Paleontology*, 73(3): 529-539.
- Gutiérrez Alonso, G., Fernández-Suárez, J. & Weil, A.B. (2004): Orocline triggered lithospheric delamination. *GSA Spec. Paper*, 383: 121-130.
- Gutiérrez-Marco, J.G., Robardet, M. & Piçarra, J.M. (1998): Silurian stratigraphy and paleogeography of the Iberian Peninsula (Spain and Portugal). *Temas Geológico-Mineros ITGE*, 23: 13-44.
- Gutiérrez-Marco, J.G., Robinson, M., Rábano, I.,



- Sarmiento, G.N., San José Lancha, M.A. & Herranz Araújo, P. (2002): Ordovician. In: Gibbons, W. and Moreno, T., eds., *Geology of Spain*: London, Geological Society, p. 31-49.
- Haq, B.U., Hardenbol, J. & Vail, P.R. (1987): Chronology of Fluctuating Sea Level Since the Triassic. *Science*, 235: 1156-1167.
- Haq, B.U. (1991): Sequence stratigraphy, sea-level change, and significance for the deep sea. In: MacDonald, D.I.M., ed., *Sedimentation, Tectonics and Eustasy*, v. 12, IAS Spec. Publ., p. 3-39.
- Harland, W.B. (1989): *A geological time scale*. Cambridge, Cambridge Univ. Pr. 263.
- Heckel, P.H. (1986): Sea-level curve for Pennsylvanian eustatic marine transgressive-regressive depositional cycles along midcontinent outcrop belt, North America. *Geology*, 14: 330-334.
- Hedberg, H.D. (1970): Continental margins from viewpoint of the petroleum geologist. *AAPG Bulletin*, 54: 3-43.
- Heddebaut, C. (1975): Etudes géologiques dans le massif paléozoïques basques. *Bulletin du BRGM (2ème série)*, section IV, 1: 5-30.
- Helland-Hansen, W., Kendall, C.G.S.C., Lerche, I. & Nakayama, K. (1988): A simulation of continental basin margin sedimentation in response to crustal movements, eustatic sea level change and sediment accumulation rates. *Mathematical Geology*, 20: 777-802.
- Heller, P.L., Angevine, C.L., Winslow, N.S. & Paola, C. (1988): Two-phase stratigraphic model of foreland-basin sequences. *Geology*, 16: 501-504.
- Heller, P.L. & Paola, C. (1992): The large-scale dynamics of grain-size variation in alluvial basins, 2: application to syntectonic conglomerate. *Basin Research*, 4: 91-102.
- Hemleben, C. & Reuther, C.D. (1980): Alldapic limestones of the Barcaliente Formation (Namurian A) between Luna and Cea rivers (southern Cantabrian Mountains, Spain). *Neues Jahrbuch fuer Geologie und Palaeontologie. Abhandlungen*, 159(2): 225-255.
- Heward, A.P. (1978): Alluvial fan sequence and megasequence models: with examples from Westphalian D-Stephanian B coalfields, Northern Spain. In: Miall, A., ed., *Fluvial Sedimentology*, v. Memoir 5, Canadian Society of Petroleum Geologists, p. 669-702.
- Heward, A.P. & Reading, H.G. (1980): Deposits associated with a Hercynian to Late Hercynian continental strike-slip system, Cantabrian Mts., northern Spain. In: Ballance, B.F. and Reading, H.G., eds., *Sedimentation at Oblique Slip Margins*, v. 4, IAS Spec. Publ., p. 105-125.
- Higgins, A.C., Wagner-Gentis, C.H.T. & Wagner, R.H. (1964): Basal Carboniferous Strata in Part of Northern Leon, NW Spain: Stratigraphy, Conodont and Goniatite Faunas. *Bull. Soc. Belge Géol. Paléont. Hydrol.*, 72: 205-248.
- Higgins, A.C. (1971): Conodont biostratigraphy of the late Devonian and early Carboniferous rocks of the South Central Cantabrian Cordillera. *Trab. Geol.*, 3: 179-192.
- Higgins, A.C. & Wagner-Gentis, C.H.T. (1982): Conodonts, goniatites and the biostratigraphy of the earlier Carboniferous from the Cantabrian Mountains, Spain. *Paleontology*, 25(2): 313-350.
- Hinsch (1997): Kinematische Entwicklung der variszisch angelegten Forcada Einheit, Kantabrisches Gebirge, Nord-Spanien. *Diploma thesis*, Hamburg.
- Hirt, A.M., Lowrie, W., Julivert, M. & Arboleya, M.L. (1992): Paleomagnetic results in support of a model for the origin of the Asturian arc. *Tectonophysics*, 213: 321-339.
- Holt, W.E. & Stern, T.A. (1994): Subduction, platform subsidence, and foreland thrust loading: the late Tertiary development of Taranaki basin, New Zealand. *Tectonics*, 13: 1068-1092.
- Horton, B.K. & DeCelles, P.G. (1997): The modern foreland basin system adjacent to the Central Andes. *Geology*, 25(10): 895-898.
- Hossack, J.R. (1983): A cross-section through the Scandinavian Caledonides constructed with the aid of branch-line maps. *J. Structural Geology*, 5(2): 103-111.
- Hunt, C.W. (1957): Planimetric equation. *J. Alta Soc. Petrol. Geol.*, 5: 259-264.
- Hüssner, H., Roessler, J. & Monz, R. (1997): REPRO - a 3D simulation program of reef growth models. *Zbl. Geol. Paläont. Teil I*, 9: 957-968.
- James, N.P. (1978): Facies models; 10: reefs. *Geosci. Canada*, 5: 16-26.
- James, N.P. (1983): Reef environment. In: Scholle, P.A., Bebout, D.G. and Moore, C.H., eds., *Carbonate Depositional Environments*, v. 33: Tulsa, Mem. Amer. Ass. Petrol. Geol., p. 345-440.
- Jervey, M.T. (1988): Siliciclastic sequence development in foreland basins; a numerical approach. In: James, D.P. and Leckie, D.A., eds., *Sequences, stratigraphy, sedimentology; surface*

- and subsurface, v. Memoir 15, Canadian Society of Petroleum Geologists, p. 579.
- Johnson, G.A.L. (1973): Closing of the Carboniferous Sea in Western Europe, Implications of Continental Drift to the Earth Sciences, Vol. 2; Part 8, Palaeogeographic Implications: London, Academic Press, p. 843-850.
- Johnson, J.G., Klapper, G. & Sandberg, C.A. (1985): Devonian eustatic fluctuations in Euramerica. Geological Society of America Bulletin, 96(5): 567-587.
- Jordan, T.E. (1995): Retroarc foreland and related basins. In: Busby, C.J. and Ingersoll, R.V., eds., Tectonics of sedimentary basins: Oxford, Blackwell Science, p. 331-362.
- Julivert, M. (1960): Estudio geológico de la Cuenca de Beleño (valles altos del Sella, Ponga, Nalón y Esla). Boletín Inst. Geol. Min. España, 71: 1-346.
- Julivert, M. (1971): Décollement tectonics in the Hercynian Cordillera of northwest Spain. American Journal of Science, 270: 1-29.
- Julivert, M., Marcos, A. & Truyols, J. (1972): L'évolution paléogéographique du nord-ouest de l'Espagne pendant l'Ordovicien-Silurien. Bulletin de la Société Géologique et Minéralogique de Bretagne [C], 4: 1-7.
- Julivert, M. & Marcos, A. (1973): Superimposed folding under flexural conditions in the Cantabrian zone (Hercynian Cordillera, Northwest Spain). American Journal of Science, 273: 353-375.
- Julivert, M. (1978): Hercynian Orogeny and Carboniferous Palaeogeography in Northwestern Spain: A Model of Deformation-Sedimentation Relationships. Z. dt. geol. Ges., 129: 565-592.
- Julivert, M. & Arboleya, M.L. (1984): A geometrical and kinematical approach to the nappe structure in an arcuate fold belt: the Cantabrian nappes (Hercynian chain, NW Spain). J. Structural Geology, 6(5): 499-519.
- Julivert, M. & Arboleya, L.M. (1986): Areal balancing and estimate of areal reduction in a thin-skinned fold-and-thrust belt (Cantabrian Zone, NW Spain): constraints on its emplacement mechanism. J. Structural Geology, 8(3/4): 407-414.
- Keller, M. (1988): Die La-Vid-Gruppe - Fazies, Paläogeographie und synsedimentäre Tektonik im Unter-Devon des Kantabrischen Gebirges (NW-Spanien). Dissertation thesis, Friedrich-Alexander-Universität, Erlangen-Nürnberg, 110 p.
- Keller, M. (1997): Evolution and sequence stratigraphy of an early Devonian carbonate ramp, Cantabrian Mountains, northern Spain. J. Sedimentary Research, 67(4): 638-652.
- Kendall, C.G.S.C., Moore, P., Strobel, J., Cannon, R., Perlmutter, M., Bezdek, J. & Biswas, G., Eds. (1991): Simulation of the sedimentary fill of basins. Sedimentary modeling: Computer simulations and methods for improved parameter definition, Kansas Geological Survey Bulletin 233.
- Kendall, C.G.S.C., Moore, P. & Whittle, G. (1992): A challenge: Is it possible to determine eustasy and does it matter? In: Dott, R.H.J., ed., Eustasy: The Historical Ups and Downs of a Major Geological Concept, v. 180, Geological Society of America, p. 93-106.
- Kendall, C.G.S.C., Whittle, G.L., Ehrlich, R., Moore, P.D., Cannon, R.L. & Hellmann, D.R. (1993): Computer sedimentary simulation models sequence stratigraphy. Oil and Gas Journal, 91(17): 46-51.
- Kendall, C.G.S.C. & Moore, P. (2004): SEDPAK Manual. [www.sedpak.geol.sc.edu/doc/help/index.html](http://www.sedpak.geol.sc.edu/doc/help/index.html).
- Kingston, D.R., Dishroon, C.P. & Williams, P.A. (1983): Global basin classification system. AAPG Bulletin, 67: 2175-2193.
- Kisch, H.J. (1980): Incipient metamorphism of Cambro-Silurian clastic rocks from the Jämtland Supergroup, central Scandinavian Caledonides, western Sweden: illite crystallinity and 'vitrinite' reflectance. J. geol. Soc. London, 137: 271-288.
- Klein, G.d.V. (1987): Current aspects of basin analysis. Sedimentary Geology, 50: 95-118.
- Klein, G.d.V. (1990): Pennsylvanian time scales and cycle periods. Geology, 18: 455-457.
- Kollmeier, J.M., van der Pluijm, B.A. & Van der Voo, R. (2000): Analysis of Variscan dynamics; early bending of the Cantabria-Asturias Arc, northern Spain. Earth and Planetary Science Letters, 181: 203-216.
- Kullmann, J. (1961): Die Goniatiten des Unterkarbons im Kantabrischen Gebirge (Nordspanien). I. Stratigraphie, Paläontologie der U. O. Goniatitina Hyatt. N. Jb. Geol. Pal. Abhandlungen, 113(3): 219-326.
- Kullmann, J. (1962): Die Goniatiten der Namur-Stufe (Oberkarbon) im Kantabrischen Gebirge, Nord-Spanien. Akad. Wiss. Lit. Abh. Math. Naturwiss. Kl., 6: 263-377.
- Kullmann, J. (1963): Die Goniatiten des Unterkarbons im Kantabrischen Gebirge (Nordspanien).

- II. N. Jb. Geol. Pal. Abhandlungen, 116: 269-324.
- Kullmann, J. (1965): Rugose Korallen der Cephalopodenfazies und ihre Verbreitung im Devon des südöstlichen Kantabrischen Gebirges (Nordspanien). *Abh. Math.-Naturwiss. Kl. Akad. Wiss. Liter. Mainz*, 2: 1-136.
- Kullmann, J. (1976a): Entwicklung der Lebensräume im Kantabrischen Variszikum. *Zentralblatt für Geologie und Paläontologie*, 5/6.
- Kullmann, J. (1976b): Veränderungen von marinen Vergesellschaftungen in der zeitlichen Dimension. *Zentralblatt für Geologie und Paläontologie*(5-6): 392-396.
- Kullmann, J., Reuther, C.D. & Schönenberg, R. (1977): La transición del estadio geosinclinal a la orogénesis en la formación variscica de la Cordillera Cantábrica. *Breviora Geologica Asturica*, 21(1): 3-11.
- Kullmann, J. (1979): Die "Reticuloceras-Zeit" (Oberkarbon) in der Entwicklung des Kantabrischen Variszikums. *Clausthaler Geol. Abh.*, 30: 34-44.
- Kullmann, J. & Schönenberg, R. (1980): Geodynamik und Paläökologie im kantabrischen Variszikum. *N. Jb. Geol. Pal. Abhandlungen*, 163(2): 143-148.
- Lawrence, D.T., Doyle, M. & Aigner, T. (1990): Application of stratigraphic forward models in exploration settings. *Bulletin - Houston Geological Society*, 32(5): 7.
- Leeder, M.R. (1988): Devonian-Carboniferous river systems and sediment dispersal from the orogenic belts and cratons of NW Europe. In: Harris, A.L. and Fettes, D.J., eds., *The Caledonian-Appalachian Orogen*, v. 38: London, Geological Society of London, p. 549-558.
- Leeder, M.R. (1999): *Sedimentology and Sedimentary Basins: From Turbulence to Tectonics*, Blackwell Publishing.
- Lepvrier, C. & Martínez-García, E.M. (1990): Fault development and stress evolution of the post-Hercynian Asturian Basin (Asturias and Cantabria, northwestern Spain). *Tectonophysics*, 184: 345-356.
- Leyva, F., Granados, L.F., Solovieva, M.N., Reitlinger, E.A., Martínez Díaz, C., Laveine, J.P., Loboziak, S., Brousmiche, C., Candilier, A.M. & Horvath, V. (1985): La estratigrafía del Carbonífero Medio en el Sector Central de la Unidad Estructural de La Sobia-Bodón (Cuencas de Quirós-Teverga). *C. R. X. Int. Congr. Strat. Geol. Carb. Madrid*, 1983, 1: 213-230.
- Linnemann, U. & Heuse, T. (2000): The Ordovician of the Schwarzburg Anticline: Geotectonic setting, biostratigraphy and sequence stratigraphy (Saxo-Thuringian Terrane, Germany). *Zeitschrift der Deutschen Geologischen Gesellschaft*, 151: 471-491.
- Liñán, E., Fernández-Nieto, C. & Gámez, J.A. (1993): Problemática del límite Cámbrico Inferior-Medio en Murero (Cadenas Ibéricas, España). *Rev. Esp. Pal.*, No. Extraordinario: 26-39.
- Liñán, E., Gonçalves, F., Gámez Vintaned, J.A. & Gozalo, R. (1997): Evolución paleogeográfica del Cámbrico de la Zona de Ossa Morena basada en el registro fósil. In: A, A.A. and Pereira, M.F., eds., *Estudo sobre a Geologia da Zona de Ossa Morena (Maciço Ibérico)*, Livro de Homenagem ao Professor Francisco Gonçalves, University of Évora, p. 1-26.
- Liñán, E., Gozalo, R., Palacios, T., Gámez Vintaned, J.A., Ugidos, J.M. & Mayoral, E. (2002): Cambrian. In: Gibbons, W. and Moreno, T., eds., *The Geology of Spain*: London, The Geological Society, p. 17-29.
- Lippolt, H.J., Hess, J.C. & Burger, K. (1984): Isotopische Alter von pyroklastischen Sanidinen aus Kaolin-Kohlentonsteinen als Korrelationsmarken für das mitteleuropäische Oberkarbon. *Fortschr. Geol. Rheinld. u. Westf.*, 32: 119-150.
- Liu, K., Liang, T.C.K., Paterson, L. & Kendall, C.G.S.C. (1998): Computer simulation of the influence of basin physiography on condensed section deposition and maximum flooding. *Sedimentary Geology*, 122: 181-191.
- Llopis Lladó, N. (1965): Sur la paléogéographie du Dévonien du Nord de l'Espagne. *Compte Rendu Sommaire des séances de la Société Géologique de France*, 9: 290-292.
- Lobato, L., García-Alcalde, J.L., Sánchez de Posada, L.C. & Truyols, J. (1984): Cartografía del mapa geológico de España, Escala 1:50.000, No.104 (Boñar). Madrid, IGME.
- Loevezijs, v.G.B.S. (1986): Stratigraphy and facies of the Nocado, Fueyo and Ermita formations (Upper Devonian to lowermost Carboniferous) in León, N Spain. *Scripta Geol.*, 81: 1-116.
- Longman, M.W. (1981): A process approach to recognizing facies of reef complexes. *Spec. Publ. Soc. Econ. Paleont. Min.*, 30: 9-40.
- Lorenz, V. & Nichols, I. (1984): Plate and intraplate processes of Hercynian Europe during the Late Palaeozoic. *Tectonophysics*, 107: 25-56.
- Lotze, F. (1945): Zur Gliederung der Varisciden der Iberischen Meseta. *Geotektonische Forschun-*



- gen, 6: 78-92.
- Lotze, F. (1961): Das Kambrium Spaniens. Teil I: Stratigraphie. Akademie der Wissenschaften und der Literatur, Abh. der Math.-Natwiss. Kl., 6-8: 411.
- Lugo, J. & Mann, P. (1995): Jurassic-Eocene tectonic evolution of Maracaibo Basin, Venezuela. In: Tankard, A.J., Suarez, S. and Welsink, H., eds., Petroleum basins of South America, v. Memoir 62, AAPG, p. 699-725.
- Marcos, A. (1968): La tectónica de la unidad de la Sobia-Bodon. Trabajos de Geología, 2: 59-87.
- Marcos, A. (1973): Las Series del Paleozoico Inferior y la estructura herciniana del Occidente de Asturias (NW de España). Trab. Geol. Univ. Oviedo, 6: 1-113.
- Marcos, A. & Pulgar, J.A. (1982): An approach to the tectonostratigraphic evolution of the Cantabrian foreland thrust and fold belt, Hercynian Cordillera of NW Spain. Neues Jahrbuch fuer Geologie und Palaeontologie. Abhandlungen, 163(2): 256-260.
- Marschik, R. (1992): Der Übergang von der Diagenese zur sehr niedergradigen Metamorphose im externen Varistikum (Kantabrische Zone), NW Spanien. Diploma thesis, University of Heidelberg, Heidelberg, 70 p.
- Martínez Catalán, J.R. (1990): A non-cylindrical model for the northwest Iberian allochthonous terranes and their equivalents in the Hercynian belt of Western Europe. Tectonophysics, 179: 253-272.
- Martínez Chacon, M.L. & Winkler Prins, C.F. (1993): Carboniferous Brachiopods and the Palaeogeographic Position of the Iberian Peninsula. Compte Rendu - International Congress on Carboniferous Stratigraphy and Geology, 1: 573-580.
- Martínez-García, E. (1971): The age of the Caliza de Montaña in the eastern Cantabrian Mountains. Trabajos de Geología, 3: 267-276.
- Martínez-García, E., Wagner, R.H., Lobato, L., Fernandez, L. & Alonso, S.L. (1983): Carbonífero y Permiano de España. Madrid, Inst. Geol. y Minero España.
- Massa, D. & Bourrhouilh, R. (2000): Upper Ordovician carbonate mud-mound of northern Ghadamis Basin, Libya: a review. Sedimentary Basins of Libya: Second Symposium Geology of Northwest Libya, Tripoli, Gutenberg Press, Malta.
- Matas, J. & Rodríguez Fernández, L.R. (1984): Cartografía del mapa geológico de España, Escala 1:50.000, No.129 (La Robla). Madrid, IGME.
- Matte, P. & Ribeiro, A. (1975): Forme et orientation de l'épisode de déformation dans la virgation hercynienne de Galice. Relations avec le plissement et hypothèse sur la genèse de l'arc Ibero-Armoricaine. Académie de Sci. Comptes Rendus, 280: 2825-2828.
- Matte, P. (1986): Tectonics and plate tectonics model for the Variscan belt of Europe. Tectonophysics, 126: 329-374.
- Matte, P. (1991): Accretionary history and crustal evolution of the Variscan Belt in Western Europe. In: Hatcher, R.D., Jr. and Zonenshain, L., eds., Accretionary tectonics and composite continents.: Tectonophysics, v. 196: Amsterdam, Netherlands, Elsevier, p. 309-337.
- Matte, P. (2001): The Variscan collage and orogeny (480-290 Ma) and the tectonic definition of the Armorican microplate: a review. Terra Nova, 13: 122-128.
- Maxwell, J.C. (1964): Influence of depth, temperature, and geologic age on porosity of quartzose sandstone. AAPG Bulletin, 48: 697-709.
- McClay, K.R. (1987): The mapping of geological structures, Open University Press 164.
- McClay, K.R., Ed. (1992): Thrust Tectonics. Glossary of thrust tectonic terms.
- McKenzie, D. & Fairhead, D. (1997): Estimates of the effective elastic thickness of the continental lithosphere from Bouguer and free air gravity anomalies. Journal of Geophysical Research, 102(B12): 27523-27552.
- McKerrow, W.S. & Van Staal, C.R. (2000): The Palaeozoic time scale reviewed. In: Franke, W., Haak, V., Oncken, O. and Tanner, D., eds., Orogenic Processes: Quantification and Modelling in the Variscan Belt, v. 179: London, Geological Society, p. 5-8.
- Meer Mohr, v.d., C. (1969): The stratigraphy of the Cambrian Lancara Fm. between the Luna River and the Esla River in the Cantabrian Mountains, Spain. Leidse Geol. Meded., 43.
- Meischner, D. (1964): Alldapische Kalke, Turbidite in ríffnahen Sedimentations-Becken. In: Bouma, A.H. and Brouwer, A., eds., Turbidites: Dev. in Sedimentol., v. 3: Amsterdam, Elsevier, p. 156-191.
- Menéndez-Álvarez, J.R. (1991): Conodontos del Carbonífero Inferior y Medio de la Cordillera Cantábrica. Doctoral thesis, Universidad de Oviedo, Oviedo, 283 p.
- Menning, M., Weyer, D., Drozdowski, G., Van Amerom, H.W.J. & Wendt, I. (2000): A Carboniferous Time Scale 2000: Discussion and Use of Geological Parameters as Time Indica-

- tors from Central and Western Europe. *Geol. Jb.*, A 156: 3-44.
- Menning, M. & German Stratigraphic Commission (2002): A geologic time scale 2002. In: Commission, G.S., ed., *Stratigraphic Table of Germany 2002*.
- Miall, A.D. (1999): *Principles of sedimentary basin analysis*. Berlin Heidelberg, Springer 616.
- Mitchell, A.H.G. & Reading, H.G. (1986): Sedimentation and tectonics. In: Reading, H.G., ed., *Sedimentary Environments and Facies*: Oxford, Blackwell Scientific Publications, p. 471-519.
- Mitchum, R.M., Vail, P.R. & Thompson, S. (1977): Seismic Stratigraphy and global changes of sea level, Part 2: the depositional sequence as a basic unit for stratigraphic analysis. In: Payton, C.E., ed., *Seismic Stratigraphy - Applications to Hydrocarbon Exploration*, v. 26: Tulsa, AAPG Memoir, p. 53-62.
- Mitchum, R.M., Sangree, J.B., Vail, P.R. & Wornardt, W.W. (1991): Integrated well-log, seismic, and biostratigraphic approach to sequence stratigraphy in late Cenozoic expanded sections, Gulf of Mexico. *AAPG Bulletin*, 75(3): 637pp.
- Mitra, S. (1986): Duplex Structures and Imbricate Thrust Systems: Geometry, Structural Position, and Hydrocarbon Potential. *AAPG Bulletin*, 70(9): 1087-1112.
- Moore, L.R., Neves, R., Wagner, R.H. & Wagner-Gentis, C.H.T. (1971): The stratigraphy of Namurian and Westphalian rocks in the Villamanin area of northern León, N.W. Spain. *Trabajos de Geologia*, 3.
- Morley, C.K. (1988): Out-of-sequence thrusts. *Tectonics*, 7(3): 539-561.
- Näglér, T.F., Schäfer, H.J. & Gebauer, D. (1995): Evolution of the Western European continental crust: implications from Nd and Pb isotopes in Iberian sediments. *Chemical Geology*, 121: 345-357.
- Nichols, G. (1999): *Sedimentology and stratigraphy*. Malden, Mass, Blackwell Science 355 p.
- Nijman, W. & Savage, J.F. (1989): Persistent basement wrenching as controlling mechanism of Variscan thin-skinned thrusting and sedimentation, Cantabrian Mountains Spain. *Tectonophysics*, 169: 281-302.
- Nordlund, U. (1996): Formalizing geological knowledge - with an example of modeling stratigraphy using fuzzy logic. *Journal of Sedimentary Research*, 66: 689-698.
- Nordlund, U. (1999): FUZZIM: forward stratigraphic modeling made simple. *Computers & Geosciences*, 25: 449-456.
- Nystuen, J.P. (1998): History and development of sequence stratigraphy. In: Grandstein, S., Milton, ed., *sequence stratigraphy - concepts and applications*, v. NPF Special Publication, Elsevier, p. 31-116.
- Odin, G.S. & Gale, N.H. (1982): Mise a jour de l'échelle des temps caledoniens et hercyniens. Translated Title: Updated Caledonian and Hercynian time scales. *Comptes-Rendus des Seances de l'Academie des Sciences, Serie 2: Mecanique-Physique, Chimie, Sciences de l'Univers, Sciences de la Terre*, 294(7): 453-456.
- Oele, E. (1964): Sedimentological aspects of four Lower-Paleozoic formations in the Northern part of the Province of León (Spain). *Leidse Geol. Meded.*, 30: 1-100.
- Oriel, S.S. & Moore, D.W. (1986): Structure and petroleum potential of Palisades Roadless Area, Idaho-Wyoming thrust-belt salient near Jackson, Wyoming. USGS research on energy resources, Denver, CO, United States, U. S. Geological Survey.
- Parés, J.M., Van der Voo, R., Stamatakis, J. & Pérez-Estaún, A. (1994): Remagnetizations and post-folding oroclinal rotations in the Cantabrian/Asturian arc, northern Spain. *Tectonics*, 13(6): 1461-1471.
- Paris, F. & Robardet, M. (1977): Paléogéographie et relations ibéro-armoricaines au Paléozoïque anté-Carbonifère. *Bulletin de la Société Géologique de France*, 19(7): 1121-1126.
- Paris, F. (1993): Evolution paléogéographique de l'Europe au Paléozoïque inférieur: le test des Chitinozoaires. *Comptes Rendus de l'Académie des Sciences, Paris*, 316(sér. II): 273-280.
- Paulsen, T. & Marshak, S. (1998): Charleston transverse zone, Wasatch Mountains, Utah; structure of the Provo Salient's northern margin, Sevier fold-thrust belt. *Geological Society of America Bulletin*, 110(4): 512-522.
- Perroud, H. & Bonhommet, N. (1981): Palaeomagnetism of the Ibero-Armorican arc and the Hercynian orogeny in Western Europe. *Nature*, 292(5822): 445-448.
- Perroud, H. (1986): Paleomagnetic evidence for tectonic rotations in the Variscan mountain belt. *Tectonics*, 5(2): 205-214.
- Pérez-Estaún, A., Bastida, F., Alonso, J.L., Marquinez, J., Aller, J., Alvarez-Marrón, J., Marcos, A. & Pulgar, J.A. (1988): A thin-skinned

- tectonics model for an arcuate fold and thrust belt: the Cantabrian zone (Variscan Ibero-Armorican Arc). *Tectonics*, 7(3): 517-537.
- Pérez-Estaún, A. & Bastida, F. (1990): Cantabrian Zone: Structure. In: Dallmeyer, R.D. and Martinez Garcia, E., eds., *Pre-Mesozoic Geology of Iberia*: Berlin.
- Pérez-Estaún, A., Pulgar, J.A., Banda, E., Álvarez-Marrón, J. & group, E.-N. (1994): Crustal structure of the external variscides in north-west Spain from deep seismic reflection profiling. *Tectonophysics*, 232: 91-118.
- Pérez-Estaún, A., Pulgar, J.A., Álvarez-Marrón, J., ESCI-N group (1995): Crustal structure of the Cantabrian Zone: seismic image of a Variscan foreland thrust and fold belt (NW Spain). *Rev. Soc. Geol. Espana*, 8(4).
- Pigram, D.J., Davies, P.J., Feary, D.A. & Symonds, P.A. (1989): Tectonic controls on carbonate platform evolution in southern Papua New Guinea: passive margin to foreland basin. *Geology*, 17: 199-202.
- Posamentier, H.W., Jervey, M.T. & Vail, P.R. (1988): Eustatic Controls on clastic deposition I - conceptual framework. *SEPM Special Publications*, 42.
- Posamentier, H.W. (1991): An overview of sequence-stratigraphic concepts. In: Leckie, D.A., Posamentier, H.W. and Lovell, R.W.W., eds., *Proceedings of 1991 NUNA Conference on High-Resolution Sequence Stratigraphy*: Toronto, Geol. Ass. Canada, p. 62-74.
- Potent, S. & Reuther, C.-D. (2000): Kinematik der Faltungs- und Überschiebungsprozesse der variszisch angelegten Montuerto-Struktur im südlichen Kantabrischen Gebirge, Nord-Spanien. *Mitt. Geol.-Paläont. Inst. Univ. Hamburg*, 84: 83-110.
- Potent, S. (2000): Kinematische Analyse der variszisch angelegten Montuerto-Syncline, südliches Kantabrisches Gebirge, Nord-Spanien. Diploma thesis, Universität Hamburg, Hamburg.
- Price, R.A. (1964): Flexural slip folds in the Rocky Mountains, southern Alberta and British Columbia. *Geol. Surv. Can.*, 78: 16pp.
- Price, R.A. (1973): Large scale gravitational flow of supracrustal rocks, southern Canadian Rockies. In: DeJong, K.A. and Scholten, R.A., eds., *Gravity and Tectonics*: New York, Wiley, p. 491-502.
- Prost, A.E. & Becq-Giraudon, J.F. (1989): Evidence for mid-Permian compressive tectonics in Western Europe supported by a comparison with the Alleghanian geodynamic evolution. *Tectonophysics*, 169(4): 333-340.
- Pryor, W.A. (1973): Permeability-porosity patterns and variations in some Holocene sand bodies. *AAPG Bulletin*, 57: 162-189.
- Pulgar, J.A., Gallart, J., Fernández-Viejo, G., Pérez-Estaún, A. & Álvarez-Marrón, J. (1996): Seismic image of the Cantabrian Mountains in the western extension of the Pyrenees from integrated ESCIN reflection and refraction data. *Tectonophysics*, 264: 1-19.
- Quinlan, G.M. & Beaumont, C. (1984): Appalachian thrusting, lithospheric flexure, and the Paleozoic stratigraphy of the Eastern Interior of North America. *Canadian Journal of Earth Sciences*, 21(973-996).
- Ramsay, J.G. (1967): *Folding and fracturing of rocks*. New York, McGraw-Hill 568 p.
- Ramsay, J.G. & Huber, M.I. (1987): *The Techniques of Modern Structural Geology*.
- Ranalli, G. (1994): Nonlinear flexure and equivalent mechanical thickness of the lithosphere. *Tectonophysics*, 240: 107-114.
- Raven, J.G.M. (1983): Conodont biostratigraphy and depositional history of the Middle Devonian to Lower Carboniferous in the Cantabrian Zone (Cantabrian Mountains, Spain). *Leidse Geol. Meded.*, 52(2): 265-339.
- Raven, J.G.M. & van der Pluijm, B.A. (1986): Metamorphic fluids and transtension in the Cantabrian Mountains of northern Spain: an application of the conodont colour alteration index. *Geol. Mag.*, 123(6): 673-681.
- Rácz, L. (1966): Carboniferous calcareous algae and their associations in the San Emiliano and Lois-Ciguera Formations (Prov. León, NW Spain). *Leidse Geol. Meded.*, 31: 5-112.
- Reijers, T.J.A. (1973): Stratigraphy, sedimentology and palaeogeography of Eifelian, Givetian and Frasnian strata between the River Porma and the Embalse de la Luna, Cantabrian Mountains, Spain. *Geologie en Mijnbouw*, 52(3): 115-124.
- Reijers, T.J.A. (1980): Sedimentary mechanisms in Spanish Devonian carbonates. *Geol. en Mijnbouw*, 59(1): 87-96.
- Reijers, T.J.A. (1984): The Peñolas structure in the Peña Corada unit, Cantabrian Mountains (Spain). *Boletín Geológico y Minero*, 155(3): 214-224.
- Reitlinger, E.A., Semichatova, S.V., Byusheva, T.V., Chizhova, V.A., Kononova, L.I., Lipina, O.A., Aisenverg, D.E., Antropov, I.A., Brazhnikova, N.E., Durkina, A.V., Fedorova, T.I., Groz-



- dilova, L.P., Kedo, G.J., Khalymbadzha, V.G., Lapina, N.M., Martynova, M.N., Nasikanova, O.H., Nechaeva, M.A., Rozhdestvenskaya, A.A., Samoilova, R.B., Tkacheva, U.D., Umnova, B.T. & Nenastieva, V.E. (1979): The Devonian-Carboniferous boundary in the USSR. In: Wagner, R.H., Higgins, A.C. and Meyen, S.V., eds., *The Carboniferous of the U.S.S.R.; reports presented to the I.U.G.S. Subcommittee on Carboniferous Stratigraphy at the 8th international congress on Carboniferous stratigraphy and geology*, v. 4, Occasional Publication Yorkshire Geological Society, p. 23-42.
- Remane, J. (2000): International Stratigraphic Chart and Explanatory note to the international stratigraphic chart, IUGS/UNESCO 16.
- Reuther, C.D. (1977): Das Namur im südlichen Kantabrischen Gebirge (Nordspanien). *Clausthaler Geol. Abh.*, 28.
- Ribeiro, A., Quesada, C. & Dallmeyer, R.D. (1990): Geodynamic evolution of the Iberian Massif. In: Dallmeyer, R.D. and Martínez-García, E., eds., *Pre-Mesozoic Geology of Iberia*: Berlin, Springer-Verlag, p. 399-409.
- Rich, J.L. (1934): Mechanics of low-angle overthrust faulting as illustrated by Cumberland thrust block, Virginia, Kentucky, and Tennessee. *AAPG Bulletin*, 18: 1584-1596.
- Riding, R. (1974): Model of the Hercynian fold belt. *Earth and Planetary Science Letters*, 245: 125-135.
- Rinklef, J. (1987): Kartierung im kantabrischen Paläozoikum bei Cármenes (Provinz León, NW-Spanien) mit der Beschreibung präorogener Flachwassersedimente des Westfalium (Los Pontedos Formation, Cármenes Formation) im Hangenden der Valdeteja Formation. Unveröff. Diplomarbeit, Tübingen.
- Robardet, M. (1976): L'originalité du segment hercynien sud-ibérique au Paléozoïque inférieur: Ordovicien, Silurien et Dévonien dans le nord de la province de Séville (Espagne). *Comptes Rendus de l'Académie des Sciences, Paris*, 283(série D): 999-1002.
- Robardet, M. & Gutiérrez-Marco, J.G. (1990): Sedimentary and faunal domains in the Iberian Peninsula during Lower Paleozoic times. In: Dallmeyer, R.D. and Martínez-García, E., eds., *Pre-Mesozoic Geology of Iberia*: Berlin, Springer-Verlag, p. 383-395.
- Robardet, M., Bonjour, J.L., Paris, F., Morzadec, P. & Racheboeuf, P.R. (1994): Ordovician, Silurian, and Devonian of the Medio-North-Armorican Domain. In: Keppie, J.D., ed., *Pre-Mesozoic Geology in France and Related Areas*: Berlin, Springer-Verlag, p. 142-151.
- Robardet, M. (2002): Alternative approach to the Variscan Belt in southwestern Europe: Pre-orogenic paleobiogeographical constraints. In: Martínez Catalán, J.R., Hatcher, R.D., Jr., Arenas, R. and Díaz García, F., eds., *Variscan-Appalachian dynamics: The building of the late Paleozoic basement*, v. 364: Boulder, Colorado, Geological Society of America Special Paper, p. 1-15.
- Robardet, M. & Gutiérrez-Marco, J.C. (2002): Silurian. In: Gibbons, W. and Moreno, T., eds., *The Geology of Spain*: London, The Geological Society, p. 51-66.
- Rodríguez, F.L.R. (1983): Evolucion estructural de la Zona Cantábrica durante el Carbonífero.
- Roeder, D., Gilbert, O.E., Jr & Witherspoon, W.D. (1978): Evolution and macroscopic structure of Valley and Ridge thrust belt, Tennessee and Virginia. *Studies in Geology*, 2.
- Roest, W.R. & Srivastava, S.P. (1991): Kinematics of the plate boundaries between Eurasia, Iberia and Africa in the North Atlantic from the Late Cretaceous to the present. *Geology*, 19: 613-616.
- Ross, C.A. & Ross, J.R.P. (1987): Late Paleozoic sea levels and depositional sequences. *Cushman Foundation for Foraminiferal Research, Special Publication*, 24: 137-149.
- Ross, C.A. & Ross, J.R.P. (1988): Late Paleozoic transgressive-regressive deposition. In: Wilgus, C., K., Hastings, B., S, Ross, C., A, Posamentier, H., W, Van Wagoner, J. and Kendall, C., St, eds., *Sea-level changes; an integrated approach*: Special Publication - Society of Economic Paleontologists and Mineralogists, v. 42: Tulsa, OK, United States, SEPM (Society for Sedimentary Geology), p. 227-247.
- Ross, W.C., Halliwell, B.A., May, J.A., Watts, D.E. & Syvitski, J.P.M. (1994): Slope readjustment: A new model for the development of submarine fans and aprons. *Geology*, 22: 511-514.
- Ross, C.A. & Ross, J.R.P. (1996): Silurian sea-level fluctuations. In: Witzke, B.J., Ludvigson, G.A. and Day, J., eds., *Paleozoic Sequence Stratigraphy: Views from the North American Craton*, v. 187-192: Boulder, Colorado, Geological Society of America Spec. Paper, p. 203-211.
- Rupke, J. (1965): The Esla Nappe, Cantabrian Mountains (Spain). *Leidse Geol. Meded.*, 32: 74 p.
- Samankassou, E. (2001): Internal structure and depositional environment of Late Carbonifer-

- ous mounds from the San Emiliano Formation, Cármenes Syncline, Cantabrian Mountains, Northern Spain. *Sedimentary Geology*, 145: 235-252.
- San José, M.A., Pieren, A.P., García Hidalgo, J.F., Vilas, L., Herranz, P., Peláez, J.R. & Perejón, A. (1990): Autochthonous sequences in the Central Iberian Zone: ante-Ordovician stratigraphy. In: Dallmeyer, R.D. and Martínez García, E., eds., *Pre-Mesozoic Geology of Iberia*: Berlin, Springer-Verlag, p. 147-159.
- Savage, J.F. & Boschma, D. (1980): Geological maps of the southern Cantabrian Mountains (Spain). *Leidse Geol. Meded.*, 50(2): 75-114.
- Sánchez de la Torre, L. & Gonzalez Lastra, J. (1978): Esquema de distribucion de ambientes y facies sedimentarias en el Carbonífero Inferior de la Cordillera Cantábrica. *Trab. Geol. Univ. Oviedo*, 10: 401-406.
- Sánchez de la Torre, S., Agueda Villar, J.A., Colmenero Navarro, J.R., García-Ramos, J.C. & Gonzáles Lástra, J. (1983): Evolucion sedimentaria y paleogeografica del Carbonifero en la Cordillera Cantabrica, Carbonifero y Permico de Espana: Madrid, IGME, p. 133-150.
- Sánchez de Posada, L.C., Martínez Chacón, M.L., Méndez Fernández, C., Menéndez-Álvarez, J.R., Truyols, J. & Villa, E. (1990): Carboniferous Pre-Stephanian rocks of the Asturian-Leonese Domain (Cantabrian Zone). In: Dallmeyer, R.D. and Martínez García, E., eds., *Pre-Mesozoic Geology of Iberia*: Berlin, Springer-Verlag.
- Sánchez de Posada, L.C., García López, S. & Villa, E. (1998): The Paleozoic of the Cantabrian Zone. In: Lamolda, M.A., ed., *24° Coloquio Europeo de Micropaleontología: Libro Guía*: Madrid, p. 11-22.
- Scaturro, D.M., Strobel, J.S., Kendall, C.G.S.C., Wendte, J.C., Biswas, G., Bezdek, J. & Cannon, R. (1989): Judy Creek: A case study for a two-dimensional sediment deposition simulation. In: Crevello, P.D., Wilson, J.L., Sarg, J.F. and Read, J.F., eds., *Controls on Carbonate Platform and Basin Development*, v. 44, The Society of Economic Paleontologists and Mineralogists, p. 63-76.
- Schlager, W. (1981): The paradox of drowned reefs and carbonate platforms. *Geological Society of America Bulletin*, 92: 197-211.
- Schlager, W., Reijmer, J.J.G. & Droxler, A. (1994): Highstand shedding of carbonate platforms. *J Sed Research*, B64(3): 270-281.
- Schlater, J.G. & Christie, P.A.F. (1980): Continental stretching: an explanation of the post-mid-Cretaceous subsidence of the central North Sea basin. *Journal of Geophysical Research*, 85: 3711-3739.
- Schmoker, J.W. & Halley, R.B. (1982): Carbonate porosity versus depth: a predictable relation for south Florida. *AAPG Bulletin*, 66: 2564-2570.
- Schönenberg, R. & Neugebauer, J. (1997): Einführung in die Geologie Europas. Freiburg, Rombach 384.
- Sdzuy, K. (1961): Das Kambrium Spaniens. Teil II: Trilobiten. *Akademie der Wissenschaften und der Literatur, Abh. der Math.-Natwiss. Kl.*, 7-8: 217-408 (499-690).
- Seibert, P. (1980): Geologische Kartierung im Paläozoikum zwischen Lavandera und Valdeteja (Provinz León, NW-Spanien) unter besonderer Berücksichtigung der Alba-Griotte Formation. Diploma thesis, Eberhard-Karls-Universität, Tübingen.
- Seibert, P. (1988): Fazies und Paläogeographie des Unter-Karbon (Alba-Formation) im Kantabrischen Gebirge (N-Spanien). Dissertation thesis, Eberhard-Karls-Universität Tübingen, 208 p.
- Sinclair, H.D. & Allen, P.A. (1992): Vertical vs. horizontal motions in the Alpine orogenic wedge: stratigraphic response in the foreland basin. *Basin Research*, 4: 215-232.
- Sinclair, H.D. (1997): Tectonostratigraphic model for underfilled peripheral foreland basins: An Alpine perspective. *GSA Bulletin*, 109(3): 324-346.
- Sjerp, N. (1967): The geology of the San Isidro-Porma area (Cantabrian mountains, Spain). *Leidse Geol. Meded.*, 39: 55-128.
- Sloss, L.L., Krumbein, W.C. & Dapples, E.C. (1949): Integrated facies analysis. In: Longwell, C.R., ed., *Sedimentary Facies in Geologic History*, v. 39, *Geol. Soc. Am. Mem.*, p. 91-124.
- Staalduinen, v.C.J. (1973): Geology of the area between the Luna and Torío rivers, southern Cantabrian Mountains, NW Spain. *Leidse Geol. Meded.*, 49(2): 167-205.
- Stewart, S.A. (1995): Paleomagnetic analysis of fold kinematics and implications for geological models of the Cantabrian/Asturian arc, north Spain. *J. Geophysical Research*, 100(B10): 20079-20094.
- Stockmal, G.S., Beaumont, C. & Boutilier, R. (1986): Geodynamic models of convergent margin tectonics: transition from rifted margin to overthrust belt and consequences for

- foreland-basin development. AAPG Bulletin, 70(2): 181-190.
- Strobel, J., Cannon, R., Kendall, C.G.S.C., Biswas, G. & Bezdek, J. (1989): Interactive (Sedpak) Simulation of Clastic and Carbonate Sediments in Shelf to Basin Settings. *Computers & Geosciences*, 15(8): 1279-1290.
- Stüwe, K. (2000): *Geodynamik der Lithosphäre*, Springer-Verlag 405 p.
- Suárez de Centi, C., García-Ramos, J.C. & Valenevela, M. (1989): Icnofosiles del Silurico de la zona cantabrica. *Boletín Geológico y Minero*, 100(3): 339-394.
- Suárez Rodríguez, N., Heredia, N., López Díaz, J.M., Toyos, L.R., Rodríguez Fernandez, L.R. & Gutierrez, G. (1990): Cartografía del mapa geológico de España, Escala 1:50.000, No.102 (Los Barrios de Luna). Madrid, IGME.
- Suppe, J. (1983): Geometry and kinematics of fault-bend folding. *American Journal of Science*, 283: 684-721.
- Suppe, J. (1985): *Principles of structural geology*, Prentice Hall 536.
- Syvitski, J.P.M., Smith, J.N., Calabrese, E.A. & Boudreay, B.P. (1988): Basin sedimentation and the growth of prograding deltas. *Journal of Geophysical Research*, 93: 6895-6908.
- Tait, J.A., Bachtadse, V., Franke, W. & Soffel, H.C. (1997): Geodynamic evolution of the European Variscan fold belt: palaeomagnetic and geological constraints. *Geol. Rundschau*, 86: 585-598.
- Tait, J., Schätz, M., Bachtadse, V. & Soffel, H. (2000): Palaeomagnetism and Palaeozoic palaeogeography of Gondwana and European terranes. In: Franke, W., Haak, V., Oncken, O. and Tanner, D., eds., *Orogenic Processes: Quantification and Modelling in the Variscan Belt*, v. 179: London, Geological Society, p. 21-34.
- Tetzlaff, D.M. & Harbaugh, J.W. (1989): *Simulating Clastic Sedimentation; Computer Methods in the Geosciences*. New York, Van Nostrand Reinhold 202.
- Thompson, M.L. (1964): Early Pennsylvanian microfaunas of the Illinois Basin. *Transactions of the Illinois State Academy of Science*, 57(1): 3-23.
- Truyols, J., Alvarez, F., Arbizu, M., Garcia Alcade, J.L., Garcia Lopez, S., Martinez Chacon, M.L., Mendez, B.I., Mendez-Fernandez, C., Menendez, J.R., Sanchez de Posada, L.C., Soto, F., Rodriguez Fernandez, L.R. & Lobato, L. (1984): Memoria explicativa de la Hoja no. 104 (Boñar) del Mapa Geológico Nacional E. 1:50.000, Inst. Geol. Min España 77.
- Truyols, J., Arbizu, M., Garcia Alcade, J.L., Garcia Lopez, S., Mendez, B.I., Soto, F. & Tuyols Massonniu, M. (1990): The Asturian-Leonese Domain (Cantabrian Zone). In: Dallmeyer, R.D. and Martinez Garcia, E., eds., *Pre-Mesozoic Geology of Iberia*: Berlin.
- Truyols Santonya, J. & Sánchez de Posada, L. (1983): El carbonifero inferior y medio de la Región de Pliegues y Mantos. In: Tuyol, J., ed., *Carbonifero y Permico de España*: Madrid, IGME, p. 39-59.
- Turcotte, D.L. & Schubert, G. (1982): *Geodynamics- applications of continuum physics to geological problems*, Wiley 450 p.
- Turcotte, D.L. & Schubert, G. (2002): *Geodynamics*, Cambridge University Press 456 p.
- Ugidos, J.M., Armenteros, I., Barba, P., Valladares, M.I. & Colmenero, J.R. (1997a): Geochemistry and petrology of recycled orogen-derived sediments: a case study from Upper Precambrian siliciclastic rocks of the Central Iberian Zone, Iberian Massif, Spain. *Precambrian Research*, 84: 163-180.
- Ugidos, J.M., Valladares, M.I., Recio, C., Rogers, G., Fallick, A.E. & Stephens, W.E. (1997b): Provenance of Upper Precambrian/Lower Cambrian shales in the Central Iberian Zone, Spain: evidence from a chemical and isotopic study. *Chemical Geology*, 136: 55-70.
- Ugidos, J.M., Valladares, M.I., Barba, P., Armenteros, I. & Colmenero, J.R. (1999): Geochemistry and Sm-Nd isotope systematics on the Upper Precambrian-Lower Cambrian sedimentary successions in the Central Iberian Zone, Spain. *Journal of Conference Abstracts*, 4(Annual meeting of IGCP Project): 1021-1021.
- Vail, P.R., Mitchum, R.M. & Thompson, S. (1977a): Seismic stratigraphy and global changes of sea level; Part 4. Global cycles of relative changes of sea level. In: Payton, C.E., ed., *Seismic Stratigraphy - Applications to Hydrocarbon Exploration*, v. AAPG Memoir 26, p. 83-97.
- Vail, P.R., Mitchum, R.M. & Thompson, S. (1977b): Seismic stratigraphy and global changes of sea level; Part 3. Relative changes of sea-level from coastal onlap. In: Payton, C.E., ed., *Seismic Stratigraphy - Applications to Hydrocarbon Exploration*, v. AAPG Memoir 26, p. 63-81.
- Vail, P.R., Mitchum Jr., R.M., Todd, R.G., Widmier, J.M., Thompson, S., Dangree, J.B., Bubbs, J.N. & Hatlelid, W.G. (1977c): Seismic stratigra-



- phy and global changes of sealevel. In: Payton, C.E., ed., *Seismic Stratigraphy - Applications to Hydrocarbon Exploration*, v. AAPG Memoir 26, p. 49-212.
- Vail, P.R., Audemard, F., Bowman, S.A., Eisner, P.N. & Pérez-Cruz, C. (1991): The stratigraphic signatures of tectonics, eustasy and sedimentology - an overview. In: Einsele, G., Ricken, W. and Seilacher, A., eds., *Cycles and Events in Stratigraphy*: Berlin, Springer-Verlag, p. 619-659.
- Valladares, M.I., Ugidos, J.M., Barba, P., Armenteros, I. & Colmenero, J.R. (1999): Upper Proterozoic-Lower Cambrian shales in the Central Iberian Zone: Chemical features and implications for other peri-Gondwanan areas. *Journal of Conference Abstracts*, 4(Annual meeting of IGCP Project 376): 1021-1022.
- Valladares, M.I., Barba, P., Ugidos, J.M., Colmenero, J.R. & Armenteros, I. (2000): Upper Neoproterozoic-Lower Cambrian sedimentary successions in the Central Iberian Zone (Spain): sequence stratigraphy, petrology and chemostratigraphy. Implications for other European zones. *Int. J. Earth Sci.*, 89: 2-20.
- Valladares, M.I., Ugidos, J.M., Barba, P. & Colmenero, J.R. (2002): Contrasting geochemical features of the Central Iberian Zone shales (Iberian Massif, Spain): implications for the evolution of Neoproterozoic-Lower Cambrian sediments and their sources in other peri-Gondwanan areas. *Tectonophysics*, 352: 121-132.
- Van Adrichem Boogaert, H.A. (1967): Devonian and Lower Carboniferous conodonts of the Cantabrian Mountains (Spain) and their stratigraphic application. *Leidse Geol. Meded.*, 39: 129-192.
- Van den Bosch, W.J. (1969): The relationship between orogenesis and sedimentation in the SW part of the Cantabrian Mountains (NW Spain). *Leidse Geol. Meded.*, 44: 227-233.
- Van der Ark, P. (1982): Conodonten, onderom en afzettingsmilieu van de Basis van de Alba-Formation in het Cantabrisch Gebergte (Spanje). *Geol. en. Min. Inst. te Leiden, Int. Report*.
- Van der Pluijm, B.A. & Kaars-Sijpesteijn, C.H. (1984): Chlorite-mica aggregates; morphology, orientation, development and bearing on cleavage formation in very-low-grade rocks. *J. Structural Geology*, 6(4): 399-407.
- Van der Voo, R., Stakamatos, J.A. & Parés, J.M. (1997): Kinematic constraints on thrust-belt curvature from syndeformational magnetizations in the Lagos del Valle syncline in the Cantabrian Arc, Spain. *Journal of Geophysical Research*, 102: 10105-10119.
- Van Ginkel, A.C. (1965): Carboniferous fusulinids from the Cantabrian Mountains (Spain). *Leidse Geol. Meded.*, 34.
- Van Ginkel, A.C. (1971): Fusulinids from uppermost Myachkovian and Kasimovian strata of northwestern Spain. *Leidse Geol. Meded.*, 47(1): 115-161.
- Van Ginkel, A.C. & Villa, E. (1987): The age of the San Emiliano formation in the Villamanin area (Bernesga River Valley). *Geobios*, 29(2).
- Van Wagoner, J.C., Posamentier, H.W., Mitchum Jr., R.M., Vail, P.R., Sarg, J.F., Loutit, T.S. & Hardenbol, J. (1988a): An overview of the fundamentals of sequence stratigraphy and key definitions. In: Wilgus, C.K., Hastings, B.S., Kendall, C.G.S.C., Posamentier, H.W., Ross, C.A. and Van Wagoner, J.C., eds., *Sea-Level Changes: An Integrated Approach*, v. 42: Tulsa, SEPM Special Publication, p. 39-45.
- Van Wagoner, J.C., Posamentier, H.W., Mitchum Jr., R.M., Vail, P.R., Sarg, J.F., Loutit, T.S. & Hardenbol, J. (1988b): An overview of the fundamentals of sequence stratigraphy and key definitions. In: Wilgus, C.K., Hastings, B.S., Kendall, C.G.S.C., Posamentier, H.W., Ross, C.A. and Van Wagoner, J.C., eds., *Sea-Level Changes: An Integrated Approach*, v. 42: Tulsa, SEPM Special Publication, p. 39-45.
- Van Wagoner, J.C. (1995): Overview of sequence stratigraphy of foreland basin deposits: terminology, summary of papers, and glossary of sequence stratigraphy. In: Van Wagoner, J.C. and Bertram, G.T., eds., *Sequence Stratigraphy of Foreland Basin Deposits - Outcrop and Subsurface. Examples from the Cretaceous of North America*, v. Memoir 64, AAPG, p. IX-XXI.
- Vera, J.A., Ed. (2004): *Geología de España*. Madrid, SGE-IGME.
- Verhoef, J. & Srivastava, S.P. (1989): Correlation of sedimentary basins across the North Atlantic as obtained from gravity and magnetic data, and its relation to early evolution of the North Atlantic. In: Tankard, A.J. and Balkwill, H.R., eds., *Extensional tectonics and stratigraphy of the North Atlantic margins*: AAPG Memoir, v. 46, p. 131-147.
- Veselovsky, Z. (2004): Integrated numerical modelling of a polyhistory basin, Southern Cantabrian Basin (Palaeozoic, NW-Spain). *GAEA heidelbergensis*, 13: 225.
- Vidal, G., Palacios, T., Moczydlowska, M. & Gu-

- banov, A.P. (1999): Age constraints from small shelly fossils on the early Cambrian terminal Cadomian Phase in Iberia. *Geologiska Föreningens i Stockholm Förhandlingar*, 121: 137-143.
- Vilas Minondo, L. (1971): El Paleozoico Inferior y Medio de la Cordillera Cantabrica entre los ríos Porma y Bernesga (León). *Memoria del IGME*, 80: 66-155.
- Villa, E. (1982): Observaciones sobre la edad de la formación Valdeteja (Carbonífero de la Cordillera Cantabrica) en su área-tipo. *Rev. Esp. Micropal.*, 14: 63-72.
- Villa, E. (1985): Foraminíferos de la región oriental de Asturias (Cordillera Cantabrica, N. de España). *Compte Rendu - International Congress on Carboniferous Stratigraphy and Geology*, 1: 333-344.
- Villa, E., Horvath, V., Martínez Chacón, M.L. & Sanchez de Posada, L.C. (1988): Datos paleontológicos y edad de la sección de Villamanín (Carbonífero, C. Cantabrica NW de España). *Congreso Geológico de España*, 1 (comunicaciones): 337-341.
- Villa, E., Sánchez de Posada, L.C., Fernández, L.P., Martínez-Chacón, M.L. & Stavros, C. (2001): Foraminifera and Biostratigraphy of the Valdeteja Formation Stratotype (Carboniferous, Cantabrian Zone, NW Spain). *Facies*, 45: 59-86.
- Wagner, R.H. (1963): A general account of the Palaeozoic Rocks between the Rivers Porma and Bernesga (León, NW. Spain). *Boletín Geológico y Minero*, 49.
- Wagner, R.H., Winkler Prins, C.F. & Riding, R.E. (1971): Lithostratigraphic units of the lower part of the Carboniferous in northern León, Spain. *Trabajos de Geología*, 4: 603-663.
- Wagner, R.H. & Fernandez Garcia, L. (1971): The Lower Carboniferous and Namurian rocks north of La Robla (León). *Trabajos de Geología*, 4: 507-531.
- Wagner, R.H. (1971): The Westphalian D floras of the Olloniego and Esperanza Formations in the Central Asturian Coalfield. *Trabajos de Geología*, 4: 461-505.
- Wagner, R.H. & Winkler Prins, C.F. (1979): The lower Stephanian of Western Europe. *C.R. Viii Congr.Int. Strat. Géol. Carbonifère*, Moskva.
- Wagner, R.H. & Bowman, M.B.J. (1983): The position of the Bashkirian/Moscovian boundary in West European chronostratigraphy. *Newsl. Stratigr.*, 12(3): 132-161.
- Wagner, R.H., Martínez García, E., Winkler Prins, C.F. & Lobato, L. (1983): Carboniferous stratigraphy of the Cantabrian Mountains. *Xth ICC Madrid, Field Trip A*: 1-220.
- Wagner, R.H. & Winkler Prins, C.F. (1991): Major subdivisions of the Carboniferous system. *XI Compte Rendu - International Congress on Carboniferous Stratigraphy and Geology*, 1: 213-245.
- Wagner, R.H. & Winkler Prins, C.F. (1994): Correlation between West-East European Chronostratigraphic Units. *Carboniferous Newsletter*, 12: 11-12.
- Wagner, R.H., Sánchez de Posada, L.C., Martínez Chacón, M.L., Fernández, L.P., Villa, E. & Winkler Prins, C.F. (2002): The Asturian stage: A preliminary proposal for the definition of a substitute for Westphalian D. In: Hills, L.V., Henderson, M. and Wayne Bamber, E., eds., *Carboniferous and Permian of the World: XIV ICCP Proceedings*, v. 19: Calgary, Canadian Society of Petroleum Geologists, p. 832-850.
- Wagner, R.H. & Winkler Prins, C.F. (2002): Stages of the Carboniferous system. *Newsl. Carb. Stratigr.*, 20: 14-16.
- Warr, L.N. (1996): Standardized clay mineral crystallinity data from the very low-grade metamorphic facies rocks of southern New Zealand. *Eur. J. Mineral.*, 8: 115-127.
- Waschbusch, P.J. & Royden, L.H. (1992): Spatial and temporal evolution of foredeep basins: lateral strength variations and inelastic yielding in continental lithosphere. *Basin Research*, 4: 179-196.
- Watts, A.B. (1992): The effective elastic thickness of the lithosphere and the evolution of foreland basins. *Basin Research*, 4(169-178).
- Watts, A.B. (2001): *Isostasy and flexure of the lithosphere*, Cambridge Univ. Press 458 p.
- Weil, A.B., Van der Voo, R., Van der Pluijm, B.A. & Parés, J. (2000): The formation of an orocline by multiphase deformation: a paleomagnetic investigation of the Cantabria-Asturias Arc (northern Spain). *Journal of Structural Geology*, 22: 735-756.
- Weil, A.B., Van der Voo, R. & Van der Pluijm, B.A. (2001): Oroclinal bending and evidence against the Pangea megashear: The Cantabria-Asturias arc (northern Spain). *Geology*, 29(11): 991-994.
- Weil, A.B., Gutiérrez-Alonso, G. & Fernández-Suárez, J. (2003): Orocline triggered lithosphere delamination. *GSA - Annual Meeting*, Seattle, GSA.
- Welte, D.H., Horsfield, B. & Baker, D.R. (1997):

- Petroleum and basin evolution, Springer-Verlag 535 p.
- Wheeler, H.E. (1958): Time-stratigraphy. AAPG Bulletin, 42: 1047-1063.
- White, T., Furlong, K. & Arthur, M. (2002): Forebulge migration in the Cretaceous Western Interior basin of the central United States. Basin Research, 14: 43-54.
- Whiting, B.M. & Thomas, W.A. (1994): Three-dimensional controls on subsidence of a foreland basin associated with a thrust-belt recess: Black Warrior basin, Alabama and Mississippi. Geology, 22: 727-730.
- Whittington, H.B. & Hughes, C.P. (1972): Ordovician geography and faunal provinces deduced from trilobite distribution. Philosophical Transactions of the Royal Soc. London, B, Biological Sciences, 263: 235-278.
- Wilson, J.T. (1970): Continents adrift: Readings from Scientific American. New York, Freeman and Company.
- Wilson, J.L. (1975): Carbonate facies in geologic history. Berlin - Heidelberg - New York, Springer 471.
- Windley, B.F. (1995): The Evolving Continents. Chichester, John Wiley & Sons 525.
- Winkler Prins, C.F. (1968): Carboniferous Productinida and Chonetidina of the Cantabrian Mountains (NW Spain): Systematics, Stratigraphy and Palaeoecology. Leidse Geol. Meded., 43: 41-155.
- Winkler Prins, C.F. (1971): The road section east of Valdeteja with its continuation along the Arroyo de Barcaliente (Curueño Valley, Leon). Trabajos de Geologia, 4: 677-686.
- Winkler Prins, C.F. (1979): Brachiopods and the Main Classification of the Carboniferous. Neuvième Congrès International de Stratigraphie et de Géologie du Carbonifère, Washington and Champaign-Urbana, Southern Illinois University Press.
- Winkler Prins, C.F. (1982): Brachiopods and the Lower/Middle Carboniferous (Mississippian/Pennsylvanian) Boundary. In: Ramsbottom, W.H.C., Saunders, W.B. and Owens, B., eds., Biostratigraphic Data for a Mid-Carboniferous Boundary, v. 11: Leeds, IUGS Publication.
- Winkler Prins, C.F. (1990): SCCS Working Group on the Subdivision of the Upper Carboniferous S.L. ("Pennsylvanian"): A Summary Report. CFS-Courier, 130: 297-306.
- Woodward, N.B., Gray, D.R. & Spears, D.B. (1986): Including strain data in balanced cross-sections. J. Structural Geology, 8(3/4): 313-324.
- Woodward, N.B., Boyer, S.E. & Suppe, J. (1989): Balanced Geological Cross-Sections: An Essential Technique in Geological Research and Exploration, AGU.
- Wuellner, D.E., Lehtonen, L.R. & James, W.C. (1986): Sedimentary tectonic development of the Marathon and Val Verde basins, west Texas, U.S.A.: a Permo-Carboniferous migrating foredeep. In: Allen, P.A. and Homewood, P., eds., Foreland Basins, v. 8, Spec. Publ. Int. Ass. Sed., p. 347-368.
- Young, T.P. (1990): Ordovician sedimentary facies and faunas of Southwest Europe: palaeogeographic and tectonic implications. In: McKerrow, W.S. and Scotese, C.R., eds., Palaeozoic Palaeogeography and Biogeography: Memoirs, v. 12: London, Geological Society, p. 421-430.
- Zamarreño, I. & Julivert, M. (1967): Estratigrafía del Cámbrico del oriente de Asturias y estudio petrográfico de las facies carbonatadas. Trabajos de Geologia, 1: 135-163.
- Zamarreño, I. (1972): Las litofacies carbonatadas del Cámbrico de la Zona Cantábrica (NW España) y su distribución geográfica. Trabajos de Geologia, 5: 3-118.
- Zühlke, R., Bouaouda, M.S., Ouajhain, B., Bechstädt, T. & Leinfelder, R.R. (2004): Quantitative Meso-/ Cenozoic development of the eastern central Atlantic continental shelf, western High Atlas, Morocco. Marine and Petroleum Geology, 21(2): 225-276.



**LIST OF FIGURES**

Fig. 1.1: Schematic workflow of the study	2
Fig. 1.2: Sketch of the orogenic cycle	3
Fig. 1.3: Successive flexural response of the lithosphere to an applied linear load	4
Fig. 1.4: Schematic zonation within a foreland basin system	5
Fig. 1.5: Experimental results for compensation of an applied load	5
Fig. 1.6: Underfilled and overfilled basin stages	6
Fig. 1.7: Consistency of bed length during deformation	9
Fig. 1.8: Controlling factors and the concept of reverse basin modeling	11
Fig. 2.1: Paleogeographical sketch during the Lower Ordovician	14
Fig. 2.2: Schematic plate tectonic setting of the Mid-European Variscides	15
Fig. 2.3: Overview of the structure of the European Variscides	15
Fig. 2.4: Zonation of the Variscan belt in the Iberian Peninsula	16
Fig. 2.5: Cross-section through the Cantabrian fold-and-thrust belt	17
Fig. 2.6: Development of the Asturian Arc and late-Variscan delamination	18
Fig. 2.7: Stratigraphic chart of the formations	20
Fig. 2.8: Lower Ordovician paleogeography of the northern Iberian Peninsula	21
Fig. 2.9: Schematic cross-section through the Lower Ordovician sedimentary setting	21
Fig. 2.10: Sketch of the paleogeographic setting during the Bashkirian	22
Fig. 2.11: Paleogeography of the Cantabrian Basin (Namurian A - Westphalian D)	22
Fig. 3.1: Synthetic overview of basin architecture along the Torío Transect	25
Fig. 3.2: Outcrop photo of the Barrios Fm. (northwest of Montuerto, Pozo Unit)	27
Fig. 3.3: Carboniferous time scale	29
Fig. 3.4: Sandstones of the Ermita Fm. (Arroyo de Barcaliente, Bodón Unit)	30
Fig. 3.5: Contact Vegamián Fm. to Alba Fm. (Arroyo de Barcaliente, Bodón Unit)	31
Fig. 3.6: Typical succession of the Alba Fm. (Mirador de Vegamián, Forcada Unit)	33
Fig. 3.7: View into the Arroyo de Barcaliente, type section of the Barcaliente Fm.	33
Fig. 3.8: Thin sections of the Barcaliente Fm.	34
Fig. 3.9: Characteristic regular bedding of the lower part of the Barcaliente Fm.	34
Fig. 3.10: Components of the Porma Breccia (Arroyo de Barcaliente, Bodón Unit)	36
Fig. 3.11: Siliciclastic turbidites of the Olleros Fm. (Alba Syncline)	38
Fig. 3.12: Setting at the eastern margin of the Valdeteja platform (Oville, Bodón Unit)	39
Fig. 3.13: Panoramic view of the top of the Valdeteja Fm. (Bodón Unit)	39
Fig. 3.14: Outcrop photo of the Valdeteja Fm. (Correcilla Unit)	40
Fig. 3.15: Slope deposits at the top of the Valdeteja Fm. (Valdorria, Gayo Unit)	41
Fig. 3.16: Lateral interfingering of Valdeteja and San Emiliano Fm. (Bodón Unit)	41
Fig. 3.17: Slope deposits of the Valdeteja Fm. at its type section	41

---

Fig. 3.18: Depositional environments in the type section of the Valdeteja Fm.	42
Fig. 3.19: Macroscopic fossils within the slope deposits of the Valdeteja Fm.	42
Fig. 3.20: Thin sections of slope deposits of the Valdeteja Fm.	43
Fig. 3.21: Platform margin deposits (Valdeteja, Bodón Unit)	44
Fig. 3.22: Thin sections of platform margin deposits of the Valdeteja Fm.	45
Fig. 3.23: Intra-platform basin and platform interior deposits (Bodón Unit)	46
Fig. 3.24: Thin section of the platform interior	46
Fig. 3.25: Birds-eyes structures (Las Majadas del Caserio, Bodón Unit)	46
Fig. 3.26: Bedding within intra-platform basin deposits	47
Fig. 3.27: Thin sections of the intra-platform environment	48
Fig. 3.28: Morphology of the Forcoso Zone (northern Curueño Valley, Forcada Unit)	50
Fig. 3.29: Shales of the Forcoso Zone (east of Oville, Bodón Unit)	50
Fig. 3.30: Fining-upward cycle of the Forcoso Zone (Llamazares, Forcada Unit)	50
Fig. 3.31: Thin sections of detrital limestones of the Forcoso Zone	51
Fig. 3.32: Alternating lithologies of the San Emiliano Fm. (Valverde, Bodón Unit)	52
Fig. 3.33: Terminology of time-equivalent deposits of the San Emiliano Fm.	53
Fig. 3.34: Characteristic succession of the San Emiliano Fm. (Bodón Unit)	54
Fig. 3.35: Nodules within the San Emiliano Fm. (Nocedo de Curueño, Gayo Unit)	55
Fig. 3.36: Thin sections of the San Emiliano Fm.	56
Fig. 4.1: Interpreted aerial photograph of the eastern Bodón Unit	64
Fig. 4.2: Interpreted aerial photograph of the eastern Gayo Unit	65
Fig. 4.3: Correlation of measured and interpreted stratigraphic profiles	66
Fig. 4.4: Time-distance plots (Wheeler plots) of the transects	68
Fig. 4.5: Disconformity in the uppermost part of the Señaras Mb. (Bodón Unit)	70
Fig. 4.6: Reciprocal sedimentation model for foreland basins	71
Fig. 4.7: Panoramic view of the type section of the Valdeteja Fm.	72
Fig. 4.8: Stratal patterns within the Valdeteja Fm. (Nocedo de Curueño, Gayo Unit)	72
Fig. 4.9: Clinoforms of the late HST of Bas 1 (Nocedo de Curueño, Gayo Unit)	73
Fig. 4.10: Erosional surfaces at the top of the Valdeteja Fm.	73
Fig. 4.11: Truncation of clinoforms (Las Majadas del Caserio, Bodón Unit)	75
Fig. 4.12: Cyclic pattern (Las Majadas del Caserio, Bodón Unit)	76
Fig. 5.1: Geological map of the study area and used terminology	80
Fig. 5.2: Staircase trajectory thrust and smooth-trajectory thrust	82
Fig. 5.3: Footwall cut-off lines and points	82
Fig. 5.4: Progressive geometrical development of a fault-bend fold	83
Fig. 5.5: 3D-diagram of the footwall of a thrust fault	83
Fig. 5.6: Outcrop photos demonstrating examples of deformational style	86
Fig. 5.7: Classification of duplexes	87

Fig. 5.8: Re-constructed cross-section A-B	88
Fig. 5.9: Genetical model of the development of the Correcilla Thrust Sheet	89
Fig. 5.10: Re-constructed cross-section E-F	90
Fig. 5.11: View into the Montuerto Syncline	91
Fig. 5.12: Restored sections of cross-sections A-B and E-F	93
Fig. 6.1: Comparison of 1D-curves of compaction induced subsidence rates	98
Fig. 6.2: Composite eustatic sea-level curve	99
Fig. 6.3: Effects of varying $T_e$ -values	100
Fig. 6.4: Logarithmic plot of initial porosities versus burial depth	102
Fig. 6.5: Graphic output of PHIL <sup>TM</sup> of the Torío Transect	103
Fig. 6.6: Spectral plots of the subsidence rates of the Torío Transect	104
Fig. 6.7: Spectral plots of subsidence rates of the Curueño Transect	105
Fig. 6.8: Stages of the Paleozoic basin fill	107
Fig. 6.9: Stages of the Bernesga-Transect by Veselovsky (2004)	108
Fig. 6.10: Graphic output of PHIL <sup>TM</sup> of Bodón and Curueño Transect	110
Fig. 6.11: 1D-curves of thermo-tectonic subsidence rates	112
Fig. 6.12: Spectral plot of Upper Carboniferous subsidence rates of the Torío-Transect	115
Fig. 6.13: Spectral plot of Upper Carboniferous subsidence rates of the Bodón Transect	116
Fig. 7.1: Calculation of the distribution of siliciclastic sediments with SEDPAK	118
Fig. 7.2: Overview of the definition of depositional factors for siliciclastic sediments	119
Fig. 7.3: User defined curve for the rate of carbonate accumulation	119
Fig. 7.4: Calculation of carbonate deposition with SEDPAK software	120
Fig. 7.5: Solidity-depth curves as used by SEDPAK	121
Fig. 7.6: Predicted facies distribution during the Serpukhovian	123
Fig. 7.7: Predicted facies distribution during the Bashkirian	124
Fig. 7.8: Sketch of a prograding system	125
Fig. 7.9: Example of an out-of-grade margin	126
Fig. 7.10: Carbonate production curve	127
Fig. 7.11: Semi-quantitative influence of parameters on the model	128
Fig. 7.12: Factors influencing the siliciclastic depositional system	129
Fig. 7.13: Model run with the initial eustatic sea-level curve	129
Fig. 7.14: Comparison of the initial eustatic sea-level curve and the adjusted curve	130
Fig. 8.1: Distribution of formations during the Bashkirian - Moscovian	134
Fig. 8.2: Interpreted schematic plan view of the distribution of formations	134
Fig. 8.3: Distribution of formations in relation to the approaching orogen	135
Fig. A.1: Overview of the positions of stratigraphic profiles	165



**LIST OF TABLES**

Tab. 5.1: Results of the balanced cross-sections	94
Tab. 7.1: Density values as predefined by SEDPAK	121
Tab. 7.2: Carbonate parameters	127
Tab. 7.3: Repose angles	128
Tab. 7.4: Minimum and maximum values for siliciclastic volumes	128
Tab. A.1: Biostratigraphic database	258
Tab. A.2: Input values for the reverse bays model: Torío Transect	261
Tab. A.3: Input values for the reverse bays model: Bodón Transect	262
Tab. A.4: Input values for the reverse bays model: Curueño Transect	263

**LIST OF STRATIGRAPHIC PROFILES**

Forcada Unit:	
Canseco	167
Llamazares	169
Quarry Porma Lake	172
Mirador de Vegamian	176
Pallide	182
Bodón Unit:	
Lavandera	184
Coto Cabañas	191
Valverde	194
Valdeteja	199
Arroyo de Barcaliente	209
Las Majadas del Caserio	213
West of Oville	223
East of Oville	229
Gayo Unit:	
Gete	235
Coto Calvo	236
Valdorria	240
Correcilla Unit:	
Las Hoces de Vegacervera	250

## Alba Syncline:

Carbonera	255
North of Orzonaga	256

**LIST OF MOVIES**

Mov. A.1: Reverse basin model of the Torío Transect	on CD
Mov. A.2: Reverse basin model of the Bodón Transect	on CD
Mov. A.3: Reverse basin model of the Curueño Transect	on CD
Mov. A.4: Stratigraphic forward model of the Bodón Transect	on CD
Mov. A.5: Forward model: Development of the basin margin during the Bashkirian	on CD

**LIST OF ABBREVEATIONS**

°C	degree Celsius
2D, 3D	two-dimensional, three-dimensional
Ma	million years
ka	1000 years
a	year
approx.	approximately
km	kilometer
m	meter
cm	centimeter
mm	millimeter
CZ	Cantabrian Zone
WALZ	West Asturian-Leonese Zone
E	east
W	west
N	north
S	south
Fm.	formation
Mb.	member
IPB	intra-platform basin
$T_e$	effective elastic thickness
m/Ma	meter per million years
LST	lowstand systems tract
SMW	shelf-margin wedge

TST	transgressive systems tract
HST	highstand systems tract
sb	sequence boundary
ts	transgressive surface
mfs	maximum flooding surface
Depos. Envir.	depositional environment
$S_{\text{tot}}$	total subsidence rate
$S_{\text{tect}}$	thermo-tectonic subsidence rate
$S_{\text{flex}}$	flexure induced subsidence rate
$S_{\text{comp}}$	compaction induced subsidence rate



## APPENDIX I

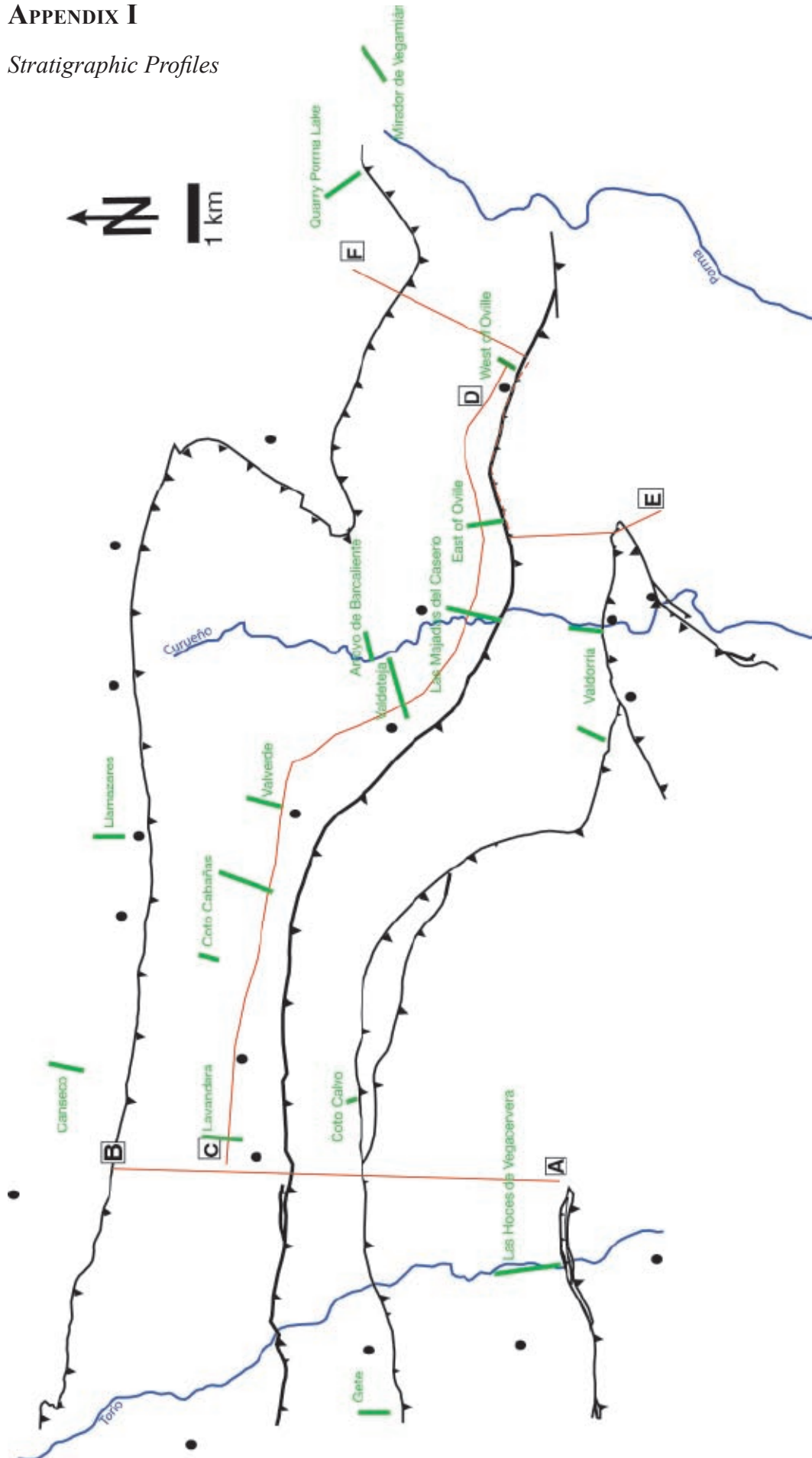
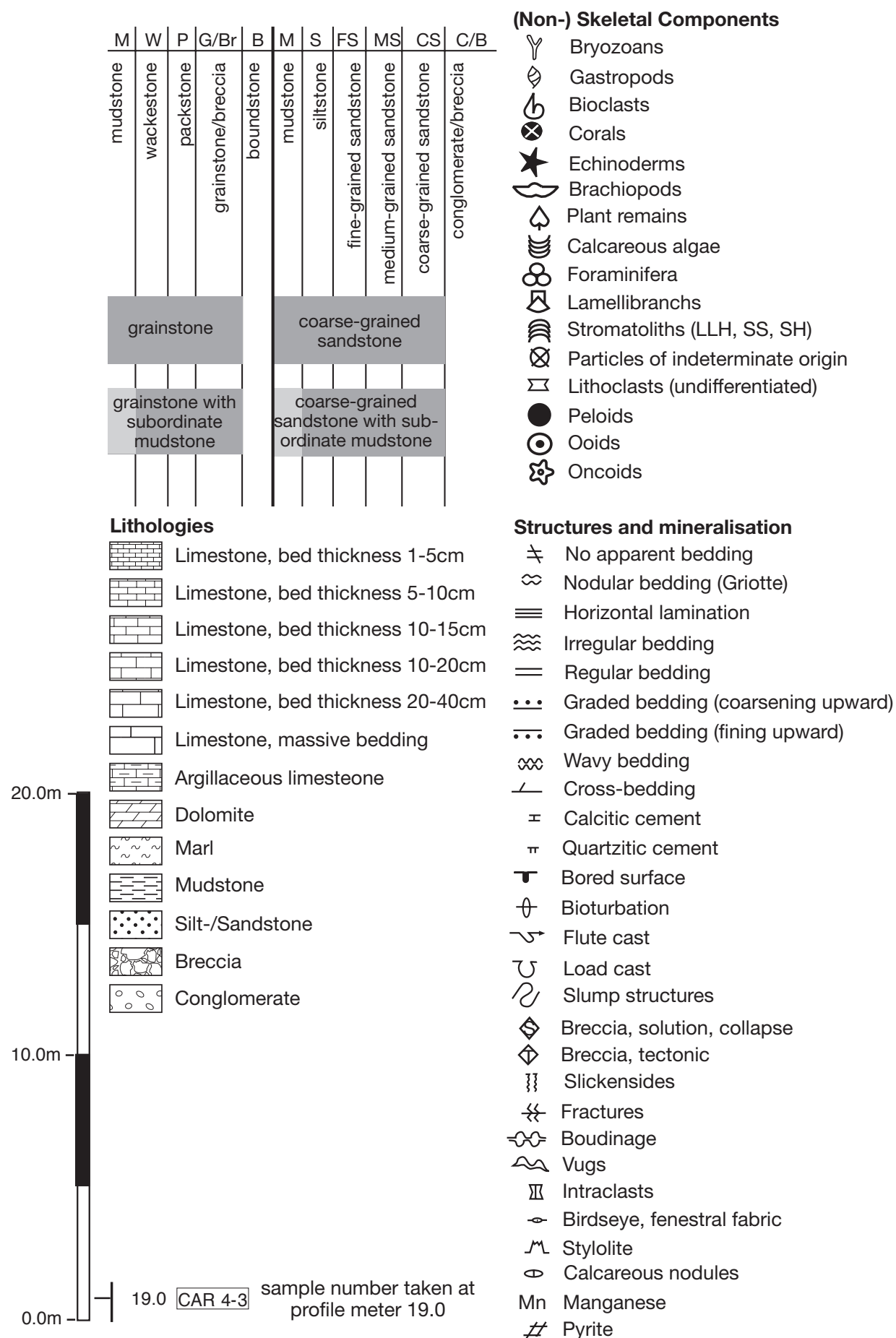
*Stratigraphic Profiles*

Fig. A.1: Overview of the positions of the recorded stratigraphic profiles within the field area, marked by thick bars. A list of the columns and the referring page numbers are given on the previous page. Selected structural elements are shown according to Figure 5.1.

## Legend



[illegible]



[illegible]

[illegible]

Llamazares				N 42° 58,142' W 005° 26,865' Altitude: 1310m		Carbonate Classification		Siliciclastic Rocks				Components										Sheet 2 / 3					
Stage	Fm .	m.	Profile / Lithology		Sample	M	W	P	G/ Br	B	M	S	FS	MS	CS	C/B	<div>☆ 𐀀 𐀁 𐀂 𐀃 𐀄 𐀅 𐀆 𐀇 𐀈 𐀉 𐀊 𐀋 𐀌 𐀍 𐀎 𐀏 𐀐 𐀑 𐀒 𐀓 𐀔 𐀕 𐀖 𐀗 𐀘 𐀙 𐀚 𐀛 𐀜 𐀝 𐀞 𐀟 𐀠 𐀡 𐀢 𐀣 𐀤 𐀥 𐀦 𐀧 𐀨 𐀩 𐀪 𐀫 𐀬 𐀭 𐀮 𐀯 𐀰 𐀱 𐀲 𐀳 𐀴 𐀵 𐀶 𐀷 𐀸 𐀹 𐀺 𐀻 𐀼 𐀽 𐀾 𐀿 𐁀 𐁁 𐁂 𐁃 𐁄 𐁅 𐁆 𐁇 𐁈 𐁉 𐁊 𐁋 𐁌 𐁍 𐁎 𐁏 𐁐 𐁑 𐁒 𐁓 𐁔 𐁕 𐁖 𐁗 𐁘 𐁙 𐁚 𐁛 𐁜 𐁝 𐁞 𐁟 𐁠 𐁡 𐁢 𐁣 𐁤 𐁥 𐁦 𐁧 𐁨 𐁩 𐁪 𐁫 𐁬 𐁭 𐁮 𐁯 𐁰 𐁱 𐁲 𐁳 𐁴 𐁵 𐁶 𐁷 𐁸 𐁹 𐁺 𐁻 𐁼 𐁽 𐁾 𐁿 𐂀 𐂁 𐂂 𐂃 𐂄 𐂅 𐂆 𐂇 𐂈 𐂉 𐂊 𐂋 𐂌 𐂍 𐂎 𐂏 𐂐 𐂑 𐂒 𐂓 𐂔 𐂕 𐂖 𐂗 𐂘 𐂙 𐂚 𐂛 𐂜 𐂝 𐂞 𐂟 𐂠 𐂡 𐂢 𐂣 𐂤 𐂥 𐂦 𐂧 𐂨 𐂩 𐂪 𐂫 𐂬 𐂭 𐂮 𐂯 𐂰 𐂱 𐂲 𐂳 𐂴 𐂵 𐂶 𐂷 𐂸 𐂹 𐂺 𐂻 𐂼 𐂽 𐂾 𐂿 𐃀 𐃁 𐃂 𐃃 𐃄 𐃅 𐃆 𐃇 𐃈 𐃉 𐃊 𐃋 𐃌 𐃍 𐃎 𐃏 𐃐 𐃑 𐃒 𐃓 𐃔 𐃕 𐃖 𐃗 𐃘 𐃙 𐃚 𐃛 𐃜 𐃝 𐃞 𐃟 𐃠 𐃡 𐃢 𐃣 𐃤 𐃥 𐃦 𐃧 𐃨 𐃩 𐃪 𐃫 𐃬 𐃭 𐃮 𐃯 𐃰 𐃱 𐃲 𐃳 𐃴 𐃵 𐃶 𐃷 𐃸 𐃹 𐃺 𐃻 𐃼 𐃽 𐃾 𐃿 𐄀 𐄁 𐄂 𐄃 𐄄 𐄅 𐄆 𐄇 𐄈 𐄉 𐄊 𐄋 𐄌 𐄍 𐄎 𐄏 𐄐 𐄑 𐄒 𐄓 𐄔 𐄕 𐄖 𐄗 𐄘 𐄙 𐄚 𐄛 𐄜 𐄝 𐄞 𐄟 𐄠 𐄡 𐄢 𐄣 𐄤 𐄥 𐄦 𐄧 𐄨 𐄩 𐄪 𐄫 𐄬 𐄭 𐄮 𐄯 𐄰 𐄱 𐄲 𐄳 𐄴 𐄵 𐄶 𐄷 𐄸 𐄹 𐄺 𐄻 𐄼 𐄽 𐄾 𐄿 𐅀 𐅁 𐅂 𐅃 𐅄 𐅅 𐅆 𐅇 𐅈 𐅉 𐅊 𐅋 𐅌 𐅍 𐅎 𐅏 𐅐 𐅑 𐅒 𐅓 𐅔 𐅕 𐅖 𐅗 𐅘 𐅙 𐅚 𐅛 𐅜 𐅝 𐅞 𐅟 𐅠 𐅡 𐅢 𐅣 𐅤 𐅥 𐅦 𐅧 𐅨 𐅩 𐅪 𐅫 𐅬 𐅭 𐅮 𐅯 𐅰 𐅱 𐅲 𐅳 𐅴 𐅵 𐅶 𐅷 𐅸 𐅹 𐅺 𐅻 𐅼 𐅽 𐅾 𐅿 𐆀 𐆁 𐆂 𐆃 𐆄 𐆅 𐆆 𐆇 𐆈 𐆉 𐆊 𐆋 𐆌 𐆍 𐆎 𐆏 𐆐 𐆑 𐆒 𐆓 𐆔 𐆕 𐆖 𐆗 𐆘 𐆙 𐆚 𐆛 𐆜 𐆝 𐆞 𐆟 𐆠 𐆡 𐆢 𐆣 𐆤 𐆥 𐆦 𐆧 𐆨 𐆩 𐆪 𐆫 𐆬 𐆭 𐆮 𐆯 𐆰 𐆱 𐆲 𐆳 𐆴 𐆵 𐆶 𐆷 𐆸 𐆹 𐆺 𐆻 𐆼 𐆽 𐆾 𐆿 𐇀 𐇁 𐇂 𐇃 𐇄 𐇅 𐇆 𐇇 𐇈 𐇉 𐇊 𐇋 𐇌 𐇍 𐇎 𐇏 𐇐 𐇑 𐇒 𐇓 𐇔 𐇕 𐇖 𐇗 𐇘 𐇙 𐇚 𐇛 𐇜 𐇝 𐇞 𐇟 𐇠 𐇡 𐇢 𐇣 𐇤 𐇥 𐇦 𐇧 𐇨 𐇩 𐇪 𐇫 𐇬 𐇭 𐇮 𐇯 𐇰 𐇱 𐇲 𐇳 𐇴 𐇵 𐇶 𐇷 𐇸 𐇹 𐇺 𐇻 𐇼 𐇽 𐇾 𐇿 𐈀 𐈁 𐈂 𐈃 𐈄 𐈅 𐈆 𐈇 𐈈 𐈉 𐈊 𐈋 𐈌 𐈍 𐈎 𐈏 𐈐 𐈑 𐈒 𐈓 𐈔 𐈕 𐈖 𐈗 𐈘 𐈙 𐈚 𐈛 𐈜 𐈝 𐈞 𐈟 𐈠 𐈡 𐈢 𐈣 𐈤 𐈥 𐈦 𐈧 𐈨 𐈩 𐈪 𐈫 𐈬 𐈭 𐈮 𐈯 𐈰 𐈱 𐈲 𐈳 𐈴 𐈵 𐈶 𐈷 𐈸 𐈹 𐈺 𐈻 𐈼 𐈽 𐈾 𐈿 𐉀 𐉁 𐉂 𐉃 𐉄 𐉅 𐉆 𐉇 𐉈 𐉉 𐉊 𐉋 𐉌 𐉍 𐉎 𐉏 𐉐 𐉑 𐉒 𐉓 𐉔 𐉕 𐉖 𐉗 𐉘 𐉙 𐉚 𐉛 𐉜 𐉝 𐉞 𐉟 𐉠 𐉡 𐉢 𐉣 𐉤 𐉥 𐉦 𐉧 𐉨 𐉩 𐉪 𐉫 𐉬 𐉭 𐉮 𐉯 𐉰 𐉱 𐉲 𐉳 𐉴 𐉵 𐉶 𐉷 𐉸 𐉹 𐉺 𐉻 𐉼 𐉽 𐉾 𐉿 𐊀 𐊁 𐊂 𐊃 𐊄 𐊅 𐊆 𐊇 𐊈 𐊉 𐊊 𐊋 𐊌 𐊍 𐊎 𐊏 𐊐 𐊑 𐊒 𐊓 𐊔 𐊕 𐊖 𐊗 𐊘 𐊙 𐊚 𐊛 𐊜 𐊝 𐊞 𐊟 𐊠 𐊡 𐊢 𐊣 𐊤 𐊥 𐊦 𐊧 𐊨 𐊩 𐊪 𐊫 𐊬 𐊭 𐊮 𐊯 𐊰 𐊱 𐊲 𐊳 𐊴 𐊵 𐊶 𐊷 𐊸 𐊹 𐊺 𐊻 𐊼 𐊽 𐊾 𐊿 𐋀 𐋁 𐋂 𐋃 𐋄 𐋅 𐋆 𐋇 𐋈 𐋉 𐋊 𐋋 𐋌 𐋍 𐋎 𐋏 𐋐 𐋑 𐋒 𐋓 𐋔 𐋕 𐋖 𐋗 𐋘 𐋙 𐋚 𐋛 𐋜 𐋝 𐋞 𐋟 𐋠 𐋡 𐋢 𐋣 𐋤 𐋥 𐋦 𐋧 𐋨 𐋩 𐋪 𐋫 𐋬 𐋭 𐋮 𐋯 𐋰 𐋱 𐋲 𐋳 𐋴 𐋵 𐋶 𐋷 𐋸 𐋹 𐋺 𐋻 𐋼 𐋽 𐋾 𐋿 𐌀 𐌁 𐌂 𐌃 𐌄 𐌅</div>										
																		Basin									
																		Intertidal									



[illegible]

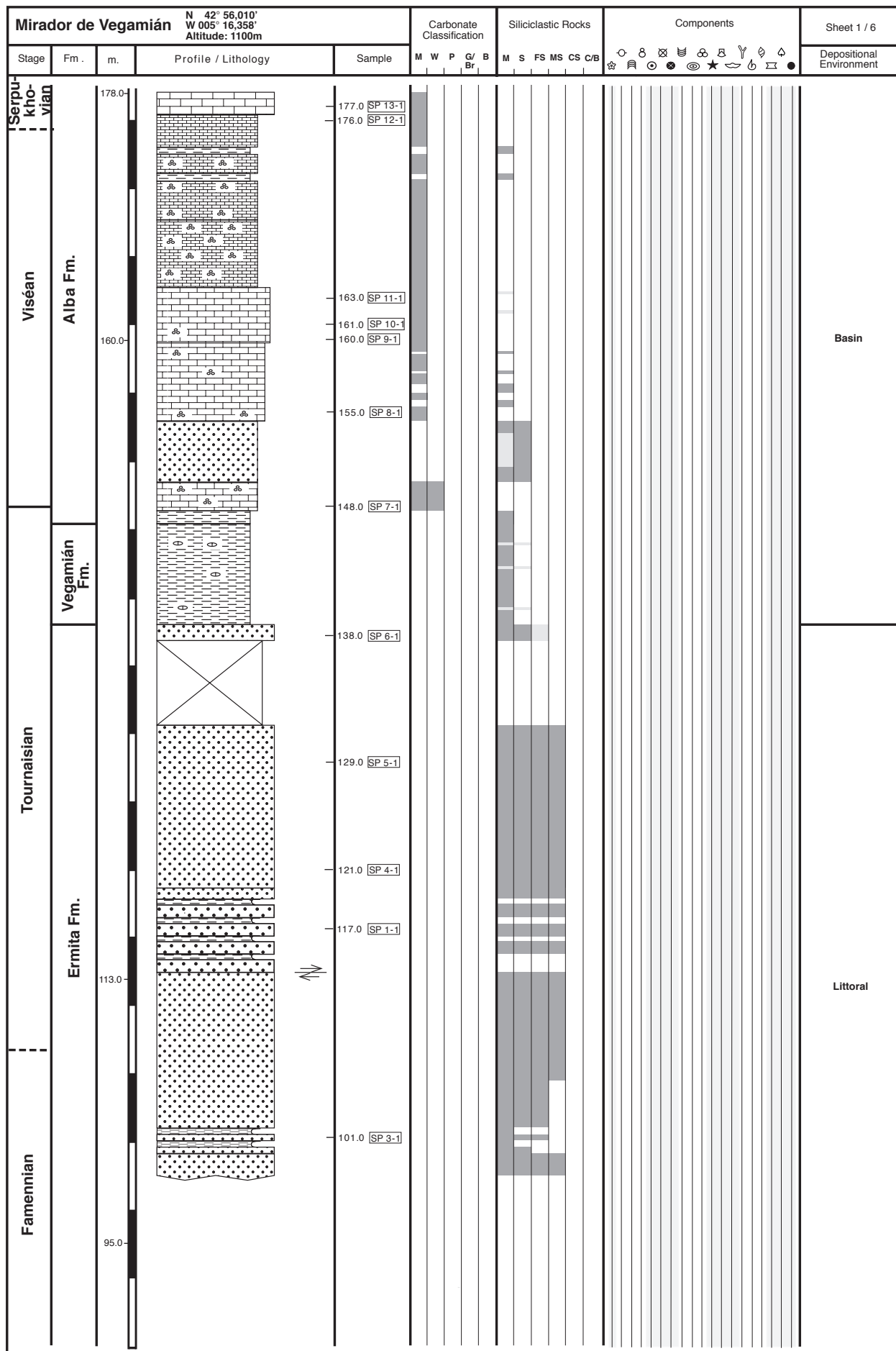
[illegible]





[illegible]

[illegible]





[illegible]

[illegible]

[illegible]

[illegible]



[illegible]

[illegible]

West of Pallide					Carbonate Classification					Siliciclastic Rocks					Components															Sheet 2 / 2
Stage	Fm .	m.	Profile / Lithology	Sample	M	W	P	G/Br	B	M	S	FS	MS	CS	C/B	<div>○ 8 ⊠ 𐀀 𐀁 𐀂 𐀃 𐀄 𐀅 𐀆 𐀇 𐀈 𐀉 𐀊 𐀋 𐀌 𐀍 𐀎 𐀏 𐀐 𐀑 𐀒 𐀓 𐀔 𐀕 𐀖 𐀗 𐀘 𐀙 𐀚 𐀛 𐀜 𐀝 𐀞 𐀟 𐀠 𐀡 𐀢 𐀣 𐀤 𐀥 𐀦 𐀧 𐀨 𐀩 𐀪 𐀫 𐀬 𐀭 𐀮 𐀯 𐀰 𐀱 𐀲 𐀳 𐀴 𐀵 𐀶 𐀷 𐀸 𐀹 𐀺 𐀻 𐀼 𐀽 𐀾 𐀿 𐁀 𐁁 𐁂 𐁃 𐁄 𐁅 𐁆 𐁇 𐁈 𐁉 𐁊 𐁋 𐁌 𐁍 𐁎 𐁏 𐁐 𐁑 𐁒 𐁓 𐁔 𐁕 𐁖 𐁗 𐁘 𐁙 𐁚 𐁛 𐁜 𐁝 𐁞 𐁟 𐁠 𐁡 𐁢 𐁣 𐁤 𐁥 𐁦 𐁧 𐁨 𐁩 𐁪 𐁫 𐁬 𐁭 𐁮 𐁯 𐁰 𐁱 𐁲 𐁳 𐁴 𐁵 𐁶 𐁷 𐁸 𐁹 𐁺 𐁻 𐁼 𐁽 𐁾 𐁿 𐂀 𐂁 𐂂 𐂃 𐂄 𐂅 𐂆 𐂇 𐂈 𐂉 𐂊 𐂋 𐂌 𐂍 𐂎 𐂏 𐂐 𐂑 𐂒 𐂓 𐂔 𐂕 𐂖 𐂗 𐂘 𐂙 𐂚 𐂛 𐂜 𐂝 𐂞 𐂟 𐂠 𐂡 𐂢 𐂣 𐂤 𐂥 𐂦 𐂧 𐂨 𐂩 𐂪 𐂫 𐂬 𐂭 𐂮 𐂯 𐂰 𐂱 𐂲 𐂳 𐂴 𐂵 𐂶 𐂷 𐂸 𐂹 𐂺 𐂻 𐂼 𐂽 𐂾 𐂿 𐃀 𐃁 𐃂 𐃃 𐃄 𐃅 𐃆 𐃇 𐃈 𐃉 𐃊 𐃋 𐃌 𐃍 𐃎 𐃏 𐃐 𐃑 𐃒 𐃓 𐃔 𐃕 𐃖 𐃗 𐃘 𐃙 𐃚 𐃛 𐃜 𐃝 𐃞 𐃟 𐃠 𐃡 𐃢 𐃣 𐃤 𐃥 𐃦 𐃧 𐃨 𐃩 𐃪 𐃫 𐃬 𐃭 𐃮 𐃯 𐃰 𐃱 𐃲 𐃳 𐃴 𐃵 𐃶 𐃷 𐃸 𐃹 𐃺 𐃻 𐃼 𐃽 𐃾 𐃿 𐄀 𐄁 𐄂 𐄃 𐄄 𐄅 𐄆 𐄇 𐄈 𐄉 𐄊 𐄋 𐄌 𐄍 𐄎 𐄏 𐄐 𐄑 𐄒 𐄓 𐄔 𐄕 𐄖 𐄗 𐄘 𐄙 𐄚 𐄛 𐄜 𐄝 𐄞 𐄟 𐄠 𐄡 𐄢 𐄣 𐄤 𐄥 𐄦 𐄧 𐄨 𐄩 𐄪 𐄫 𐄬 𐄭 𐄮 𐄯 𐄰 𐄱 𐄲 𐄳 𐄴 𐄵 𐄶 𐄷 𐄸 𐄹 𐄺 𐄻 𐄼 𐄽 𐄾 𐄿 𐅀 𐅁 𐅂 𐅃 𐅄 𐅅 𐅆 𐅇 𐅈 𐅉 𐅊 𐅋 𐅌 𐅍 𐅎 𐅏 𐅐 𐅑 𐅒 𐅓 𐅔 𐅕 𐅖 𐅗 𐅘 𐅙 𐅚 𐅛 𐅜 𐅝 𐅞 𐅟 𐅠 𐅡 𐅢 𐅣 𐅤 𐅥 𐅦 𐅧 𐅨 𐅩 𐅪 𐅫 𐅬 𐅭 𐅮 𐅯 𐅰 𐅱 𐅲 𐅳 𐅴 𐅵 𐅶 𐅷 𐅸 𐅹 𐅺 𐅻 𐅼 𐅽 𐅾 𐅿 𐆀 𐆁 𐆂 𐆃 𐆄 𐆅 𐆆 𐆇 𐆈 𐆉 𐆊 𐆋 𐆌 𐆍 𐆎 𐆏 𐆐 𐆑 𐆒 𐆓 𐆔 𐆕 𐆖 𐆗 𐆘 𐆙 𐆚 𐆛 𐆜 𐆝 𐆞 𐆟 𐆠 𐆡 𐆢 𐆣 𐆤 𐆥 𐆦 𐆧 𐆨 𐆩 𐆪 𐆫 𐆬 𐆭 𐆮 𐆯 𐆰 𐆱 𐆲 𐆳 𐆴 𐆵 𐆶 𐆷 𐆸 𐆹 𐆺 𐆻 𐆼 𐆽 𐆾 𐆿 𐇀 𐇁 𐇂 𐇃 𐇄 𐇅 𐇆 𐇇 𐇈 𐇉 𐇊 𐇋 𐇌 𐇍 𐇎 𐇏 𐇐 𐇑 𐇒 𐇓 𐇔 𐇕 𐇖 𐇗 𐇘 𐇙 𐇚 𐇛 𐇜 𐇝 𐇞 𐇟 𐇠 𐇡 𐇢 𐇣 𐇤 𐇥 𐇦 𐇧 𐇨 𐇩 𐇪 𐇫 𐇬 𐇭 𐇮 𐇯 𐇰 𐇱 𐇲 𐇳 𐇴 𐇵 𐇶 𐇷 𐇸 𐇹 𐇺 𐇻 𐇼 𐇽 𐇾 𐇿 𐈀 𐈁 𐈂 𐈃 𐈄 𐈅 𐈆 𐈇 𐈈 𐈉 𐈊 𐈋 𐈌 𐈍 𐈎 𐈏 𐈐 𐈑 𐈒 𐈓 𐈔 𐈕 𐈖 𐈗 𐈘 𐈙 𐈚 𐈛 𐈜 𐈝 𐈞 𐈟 𐈠 𐈡 𐈢 𐈣 𐈤 𐈥 𐈦 𐈧 𐈨 𐈩 𐈪 𐈫 𐈬 𐈭 𐈮 𐈯 𐈰 𐈱 𐈲 𐈳 𐈴 𐈵 𐈶 𐈷 𐈸 𐈹 𐈺 𐈻 𐈼 𐈽 𐈾 𐈿 𐉀 𐉁 𐉂 𐉃 𐉄 𐉅 𐉆 𐉇 𐉈 𐉉 𐉊 𐉋 𐉌 𐉍 𐉎 𐉏 𐉐 𐉑 𐉒 𐉓 𐉔 𐉕 𐉖 𐉗 𐉘 𐉙 𐉚 𐉛 𐉜 𐉝 𐉞 𐉟 𐉠 𐉡 𐉢 𐉣 𐉤 𐉥 𐉦 𐉧 𐉨 𐉩 𐉪 𐉫 𐉬 𐉭 𐉮 𐉯 𐉰 𐉱 𐉲 𐉳 𐉴 𐉵 𐉶 𐉷 𐉸 𐉹 𐉺 𐉻 𐉼 𐉽 𐉾 𐉿 𐊀 𐊁 𐊂 𐊃 𐊄 𐊅 𐊆 𐊇 𐊈 𐊉 𐊊 𐊋 𐊌 𐊍 𐊎 𐊏 𐊐 𐊑 𐊒 𐊓 𐊔 𐊕 𐊖 𐊗 𐊘 𐊙 𐊚 𐊛 𐊜 𐊝 𐊞 𐊟 𐊠 𐊡 𐊢 𐊣 𐊤 𐊥 𐊦 𐊧 𐊨 𐊩 𐊪 𐊫 𐊬 𐊭 𐊮 𐊯 𐊰 𐊱 𐊲 𐊳 𐊴 𐊵 𐊶 𐊷 𐊸 𐊹 𐊺 𐊻 𐊼 𐊽 𐊾 𐊿 𐋀 𐋁 𐋂 𐋃 𐋄 𐋅 𐋆 𐋇 𐋈 𐋉 𐋊 𐋋 𐋌 𐋍 𐋎 𐋏 𐋐 𐋑 𐋒 𐋓 𐋔 𐋕 𐋖 𐋗 𐋘 𐋙 𐋚 𐋛 𐋜 𐋝 𐋞 𐋟 𐋠 𐋡 𐋢 𐋣 𐋤 𐋥 𐋦 𐋧 𐋨 𐋩 𐋪 𐋫 𐋬 𐋭 𐋮 𐋯 𐋰 𐋱 𐋲 𐋳 𐋴 𐋵 𐋶 𐋷 𐋸 𐋹 𐋺 𐋻 𐋼 𐋽 𐋾 𐋿 𐌀 𐌁 𐌂 𐌃 𐌄 𐌅 𐌆 𐌇 𐌈 𐌉 𐌊 𐌋 𐌌 𐌍 𐌎 𐌏 </div>														

[illegible]



[illegible]

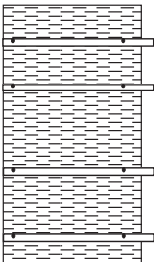

[illegible]

[illegible]

[illegible]



[illegible]

Lavandera				N 42° 57,246' W 005° 30,597' Altitude: 1310m		Carbonate Classification		Siliciclastic Rocks		Components		Sheet 7 / 7																
Stage	Fm .	m.	Profile / Lithology	Sample	M	W	P	G	B	M	S	FS	MS	CS	C/B	☆	貝	○	●	☉	★	☞	♂	♀	☐	●	Depos. Envir.	Systems Tract
Moscovian	San Emiliano Fm.	568.0-																							Prodelta	TST (Mos 2)		

[illegible]

[illegible]



[illegible]

[illegible]

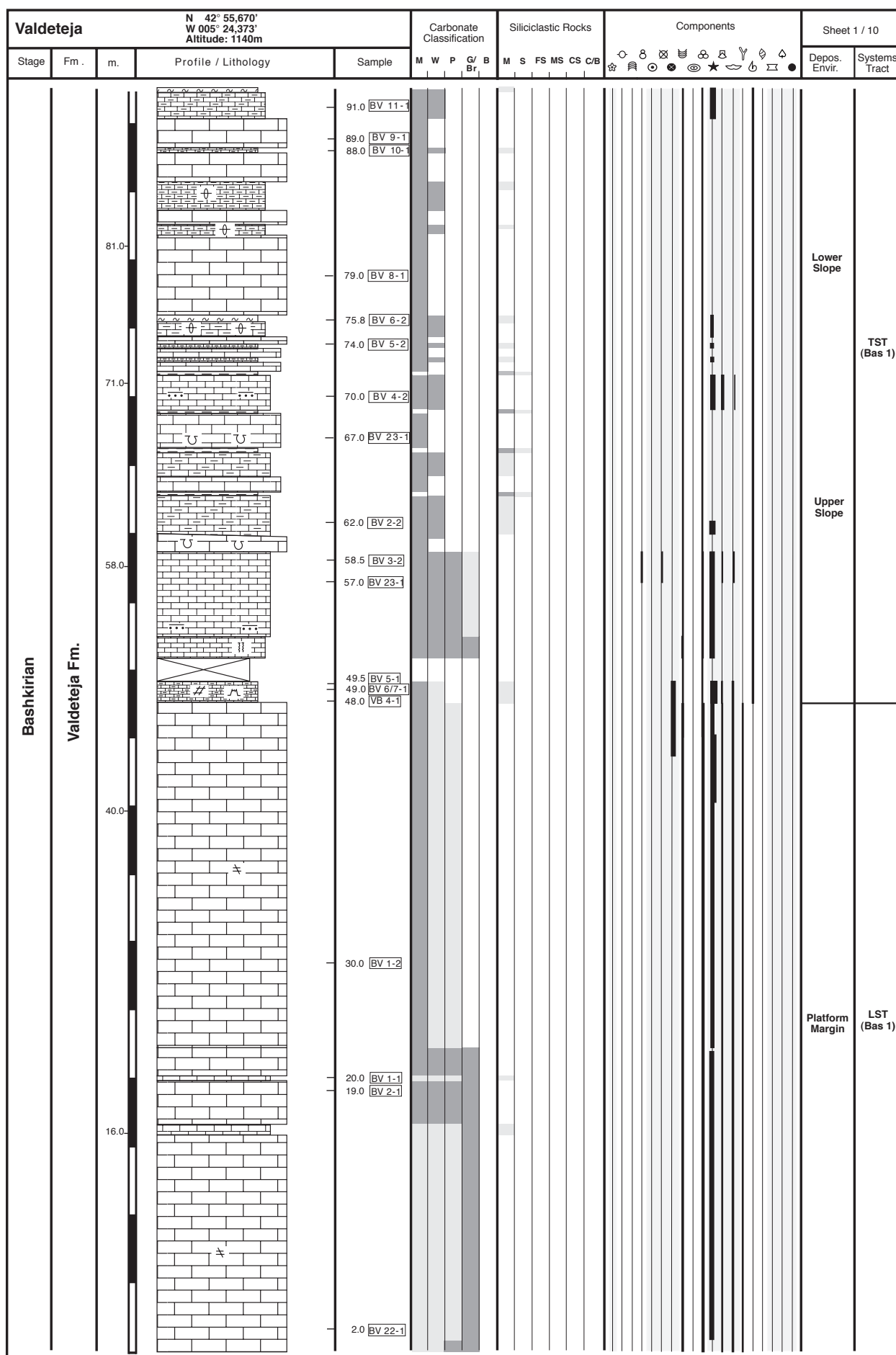
[illegible]

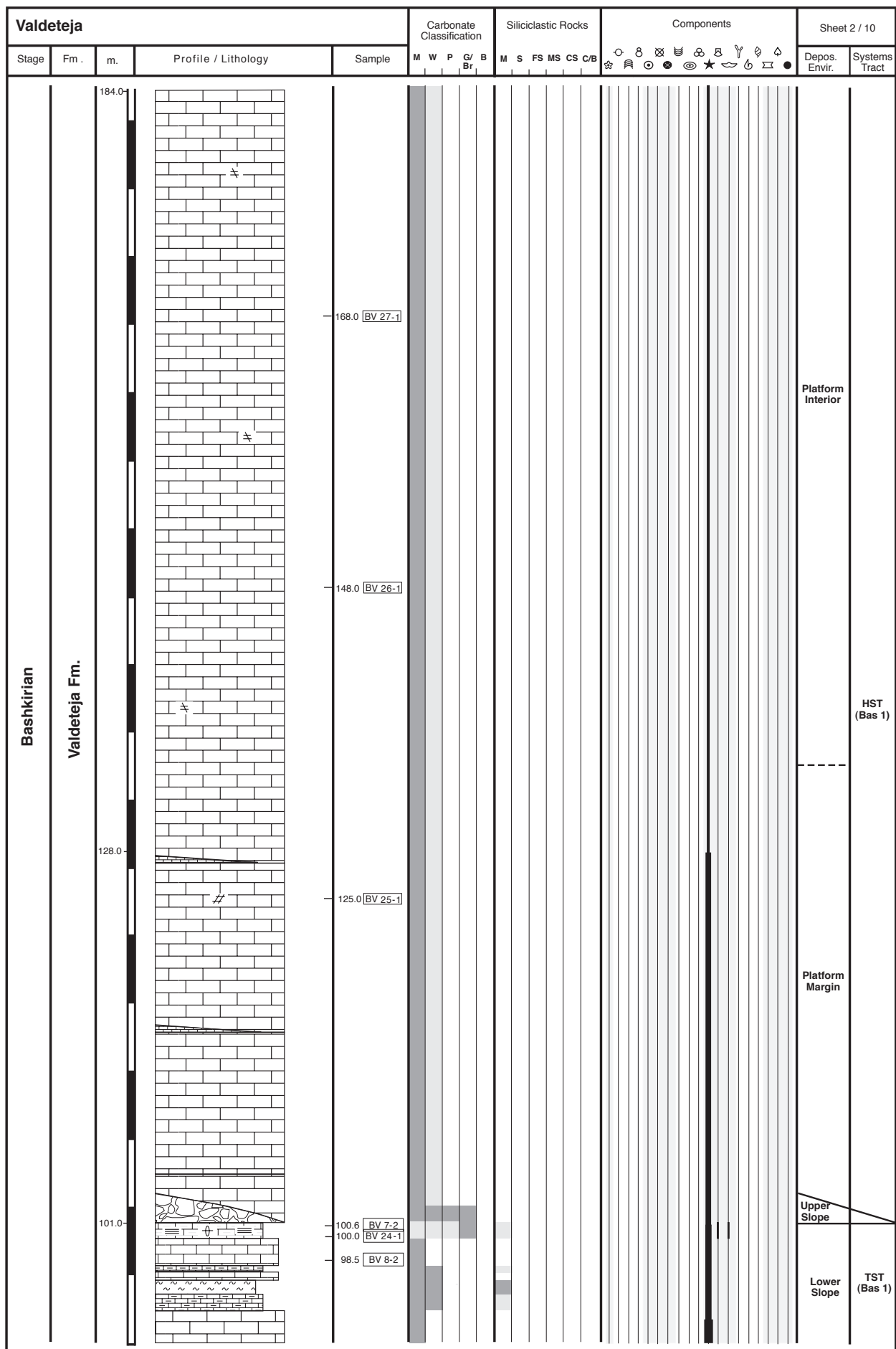
[illegible]



[illegible]

[illegible]







[illegible]

Valdeteja					Carbonate Classification					Siliciclastic Rocks							Components													Sheet 4 / 10	
Stage	Fm .	m.	Profile / Lithology	Sample	M	W	P	G/Br	B	M	S	FS	MS	CS	C/B														Depos. Envir.	Systems Tract	
Bashkirian	Valdeteja Fm.	329.0																													
		290.0		309.0 [BV 12-1]																											
				268.0 [BV 33-1]																										Platform Interior	HST (Bas 1)

Valdeteja					Carbonate Classification				Siliciclastic Rocks							Components												Sheet 5 / 10	
Stage	Fm.	m.	Profile / Lithology	Sample	M	W	P	G/Br	B	M	S	FS	MS	CS	C/B	☆	⊙	⊗	⊕	⊖	⊗	⊕	⊖	⊗	⊕	⊖	Depos. Envir.	Systems Tract	
Bashkirian	Valdeteja Fm.	422.0																									Intra-Platform Basin	LST (Bas 2)	
				408.0 BV 15-1																							Platform Interior		
																											Intra-Platform Basin		
																											Platform Interior		
																											Intra-Platform Basin	HST (Bas 1)	
		372.0		371.0 BV 14-1																							Platform Interior		
																											Intra-Platform Basin		
		337.0																									Platform Interior		

Valdeteja						Carbonate Classification				Siliciclastic Rocks							Components										Sheet 6 / 10					
Stage	Fm.	m.	Profile / Lithology	Sample	M	W	P	G/ Br	B	M	S	FS	MS	CS	C/B	○	◐	⊗	≡	⦿	⌘	⏞	⏟	⏠	⏡	⏢	⏣	●	Depos. Envir.	Systems Tract		
Bashkirian	Valdeteja Fm.	513.0-		513.0 [BV 11-2] [BV 17/18-1]																											Intra-Platform Basin	TST (Bas 2)
		499.0-		501.0 [BV 1-3]																												
		496.0 [BV 37-1]																														
		493.0 [BV 36-1]																														
		473.0-		468.0 [BV 35-1]																											Platform Margin	
		465.0 [BV 16-1]																														
		461.0 [BV 34-1]																														
		457.0 [BV 10-2]																														
452.0-																												Platform Interior	LST (Bas 2)			
432.0-																																
																														Intra-Platform Basin		



Valdeteja					Carbonate Classification		Siliciclastic Rocks						Components								Sheet 7 / 10								
Stage	Fm .	m.	Profile / Lithology	Sample	M	W	P	G/ Br	B	M	S	FS	MS	CS	C/B												Dpos. Envir.	Systems Tract	
Bashkirian	Valdeteja Fm.	600.0-		603.5 [BV 13-2]																							Intra-Platform Basin		
		581.0-		583.5 [BV 2-3] 582.5 [BV 12-2]																									
		553.0-		537.0 [BV 20-1] 536.0 [BV 21-1]																									
			</																										

Valdeteja					Carbonate Classification					Siliciclastic Rocks							Components													Sheet 8 / 10																																																																																																																																																																																																																																																																																																																																																																																																																																																																																																																																																																																																																																																																																																																																																																																																																																																																																																																																																																																																																																																																																																																																																																																																																							
Stage	Fm .	m.	Profile / Lithology	Sample	M	W	P	G/Br	B	M	S	FS	MS	CS	C/B	☆	⦶	⦶	⦶	⦶	⦶	⦶	⦶	⦶	⦶	⦶	⦶	⦶	⦶	⦶	⦶	⦶	⦶	⦶	⦶	⦶	⦶	⦶	⦶	⦶	⦶	⦶	⦶	⦶	⦶	⦶	⦶	⦶	⦶	⦶	⦶	⦶	⦶	⦶	⦶	⦶	⦶	⦶	⦶	⦶	⦶	⦶	⦶	⦶	⦶	⦶	⦶	⦶	⦶	⦶	⦶	⦶	⦶	⦶	⦶	⦶	⦶	⦶	⦶	⦶	⦶	⦶	⦶	⦶	⦶	⦶	⦶	⦶	⦶	⦶	⦶	⦶	⦶	⦶	⦶	⦶	⦶	⦶	⦶	⦶	⦶	⦶	⦶	⦶	⦶	⦶	⦶	⦶	⦶	⦶	⦶	⦶	⦶	⦶	⦶	⦶	⦶	⦶	⦶	⦶	⦶	⦶	⦶	⦶	⦶	⦶	⦶	⦶	⦶	⦶	⦶	⦶	⦶	⦶	⦶	⦶	⦶	⦶	⦶	⦶	⦶	⦶	⦶	⦶	⦶	⦶	⦶	⦶	⦶	⦶	⦶	⦶	⦶	⦶	⦶	⦶	⦶	⦶	⦶	⦶	⦶	⦶	⦶	⦶	⦶	⦶	⦶	⦶	⦶	⦶	⦶	⦶	⦶	⦶	⦶	⦶	⦶	⦶	⦶	⦶	⦶	⦶	⦶	⦶	⦶	⦶	⦶	⦶	⦶	⦶	⦶	⦶	⦶	⦶	⦶	⦶	⦶	⦶	⦶	⦶	⦶	⦶	⦶	⦶	⦶	⦶	⦶	⦶	⦶	⦶	⦶	⦶	⦶	⦶	⦶	⦶	⦶	⦶	⦶	⦶	⦶	⦶	⦶	⦶	⦶	⦶	⦶	⦶	⦶	⦶	⦶	⦶	⦶	⦶	⦶	⦶	⦶	⦶	⦶	⦶	⦶	⦶	⦶	⦶	⦶	⦶	⦶	⦶	⦶	⦶	⦶	⦶	⦶	⦶	⦶	⦶	⦶	⦶	⦶	⦶	⦶	⦶	⦶	⦶	⦶	⦶	⦶	⦶	⦶	⦶	⦶	⦶	⦶	⦶	⦶	⦶	⦶	⦶	⦶	⦶	⦶	⦶	⦶	⦶	⦶	⦶	⦶	⦶	⦶	⦶	⦶	⦶	⦶	⦶	⦶	⦶	⦶	⦶	⦶	⦶	⦶	⦶	⦶	⦶	⦶	⦶	⦶	⦶	⦶	⦶	⦶	⦶	⦶	⦶	⦶	⦶	⦶	⦶	⦶	⦶	⦶	⦶	⦶	⦶	⦶	⦶	⦶	⦶	⦶	⦶	⦶	⦶	⦶	⦶	⦶	⦶	⦶	⦶	⦶	⦶	⦶	⦶	⦶	⦶	⦶	⦶	⦶	⦶	⦶	⦶	⦶	⦶	⦶	⦶	⦶	⦶	⦶	⦶	⦶	⦶	⦶	⦶	⦶	⦶	⦶	⦶	⦶	⦶	⦶	⦶	⦶	⦶	⦶	⦶	⦶	⦶	⦶	⦶	⦶	⦶	⦶	⦶	⦶	⦶	⦶	⦶	⦶	⦶	⦶	⦶	⦶	⦶	⦶	⦶	⦶	⦶	⦶	⦶	⦶	⦶	⦶	⦶	⦶	⦶	⦶	⦶	⦶	⦶	⦶	⦶	⦶	⦶	⦶	⦶	⦶	⦶	⦶	⦶	⦶	⦶	⦶	⦶	⦶	⦶	⦶	⦶	⦶	⦶	⦶	⦶	⦶	⦶	⦶	⦶	⦶	⦶	⦶	⦶	⦶	⦶	⦶	⦶	⦶	⦶	⦶	⦶	⦶	⦶	⦶	⦶	⦶	⦶	⦶	⦶	⦶	⦶	⦶	⦶	⦶	⦶	⦶	⦶	⦶	⦶	⦶	⦶	⦶	⦶	⦶	⦶	⦶	⦶	⦶	⦶	⦶	⦶	⦶	⦶	⦶	⦶	⦶	⦶	⦶	⦶	⦶	⦶	⦶	⦶	⦶	⦶	⦶	⦶	⦶	⦶	⦶	⦶	⦶	⦶	⦶	⦶	⦶	⦶	⦶	⦶	⦶	⦶	⦶	⦶	⦶	⦶	⦶	⦶	⦶	⦶	⦶	⦶	⦶	⦶	⦶	⦶	⦶	⦶	⦶	⦶	⦶	⦶	⦶	⦶	⦶	⦶	⦶	⦶	⦶	⦶	⦶	⦶	⦶	⦶	⦶	⦶	⦶	⦶	⦶	⦶	⦶	⦶	⦶	⦶	⦶	⦶	⦶	⦶	⦶	⦶	⦶	⦶	⦶	⦶	⦶	⦶	⦶	⦶	⦶	⦶	⦶	⦶	⦶	⦶	⦶	⦶	⦶	⦶	⦶	⦶	⦶	⦶	⦶	⦶	⦶	⦶	⦶	⦶	⦶	⦶	⦶	⦶	⦶	⦶	⦶	⦶	⦶	⦶	⦶	⦶	⦶	⦶	⦶	⦶	⦶	⦶	⦶	⦶	⦶	⦶	⦶	⦶	⦶	⦶	⦶	⦶	⦶	⦶	⦶	⦶	⦶	⦶	⦶	⦶	⦶	⦶	⦶	⦶	⦶	⦶	⦶	⦶	⦶	⦶	⦶	⦶	⦶	⦶	⦶	⦶	⦶	⦶	⦶	⦶	⦶	⦶	⦶	⦶	⦶	⦶	⦶	⦶	⦶	⦶	⦶	⦶	⦶	⦶	⦶	⦶	⦶	⦶	⦶	⦶	⦶	⦶	⦶	⦶	⦶	⦶	⦶	⦶	⦶	⦶	⦶	⦶	⦶	⦶	⦶	⦶	⦶	⦶	⦶	⦶	⦶	⦶	⦶	⦶	⦶	⦶	⦶	⦶	⦶	⦶	⦶	⦶	⦶	⦶	⦶	⦶	⦶	⦶	⦶	⦶	⦶	⦶	⦶	⦶	⦶	⦶	⦶	⦶	⦶	⦶	⦶	⦶	⦶	⦶	⦶	⦶	⦶	⦶	⦶	⦶	⦶	⦶	⦶	⦶	⦶	⦶	⦶	⦶	⦶	⦶	⦶	⦶	⦶	⦶	⦶	⦶	⦶	⦶	⦶	⦶	⦶	⦶	⦶	⦶	⦶	⦶	⦶	⦶	⦶	⦶	⦶	⦶	⦶	⦶	⦶	⦶	⦶	⦶	⦶	⦶	⦶	⦶	⦶	⦶	⦶	⦶	⦶	⦶	⦶	⦶	⦶	⦶	⦶	⦶	⦶	⦶	⦶	⦶	⦶	⦶	⦶	⦶	⦶	⦶	⦶	⦶	⦶	⦶	⦶	⦶	⦶	⦶	⦶	⦶	⦶	⦶	⦶	⦶	⦶	⦶	⦶	⦶	⦶	⦶	⦶	⦶	⦶	⦶	⦶	⦶	⦶	⦶	⦶	⦶	⦶	⦶	⦶	⦶	⦶	⦶	⦶	⦶	⦶	⦶	⦶	⦶	⦶	⦶	⦶	⦶	⦶	⦶	⦶	⦶	⦶	⦶	⦶	⦶	⦶	⦶	⦶	⦶	⦶	⦶	⦶	⦶	⦶	⦶	⦶	⦶	⦶	⦶	⦶	⦶	⦶	⦶	⦶	⦶	⦶	⦶	⦶	⦶	⦶	⦶	⦶	⦶	⦶	⦶	⦶	⦶	⦶	⦶	⦶	⦶	⦶	⦶	⦶	⦶	⦶	⦶	⦶	⦶	⦶	⦶	⦶	⦶	⦶	⦶	⦶	⦶	⦶	⦶	⦶	⦶	⦶	⦶	⦶	⦶	⦶	⦶	⦶	⦶	⦶	⦶	⦶	⦶	⦶	⦶	⦶	⦶	⦶	⦶	⦶	⦶	⦶	⦶	⦶	⦶	⦶	⦶	⦶	⦶	⦶	⦶	⦶	⦶	⦶	⦶	⦶	⦶	⦶	⦶	⦶	⦶	⦶	⦶	⦶	⦶	⦶	⦶	⦶	⦶	⦶	⦶	⦶	⦶	⦶	⦶	⦶	⦶	⦶	⦶	⦶	⦶	⦶	⦶	⦶	⦶	⦶	⦶	⦶	⦶	⦶	⦶	⦶	⦶	⦶	⦶	⦶	⦶	⦶	⦶	⦶	⦶	⦶	⦶	⦶	⦶	⦶	⦶	⦶	⦶	⦶	⦶	⦶	⦶	⦶	⦶	⦶	⦶	⦶	⦶	⦶	⦶	⦶	⦶	⦶	⦶	⦶	⦶	⦶	⦶	⦶	⦶	⦶	⦶	⦶	⦶	⦶	⦶	⦶	⦶	⦶	⦶	⦶	⦶	⦶	⦶	⦶	⦶	⦶	⦶	⦶	⦶	⦶	⦶	⦶	⦶	⦶	⦶	⦶	⦶	⦶	⦶	⦶	⦶	⦶	⦶	⦶	⦶	⦶	⦶	⦶	⦶	⦶	⦶	⦶	⦶	⦶	⦶	⦶	⦶	⦶	⦶	⦶	⦶	⦶	⦶	⦶	⦶	⦶	⦶	⦶	⦶	⦶	⦶	⦶	⦶	⦶	⦶	⦶	⦶	⦶	⦶	⦶	⦶	⦶	⦶	⦶	⦶	⦶	⦶	⦶	⦶	⦶	⦶	⦶	⦶	⦶	⦶	⦶	⦶	⦶	⦶	⦶	⦶	⦶	⦶	⦶	⦶	⦶	⦶	⦶	⦶	⦶	⦶	⦶	⦶	⦶	⦶	⦶	⦶	⦶	⦶	⦶	⦶	⦶	⦶	⦶	⦶	⦶	⦶	⦶	⦶	⦶	⦶	⦶	⦶	⦶	⦶	⦶	⦶	⦶	⦶	⦶	⦶	⦶	⦶	⦶	⦶	⦶	⦶	⦶	⦶	⦶	⦶	⦶	⦶	⦶	⦶	⦶	⦶	⦶	⦶	⦶	⦶	⦶	⦶	⦶	⦶	⦶	⦶	⦶	⦶	⦶	⦶	⦶	⦶	⦶	⦶	⦶	⦶	⦶	⦶	⦶	⦶	⦶	⦶	⦶	⦶	⦶	⦶	⦶	⦶	⦶	⦶	⦶	⦶	⦶	⦶	⦶	⦶	⦶	⦶	⦶	⦶	⦶	⦶	⦶	⦶	⦶	⦶	⦶	⦶	⦶	⦶	

[illegible]

[illegible]





[illegible]

[illegible]

[illegible]





[illegible]

[illegible]

[illegible]



[illegible]

[illegible]

Las Majadas del Caserio					Carbonate Classification					Siliciclastic Rocks					Components														Sheet 7 / 10																																																																																																																																																																																																																			
Stage	Fm.	m.	Profile / Lithology	Sample	M	W	P	G/Br	B	M	S	FS	MS	CS	C/B																																																																																																																																																																																																																																	

[illegible]



[illegible]

[illegible]

West of Oville														Components							Sheet 1 / 6				
<div>N 42° 54,822' W 005° 20,389' Altitude: 1360m</div>						Carbonate Classification				Siliciclastic Rocks														Depositional Environment	
Stage	Fm .	m.	Profile / Lithology		Sample	M	W	P	G/ Br	B	M	S	FS	MS	CS	C/B									
Serpukhovian	Barcaliente Fm.	0.0-																			Basin				
Bashkirian	Forcoso Fm.	44.0-																							

[illegible]



[illegible]

[illegible]

[illegible]

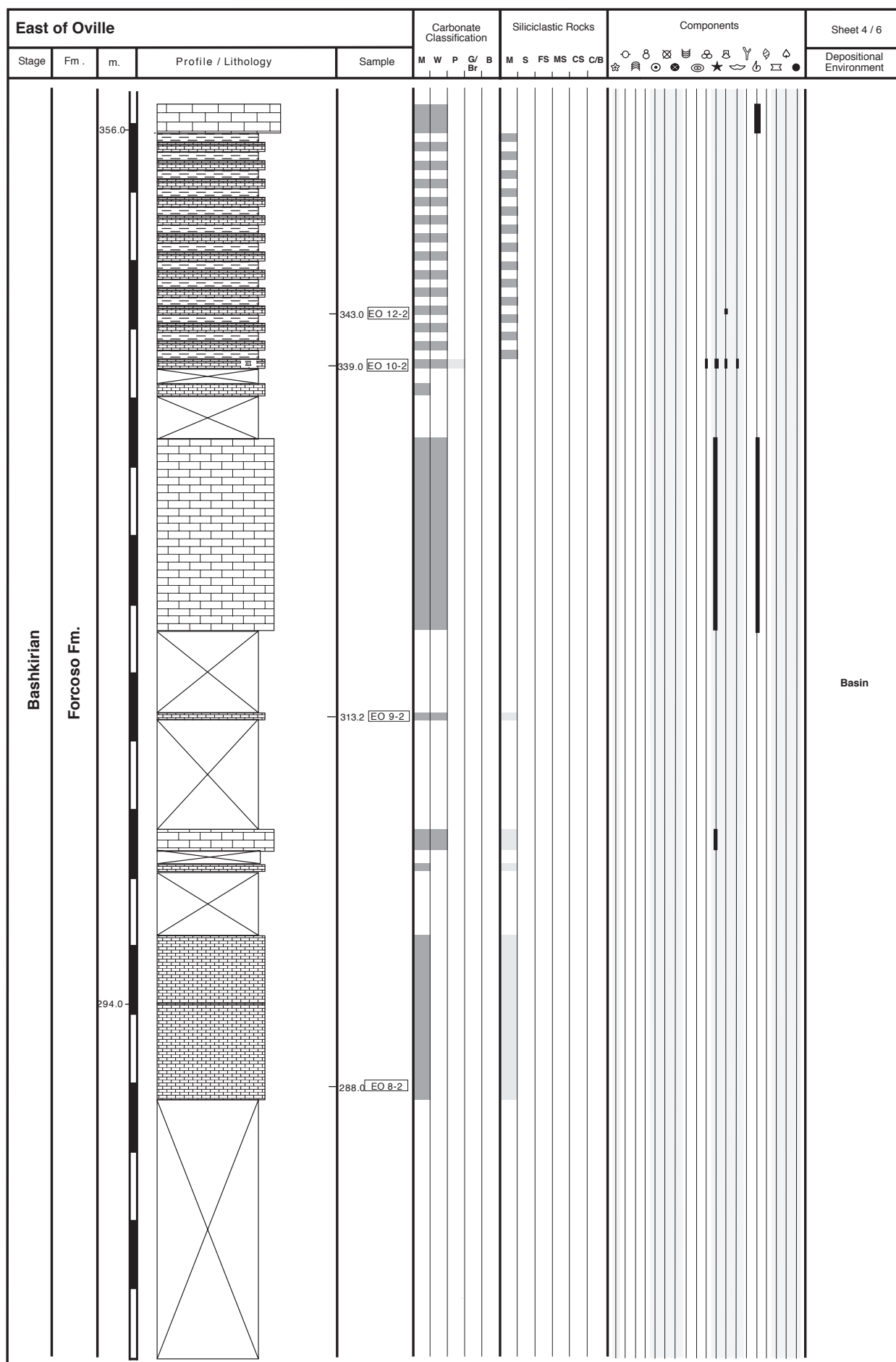
[illegible]



[illegible]

[illegible]

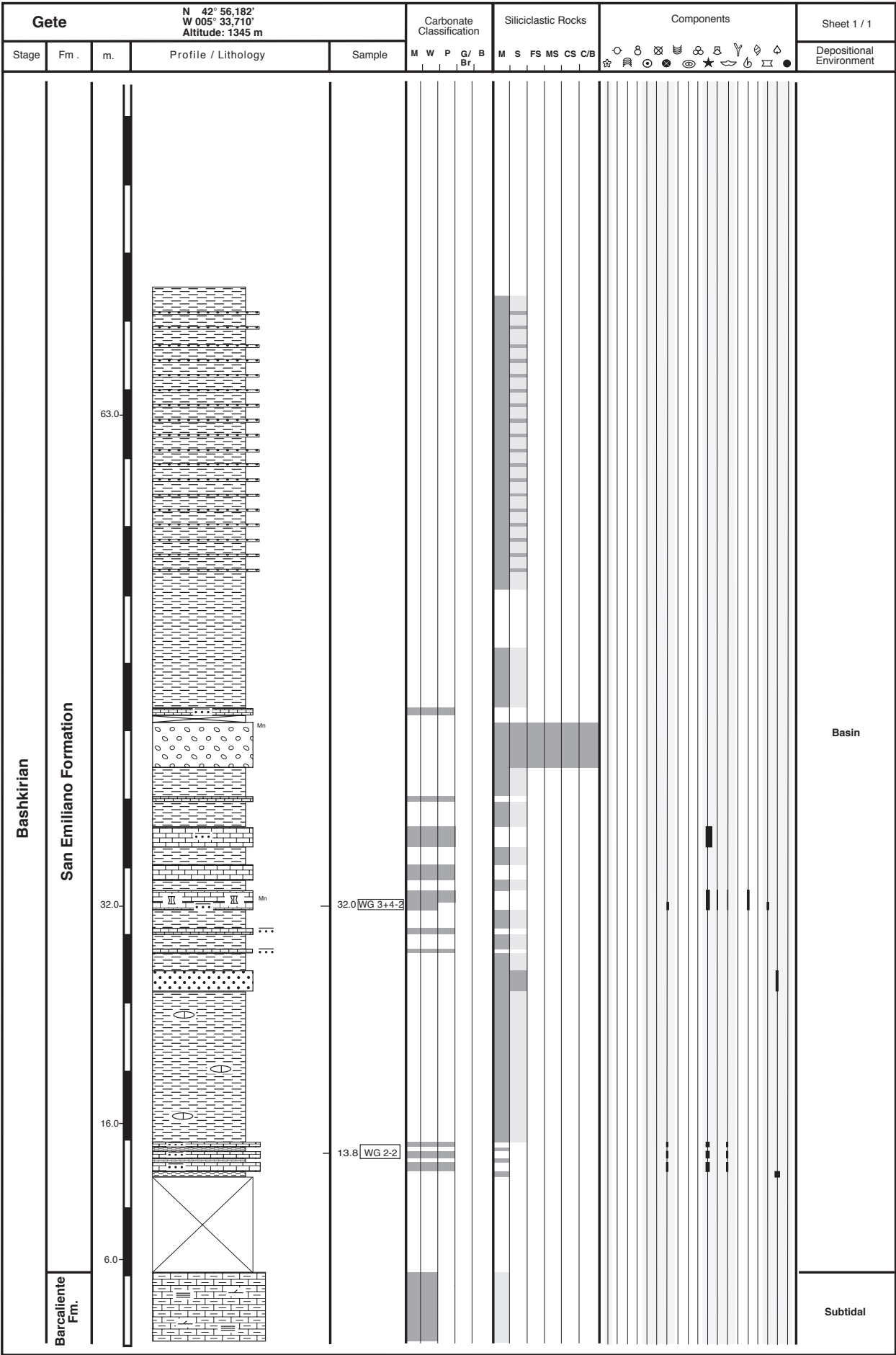
[illegible]



[illegible]



[illegible]



[illegible]

[illegible]

**Slope (?)**



Coto Calvo					Carbonate Classification					Siliciclastic Rocks					Components												Sheet 4 / 4
Stage	Fm .	m.	Profile / Lithology	Sample	M	W	P	G/Br	B	M	S	FS	MS	CS	C/B	<div><div><div><div>○</div><div>⊗</div><div>⊙</div><div>⊛</div><div>⊞</div><div>⊠</div><div>⊡</div><div>⊢</div><div>⊣</div><div>⊤</div><div>⊥</div><div>⊦</div><div>⊧</div><div>⊨</div><div>⊩</div><div>⊪</div><div>⊫</div><div>⊬</div><div>⊭</div><div>⊮</div><div>⊯</div><div>⊰</div><div>⊱</div><div>⊲</div><div>⊳</div><div>⊴</div><div>⊵</div><div>⊶</div><div>⊷</div><div>⊸</div><div>⊹</div><div>⊺</div><div>⊻</div><div>⊼</div><div>⊽</div><div>⊾</div><div>⊿</div></div><div><div>○</div><div>⊗</div><div>⊙</div><div>⊛</div><div>⊞</div><div>⊠</div><div>⊡</div><div>⊢</div><div>⊣</div><div>⊤</div><div>⊥</div><div>⊦</div><div>⊧</div><div>⊨</div><div>⊩</div><div>⊪</div><div>⊫</div><div>⊬</div><div>⊭</div><div>⊮</div><div>⊯</div><div>⊰</div><div>⊱</div><div>⊲</div><div>⊳</div><div>⊴</div><div>⊵</div><div>⊶</div><div>⊷</div><div>⊸</div><div>⊹</div><div>⊺</div><div>⊻</div><div>⊼</div><div>⊽</div><div>⊾</div><div>⊿</div></div><div><div>○</div><div>⊗</div><div>⊙</div><div>⊛</div><div>⊞</div><div>⊠</div><div>⊡</div><div>⊢</div><div>⊣</div><div>⊤</div><div>⊥</div><div>⊦</div><div>⊧</div><div>⊨</div><div>⊩</div><div>⊪</div><div>⊫</div><div>⊬</div><div>⊭</div><div>⊮</div><div>⊯</div><div>⊰</div><div>⊱</div><div>⊲</div><div>⊳</div><div>⊴</div><div>⊵</div><div>⊶</div><div>⊷</div><div>⊸</div><div>⊹</div><div>⊺</div><div>⊻</div><div>⊼</div><div>⊽</div><div>⊾</div><div>⊿</div></div><div><div>○</div><div>⊗</div><div>⊙</div><div>⊛</div><div>⊞</div><div>⊠</div><div>⊡</div><div>⊢</div><div>⊣</div><div>⊤</div><div>⊥</div><div>⊦</div><div>⊧</div><div>⊨</div><div>⊩</div><div>⊪</div><div>⊫</div><div>⊬</div><div>⊭</div><div>⊮</div><div>⊯</div><div>⊰</div><div>⊱</div><div>⊲</div><div>⊳</div><div>⊴</div><div>⊵</div><div>⊶</div><div>⊷</div><div>⊸</div><div>⊹</div><div>⊺</div><div>⊻</div><div>⊼</div><div>⊽</div><div>⊾</div><div>⊿</div></div><div><div>○</div><div>⊗</div><div>⊙</div><div>⊛</div><div>⊞</div><div>⊠</div><div>⊡</div><div>⊢</div><div>⊣</div><div>⊤</div><div>⊥</div><div>⊦</div><div>⊧</div><div>⊨</div><div>⊩</div><div>⊪</div><div>⊫</div><div>⊬</div><div>⊭</div><div>⊮</div><div>⊯</div><div>⊰</div><div>⊱</div><div>⊲</div><div>⊳</div><div>⊴</div><div>⊵</div><div>⊶</div><div>⊷</div><div>⊸</div><div>⊹</div><div>⊺</div><div>⊻</div><div>⊼</div><div>⊽</div><div>⊾</div><div>⊿</div></div></div></div>	Depositional Environment										
Bashkirian	Valdeteja Fm.	282.0	<div><div><div><div></div><div></div><div></div><div></div><div></div><div></div><div></div><div></div><div></div><div></div><div></div><div></div><div></div><div></div><div></div><div></div><div></div><div></div><div></div><div></div><div></div><div></div><div></div><div></div><div></div><div></div><div></div><div></div><div></div><div></div><div></div><div></div><div></div><div></div><div></div><div></div><div></div><div></div><div></div><div></div><div></div><div></div><div></div><div></div><div></div><div></div><div></div><div></div><div></div><div></div><div></div><div></div><div></div><div></div><div></div><div></div><div></div><div></div><div></div><div></div><div></div><div></div><div></div><div></div><div></div><div></div><div></div><div></div><div></div><div></div><div></div><div></div><div></div><div></div><div></div><div></div><div></div><div></div><div></div><div></div><div></div><div></div><div></div><div></div><div></div><div></div><div></div><div></div><div></div><div></div><div></div><div></div><div></div><div></div><div></div><div></div><div></div><div></div><div></div><div></div><div></div><div></div><div></div><div></div><div></div><div></div><div></div><div></div><div></div><div></div><div></div><div></div><div></div><div></div><div></div><div></div><div></div><div></div><div></div><div></div><div></div><div></div><div></div><div></div><div></div><div></div><div></div><div></div><div></div><div></div><div></div><div></div><div></div><div></div><div></div><div></div><div></div><div></div><div></div><div></div><div></div><div></div><div></div><div></div><div></div><div></div><div></div><div></div><div></div><div></div><div></div><div></div><div></div><div></div><div></div><div></div><div></div><div></div><div></div><div></div><div></div><div></div><div></div><div></div><div></div><div></div><div></div><div></div><div></div><div></div><div></div><div></div><div></div><div></div><div></div><div></div><div></div><div></div><div></div><div></div><div></div><div></div><div></div><div></div><div></div><div></div><div></div><div></div><div></div><div></div><div></div><div></div><div></div><div></div><div></div><div></div><div></div><div></div><div></div><div></div><div></div><div></div><div></div><div></div><div></div><div></div><div></div><div></div><div></div><div></div><div></div><div></div><div></div><div></div><div></div><div></div><div></div><div></div><div></div><div></div><div></div><div></div><div></div><div></div><div></div><div></div><div></div><div></div><div></div><div></div><div></div><div></div><div></div><div></div><div></div><div></div><div></div><div></div><div></div><div></div><div></div><div></div><div></div><div></div><div></div><div></div><div></div><div></div><div></div><div></div><div></div><div></div><div></div><div></div><div></div><div></div><div></div><div></div><div></div><div></div><div></div><div></div><div></div><div></div><div></div><div></div><div></div><div></div><div></div><div></div><div></div><div></div><div></div><div></div><div></div><div></div><div></div><div></div><div></div><div></div><div></div><div></div><div></div><div></div><div></div><div></div><div></div><div></div><div></div><div></div><div></div><div></div><div></div><div></div><div></div><div></div><div></div><div></div><div></div><div></div><div></div><div></div><div></div><div></div><div></div><div></div><div></div><div></div><div></div><div></div><div></div><div></div><div></div><div></div><div></div><div></div><div></div><div></div><div></div><div></div><div></div><div></div><div></div><div></div><div></div><div></div><div></div><div></div><div></div><div></div><div></div><div></div><div></div><div></div><div></div><div></div><div></div><div></div><div></div><div></div><div></div><div></div><div></div><div></div><div></div><div></div><div></div><div></div><div></div><div></div><div></div><div></div><div></div><div></div><div></div><div></div><div></div><div></div><div></div><div></div><div></div><div></div><div></div><div></div><div></div><div></div><div></div><div></div><div></div><div></div><div></div><div></div><div></div><div></div><div></div><div></div><div></div><div></div><div></div><div></div><div></div><div></div><div></div><div></div><div></div><div></div><div></div><div></div><div></div><div></div><div></div><div></div><div></div><div></div><div></div><div></div><div></div><div></div><div></div><div></div><div></div><div></div><div></div><div></div><div></div><div></div><div></div><div></div><div></div><div></div><div></div><div></div><div></div><div></div><div></div><div></div><div></div><div></div><div></div><div></div><div></div><div></div><div></div><div></div><div></div><div></div><div></div><div></div><div></div><div></div><div></div><div></div><div></div><div></div><div></div><div></div><div></div><div></div><div></div><div></div><div></div><div></div><div></div><div></div><div></div><div></div><div></div><div></div><div></div><div></div><div></div><div></div><div></div><div></div><div></div><div></div><div></div><div></div><div></div><div></div><div></div><div></div><div></div><div></div><div></div><div></div><div></div><div></div><div></div><div></div><div></div><div></div><div></div><div></div><div></div><div></div><div></div><div></div><div></div><div></div><div></div><div></div><div></div><div></div><div></div><div></div><div></div><div></div><div></div><div></div><div></div><div></div><div></div><div></div><div></div><div></div><div></div><div></div><div></div><div></div><div></div><div></div><div></div><div></div><div></div><div></div><div></div><div></div><div></div><div></div><div></div><div></div><div></div><div></div><div></div><div></div><div></div><div></div><div></div><div></div><div></div><div></div><div></div><div></div><div></div><div></div><div></div><div></div><div></div><div></div><div></div><div></div><div></div><div></div><div></div><div></div><div></div><div></div><div></div><div></div><div></div><div></div><div></div><div></div><div></div><div></div><div></div><div></div><div></div><div></div><div></div><div></div><div></div><div></div><div></div><div></div><div></div><div></div><div></div><div></div><div></div><div></div><div></div><div></div><div></div><div></div><div></div><div></div><div></div><div></div><div></div><div></div><div></div><div></div><div></div><div></div><div></div><div></div><div></div><div></div><div></div><div></div><div></div><div></div><div></div><div></div><div></div><div></div><div></div><div></div><div></div><div></div><div></div><div></div><div></div><div></div><div></div><div></div><div></div><div></div><div></div><div></div><div></div><div></div><div></div><div></div><div></div><div></div><div></div><div></div><div></div><div></div><div></div><div></div><div></div><div></div><div></div><div></div><div></div><div></div><div></div><div></div><div></div><div></div><div></div><div></div><div></div><div></div><div></div><div></div><div></div><div></div><div></div><div></div><div></div><div></div><div></div><div></div><div></div><div></div><div></div><div></div><div></div><div></div><div></div><div></div><div></div><div></div><div></div><div></div><div></div><div></div><div></div><div></div><div></div><div></div><div></div><div></div><div></div><div></div><div></div><div></div><div></div><div></div><div></div><div></div><div></div><div></div><div></div><div></div><div></div><div></div><div></div><div></div><div></div><div></div><div></div><div></div><div></div><div></div><div></div><div></div><div></div><div></div><div></div><div></div><div></div><div></div><div></div><div></div><div></div><div></div><div></div><div></div><div></div><div></div><div></div><div></div><div></div><div></div><div></div><div></div><div></div><div></div><div></div><div></div><div></div><div></div><div></div><div></div><div></div><div></div><div></div><div></div><div></div><div></div><div></div><div></div><div></div><div></div><div></div><div></div><div></div><div></div><div></div><div></div><div></div><div></div><div></div><div></div><div></div><div></div><div></div><div></div><div></div><div></div><div></div><div></div><div></div><div></div><div></div><div></div><div></div><div></div><div></div><div></div><div></div><div></div><div></div><div></div><div></div><div></div><div></div><div></div><div></div><div></div><div></div><div></div><div></div><div></div><div></div><div></div><div></div><div></div><div></div><div></div><div></div><div></div><div></div><div></div><div></div><div></div><div></div><div></div><div></div><div></div><div></div><div></div><div></div><div></div><div></div><div></div><div></div><div></div><div></div><div></div><div></div><div></div><div></div><div></div><div></div><div></div><div></div><div></div><div></div><div></div><div></div><div></div><div></div><div></div><div></div><div></div><div></div><div></div><div></div><div></div><div></div><div></div><div></div><div></div><div></div><div></div><div></div><div></div><div></div><div></div><div></div><div></div><div></div><div></div><div></div><div></div><div></div><div></div><div></div><div></div><div></div><div></div><div></div><div></div><div></div><div></div><div></div><div></div><div></div><div></div><div></div><div></div><div></div><div></div><div></div><div></div><div></div><div></div><div></div><div></div><div></div><div></div><div></div><div></div><div></div><div></div><div></div><div></div><div></div><div></div><div></div><div></div></div></div></div>																								

[illegible]

[illegible]

Valdorria					Carbonate Classification					Siliciclastic Rocks					Components													Sheet 3 / 10		
Stage	Fm .	m.	Profile / Lithology	Sample	M	W	P	G	B	M	S	FS	MS	CS	C/B													Depos. Envir.	Systems Tract	
Bashkirian	Valdeteja Formation	231.0-																											Slope (?)	HST (Bas 1)

[illegible]



[illegible]

[illegible]

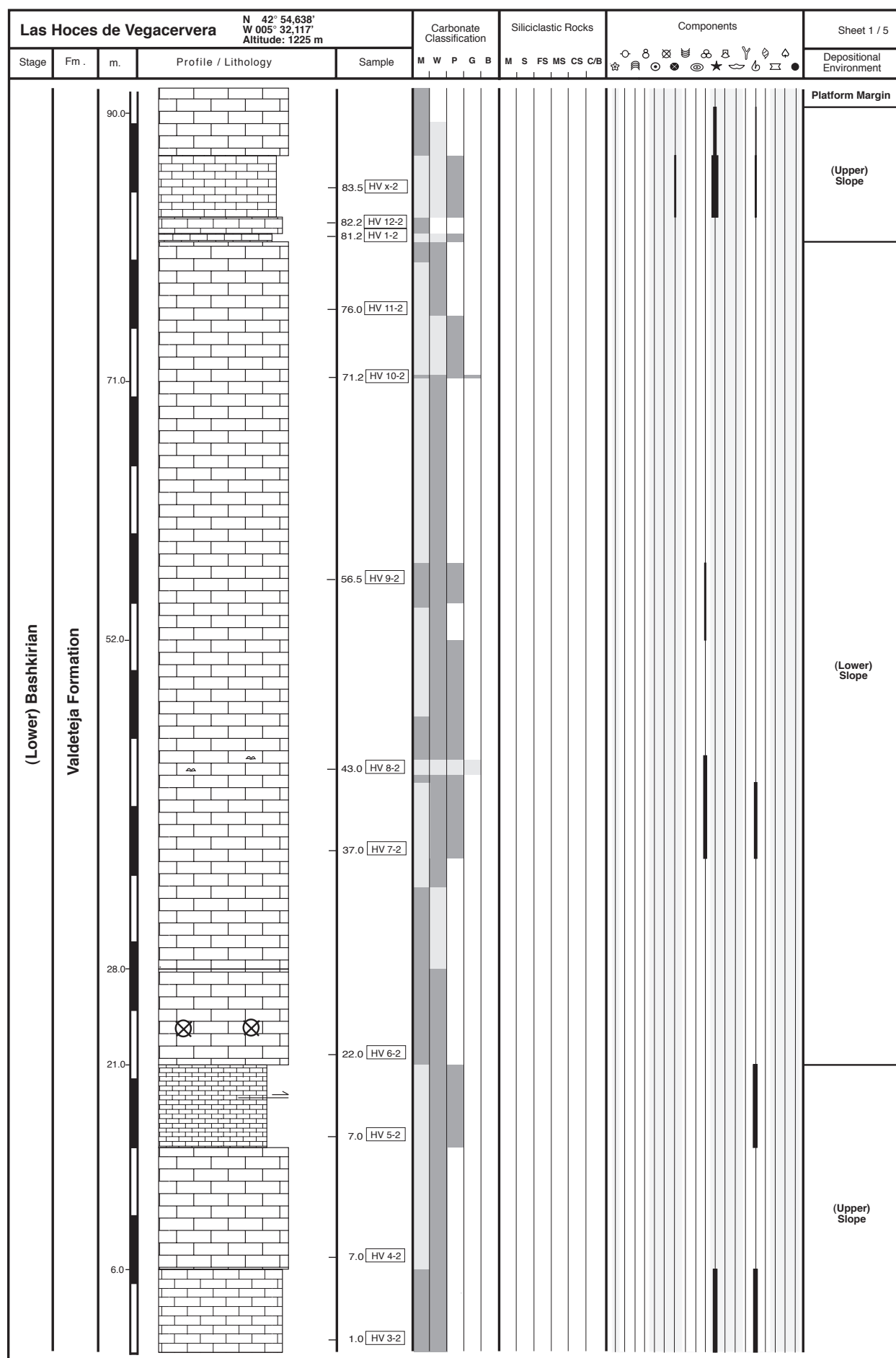
[illegible]

[illegible]

[illegible]



[illegible]



[illegible]

[illegible]

[illegible]



[illegible]

**Cuevas Fm.**

[illegible]



## APPENDIX II

## Biostratigraphic Data

Table A.1: Biostratigraphic database.

Location	Tectonic Unit	Formation	Position in Formation (m above base)	Age	Method	Reference
Arroyo de Barcaliente	Bodón	Barcaliente	up to 105	Ambergian - Upper Namurian A	conodonts	Menendez Alvarez 1991
Arroyo de Barcaliente	Bodón	Barcaliente	Base	Ambergian - Upper Namurian A	ammonites	Kullman 1962, Wagner et al. 1971
Arroyo de Barcaliente	Bodón	Barcaliente	105 - 150	Boundary Ambergian - Chokierian	conodonts	Menendez Alvarez 1991
Arroyo de Barcaliente	Bodón	Barcaliente	Top	R1a - Lower Namurian B	goniatites	Kullmann, 1962, 1963, 1979; Sjerp, 1967
Arroyo de Barcaliente	Bodón	Barcaliente	Top	Lower Bashkirian - Lower Namurian B	foraminifers	Villa 1982
Arroyo de Barcaliente	Bodón	Barcaliente	Top	Kinderscoutian - Lower Namurian B	conodonts	Menendez Alvarez 1991
Type locality	Bodón	Barcaliente	Top	Syranian or older	foraminifers	Villa et al. 2001
North of Villamanin	Bodón	caliza masiva	Base	Upper Bashkirian	Fusulinids, microflora	Moore et al. 1971, Villa et al. 1988
North of Villamanin	Bodón	caliza masiva	Base	Upper Bashkirian	brachiopods	Martinez Chacon in Truyols & Sanchez de Posada 1983
North of Villamanin	Bodón	caliza masiva	Top	Vereian - Lower Moscovian	foraminifers	Villa et al. 1988
Porma Lake, westernmost viewpoint	Forcada	Forcoso	Base	R1a - Lower Namurian B	goniatites	Kullmann 1979
East of Oville	Bodón	Forcoso	Base	R1 - Namurian B	goniatites	Reuther 1977
Tolbia de Arriba	Forcada	Forcoso	350	Boundary Bashkirian/Moscovian	germs, calcareous algae	Rác 1966, in: Evers 1967
Tolbia de Arriba	Forcada	Forcoso	Base	R1 - Namurian B	goniatites	Reuther 1977
Llamazares	Forcada	Forcoso	Base	R1 - Namurian B	goniatites	Reuther 1977
East of Oville	Bodón	Forcoso	110	Westphalian A	goniatites	Frankenfeld 1976, Reuther 1977
Tolbia de Arriba	Forcada	Forcoso	350	Lower Moscovian	calcareous algae	Rác 1966
Fonfria	Pedroso Syncline	Olleros	Base	R1 - Namurian B	goniatites	Reuther 1977
Type locality	Bodón	San Emiliano	960	Boundary Bashkirian/Moscovian	plant macrofossils	Wagner & Bowman 1983
Type locality	Bodón	San Emiliano	780	Uppermost Bashkirian	plant macrofossils	Wagner & Bowman 1983
Type locality	Bodón	San Emiliano	1120	Lowermost Moscovian	plant macrofossils,	Wagner & Bowman 1983
Type locality	Bodón	San Emiliano	"Top"	(Upper?) Westphalian A	plant macrofossils	Wagner & Bowman 1983
Type locality	Bodón	San Emiliano	Base	Yeadonian (Namurian C)	miospores	Wagner & Bowman 1983
North of Gete	Gayo	San Emiliano	Base	R2 - Namurian B	goniatite	Eichmüller 1985
North of Valverde	Bodón	San Emiliano	485	Lower Upper Bashkirian	calcareous algae	Rác 1966
R24: North of Lavandera	Bodón	San Emiliano	400	Uppermost Bashkirian/close to Moscovian	calcareous algae	Rác 1966
R36: North of Pedrosa	Bodón	San Emiliano	Base	Lower Upper Bashkirian	calcareous algae	Rác 1966
R401: North of Cármenes	Bodón	San Emiliano	Base	Lower Upper Bashkirian	calcareous algae	Rác 1966
R449: West of Pedrosa	Bodón	San Emiliano	youngest carbonate unit	Uppermost Bashkirian/close to Moscovian	calcareous algae	Rác 1966



Table A.1 (continued)

R42&43: West of Almuzara (southern limb)	Bodón	San Emiliano	corresponds to oldest carbonate unit	Uppermost Bashkirian/close to Moscovian	calcareous algae	Rác 1966
North of Valverdin	Bodón	San Emiliano	270	Middle Westphalian C	calcareous algae	Rinklef 1987
North of Pedrosa	Bodón	San Emiliano	298	Westphalian C	corals	Boll 1985
North of Valverdin	Bodón	San Emiliano	285	Westphalian C	corals	Boll 1986
Type locality	Bodón	San Emiliano	Top	Kashirsky - Westphalian B	fusulinids	Fernández Rodríguez-Arango et al. 1981, Leyva et al. 1985, Truyols et al. 1982, Wagner & Bowman 1983
Type locality	Bodón	San Emiliano	Base	Yeadonian - Namurian C	miospores	Bowman 1982
Type locality	Bodón	San Emiliano	Base La Majua Mb.	Tashastinsky - Lower Upper Bashkirian	foraminifers	Van Ginkel 1965
Type locality	Bodón	San Emiliano	Base Candemuela Mb.	Boundary Bashkirian/Moscovian	foraminifers	Van Ginkel 1965, 1987, Leyva et al. 1985
Type locality	Bodón	Valdeteja	7	Upper boundary Millerella Zone	fusulinids	Eichmüller 1985
Type locality	Bodón	Valdeteja	107	Upper boundary Pseudostaffella antiqua Subzone	fusulinids	Eichmüller 1985
Type locality	Bodón	Valdeteja	757	Upper boundary Profusulinella Subzone A	fusulinids	Eichmüller 1985
Type locality	Bodón	Valdeteja	814	Upper boundary Profusulinella Subzone A	fusulinids	Eichmüller 1985
Las Majadas	Bodón	Valdeteja	43	Upper boundary Pseudostaffella antiqua Subzone	fusulinids	Eichmüller 1985
West of Oville	Bodón	Valdeteja	186	Upper boundary Profusulinella Subzone A	fusulinids	Eichmüller 1985
West of Oville	Bodón	Valdeteja	50	Upper boundary Millerella Zone	fusulinids	Eichmüller 1985
Gete	Gayo	Valdeteja	107	Upper boundary Pseudostaffella antiqua Subzone	fusulinids	Eichmüller 1985
Gete	Gayo	Valdeteja	164	Upper boundary Pseudostaffella antiqua Subzone	fusulinids	Eichmüller 1985
Caldas de Nocado	Gayo	Valdeteja	450	Upper boundary Profusulinella Subzone A	fusulinids	Eichmüller 1985
Caldas de Nocado	Gayo	Valdeteja	221	Upper boundary Pseudostaffella antiqua Subzone	fusulinids	Eichmüller 1985
Las Hoces de Vegacervera (southern limb)	Correcilla	Valdeteja	29	Upper boundary Millerella Zone	fusulinids	Eichmüller 1985
Las Hoces de Vegacervera (northern limb)	Correcilla	Valdeteja	200	Upper boundary Pseudostaffella antiqua Subzone	fusulinids	Eichmüller 1985
Las Hoces de Vegacervera (northern limb)	Correcilla	Valdeteja	481	Akavassky horizon (thin section VV 3-2)	fusulinids	pers.com. E. Villa 2003
Caldas de Nocado	Gayo	Valdeteja	537	Askynbashsky horizon (thin section VV 8-2)	fusulinids	pers.com. E. Villa 2003
Caldas de Nocado	Gayo	Valdeteja	548	Upper Bashkirian (thin section VV 10-2)	fusulinids	pers.com. E. Villa 2003

Table A.1 (continued)

Las Majadas del Caserio	Bodón	Valdeteja	530	Upper Bashkirian	fusulinids	Villa 1982
Las Majadas del Caserio	Bodón	Valdeteja	300	Lowermost Upper Bashkirian (Tashatinsky)	fusulinids	Villa 1982
Las Majadas del Caserio	Bodón	Valdeteja	Base	R1 - Namurian B	goniatites	Reuther 1977
Type locality	Bodón	Valdeteja	47	Lower Bashkirian	brachiopods, corals	Wagner et al. 1971, Winkler Prins 1968
Las Majadas del Caserio	Bodón	Valdeteja	665	Early Moscovian (Vereisky)	foraminifers	Villa 1982
Type locality	Bodón	Valdeteja	Top	Askynbashsky - Uppermost Lower Bashkirian	foraminifers	van Ginkel 1987
Las Majadas del Caserio	Bodón	Valdeteja	210	Boundary between Idiognathoides delicatus und -parvus	conodonts	Menendez Alvarez 1991
Las Majadas del Caserio	Bodón	Valdeteja	15	Marsdenian or younger	conodonts	Menendez Alvarez 1991
Type locality	Bodón	Valdeteja	Base	Namurian B	goniatites	Reuther 1977
Viadangos de Arbas	Bodón	Valdeteja	Top	Upper Namurian B	spores	Moore et al. 1971
Type locality	Bodón	Valdeteja	Top	Vereian - Lower Moscovian	foraminifers	Villa et al. 2001
Type locality	Bodón	Valdeteja	Base	Lower Bashkirian	foraminifers	Villa et al. 2001
Type locality	Bodón	Valdeteja	42 ( <i>Cladochonus</i> Band)	Akavasian - Lower Bashkirian	foraminifers	Villa et al. 2001
Type locality	Bodón	Valdeteja	540 ( <i>Chaoiella</i> Band)	Upper Bashkirian	foraminifers	Villa et al. 2001
Type locality	Bodón	Valdeteja	541 ( <i>Chaoiella</i> Band)	Yeadonian - Upper Bashkirian	conodonts	Menendez Alvarez 1991
Type locality	Bodón	Valdeteja	515 ( <i>Fenestella-Composita</i> Band)	Upper Bashkirian	foraminifers	Villa et al. 2001
Type locality	Bodón	Valdeteja	670 ( <i>Echinoconchus</i> Band)	Uppermost Bashkirian	foraminifers	Villa et al. 2001
Type locality	Bodón	Valdeteja	705 ( <i>Linoproductus</i> Band)	Vereian - Lower Moscovian	foraminifers	Villa et al. 2001
Type locality	Bodón	Valdeteja	Base	Marsdenian - Lower Bashkirian (- <i>delicatus</i> )	conodonts	Menendez Alvarez 1991
Type locality	Bodón	Valdeteja	210	Upper Bashkirian ( <i>Ides. Tuberculatus</i> )	conodonts	Menendez Alvarez 1991
San Emiliano	Bodón	Valdeteja	Top	Lower Bashkirian (Krasnopolvansky)	foraminifers	Leyva et al. 1985
Type locality	Bodón	San Emiliano	Candemuela Mb.	Vereisky - Westfalian A/B	foraminifers	Leyva et al. 1985
Genicera/Valverdín	Bodón	San Emiliano	second limestone unit	Moscovian (undetermined)	brachiopods	Martinez Chacon in Fernandez Gonzalez 1990
Ollerios de Alba	Abelgas-Bregón	Ollerios	300	Serpukhovian (- <i>bolandensis</i> )	conodonts	Menendez Alvarez 1991
Ollerios de Alba	Abelgas-Bregón	Ollerios	Top	Namurian B	conodonts	Wagner & Fernandez Garcia 1971
Ollerios de Alba	Abelgas-Bregón	Ollerios	Base	Amsbergian - Serpukhovian	conodonts	Becker et al. 1975
Type locality	Bodón	Barcaliente	Top	R1 - Namurian B	goniatites	Braun 1981
Type locality	Bodón	Barcaliente	Top	Namurian B-C	conodonts	Braun 1981

## Stratigraphic Data

Table A.2: Input values for the reverse basin model: Torío Transect. Th: thickness, WD: water depth

	Formation	Age (Ma)	Forcada Unit		Bodón Unit		Gayo Unit		Correcilla Unit	
			Th (m)	WD (m)	Th (m)	WD (m)	Th (m)	WD (m)	Th (m)	WD (m)
Meso-/Cenozoic	Vegaquemada	34	150	-10	150	-10	150	-10	150	-10
	Hiatus	40	0	-40	0	-40	0	-40	0	-40
	Boñar	67	100	0	100	0	100	0	100	0
	Hiatus	77	0	-40	0	-40	0	-40	0	-40
	Utrillas/Voznuevo	94	750	-20	750	-20	750	-20	750	-20
Carboniferous	Hiatus	105	0	-50	0	-50	0	-50	0	-50
	San Emiliano	312	80	35	100	35	0	-25	0	-10
	Valdeteja/Forcoso/San Emiliano	313.5	20	40	20	40	15	-2	15	-5
	Valdeteja/Forcoso/San Emiliano	314	20	65	20	45	15	40	10	35
	Valdeteja/Forcoso/San Emiliano	314.5	38	60	40	35	30	40	30	40
	Valdeteja/Forcoso/San Emiliano	315	15	120	120	45	30	60	90	60
	Valdeteja/Forcoso/San Emiliano	315.5	28	160	260	55	35	65	100	65
	Valdeteja/Forcoso/San Emiliano	316.5	28	160	205	35	90	75	112	40
	Valdeteja/Forcoso/San Emiliano	317.5	28	160	140	25	50	80	112	10
	Valdeteja/Forcoso	318.5	56	160	100	30	308	35	200	15
	Barcaliente	319.5	180	30	187	22	190	24	190	24
	Alba	322	41	200	25	150	30	100	18	100
	Vegamián	347	1	100	2	90	3	80	2	80
	Baleas /Ermita	353	2	8	2	10	2	10	10	8
	Ermita	355	6	8	8	8	10	6	10	8
Devonian	Hiatus	358	0	-50	0	-35	0	-30	0	-30
	Huergas	385	0	-40	0	-30	0	-20	30	15
	Santa Lucía	391	0	-35	0	-28	0	-10	189	4
	Esla	396	0	-30	0	-27	48	40	92	40
	Abelgas	402	0	-27	0	-25	90	-1	110	-1
	San Pedro	415	0	-26	0	-24	22	10	20	10
Silurian	Formigoso	428	0	-23	0	-22	85	15	98	15
Ordovician	Hiatus	435	0	-30	0	-30	0	-30	0	-30
	Capas de Getino	459	0	-30	0	-20	0	-10	20	40
	Hiatus	465	0	-30	0	-30	0	-30	0	-30
	Barrios (La Matosa Mb.)	500	53	-5	194	2	200	3	170	3
Cambrian	Oville	505	170	-3	160	3	140	4	140	7
	Láncara	513	48	180	70	190	70	195	70	200
	Herrera	525	700	200	700	200	700	200	700	200
	Base Herrera	560								



Table A.4: Input values for the reverse basin model: Curueño Transect.

	Formation	Age (Ma)	Forcada Unit		Bodón Unit		Gayo Unit (North)		Gayo Unit (South)	
			Th (m)	WD (m)	Th (m)	WD (m)	Th (m)	WD (m)	Th (m)	WD (m)
Meso-/Cenozoic	Vegaquemada	34	150	-10	150	-10	150	-10	150	-10
	Hiatus	40	0	-40	0	-40	0	-40	0	-40
	Boñar	67	100	0	100	0	100	0	100	0
	Hiatus	77	0	-40	0	-40	0	-40	0	-40
	Utrillas/Voznuevo	94	750	-20	750	-20	750	-20	750	-20
	Hiatus	105	0	-50	0	-50	0	-50	0	-50
Carboníferous	San Emiliano	312	40	-10	25	-15	0	-18	0	-21
	San Emiliano	313.5	84	170	60	165	84	130	80	160
	San Emiliano	315	84	170	84	165	84	100	84	160
	Valdeteja/Forcoso	316.5	28	170	23	165	0	0	110	160
	Valdeteja/Forcoso	317.5	28	170	23	165	400	60	30	160
	Valdeteja/Forcoso	318.5	56	170	50	165	86	80	56	160
	Barcaliente	319.5	140	40	170	40	140	30	144	35
	Alba	322	41	200	35	150	20	100	14	100
	Vegamián	347	7	100	2	90	2	80	2	80
	Ermita/Baleas	353	3	7	4	8	4	8	4	10
Devonian	Ermita	355	3	7	4	8	4	8	8	6
	Hiatus	358	0	-50	0	-45	0	-30	0	-30
	Santa Lucía	391	0	-40	0	-37	0	-10	10	5
	Esla	396	0	-37	0	-34	90	30	115	40
	Abelgas	402	0	-33	0	-31	35	-1	46	-2
	San Pedro	415	0	-30	0	-28	20	10	18	10
Silurian	Formigoso	428	0	-27	0	-25	80	15	80	15
	Hiatus	435	0	-44	0	-40	0	-30	0	-30
Ordovician	Capas de Getino	459	0	-40	0	-33	15	40	15	40
	Hiatus	465	0	-38	0	-35	0	-30	0	-30
	Barrios (La Matosa Mb.)	500	0	-10	270	2	282	3	335	3
Cambrian	Oville	505	260	-3	280	3	300	4	300	4
	Láncara	513	48	180	55	190	64	195	57	200
	Herrería	525	700	200	700	200	700	200	700	200
	Base Herrería	560								



